# *Chemistry of Oxomolybdenum Complexes with ON- and ONO- Donor Ligands*

*Thesis submitted in partial fulfillment of the requirements for the degree of*

**Doctor of Philosophy**

**by**

**Sagarika Pasayat**

Under the guidance of

**Dr. Rupam Dinda**

**Department of Chemistry**
**National Institute of Technology, Rourkela**
**Rourkela-769008, Odisha, India**

# CERTIFICATE

This is to certify that the thesis entitled **"*Chemistry of oxomolybdenum complexes with ON- and ONO- donor ligands*"** submitted by **Sagarika Pasayat** of the Department of Chemistry, National Institute of Technology, Rourkela, India, for the degree of **Doctor of Philosophy** is a record of bona fide research work carried out by her under my guidance and supervision. I am satisfied that the thesis has reached the standard fulfilling the requirements of the regulations relating to the nature of the degree. To the best of my knowledge, the matter embodied in the thesis has not been submitted to any other University/Institute for the award of any degree or diploma.

Supervisor

Place: Rourkela

Date:

Dr. Rupam Dinda,

Department of Chemistry

National Institute of Technology,

Rourkela-769008, Odisha, India

# *Acknowledgements*

This thesis is the account of five years of devoted work in the field of Synthetic Inorganic Chemistry at Department of Chemistry, National Institute of Technology, Rourkela, India, which would not have been possible without the help of many.

I would like to give my deep appreciation for my supervisor Dr. Rupam Dinda. I would like to thank him with immense pleasure for his valuable guidance and constant encouragements. Without his expertise and guidance, this thesis would not be written.

I am thankful to the Director, National Institute of Technology, Rourkela for providing me the use of all infrastructural facilities. I would also like to thank Prof. B. G. Mishra, HOD of our Department for providing me the various laboratory and instrumental facilities during my Ph.D. work.

I sincerely thank Prof. R. K. Singh, Prof. K. M. Purohit and Prof. Saurav Chatterjee for evaluating my progress reports and seminars, their helpful comments and valuable discussion during the Ph. D. program. I am sincerely thankful to all the faculty members and staff of our Department for their constant help. Helps received from Dr. Debayan Sarkar deserve special mention. I am really indebted to the members of our research group Subhashree P. Dash, Saswati and Satabdi Roy for their kind cooperation.

I am thankful to Prof. M. R. Maurya, Department of Chemistry, IIT Roorkee for the study of catalysis and his valuable suggestions during manuscript preparation. I am thankful to Professor Shyamal Kumar Chattopadhyay, HOD, Department of Chemistry, BESU, Howrah, for his generous help in electrochemical studies. I would also thankful to Dr. Surajit Das, Department of Life Science, NIT, Rourkela for the help in biological studies.

I am grateful to Professor Ekkehard Sinn, Department of Chemistry, Western Michigan University, Kalamazoo, USA, Dr. Werner Kaminsky, Department of Chemistry, University of

Last but not the least, I would like to record deep respect to my parents for selflessly extending their ceaseless and moral support at all times without which this work wouldn't be possible.


Date:                                                                                              Sagarika Pasayat

# ABSTRACT

## Chemistry of Oxomolybdenum Complexes with ON- and ONO- Donor Ligands

*Sagarika Pasayat*

*Department of chemistry, National Institute of Technology, Rourkela-769008, Odisha, India*

---

**Chapter 1:** In this chapter the scope of the present investigation is delineated briefly along with the aim of the work.

**Chapter 2:** Reaction of benzoylhydrazone of 2-hydroxybenzaldehyde ($H_2L$) with [$MoO_2(acac)_2$] proceeds smoothly in refluxing ethanol to afford an orange complex [$MoO_2L(C_2H_5OH)$] (**1**). The substrate binding capacity of complex (**1**) has been demonstrated by the formation and isolation of two mononuclear [$MoO_2L(Q)$] {where Q = imidazole (**2a**) and 1-methylimidazole (**2b**)} and one dinuclear [$(MoO_2L)_2(Q)$] {Q = 4,4'-bipyridine (**3**)} mixed-ligand oxomolybdenum complexes. All the complexes have been characterized by elemental analysis, electrochemical and spectroscopic (IR, UV−Vis and NMR) measurements. Molecular structures of all the oxomolybdenum(VI) complexes (**1**, **2a**, **2b** and **3**) have been determined by X-ray crystallography. The complexes have been screened for their antibacterial activity against *Escherichia coli, Bacillus subtilis* and *Pseudomonas aeruginosa*. The minimum inhibitory concentration of these complexes and antibacterial activity indicates the compound **2a** and **2b** as the potential lead molecule for drug designing.

**Chapter 3:** Reaction of the salicyloylhydrazone of 2-hydroxy-1-naphthaldehyde ($H_2L^1$), anthranylhydrazone of 2-hydroxy-1-naphthaldehyde ($H_2L^2$), benzoylhydrazone of 2-hydroxy-1-acetonaphthone ($H_2L^3$) and anthranylhydrazone of 2-hydroxy-1-acetonaphthone ($H_2L^4$; general abbreviation $H_2L$) with [$MoO_2(acac)_2$] afforded a series of  5- and 6- coordinate Mo(VI) complexes of the type [$MoO_2L^{1-2}(ROH)$] [where R = $C_2H_5$ (**1**) and $CH_3$ (**2**)], and [$MoO_2L^{3-4}$] (**3** and **4**). The substrate binding capacity of **1** has been demonstrated by the formation of one mononuclear mixed-ligand dioxomolybdenum complex [$MoO_2L^1(Q)$] {where Q = γ-picoline (**1a**)}. Molecular structure of all the complexes (**1**, **1a**, **2**, **3** and **4**) is determined by X-ray crystallography, demonstrating the dibasic tridentate behavior of ligands. All the complexes have been characterized by elemental analysis, electrochemical and spectroscopic (IR, UV−Vis and

NMR) measurements. The complexes have been screened for their antibacterial activity against *Escherichia coli, Bacillus subtilis, Proteus vulgaris* and *Klebsiella pneumoniae*. The minimum inhibitory concentration of these complexes and antibacterial activity indicates **1** and **1a** as the potential lead molecule for drug designing. Catalytic potential of these complexes was tested for the oxidation of benzoin using 30% aqueous $H_2O_2$ as an oxidant in methanol. At least four reaction products benzoic acid, benzaldehyde-dimethylacetal, methylbenzoate and benzil were obtained with the 95-99% conversion under optimized reaction conditions. Oxidative bromination of salicylaldehyde, a functional mimic of haloperoxidases, in aqueous $H_2O_2$/KBr in the presence of $HClO_4$ at room temperature has also been carried out successfully.

**Chapter 4:** Report of synthesis and characterization of two novel dimeric $[(Mo^{VI}O_2)_2L]$ (**1**) and tetrameric $[\{(C_2H_5OH)LO_3Mo_2^{VI}\}_2(\mu\text{-}O)_2]\cdot C_2H_5OH$ (**2**) dioxomolybdenum(VI) complexes with *N*,*N*'-disalicyloylhydrazine ($H_2L$), which is formed by the self combination of salicyloyl hydrazide. Both the complex was characterized by various spectroscopic techniques (IR, UV–Vis and NMR) and also by electrochemical study. The molecular structures of both the complexes have been confirmed by X-ray crystallography. All these studies indicate that the *N*,*N*'-disalicyloylhydrazine ($H_2L$) has the normal tendency to form both dimeric and tetrameric complexes coordinated through the dianionic tridentate manner.

**Chapter 5:** Two novel dioxomolybbdenum(VI) complexes containing the $MoO_2^{2+}$ motif are reported where unexpected coordination due to ligand rearrangement through metal mediated interligand C–C bond formation is observed. The ligand transformations are probably initiated by molybdenum assisted C–C bond formation in the reaction medium. The ligands ($H_2L'^{1-2}$) are tetradentate C–C coupled $O_2N_2-$ donor systems formed *in situ* during the synthesis of the complexes by the reaction of bis(acetylacetonato)dioxomolybdenum(VI) with Schiff base ligands of 2-aminophenol with 2-pyridine carboxaldehyde ($HL^1$) and 2-quinolinecarboxaldehyde ($HL^2$). The reported dioxomolybdenum(VI) complexes $[MoO_2L'^1]$ (**1**) and $[MoO_2L'^2]$ (**2**) coordinated with the $O_2N_2-$ donor rearranged ligand are expected to have better stability of the molybdenum in +6 oxidation state than the corresponding $ON_2$–donor ligand precursor. Both the complexes are fully characterized by several physicochemical techniques and the novel structural features through single crystal X-ray crystallography.

**Chapter 6:** In this chapter we present a detailed account of the synthesis, structure, spectroscopic, electrochemical properties and study of biological activity of some oxomolybdenum(VI) complexes with special reference to their H–bonded molecular and supramolecular structures. Reaction of bis(acetylacetonato)dioxomolybdenum(VI) with three different hydrazides (isonicotinoyl hydrazide, anthraniloyl hydrazide and 4-nitrobenzoyl hydrazide) afforded two di-oxomolybdenum(VI) complexes {[$MoO_2L^1(CH_3OH)$] (**1**) and [$MoO_2L^3$] (**3**)} and one mono-oxomolybdenum(VI) complex {[$MoOL^2(O–N)$] (**2**)} (where L = Intermediate *in situ* ligand formed by the reaction between acetyl acetone and the corresponding acid hydrazide, and O–N = 4-nitrobenzoylhydrazide). All the complexes have been characterized by elemental analysis, electrochemical and spectroscopic (IR, UV–Vis and NMR) measurements. Molecular structures of all the complexes (**1**, **2** and **3**) have been determined by X-ray crystallography. The complexes have been screened for their antibacterial activity against *Escherichia coli, Bacillus subtilis* and *Pseudomonas aeruginosa*. The Minimum inhibitory concentration of these complexes and antibacterial activity indicates **1** as the potential lead molecule for drug designing.

---

**Keywords:** Aroylhydrazones **/** Schiff bases / Dioxomolybdenum(VI) complexes **/** X-ray crystal structure / Biological activity / Catalytic oxidation of benzoin / Oxidative bromination

**Table of Contents**

# Preface

The present dissertation describes the design, synthesis, full characterization and the exploration of chemical, electrochemical, catalytic and biological reactivity of a series of oxomolybdenum(VI) complexes of some selected multidentate NO- and/or ONO- donor ligands. Structures of seventeen important oxomolybdenum(VI) complexes are determined by single crystal X-ray analysis. Structure-reactivity relations are discussed and implications of structure determination on the design of new complexes using the structurally characterized compounds as precursors are elaborated. All the complexes described in this dissertation are characterized by various physicochemical techniques such as elemental analysis, measurement of magnetic susceptibility at room temperature in solid state, measurement of conductivity in solution and by various spectroscopic techniques (UV-Vis, IR, NMR). Electrochemical characteristics of the complexes were studied by cyclic voltammetry and, as pointed out before, single crystal X-ray crystallography is used to find out crystal and molecular structure of all the compounds of oxomolybdenum(VI) complexes. Biological (antimicrobial activity) and catalytic activities of some of the above complexes particularly oxidation of alkenes, aromatic alcohols and oxidative bromination of aromatic aldehydes were also studied. The subject matter of this dissertation is divided into six chapters containing the chemistry of oxomolybdenum(VI) ligated to selected NO- and/or ONO- donors ligands and a *brief resume* of the work embodied in this dissertation and *concluding remarks*.

*Chapter 1* is a general introduction to the entire work described in the present dissertation and spells out the objectives of the thesis. The objectives of the works are placed at the end of the **general introduction.** The entire subject matter of this dissertation is organized as follows:

*Chapter 2* contains synthesis and characterization of the oxomolybdenum(VI) complex [MoO$_2$L(C$_2$H$_5$OH)] (**1**) of benzoylhydrazone of *2*-hydroxybenzaldehyde (H$_2$L). The substrate binding capacity of **1** has been demonstrated by the formation and isolation of two mononuclear [MoO$_2$L(Q)] {where Q = imidazole (**2a**) and 1-methylimidazole (**2b**)} and one dinuclear [(MoO$_2$L)$_2$(Q)] {Q = 4,4'-bipyridine (**3**)} mixed-ligand oxomolybdenum(VI) complexes. All the complexes have been characterized by elemental analysis, spectroscopic (IR, UV–Vis and NMR) and cyclic voltammetry measurements. Molecular structures of all the oxomolybdenum(VI) complexes (**1**, **2a**, **2b** and **3**) have been determined by X-ray crystallography. The complexes

have been screened for their antibacterial activity against *Escherichia coli, Bacillus subtilis* and *Pseudomonas aeruginosa*. The minimum inhibitory concentration of these complexes and antibacterial activity indicates the compound **2a** and **2b** as the potential lead molecule for drug designing.

*Chapter 3* deals with the synthesis, characterization and reactivity of a series of 5- and 6-coordinated oxomolybdenum(VI) complexes of the type $[MoO_2L^{1-2}(ROH)]$ [where R = $C_2H_5$ (**1**) and $CH_3$ (**2**)], and $[MoO_2L^{3-4}]$ (**3** and **4**) of four different ONO donor ligands: salicyloylhydrazone of 2-hydroxy-1-naphthaldehyde ($H_2L^1$), anthranylhydrazone of 2-hydroxy-1-naphthaldehyde ($H_2L^2$), benzoylhydrazone of 2-hydroxy-1-acetonaphthone ($H_2L^3$) and anthranylhydrazone of 2-hydroxy-1-acetonaphthone ($H_2L^4$; general abbreviation $H_2L$). The substrate binding capacity of **1** has been demonstrated by the formation of one mononuclear mixed-ligand dioxidomolybdenum complex $[MoO_2L^1(Q)]$ {where Q = γ-picoline (**1a**)}. Molecular structure of all the complexes (**1**, **1a**, **2**, **3** and **4**) is determined by X-ray crystallography, demonstrating the dibasic tridentate behavior of ligands. The complexes have been screened for their antibacterial activity against *Escherichia coli, Bacillus subtilis, Proteus vulgaris* and *Klebsiella pneumoniae*. The minimum inhibitory concentration of these complexes and antibacterial activity indicates **1** and **1a** as the potential lead molecule for drug designing. Catalytic potential of these complexes was tested for the oxidation of benzoin using 30% aqueous $H_2O_2$ as an oxidant in methanol. At least four reaction products benzoic acid, benzaldehyde-dimethylacetal, methylbenzoate and benzil were obtained with the 95-99% conversion under optimized reaction conditions. Oxidative bromination of salicylaldehyde, a functional mimic of haloperoxidases, in aqueous $H_2O_2$/KBr in the presence of $HClO_4$ at room temperature has also been carried out successfully.

*Chapter 4* describes the report of synthesis and characterization of two novel dimeric $[(Mo^{VI}O_2)_2L]$ (**1**) and tetrameric $[\{(C_2H_5OH)LO_3Mo_2^{VI}\}_2(\mu-O)_2]\cdot C_2H_5OH$ (**2**) dioxomolybdenum(VI) complexes with *N,N'*-disalicyloylhydrazine ($H_2L$), which is formed by the self combination of acid hydrazide. Both the complex was characterized by various spectroscopic techniques (IR, UV–Vis and NMR) and also by electrochemical study. The molecular structures of both the complexes have been confirmed by X-ray crystallography. All these studies indicate that the *N,N'*-disalicyloylhydrazine ($H_2L$) has the normal tendency to form both dimeric and tetrameric complexes coordinated through the dianionic tridentate manner.

In *chapter 5* two novel dioxomolybbdenum(VI) complexes containing the $MoO_2^{2+}$ motif are reported where unexpected coordination due to ligand rearrangement through metal mediated interligand C–C bond formation is observed. These ligand transformations are probably initiated by molybdenum assisted C–C bond formation in the reaction medium. It is checked and confirmed that, the reactions using other metal precursors $[VO(acac)_2$ or $Cu(acac)_2]$ do not initiate this type of ligand rearrangement. The ligands $(H_2L^{'})$ are tetradentate C–C coupled $O_2N_2$– donor systems formed *in situ* during the synthesis of the complexes from bis(acetylacetonato)dioxomolybdenum(VI) with Schiff base ligands of 2-aminophenol with 2-pyridinecarboxaldehyde $(HL^1)$ and 2-quinolinecarboxaldehyde $(HL^2)$. The reported dioxomolybdenum(VI) complexes $[MoO_2L^{'1}]$ (**1**) and $[MoO_2L^2]$ (**2**) coordinated with the $O_2N_2$– donor rearranged ligand are expected to have better stability of the +6 oxidation state of molybdenum than the corresponding ONN– donor ligand precursor. Both the complexes are fully characterized by several physicochemical techniques and the novel structural features through single crystal X-ray crystallography.

The essence of the work presented in *chapter 6* is the detailed account of the synthesis, structure, spectroscopic, electrochemical properties and study of biological activity of some oxomolybdenum(VI) complexes with special reference to their H-bonded molecular and supramolecular structures. Reaction of bis(acetylacetonato)dioxomolybdenum(VI) with three different hydrazides (isonicotinoyl hydrazide, anthraniloyl hydrazide and 4-nitrobenzoyl hydrazide) afforded two dioxomolybdenum(VI) complexes $\{[MoO_2L^1(CH_3OH)]$ (**1**) and $[MoO_2L^3]$ (**3**)$\}$ and one mono-oxomolybdenum(VI) complex $\{[MoOL^2(O-N)]$ (**2**)$\}$ (where L = Intermediate *in situ* ligand formed by the reaction between acetyl acetone and the corresponding acid hydrazide, and O–N = 4-nitrobenzoylhydrazide). All the complexes have been characterized by elemental analysis, electrochemical and spectroscopic (IR, UV–Vis and NMR) measurements. Molecular structures of all the complexes (**1**, **2** and **3**) have been determined by X-ray crystallography. The complexes have been screened for their antibacterial activity against *Escherichia coli, Bacillus subtilis* and *Pseudomonas aeruginosa*. The minimum inhibitory concentration of these complexes and antibacterial activity indicates **1** as the potential lead molecule for drug designing.

# Chapter 1

## Scope of the Present Investigation

# Chapter 1

## Scope of the present investigation

**Abstract:** In this chapter the scope of the present investigation is delineated briefly along with the aim of the work.

### 1.1 Review on oxomolybdenum complexes with ON- and ONO- donor ligands

The studies described in the present thesis involve coordination complexes of molybdenum featuring ON- and/or ONO- donor ligands in relation to their biological and catalytic activities. The coordination chemistry of metal complexes with Schiff base ligands has attracted continuing attention for the synthetic chemist due to their ease of synthesis and stability under a variety of oxidative and reductive conditions. Molybdenum is one of the versatile transition metal with a large number of stable and accessible oxidation states ranging from –2 to +6 [1]. Within the second series of transition metals only molybdenum represents a biometal, important for microorganisms, plant and animals. Co-ordination numbers of Mo are from 4 to 8. Mo complexes show varied stereochemistry. It can form compounds with inorganic and organic ligands, with particular preference for oxygen, sulphur, fluorine and chlorine donor atoms. Again, coordination chemistry of molybdenum(VI) assumed special importance due to the following reasons:

1) Molybdenum complexes have long standing application in the catalysis of chemical and petrochemical processes in various industries like ammoxidation of propene [2], epoxidation of olefin [3], olefin metathesis [4], isomerization of allylic alcohols [5], oxidative bromination of salicylaldehyde etc. [6].

2) Mo(VI) complexes have played a versatile role in biology [6]. Molybdenum(VI) is found to be present at the active centers of oxotransfer molybdoenzymes and nitrogen fixing enzymes - the nitrogenases [7]. It is the heaviest metal which is essential for life and its biological importance was first recognized in the field of agriculture.

3) The discovery of several oxotransferase enzymes like xanthine oxidase and DMSO reductase [8, 9] containing NSO donor points around the Mo(VI) center .

4) Unlike most transition metals, molybdenum(VI) is relatively harmless to the environment [10].

5) Molybdenum(VI) with Schiff base complexes are of significant interest and attention because of their biological activity including anticancer [11], antibacterial [12], antifungal [13] and antitumor [14] properties.

In this context, role of the coordination environment around the central metal (molybdenum) ion is most important. Variation in the coordination environment can only bring about corresponding variation in the properties of the complexes. Chemistry of oxomolybdenum(VI) by ligands of various types has been of significant importance in this regard. Review on some of the recent reports of the oxomolybdenum complexes with ON-donor environments, which are drawing much current attention, are highlighted below.

R. Sillanpää and coworkers reported the synthesis and characterization of few monomeric cis dioxomolybdenum(VI) complexes of some tridentate Schiff base ligands obtained by condensing salicylaldehyde with substituted aminoalcohols [15]. These ligands were found to coordinate through the deprotonated phenolate oxygen, the azomethine nitrogen and the deprotonated alkoxide oxygen. Structures of four complexes were determined and each one showed that the sixth coordination position around the Mo(VI) center is taken up by a MeOH molecule, which is used as solvent for the preparation of the complexes (**Fig.1.1**). The complexes are reported to act as inhibitors in the oxidation of aldehydes by oxygen.
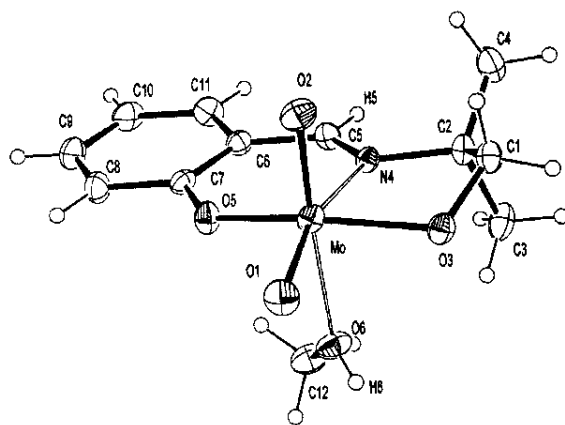


**Fig.1.1**

B. Modec and his coworkers [16] have reported the preparation and structure of the two cluster species of $[Mo_8O_{16}(OCH_3)_8Py_4]\cdot 2CH_3OH$ (Py = pyridine, $C_5H_5N$) (**1**) and $[Mo_8O_{16}(OCH_3)_8(4\text{-}MePy)_4]$ (4-MePy = 4-methylpyridine, $C_6H_7N$) (**2**). Both products were synthesized by the solvothermal reactions. The two distinct geometries of $[Mo_8O_{16}(OCH_3)_8Py_4]$, one encountered in complex (**1**) and the other being the cyclic $[Mo_8O_{16}(OCH_3)_8Py_4]$, make a pair of structural isomers whose differences can be interpreted in terms of different arrangement of constituent $\{Mo_2O_4\}^{2+}$ blocks and connectivity among them.
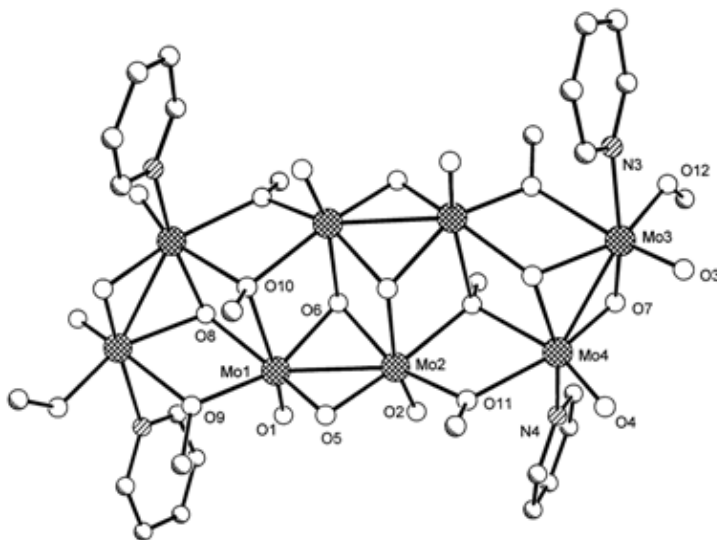


**Fig.1.2**

These cluster (**Fig.1.2**) complexes are formed by the reactions of $(PyH)_2[MoOCl_5]$ with methanol and pyridine or alkyl-substituted pyridines (R-Py). Its reactivity is a further demonstration of the propensity of molybdenum in the +5 oxidation state to hydrolyze with the formation of dimers, i.e. $\{Mo_2O_3\}^{4+}$ or $\{Mo_2O_4\}^{2+}$, through one or two bridging oxygen atoms, with or without the metal–metal bond respectively.

In 2002 M. Cindric et al. reported [17] the synthesis and characterization of three acetato complexes of Mo(VI) (along with other related Mo(V) and Mo(IV) complexes). They are $[MoO_2(OCOCH_3)_2]$ (**1**), $Na_2[Mo_2O_4(OCOCH_3)_6]\cdot CH_3COONa\cdot CH_3COOH$ (**2**) and $K[MoO_2(OCOCH_3)_3]\cdot CH_3COOH$ (**3**). Crystal structures of (**2**) and (**3**) were determined by single crystal X-ray diffraction analysis.

In the same year (2002) H. K. Lee and his group reported [18] the synthesis and catalytic activity of dioxomolybdenum(VI) alkyl complex supported by a $N_2O$-type ancillary ligand. Initially they synthesized a series of cis-dioxomolybdenum(VI) complexes $MoO_2(L^n)Cl$ (n = 1-5) (**Fig.1.3**) by the reaction of $MoO_2Cl_2(DME)$ (DME = 1,2-dimethoxyethane) with 2-N-(2-pyridylmethyl)aminophenol ($HL^1$) or its N-alkyl derivatives ($HL^n$) (n = 2-5) in the presence of triethylamine.
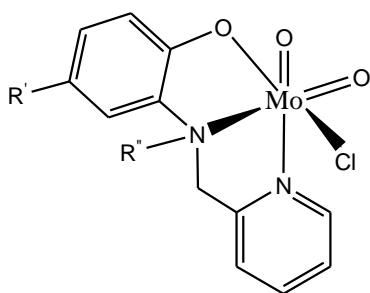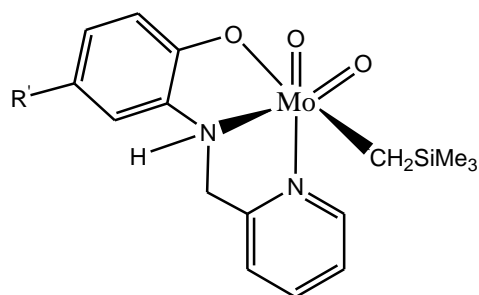


**Fig.1.3**                                             **Fig.1.4**

The dioxomolybdenum(VI) alkyl complexes (**Fig.1.4**) were prepared by the treatment of $MoO_2(L^1)Cl$ or $[MoO_2(L^1)]_2O$ with the Grignard reagent $Me_3SiCH_2MgCl$. They have also reported the catalytic properties of selected dioxo-Mo(VI)-chloro and μ-oxo complexes towards epoxidation of styrene by tert-butyl hydroperoxide (TBHP).

An interesting report on the synthesis and characterization of three non-oxo molybdenum(VI) complexes by Jeong et al. appeared in 2002 [19]. These three non-oxo-molybdenum(VI) bis(imido) complexes are $[T_p^*Mo(Nmes)_2Cl]$ (**1**), $[T_p^*Mo(Nmes)_2(CH_3)]$ (**2**) and $[T_p^*Mo(Nmes)_2(OH)]$ (**3**), where $T_p^* =$ hydrotris (3,5- dimethyl –1-pyrazolyl) borate. Structures of (**1**) (**Fig.1.5**) and (**3**) were solved by single crystal X-ray analyses. Structure of (**1**) reveals that the non-oxo Mo(VI) centre is present in a distorted octahdral $N_5Cl$ coordination. High reactivity of complex (**1**) centered at the coordinated Cl indicates that (**1**) may be used as the precursor of new non-oxo Mo(VI) complexes.
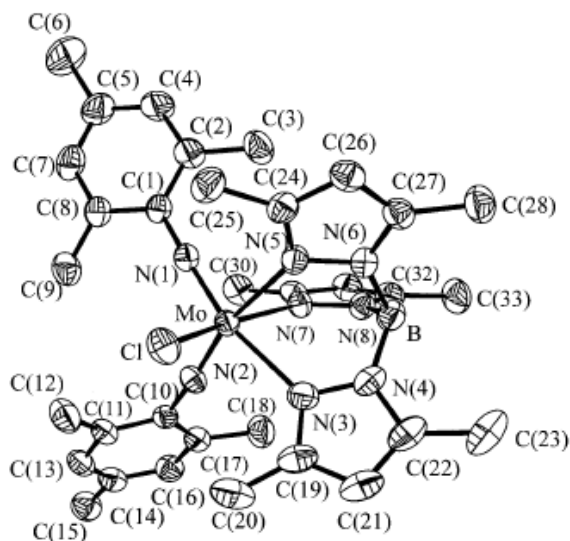
**Fig.1.5**

Rana et al. has published the synthesis and crystal structure of cis-dioxomolybdenum(VI) complexes of some potentially pentadentate but functionally tridentate (ONS) donor ligands [20]. These complexes, $MoO_2LH(R-/OH)$ (R-/CH$_3$) (where LH = L$^{1-4}$H) (**Fig.1.6**) were synthesized by the reaction of the thiocarbodihydrazone of substituted salicylaldehyde (ONSNO donor, $H_3L^{1-4}$) with $MoO_2(acac)_2$. All the complexes were characterized by IR, UV–Vis and $^1H$ NMR spectroscopy, magnetic susceptibility measurement, molar conductivities in solution and by cyclic voltammetry. Two of the complexes $[MoO_2(L^2H)(MeOH)]$ (**Fig.1.7**) and $[MoO_2(L^4H)(MeOH)]$ were crystallographically characterized.

9
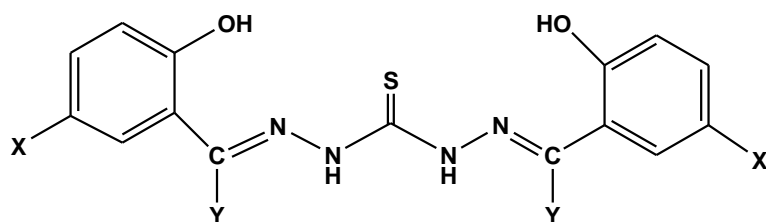
| X | Y | Ligand |
|---|---|---|
| H | H | $H_3L^1$ |
| Br | H | $H_3L^2$ |
| NO$_2$ | H | $H_3L^3$ |
| H | CH$_3$ | $H_3L^4$ |

**Fig.1.6**

Oxomolybdenum(IV) complexes of the formula $[MoO(LH)]_n$ (**1–4**) were prepared by a general method of refluxing the appropriate $[Mo^{VI}O_2(LH)(R\text{-}OH)]$ complexes with PPh$_3$ in 1:1.5 molar proportions in dry degassed CH$_3$CN under dry dinitrogen atmosphere. The oxo-abstraction property of these Mo(IV) complexes from substrates like triphenylphosphine oxide and pyridine N-oxide was demonstrated by the formation and the isolation of the precursor Mo(VI) complexes. Such reactions are reminiscent of $Mo^{IV}O^{+2}$ complexes, which mimic the active centers of the reduced forms of oxidoreductase molybdoenzymes.



**Fig.1.7**

10
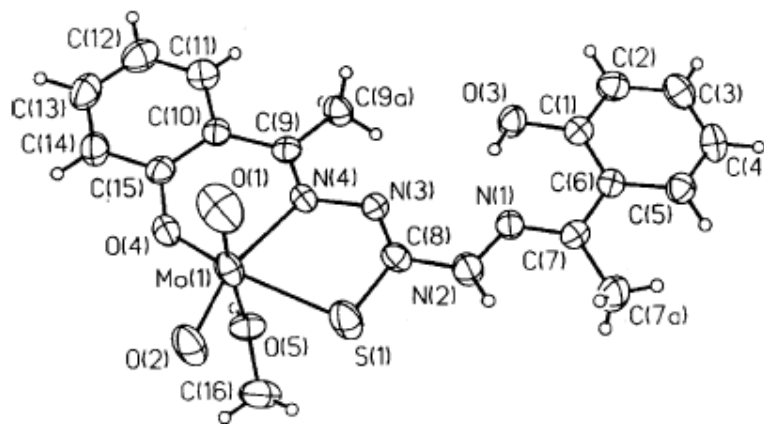
In 2004, A. Lehtonen and V.G. Kessler published the synthesis and characterization of dioxomolybdenum(VI) complexes of two equivalents of tris(2-hydroxy-3,5-dimethylbenzyl)amine (H$_3$Lig) with the alcoholic solution of MoO$_2$(acac)$_2$ [21]. A yellow crystalline anionic complex LigH$_4$[MoO$_2$Lig] was formed and characterized by the single crystal X-ray crystallography. The structure of the complex (**Fig.1.8**) revealed that the asymmetric unit of metal complex consists of one [MoO$_2$Lig]$^-$ anion, one HLig$^+$ cation and two molecules of MeOH. In the Mo centered unit, the phenoxide groups of the tetradentate ligand are bonded to cis-MoO$_2$$^{2+}$ ion in xy-plane, while the amino nitrogen completes the distorted octahedral coordination.
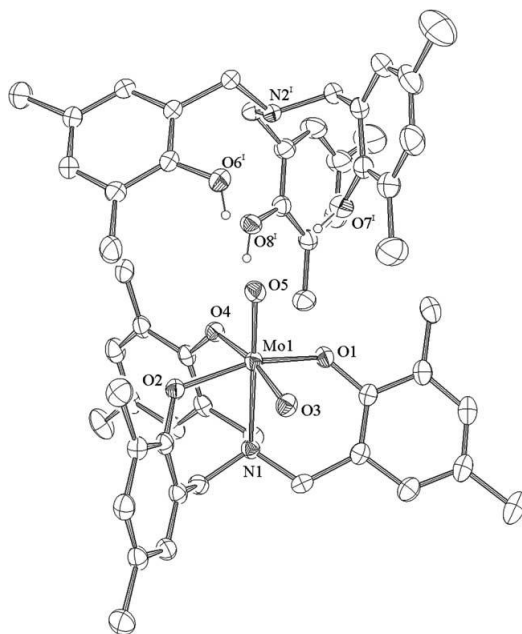


**Fig.1.8**

A. Lehtonen and R. Sillanpää also prepared several oxomolybdenum(VI) complexes with tri- and tetradentate ligand derived from aminobis(phenolate) [22]. Tridentate aminobis(phenol) ligands can form monomeric dioxomolybdenum(VI) complex in which the sixth coordination site is occupied by solvent methanol. In the absence of methanol, the coordination sphere around oxophilic Mo(VI) ion was completed by dimerization through oxygen bridges (**Fig.1.9**).
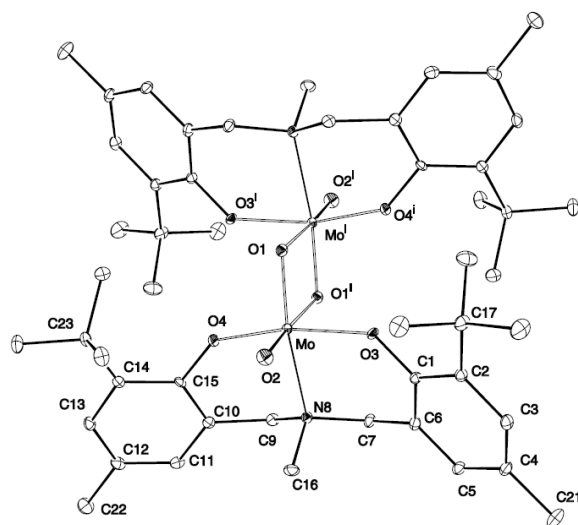
**Fig.1.9**

Potentially tetradentate aminobis(phenol) ligands ($H_2L^n$), which carry either a dimethylamino, a pyridyl or a methoxy sidearm donor were used in the preparation of new tungsten and molybdenum complexes [23]. The spectral analyses and crystal structure investigations revealed that the dianionic aminobis(phenolate) backbones of the ligands have coordinated as ONO donors (**Fig.1.10**).
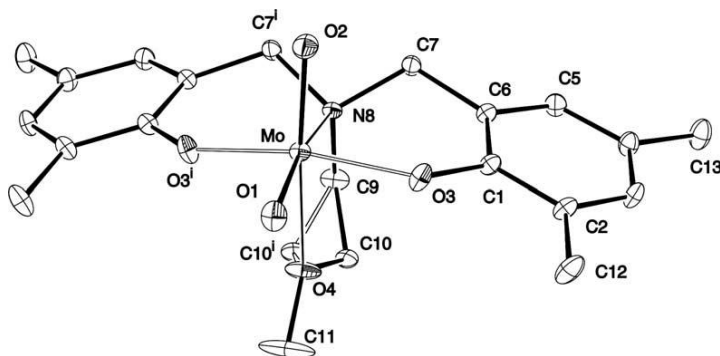


**Fig. 1.10**

M. Masteri-Farahani and his coworkers published a paper on the synthesis and characterization of molybdenum complexes with bidentate Schiff base ligands supported on MCM-41 mesoporous material [24]. Characterization of these materials was carried out with FT-IR, atomic absorption spectroscopy, powder X-ray diffraction (XRD) and BET nitrogen adsorption–desorption methods. Reaction of amine groups of AmpMCM-41 and carbonyl groups of aldehyde or ketone are condensed to formed ON- and NN-donor Schiff base ligands. Reaction of the supported Schiff base ligands with $MoO_2(acac)_2$ in refluxing absolute ethanol formed the corresponding molybdenum complexes on MCM-41 surface. Catalytic activities of the prepared molybdenum catalysts were also investigated in the epoxidation of cyclooctene, cyclohexene, 1-octene and 1-hexene with TBHP. The ON– donor type catalyst (MoO$_2$acacAmpMCM-41) mostly exhibits more epoxidation activity than NN– donor type catalyst (MoO$_2$pycaAmpMCM-41).

S. N. Rao and their group reported [25] the catalytic air oxidation of olefins by using molybdenum dioxo complexes with dissymmetric tridentate ONS donor Schiff base ligands derived from o-hydroxyacetophenone and S-benzyldithiocarbazate or S-methyldithiocarbazate. The corresponding metal complexes oxidized 1-hexene, cyclohexene and styrene at 60ºC and 1 atm O$_2$ in DMF with a high percentage conversion in the range 86–98%, which obey pseudo-first order kinetics.
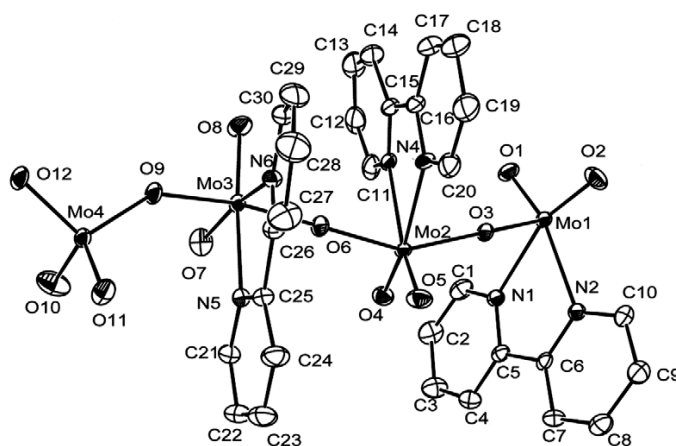


**Fig.1.11**

Another interesting report on the synthesis and structure (**Fig.1.11**) of one-dimensional chain oxomolybdenum polymer [$Mo_4O_{12}(2,2'\text{-bpy})_3$] with three {$MoO_4N_2$} octahedral and one {$MoO_4$} tetrahedral unit [26]. This reaction was carried out by the hydrothermal reaction of $(NH_4)_6Mo_7O_{24}.4H_2O$, $MnCl_2.4H_2O$, 2,2′-dipyridyl N,N´-dioxide, and $H_2O$ in the mole ratio 1.00:1.67:3.33:3333 at 200 ºC for 6 days.

The new complexes, [$(\mu\text{-CO})_2Cr_2(\eta^4\text{-H}_2L)_2$], (**1**); [$(\mu\text{-CO})M_2(CO)_2(\eta^4\text{-H}_2L)_2$], [M = Mo; (**2**), W; (**3**)]; [$(\mu\text{-CO})_2Cr_2(\eta^4\text{-H}_2L')_2$], (**4**) and [$(\mu\text{-CO})M_2(CO)_2(\eta^4\text{-H}_2L')_2$], [M = Mo; (**5**), W; (**6**)] were synthesized by Karahan et al. in 2008 [27]. All the complexes were synthesized by the photochemical reactions of $M(CO)_5THF$ (M = Cr, Mo, W) with tetradentate Schiff base ligands, {N,N′-bis(2-hydroxynaphtalin-1-carbaldehydene)-1,2-bis(p-aminophenoxy)ethane (H$_2$L) and N,N′-bis(2-hydroxynaphtalin-1-carbaldehydene)-1,4-bis(p-aminophenoxy)butane (H$_2$L′)}. The complexes were characterized by elemental analyses, LC-mass spectrometry, magnetic studies, FTIR, and $^1$H-NMR spectroscopy. The mass spectra fragmentations showed good accordance with the expected structures of all the complexes.



$LR^n$
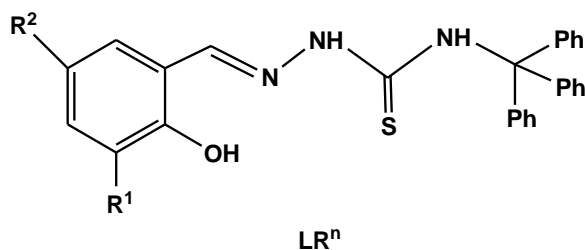
H$_2$L (R$^1$ = H, R$^2$ = H)
H$_2$LF (R$^1$ = H, R$^2$ = F)
H$_2$LCl (R$^1$ = H, R$^2$ = Cl)
H$_2$LBr (R$^1$ = H, R$^2$ =Br)
 H$_2$LI (R$^1$ = H, R$^2$ = I)
H$_2$LMe (R$^1$ = H, R$^2$ = Me)
H$_2$LMeO (R$^1$ = H, R$^2$ = MeO)
H$_2$LNO$_2$ (R$^1$ = H, R$^2$ = NO$_2$)
H$_2$L$_3$-MeO (R$^1$ = MeO, R$^2$ = H)
H$_2$LCl$_2$ (R$^1$ = Cl, R$^2$ = Cl)
H$_2$LBrCl (R$^1$ = Br, R$^2$ = Cl)

**Fig.1.12**

A series of homologous mononuclear dioxomolybdenum complexes were reported [28]. The ligands were derived from the prototype 2-hydroxybenzaldehyde-4-triphenylmethylthiosemicarbazone ($H_2L$) (**Fig.1.12**) behave as a tridentate ONS donor set to the central metal atom. X-ray crystal structures of $[MoO_2(LR^n)(dmf)]$ and $[MoO_2(LR^n)(MeOH)]$ were determined. From the variation of substituents in this ligand library, the influences of electronic ligand effects on the spectroscopic, electrochemical, and functional properties of these biomimetic model complexes for molybdenum-containing oxotransferases were reported.
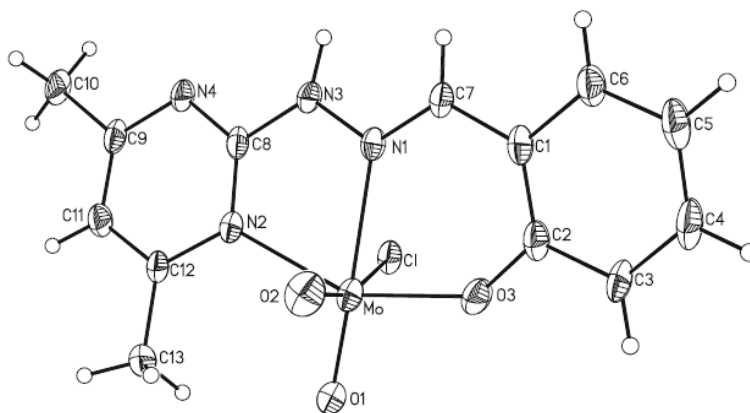


**Fig. 1.13**

Molybdenum(VI) complexes of the ligands were prepared by the condensation of 4,6-dimethyl 2-hydrazino pyrimidine with salicylaldehyde (for $HL_1$) and o-hydroxy acetophenone (for $HL_2$) respectively. When $MoO_2(acac)_2$ was used as a metal precursor in acidic medium, $HL_1$ yielded the normal ligand exchange product $[MoO_2(L_1)Cl]$ (**1**) (**Fig.1.13**). In the same reaction medium $HL_2$ produced two bis chloro dioxomolybdenum(VI) complexes $[MoO_2(L_3)Cl_2]$ (**2**) and $[Mo_2O_5(L_3)Cl_2]$ (**3**) (**Fig.1.14**), where $L_3$ is a bidentate neutral ligand 2-(3, 5-dimethyl-1-pyrazolyl) 4,6-dimethyl pyrimidine, which was afforded by an organic transformation of the used ligand.
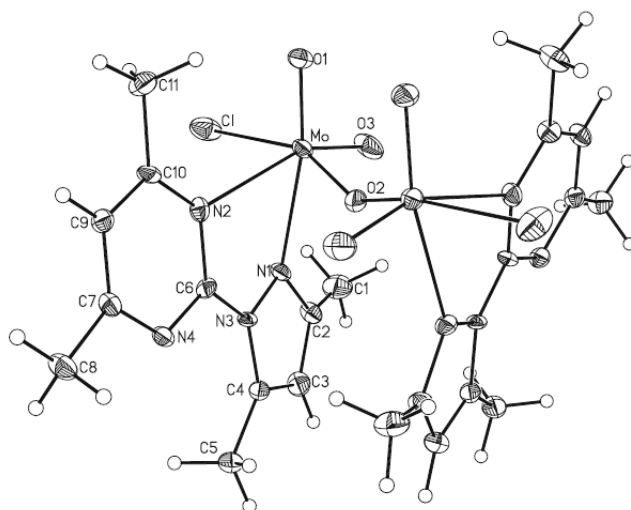
**Fig. 1.14**

The complexes were characterized by elemental analyses, electronic spectra, IR, $^1$H NMR, magnetic measurements, EPR and by cyclic voltammetry. Another pyrimidine derived hydrazone ligand (H$_2$L$'_1$) (**Fig.1.15**) was employed for complexation with MoO$_2$(acac)$_2$, a similar ligand transformation occurred and the complex [MoO$_2$(L$_4$)Cl] (**4**) (**Fig.1.16**) was produced. Complexes (**1–4**) as well as the ligand HL$_2$, have been crystallographically characterized. From X-ray crystallography it is revealed that during complex formation, the ligand transformations were initiated by a metal mediated C=N bond cleavage of the used ligands in the reaction medium [29].



H$_2$L$'_1$

**Fig.1.15**



[MoO$_2$(L$_4$)Cl] (4)
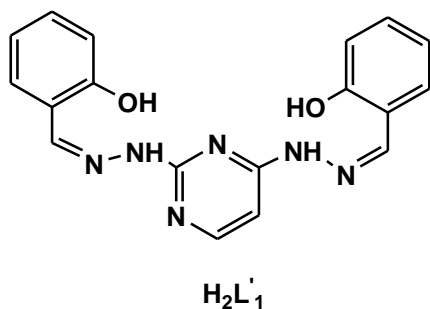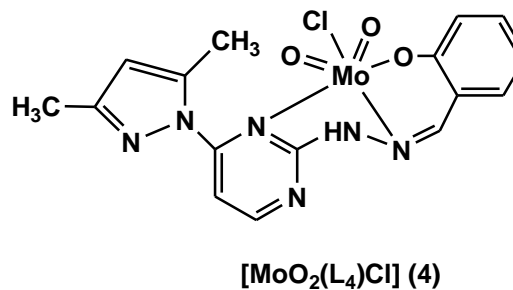
**Fig.1.16**

The synthesis of a new Mo complex [MoO$_2$(L)-(CH$_3$OH)] with 2-{(2-hydroxypropylimino)methyl}phenol ligand (H$_2$L) was reported and prepared by the reaction between 2-{(2-hydroxypropylimino)} methyl]phenol and dioxo-molybdenum(VI) acetylacetonate [30]. The [MoO$_2$(L)(CH$_3$OH)] was structurally characterized by single-crystal X-ray crystallography, having a monoclinic structure with a space group P2$_1$/c (**Fig.1.17**). Conversion of sulfides to both sulfoxides and sulfones by using UHP was efficiently enhanced under the influence of [MoO$_2$(L)(CH$_3$OH)] catalyst in ethanol under mild conditions and high turnover rates were obtained in the oxidation reactions, which highlighted the novelty of this new Mo-catalyst.
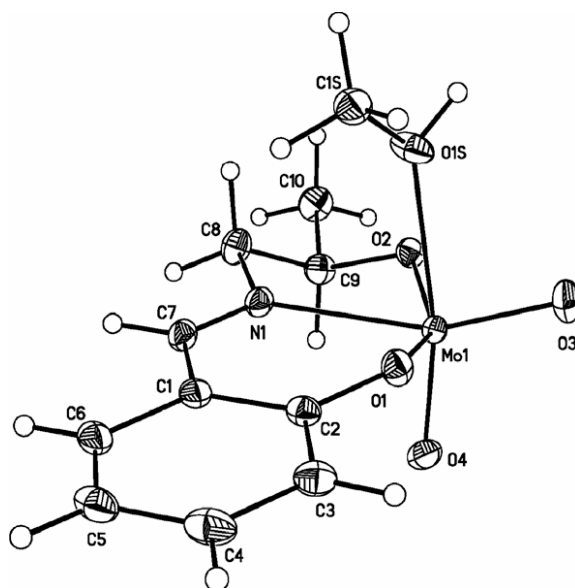


**Fig.1.17**

V. Vrdoljak and his coworkers have reported [31] some oxomolybdenum(VI) (monomeric [MoO$_2$L$^1$(CH$_3$OH)] or polymeric [MoO$_2$L$^{1-3}$]) complexes, which were prepared by the reaction of [Mo$^{VI}$O$_2$(acac)$_2$] or (NH$_4$)$_2$[Mo$^V$OCl$_5$] with different N-substituted pyridoxal thiosemicarbazone ligands (H$_2$L$^1$ = pyridoxal 4-phenylthiosemicarbazone; H$_2$L$^2$ = pyridoxal 4-methylthiosemicarbazone, H$_2$L$^3$ = pyridoxal thiosemicarbazone). In all the complexes molybdenum was coordinated with a tridentate doubly-deprotonated ligand, but in the oxomolybdenum(V) complexes [MoOCl$_2$(HL$^{1-3}$)] (**Fig.1.18**) the pyridoxal thiosemicarbazonato

ligands are tridentate monodeprotonated. Crystal and molecular structures of the pyridoxal thiosemicarbazone ligand and complexes were determined by the single crystal X-ray diffraction method.



| | |
|---|---|
| **R=Ph** | [MoOCl$_2$(HL$^1$)] (**4**) |
| **R=Me** | [MoOCl$_2$(HL$^2$)] (**5**) |
| **R=H** | [MoOCl$_2$(HL$^3$)] (**6**) |
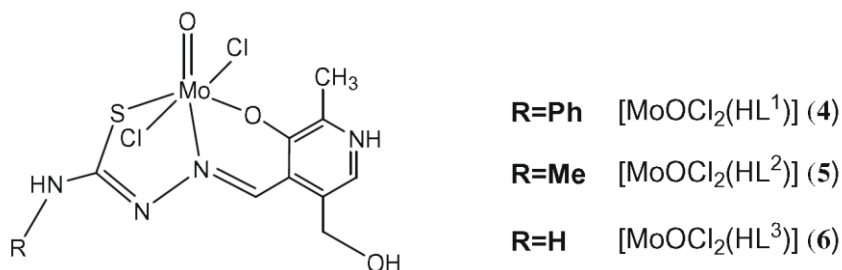
**Fig.1.18**

Nair and Thankamani have reported some new oxomolybdenum(V) and dioxomolybdenum(VI) with a Schiff base, 3-methoxysalicylaldehydeisonicotinoylhydrazone derived from 3-methoxysalicylaldehyde and isonicotinoylhydrazide [32]. The complexes have been characterized by elemental analyses, molar conductance, magnetic susceptibility data, IR, UV-Vis, EPR, $^1$H NMR and FAB mass spectral studies. The FAB mass and X-band EPR spectra indicate that the pentavalent Mo in the complex [MoO(MSINH)Cl$_2$] (**Fig.1.19**) is monomeric in nature. The anticancer and antibacterial activities of ligand, [MoO(MSINH)Cl$_2$] and [MoO$_2$(MSINH)Cl] were also investigated. The complex [MoO(MSINH)Cl$_2$] exhibits much higher activity than the ligand (MSINH) and its dioxo complex [MoO$_2$(MSINH)Cl].



X = Cl, NCS

**Fig.1.19**

18
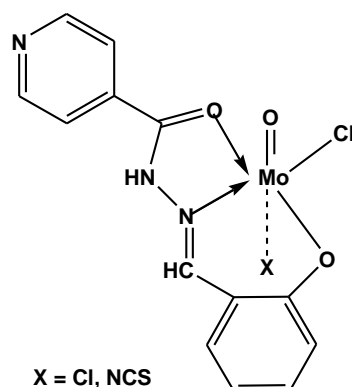
The tetradentate Schiff base N,N′-bis(salicylidene)4,5-dichloro-1.2-phenylenediamine (H₂L) with M(CO)₆ (M = Cr and Mo) under different conditions formed [Cr(CO)₂(H₂L)] and [Mo(CO)₂(L)] under reduced pressure, and the oxo complex [Cr(O)(L)] and the dioxo complex [Mo(O₂)(L)] (**Fig.1.20**) in air condition were reported by A. A. Abdel Aziz [33]. The catalytic activities of all the complexes were investigated in the epoxidation of cyclooctene, cyclohexene, 1-octene and 1-hexene with TBHP and methylene chloride as a solvent at different temperatures. The results showed that the reported molybdenum complexes have higher catalytic activity than chromium complexes. The antibacterial and antifungal activities of the new compounds were also investigated.
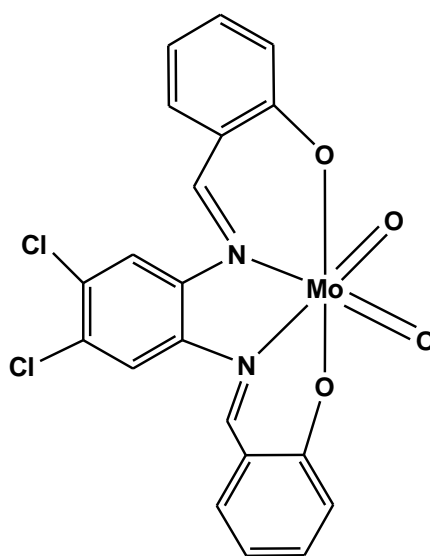


**Fig.1.20**

The oxo imido molybdenum(VI) compounds [MoO(N-t-Bu)L₂] (**Fig.1.21**) were reported by Nadia C. Mösch-Zanetti and his coworkers [34]. Reaction of [MoO(N-t-Bu)Cl₂(dme)] (dme = dimethoxyethane) with 2 equiv of the potassium salts of Schiff base ligands {KArNC(CH₃)CHC(CH₃)O} afforded oxo imido molybdenum(VI) compounds [MoO(N-t-Bu)L₂] (**1**) {with Ar = phenyl (L_Ph) (**Fig.1.22**), (**2**) with Ar = 2-tolyl (L_MePh), (**3**) with Ar = 2,6-dimethylphenyl (L_Me2Ph) and (**4**) with Ar = 2,6-diisopropylphenyl (L_i-Pr2Ph), (**5**) with (L = LPh), (**6**) with (L = L_MePh), and (**7**) with (L = L_Me2Ph)}. The complexes (**1**, **3**, **5**, and **6**) were characterized by single crystal X-ray diffraction.
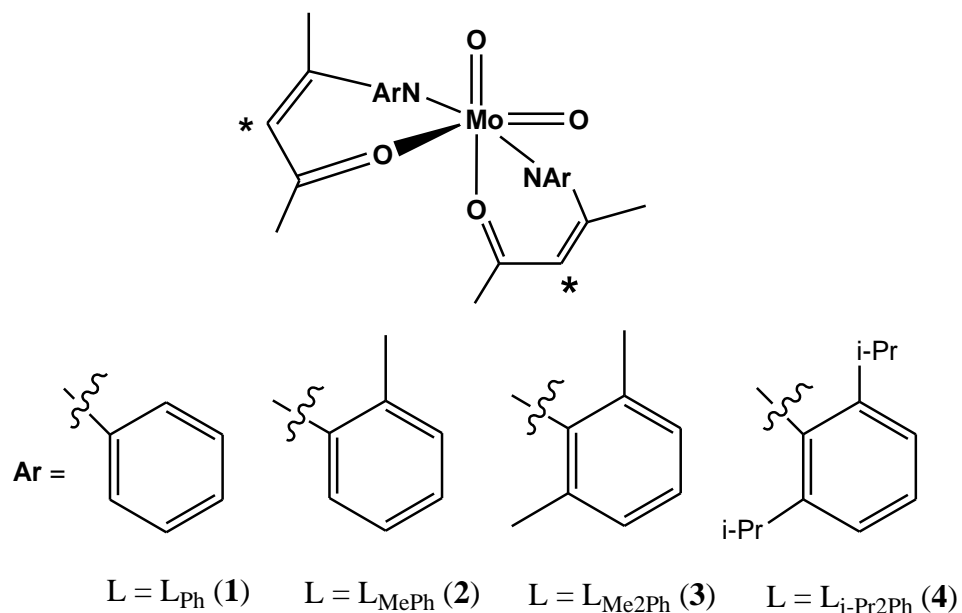
**Fig. 1.21**

The oxo imido complexes (**1** and **3**) also introduced oxygen atom transfer (OAT) by trimethyl phosphine. This oxygen transfer was analyzed kinetically by UV-Vis spectroscopy under pseudo-first order conditions.
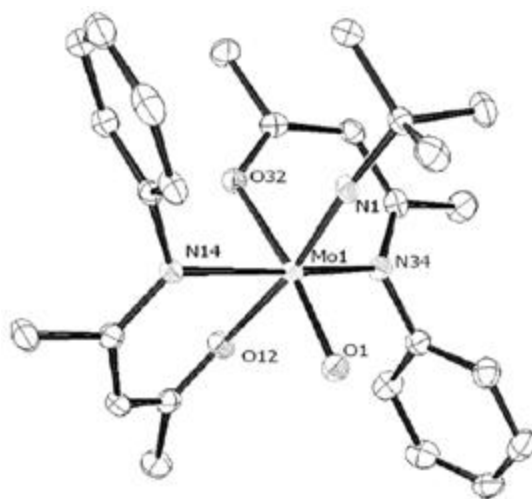


**Fig. 1.22**

The synthesis and catalytic performance of novel cis-dioxo-Mo(VI) complexes containing simple ONO tridentate Schiff base ligands in the epoxidation of various olefins using tert-butyl hydroperoxide in desired times with excellent chemo- and stereoselectivity have been described by A. Rezaeifard et al. [35]. The study of turnover numbers and the UV–Vis spectra of the Mo complexes in the epoxidation system indicate well the high efficiency and stability of the catalysts during the reaction. The electron-deficient and bulky groups on the salicylidene ring of the ligand promote the effectiveness of the catalyst.



**[MoO₂L(CH₃OH)]**

$L^1$ , R = -N(CH₂CH₃)₂, R' = H
$L^2$ , R = -OCH₃, R' = H
$L^3$ , R = -C₆H₅, R' = H
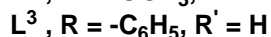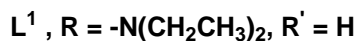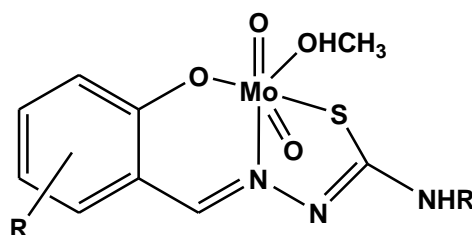
**Fig.1.23**

Synthesis, characterization and study of antitumor activity of some new thiosemicarbazonato dioxomolybdenum(VI) complexes have been reported by V. Vrdoljak and his coworkers [36]. The dioxomolybdenum(VI) [MoO₂L(CH₃OH)] complexes (**Fig.1.23**) were obtained by the reaction of [MoO₂(acac)₂] with thiosemicarbazone ligands derived from 3-thiosemicarbazide and 4-(diethylamino)salicylaldehyde ($H_2L^1$), 2-hydroxy-3-methoxybenzaldehyde ($H_2L^2$) or 2-hydroxy-1-naphthaldehyde ($H_2L^3$). All the complexes were characterized by means of chemical analyses, IR spectroscopy, TGA and NMR measurements. The molecular structures of the ligand $H_2L^2$ and complex [MoO₂L²(CH₃OH)]·CH₃OH (2a) have been determined by single crystal X-ray crystallography.
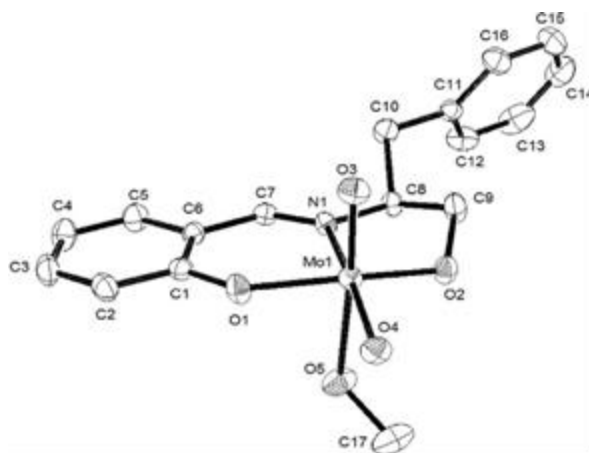
**Fig.1.24**

Z. Hu et al. has published the olefin epoxidation of Schiff base molybdenum(VI) complexes immobilized onto zirconium poly (styrene-phenylvinylphosphonate)-phosphate. Schiff base molybdenum(VI) complexes were immobilized onto a novel polymer–inorganic hybrid support, zirconium poly(styrene-phenylvinylphosphonate)-phosphate (ZPS-PVPA) [37]. The catalysts were characterized by IR, BET, XPS, SEM and TEM. Compared with other heterogeneous catalysts known from the relative literatures, the as-prepared heterogeneous catalysts showed comparable or even higher conversion and chemical selectivity, which was mainly attributed to the special structure and composition of ZPS-PVPA. Moreover, the supported catalysts were easily recovered by simple filtration and could be reused at least ten times with little loss of activity.

Chakravarthy and his co-workers have reported six new cis-dioxomolybdenum(VI) complexes (**Fig.1.24**) of chiral Schiff-base ligands, derived from condensation of various amino alcohols and substituted salicylaldehydes [38]. All the complexes were characterized by NMR, IR, ESI-MS and single crystal X-ray diffraction techniques. The octahedral geometry of the cis-dioxomolybdenum center was completed by a coordinated labile solvent molecule. In some complexes the sixth site is found to be vacant where the relatively bulky substituents hinder the coordination of the solvent. These complexes were tested for catalytic enantioselective sulfoxidation reactions using hydrogen peroxide as oxidant at low temperature which shows high

selectivity along with good to moderate enantiomeric excess. The formation of oxoperoxo Mo(VI) complexes was studied by ESI-MS from the reaction mixture during catalysis.
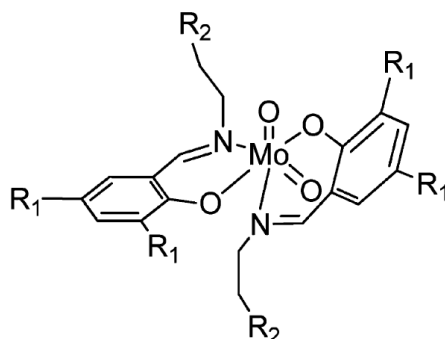


1: $R_1$ = tBu, $R_2$ = OMe; 77%
2: $R_1$ = Me, $R_2$ = OMe; 82%
3: $R_1$ = tBu, $R_2$ = NMe$_2$; 62%
4: $R_1$ = Me, $R_2$ = NMe$_2$; 63%
5: $R_1$ = tBu, $R_2$ = Et; 54%

**Fig.1.25**

M. Kooti and M. Afshari published a paper on the molybdenum Schiff base complex which was covalently anchored with silica-coated cobalt ferrite nanoparticles and used as a heterogeneous catalyst for the oxidation of alkenes [39]. The prepared catalyst was characterized by X-ray powder diffraction, transmission electron microscopy, vibrating sample magnetometry, thermogravimetric analysis, Fourier transform infrared, and inductively coupled plasma atomic emission spectroscopy. The molybdenum complex was shown to be an efficient heterogeneous catalyst for the oxidation of various alkenes using t-BuOOH as oxidant.

M. E. Judmaier and his coworker reported [40] a series of new [MoO$_2$(L$^X$)$_2$] (**Fig. 1.25**) complexes with Schiff base ligands using the uncommon $\eta^2$ coordinated [MoO$_2$($\eta^2$-tBu$_2$pz)$_2$] complex as starting material. All ligands coordinate through phenolic O atom and the imine N atom in a bidentate manner to the metal center.
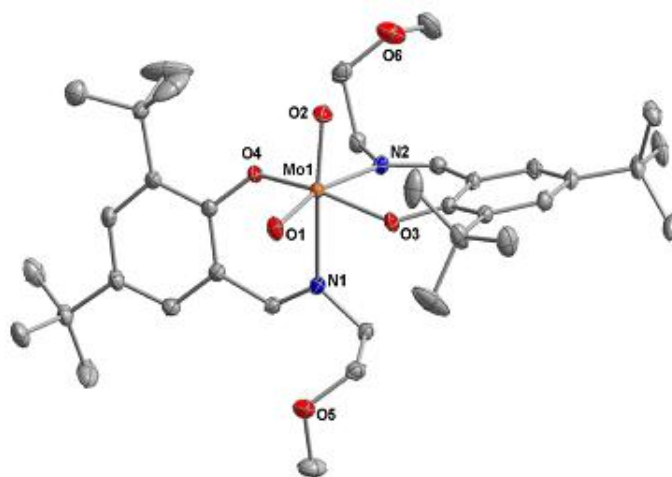
**Fig.1.26**

With the more sterically demanding ᵗBu substituent on the aryl ring (complexes **1**, **3** and **5**), a mixture of two isomers in solution was obtained, whereas only one isomer in solution was detected for methyl substituted complexes (**2**) and (**4**). Complexes (**1**) (**Fig.1.26**) and (**3**) were characterized by X-ray diffraction analyses. All the complexes were used as catalyst in the epoxidation of various alkenes where TBHP was used as oxidant. Among them, complexes (**1**) and (**2**) were highly selective in the epoxidation of styrene and the yield was very high. Complex (**3**), (**4**) and (**5**) were significantly less selective in the epoxidation of styrene.



**Fig.1.27**

24
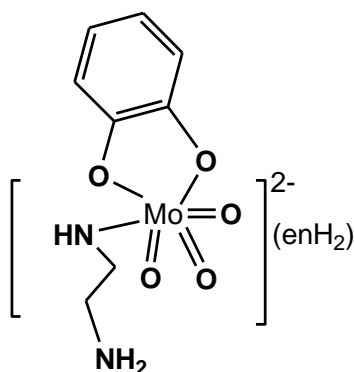
Jun Feng and his coworkers have reported the synthesis and characterization of a series of oxomolybdenum complexes with polyhydroxyl phenols [41], where two of them are tri-oxo-molybdenum complexes (**Fig.1.27**), in relation to their *in vitro* anticancer activities against human cancer cells. The structural features of all the complexes were investigated by X-ray diffraction. MTT assay tests indicated that their anticancer activities against human cancer cells decreased when the chelation number of the ligand increased.

### 1. 2. Aim of the present work

The primary aim of the present work has been to study the chemistry of oxomolybdenum(VI) complexes with ON- and/or ONO- donor ligand systems. The different ligands that have been used for this purpose are shown below along with their observed coordination modes.



$X = C_2H_5OH$, Imz, 1-MeImz, 4,4'-bipy



R = H, OH, $NH_2$

$R^1$ = H , $CH_3$

$X = C_2H_5OH$, $CH_3OH$, $\gamma$ -picoline
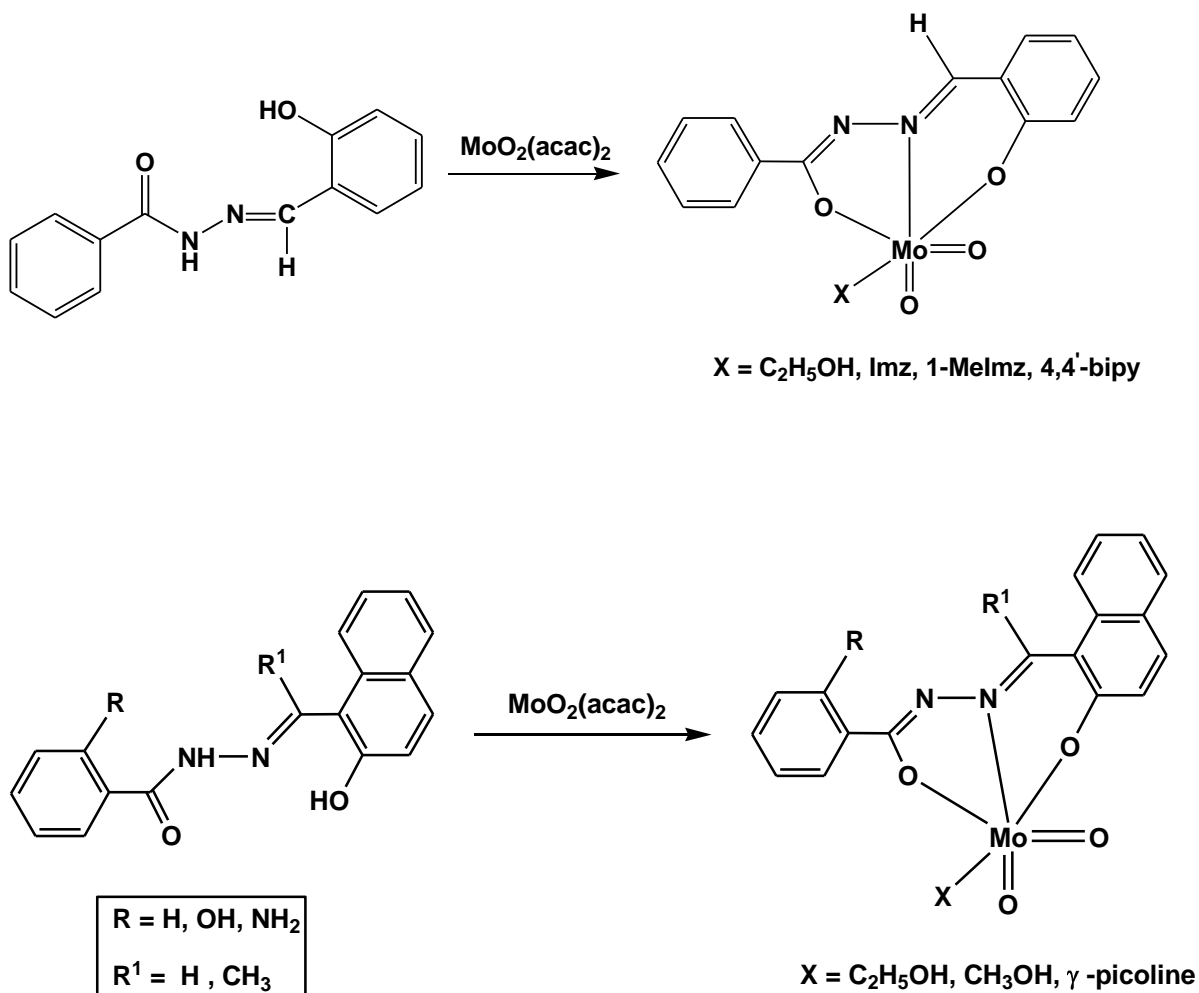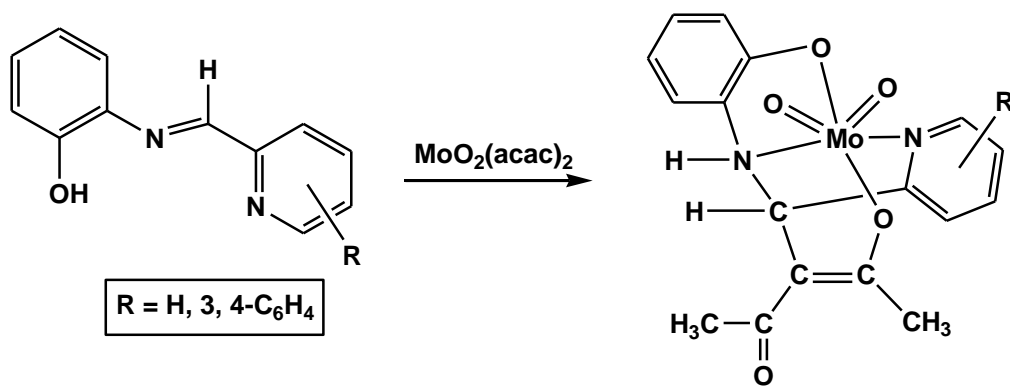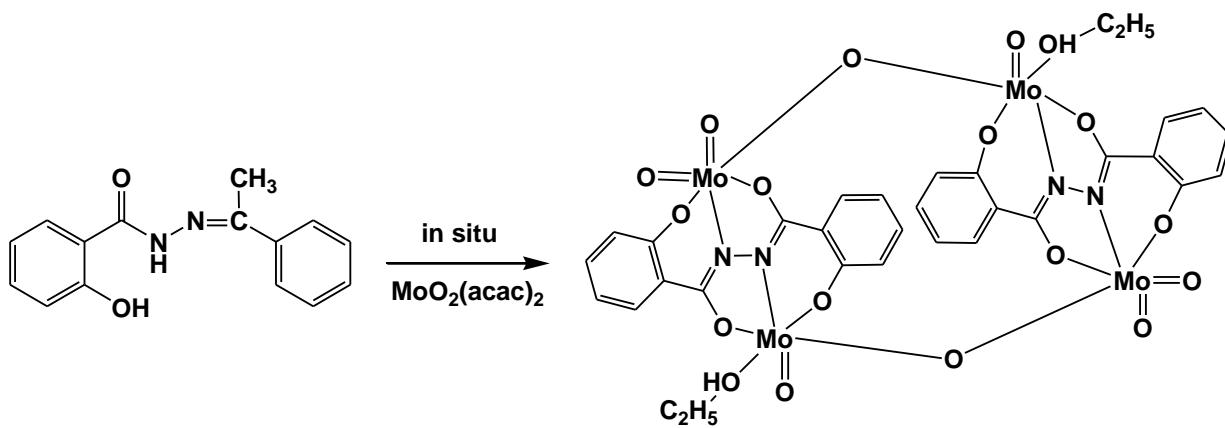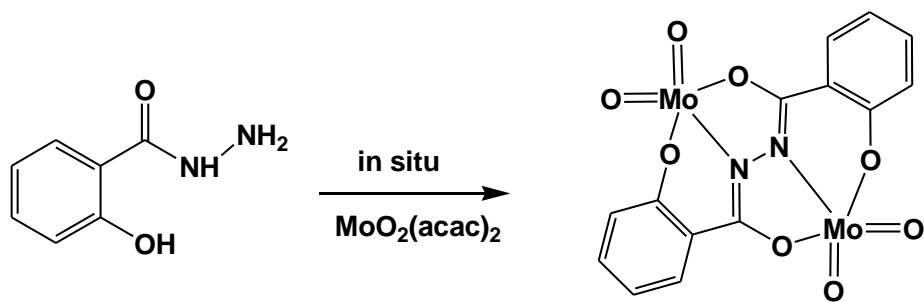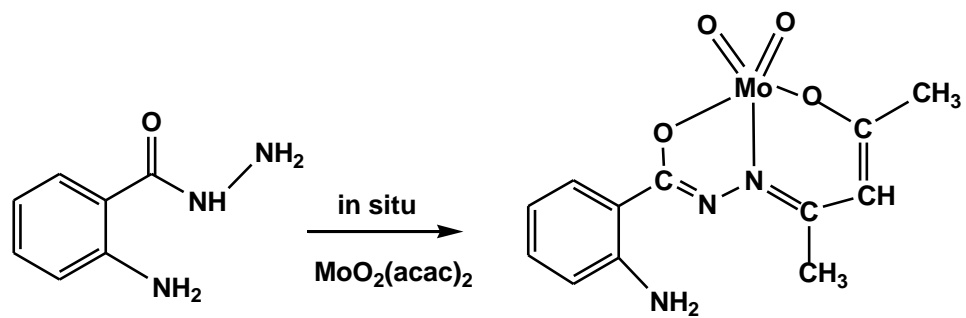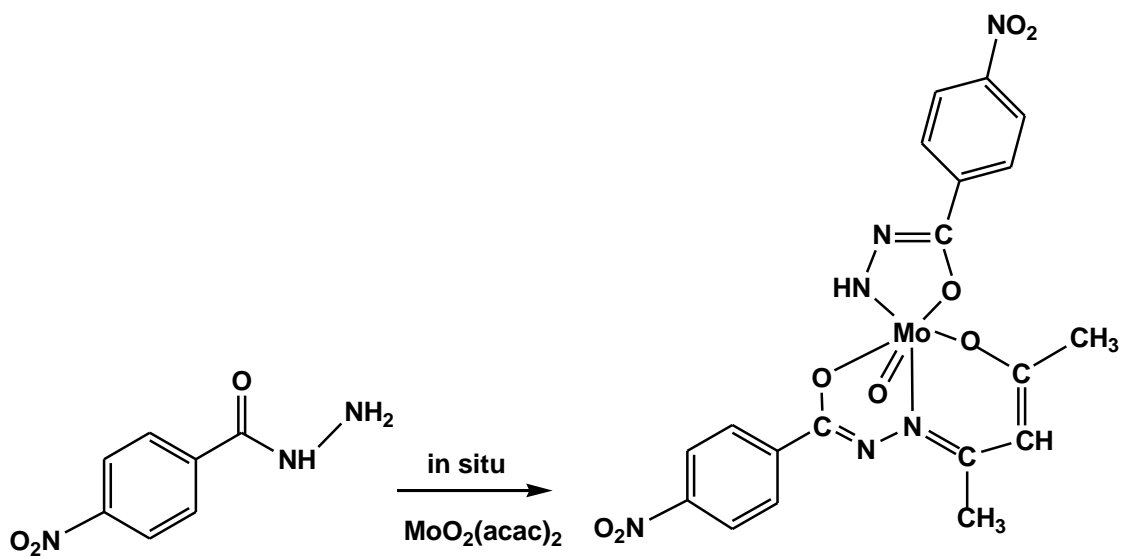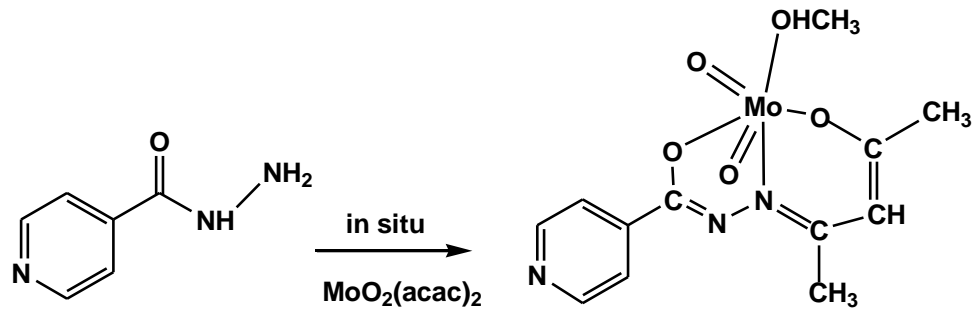
**1.3. The main objectives of the present study:**

1. To develop some ON- and/or ONO- donor mono- and binucleating ligand systems, (especially aroylhydrazones and Schiff bases) inspired by the paradigm of biologically and catalytically important oxomolybdenum complexes.

2. To develop versatile, new-generation mono- and dinuclear oxomolybdenum(VI) systems, for use as reagents in some bio- and catalytic reactions. This work uses synthetic and analytical approaches to generate and study mono- and binuclear molybdenum complexes, relying upon current mechanistic understanding of their mode of action.

3. Study the properties of these metal complexes, such as spectral, magnetic and redox behavior. Solve the X-ray structure of these complexes and develop the structure-reactivity correlation.

4. Exploration of biological (antibacterial activity) and catalytic activities of some of the above complexes particularly oxidation of alkenes, aromatic alcohols and oxidative bromination of aromatic aldehydes.

**References**

1. C.L. Rollinson, Inorg. Chem. 21 (1973) 691; Cotton and Wilkinson, 6$^{th}$ edition Wiley-Interscience, N. Y. (1999) 920.

2. R.K. Grasselli, Catal. Today 49 (1999) 141.

3. R.J. Cross, P.D. Newman, R.D. Peacock, D. Stirling, J. Mol. Catal. 144 (1999) 273.

4. K.J. Ivin, J.C. Mol, Olefin metathesis polymerisation, Academic Press, London (1997).

5. J. Belgacem, J. Kress, J.A. Osborn, J. Am. Chem. Soc. 114 (1992) 1501.

6. M.R. Maurya, S. Sikarwar, T. Joseph, S.B. Halligudi, J. Mol. Catal. A: Chem. 236 (2005) 132.

7. D. Collison, C.D. Garner, J.A. Joule, Chem. Soc. Rev. 25 (1996).

8. R. Hill, Chem. Rev. 96 (1996) 2757.

9. Nitrogen Fixation: The chemical- Biochemical Genetic Interface, A. Miller, W.E. Newton,(Eds), Plenum Press, NY, (1983). Advance in Nitrogen Fixation Research, C. Veeger, W.E. Newton, (Eds.), Nijhoff / Junk, Wageningen, (1984).

10. G.C. Tucci, J.P. Donahue, R.H. Holm, Inorg. Chem. 37 (1998) 1602.

11. B.E. Schultz, S.F. Gheller, M.C. Muetterties, M. J. Scott, R.H. Holm, J. Am. Chem. Soc. 115 (1993) 2714.

12. S.K. Sridhar, M. Saravanan, A. Ramesh, Eur. J. Med. Chem. 36 (2001) 615.

13. S.N. Pandeya, D. Sriram, G. Nath, E. De Clercq, Eur. J. Pharm. Sci. 9 (1999) 25.

14. R. Mladenova, M. Ignatova, N. Manolova, T.S. Petrova, I. Rashkov, Eur. Polym. J. 38 (2002) 989.

15. J. Liimatainen, A. Lehtonen, R. Sillanpää, Polyhedron 19 (2000) 1133.

16. B. Modec, J.V. Brenčič, R.C. Finn, R.S. Rarig, J. Zubieta, Inorg. Chim. Acta. 322 (2001) 113.

17. B. K. Colig, M. Cindric, D. M. Calogovic, V. Vrdoljak, B. Kamenar, Polyhedron 21 (2002) 147.

18. Y. Wong, D. K. P. Ng, H. K. Lee, Inorg. Chem. 41 (2002) 5276.

19. H. Y. Cho, S. G. Roh, J. H. Jeong, Polyhedron 21 (2002) 1211.

20. A. Rana, R. Dinda, P. Sengupta, L.R. Falvello, S. Ghosh, Polyhedron 21 (2002) 1023.

21. A. Lehtonen, V.G. Kessler, Inorg. Chem. Commun. 7 (2004) 691.

22. A. Lehtonen, R. Sillanpää, Polyhedron 24 (2005) 257.

23. A. Lehtonen, M. Wasberg, R. Sillanpää, Polyhedron 25 (2006) 767.

24. M. Masteri-Farahani, F. Farzaneh, M. Ghandi, J. Mol. Catal. A: Chem.248 (2006) 53.

25. S. N. Rao, N. Kathale, N.N. Rao, K.N. Munshi, Inorg. Chim. Acta 360 (2007) 4010.

26. J. Kim, W.T. Lim, B.K. Koo, Inorg. Chim. Acta 360 (2007) 2187.

27. S. Karahan, P. Köse, E. Subasi, H. Temel, Synth. React. Inorg., Met.-Org., Nano-Met. Chem. 38 (2008) 615.

28. D. Eierhoff , W. C. Tung, A. Hammerschmidt, B. Krebs, Inorg. Chim. Acta 362 (2009) 915.

29. S. Gupta, S. Pal, A.K. Barik, S. Roy, A. Hazra, T.N. Mandal, R.J. Butcher, S.K. Kar, Polyhedron 28 (2009) 711.

30. I. Sheikhshoaie, A. Rezaeifard, N. Monadi, S. Kaafi, Polyhedron 28 (2009) 733.

31.  V. Vrdoljak, J. Pisk, B. Prugovečki, D. Matković-Čalogović, Inorg. Chim. Acta 362 (2009) 4059.

32. M.L.H. Nair, D. Thankamani, Indian J. Chem. 48 (2009) 1212.

33. A.A.A. Aziz, J. Mol. Struct. 979 (2010) 77.

34. N.C. Mösch-Zanetti, D. Wurm, M. Volpe, G. Lyashenko, B. Harum, F. Belaj, J. Baumgartner, Inorg. Chem. 49 (2010) 8914.

35. A. Rezaeifard, I. Sheikhshoaie, N. Monadi, M. Alipour, Polyhedron 29 (2010) 2703.

36. V. Vrdoljak, I. Đilović, M. Rubčić, S.K. Pavelić, M. Kralj, D. Matković–Calogović, I. Piantanida, P. Novak, A. Rožman, M. Cindrić, Eur. J. Med. Chem.45 (2010) 38.

37. Z. Hu, X. Fu, Y. Li, Inorg. Chem. Commun.14 (2011) 497.

38. R.D. Chakravarthy, K. Suresh, V. Ramkumar, D.K. Chand, Inorg. Chim. Acta 376 (2011) 57.

39. M. Kooti, M. Afshari, Catal Lett 142 (2012) 319.

40. M.E. Judmaier, C. Holzer, M. Volpe, N.C. Mösch-Zanetti, Inorg. Chem.51 (2012) 9956.

41. J. Feng, X. Lu, G. Wang, S. Du, Y. Cheng, Dalton Trans. 41 (2012) 8697.

# Chapter 2

**Mixed-ligand Aroylhydrazone Complexes of Molybdenum:**

**Synthesis, Structure and Biological Activity**

# Chapter 2

**Mixed-Ligand Aroylhydrazone Complexes of Molybdenum: Synthesis, Structure and Biological Activity**

**Abstract**

Reaction of benzoylhydrazone of 2-hydroxybenzaldehyde ($H_2L$) with $[MoO_2(acac)_2]$ proceeds smoothly in refluxing ethanol to afford an orange complex $[MoO_2L(C_2H_5OH)]$ (**1**). The substrate binding capacity of **1** has been demonstrated by the formation and isolation of two mononuclear $[MoO_2L(Q)]$ {where Q = imidazole (**2a**) and 1-methylimidazole (**2b**)} and one dinuclear $[(MoO_2L)_2(Q)]$ {Q = 4,4'-bipyridine (**3**)} mixed-ligand oxomolybdenum complexes. All the complexes have been characterized by elemental analysis, electrochemical and spectroscopic (IR, UV–Vis and NMR) measurements. Molecular structures of all the oxomolybdenum(VI) complexes (**1**, **2a**, **2b** and **3**) have been determined by X-ray crystallography. The complexes have been screened for their antibacterial activity against *Escherichia coli, Bacillus subtilis* and *Pseudomonas aeruginosa*. The minimum inhibitory concentration of these complexes and antibacterial activity indicates the compound (**2a**) and (**2b**) as the potential lead molecule for drug designing.

## 2.1. Introduction

The coordination chemistry of molybdenum has become a fascinating area of research in recent time because of presence of molybdenum in metalloenzymes and its biochemical as well as catalytic importance [1–20]. The molybdenum Schiff's base complexes have continued to play the role of one of the most important models of molybdoenzymes [21–23] due to their preparative accessibility. Schiff bases derived from salicylaldehyde and amino alcohols have been widely used for the preparation of oxomolybdenum complexes containing the $MoO_2^{2+}$-core [24–26] whereas, Schiff bases obtained by the reactions of aromatic acidhydrazides with *o*-hydroxycarbonyl compounds have rarely been used in molybdenum chemistry. This type of ligands are of particular interest because $MoO_2L$ or $MoOL$ type of complex possess one or two "open" coordination sites that can be utilized for substrate binding [23, 27–29] properties and these species have frequently been considered as models of enzymatic reaction and catalytic sites. On the other hand, hydrazones –NH–N=CRR' (R and R′ = H, alkyl, aryl) are versatile ligands due to their applications in the field of analytical [30] and medicinal chemistry [31]. Hydrazone moieties are the most important pharmacophoric cores of several anti-inflammatory, antinociceptive, and antiplatelet drugs [32]. It may be relevant to mention here that though the study of antibacterial activity of aroylhydrazones complexes of many transition metals have been extensively studied [33–38], that of oxomolybdenum(VI) appears to have remained practically unexplored [39–41].

As part of our group studies on aroylhydrazone complexes [29,33,42], this chapter reports the synthesis, X-ray structure and characterization of a new mononuclear Schiff base complex $MoO_2L(C_2H_5OH)]$ (**1**), some mixed–ligand mononuclear [$MoO_2L(Imz)$] (**2a**), [$MoO_2L(1–MeImz)$] (**2b**) and diimine bridged dinuclear [$(MoO_2L)_2(\mu$-4,4'-bipy)] (**3**) cis-dioxomolybdenum(VI) complexes with aroylhydrazone as a primary ligand with special reference to their antibacterial activity.

## 2.2. Experimental

### 2.2.1. Materials

[MoO$_2$(acac)$_2$] was prepared as described in the literature [28]. Reagent grade solvents were dried and distilled prior to use. All other chemicals were reagent grade, available commercially and used as received. Commercially available TBAP (tetra butyl ammonium perchlorate) was properly dried and used as a supporting electrolyte for recording cyclic voltammograms of the complexes.

### 2.2.2. Physical Measurements

Elemental analyses were performed on a Vario ELcube CHNS Elemental analyzer. IR spectra were recorded on a Perkin-Elmer Spectrum RXI spectrometer. $^1$H NMR spectra were recorded with a Bruker Ultrashield 400 MHz spectrometer using SiMe$_4$ as an internal standard. Electronic spectra were recorded on a Lamda25, PerkinElmer spectrophotometer. Magnetic susceptibility was measured with a Sherwood Scintific AUTOMSB sample magnetometer. Electrochemical data were collected using a PAR electrochemical analyzer and a PC-controlled Potentiostat/Galvanostat (PAR 273A) at 298 K in a dry nitrogen atmosphere. Cyclic voltammetry experiments were carried out with a platinum working electrode, platinum auxiliary electrode, Ag/AgCl as reference electrode and TBAP as supporting electrolyte.

### 2.2.3. Synthesis of Ligand (**H₂L**)

The ligand benzoylhydrazone of 2-hydroxybenzaldehyde (H$_2$L) was prepared by the condensation of equimolar ratio of benzoylhydrazide 2.72 g (20.00 mmol) and 2-hydroxybenzaldehyde 1.46 g (20.00 mmol) in stirring ethanol (25 ml) for 2 hr. The resulting yellowish- white compound was filtered, washed with ethanol and dried over fused CaCl$_2$. M.P. 160$^o$C. Yield: 2.88g (61%). Anal. Calcd. for C$_{14}$H$_{12}$N$_2$O$_2$: C, 69.98; H, 5.03 ; N, 11.65. Found: C, 70.00; H, 5.01; N, 11.62%. $^1$H NMR (DMSO-d$_6$,400 MHz): $\delta$ = 12.14 (s, 1H, OH), 11.32 (s, 1H, NH), 8.66 (s, 1H, CH), 7.96–6.91 (m, 9H, Aromatic). $^{13}$C NMR (DMSO-d$_6$, 100 MHz): $\delta$ = 163.30, 157.94, 148.79, 133.27, 132.45, 131.86, 130.01, 129.02, 128.11, 119.82, 119.13, 116.89, 114.34, 112.57.

*2.2.4. Synthesis of precursor complex [MoO$_2$L(C$_2$H$_5$OH)] (1)*

0.24 g (1.00 mmol) of ligand H$_2$L was dissolved in 30 mL ethanol. When 0.32 g (1.00 mmol) of MoO$_2$(acac)$_2$ was added to the solution, the color changed to dark orange. The solution mixture was then refluxed for 3 hr. After leaving the solution for 2 days at room temperature, fine dark orange crystals were isolated and a suitable single crystal was selected for X-ray analysis. Yield: 0.31g (75%). Anal. Calcd. for C$_{16}$H$_{16}$N$_2$O$_5$Mo: C, 46.61; H, 3.91; N, 6.79. Found: C, 46.63; H, 3.89; N, 6.77%. $^1$H NMR (DMSO-d$_6$, 400 MHz): $\delta$ = 9.01 (s, 1H, CH), 8.02–6.95 (m, 9H, Aromatic), 4.37 (s, 1H, OH), 3.40 (q, 2H, CH$_2$), 1.04 (t, 3H, CH$_3$). $^{13}$C NMR (DMSO-d$_6$, 100 MHz): $\delta$ = 169.16, 159.83, 156.50, 135.42, 134.77, 132.46, 130.40, 129.28, 128.44, 122.08, 120.74, 119.03, 114.49, 112.69, 56.50, 19.01.

*2.2.5. Synthesis of mixed-ligand complexes [{MoO$_2$L(Q)}, where Q = imidazole (2a), 1-methylimidazole (2b)] and [{(MoO$_2$L)$_2$(Q)} where Q = 4,4'-bipyridine (3)]*

To a clear orange solution (obtained by refluxing) of **1** (0.50 mmol) in ethanol (30 ml) was added corresponding mixed-ligand [0.73 mmol (**2a** and **2b**), 0.30 mmol (**3**)] and the mixture was refluxed for 3 hr. Slow evaporation of the orange filtrate over 2 days produced orange-red crystals.

*[MoO$_2$L(Imz)] (2a)*: Yield: 0.25g (57%). Anal. Calcd. for C$_{17}$H$_{14}$N$_4$O$_4$Mo: C, 47.01; H, 3.23; N, 12.90. Found: C, 47.03; H, 3.20; N, 12.89%. $^1$H NMR (DMSO-d$_6$, 400 MHz): $\delta$ = 8.95 (s, 1H, CH), 7.99–6.96 (m, 9H, Aromatic), 7.74–7.01 (m, 3H, Aromatic–Imz); 7.67 (br s, 1H, NH–Imz). $^{13}$C NMR (DMSO-d$_6$, 100 MHz): $\delta$ = 169.24, 159.90, 156.52, 135.44, 134.82, 132.48, 130.36, 129.28, 129.03, 128.42, 128.10, 122.14, 120.75, 119.05, 118.34, 116.45, 113.56.

*[MoO$_2$L(1-MeImz)] (2b)*: Yield: 0.35g (78%). Anal. Calcd. for C$_{18}$H$_{16}$N$_4$O$_4$Mo: C, 48.21; H, 3.59; N, 12.50. Found: C, 48.18; H, 3.60; N, 12.48%. $^1$H NMR (DMSO-d$_6$, 400 MHz): $\delta$ = 8.96 (s, 1H, CH), 7.99–7.07 (m, 9H, Aromatic), 7.74–6.87 (m, 3H, Aromatic–1–MeImz), 3.63 (s, 3H, CH$_3$–1–MeImz). $^{13}$C NMR (DMSO-d$_6$, 100 MHz): $\delta$ = 169.19, 159.88, 156.54, 138.37, 135.43, 134.80, 132.48, 131.42, 130.37, 129.28, 129.13, 128.43, 128.16, 122.13, 121.15, 120.75, 119.03, 67.87.

*[(MoO₂L)₂(μ-4,4'-bipy)] (3)*: Yield: 0.54g (60%). Anal. Calcd. for $C_{38}H_{28}N_6O_8Mo_2$: C, 51.35; H, 3.15; N, 9.45. Found: C, 51.37; H, 3.13; N, 9.46%. $^1$H NMR (DMSO-d$_6$, 400 MHz): $\delta$ = 8.96 (s, 1H, CH), 8.71–7.82 (m, 4H, Aromatic–4,4'–bipy), 7.99–6.96 (m, 9H, Aromatic). $^{13}$C NMR (DMSO-d$_6$, 100 MHz): $\delta$ = 169.15, 159.82, 156.52, 151.03, 144.78, 135.44, 134.78, 132.48, 132.06, 130.38, 129.29, 129.13, 128.43, 126.43, 124.62, 122.10, 121.76, 120.73, 119.03.

### 2.2.6. Crystallography

Suitable single crystal of **1, 2a, 2b** and **3** were chosen for X-ray diffraction studies. Crystallographic data and details of refinement are given in **Table 2.1**. These compounds crystallized in the monoclinic space group *P2₁/c* (**1**), orthorhombic space group *Pna2₁* (**2a**), orthorhombic space group *Pca2₁* (**2b**) and monoclinic space group *P2₁/n* (**3**) respectively. The unit cell parameters and the intensity data for all the complexes were collected at ~ 293 K, on a Bruker Smart Apex CCD diffractometer using graphite monochromated Mo Kα radiation (k = 0.71073 Å), employing the *ω–2θ* scan technique. The intensity data were corrected for Lorentz, polarization and absorption effects. The structures were solved using the SHELXS97 [43] and refined using the SHELXL97 [44] computer programs. The non-hydrogen atoms were refined anisotropically.

### 2.2.7. Antibacterial activity

Antibacterial activity of the compounds (ligands and complexes) was studied against *Escherichia coli (E. coli), Bacillus and Pseudomonas aeruginosa* by agar well diffusion technique. Mueller Hinton-agar (containing 1% peptone, 0.6% yeast extract, 0.5% beef extract and 0.5% NaCl, at pH 6.9–7.1) plates were prepared and 0.5–McFarland culture (1.5 x 10$^8$ cells/mL) of the test organisms were swabbed onto the agar plate (as per CLSI guidelines, 2006). Test compounds were dissolved in DMSO at several concentrations ranging from 1000 μg/mL–1.95 μg/mL. 9 mm wide wells were dug on the agar plate using a sterile cork borer. 100 μg/mL of the solutions of the each test compound from each dilution were added into each of the wells using a micropipette. These plates were incubated for 24 h at 35 ± 2 °C. The growth of the test organisms was inhibited by diffusion of the test compounds and then the inhibition zones developed on the plates were measured [41,45]. The effectiveness of an antibacterial agent in sensitivity is based on the diameter of the zones of inhibition which is measured to the nearest

millimeter (mm). The standard drug Vancomycin was also tested for their antibacterial activity at the same concentration under the conditions similar to that of the test compounds as +ve control. DMSO alone was used as a –ve control under the same conditions for each organism.

**Table 2.1** Crystal and Refinement Data of Complexes **1, 2a, 2b and 3**

| Compound | 1 | 2a | 2b | 3 |
|---|---|---|---|---|
| Formula | $C_{16}H_{16}MoN_2O_5$ | $C_{17}H_{14}MoN_4O_4$ | $C_{18}H_{16}MoN_4O_4$ | $C_{38}H_{28}Mo_2N_6O_8$ |
| M | 412.25 | 434.26 | 448.29 | 888.54 |
| Crystal symmetry | Monoclinic | Orthorhombic | Orthorhombic | Monoclinic |
| Space group | $P2_1/c$ | $Pna2_1$ | $Pca2_1$ | $P2_1/n$ |
| $a(Å)$ | 10.4986(7) | 7.6276(14) | 17.0374(5) | 11.1975(3) |
| $b(Å)$ | 10.4410(7) | 16.640(3) | 6.7818(2) | 13.0914(4) |
| $c(Å)$ | 15.1561(11) | 13.260(3) | 32.3366(9) | 12.5884(3) |
| $\alpha$ (°) | 90 | 90 | 90 | 90 |
| $\beta$ (°) | 106.842(2) | 90 | 90 | 98.875(2) |
| $\gamma$ (°) | 90 | 90 | 90 | 90 |
| $V(Å^3)$ | 1590.09(19) | 1683.0(5) | 3736.31(19) | 1823.25(9) |
| Z | 4 | 4 | 8 | 2 |
| $D_{calc}(g.cm^{-3})$ | 1.722 | 1.714 | 1.594 | 1.618 |
| F(000) | 832 | 872 | 1808 | 880 |
| $\mu(Mo\text{-}K\alpha)(mm^{-1})$ | 0.854 | 0.811 | 0.733 | 0.749 |
| max./min.trans. | 0.9505 /0.8826 | 0.8047 / 0.7757 | 0.8100 / 0.7939 | 0.8064 /0.7794 |
| $2\theta(max)(°)$ | 30.5 | 28 | 30.50 | 30.20 |
| Reflections collected / unique | 23567/4900 | 16063/3880 | 68324/11367 | 15801/5495 |
| $R_1^a$ [I>2σ(I)] | R1 = 0.0281, wR2=0.0671 | R1 = 0.0360, wR2=0.0790 | R1 = 0.0413, wR2=0.0817 | R1 = 0.0611, wR2=0.1431 |
| $wR_2^b$ [all data] | R1 = 0.0324, wR2=0.0690 | R1 = 0.0455, wR2=0.0835 | R1 = 0.0716, wR2=0.0920 | R1 = 0.1310, wR2=0.1742 |
| S[goodness of fit] | 1.079 | 1.077 | 1.012 | 1.037 |
| min./max. res.(e.Å$^{-3}$) | 0.779 / -0.809 | 0.997 / -0.518 | 0.413 / -0.571 | 2.525 / -0.696 |

$^aR_1 = \Sigma ||F_O|-|F_C||/\Sigma |F_O|$.

$^bwR_2 = \{\Sigma [w (F_O^2 - F_C^2)^2]/\Sigma [w (F_O^2)^2]\}^{1/2}$

## 2.3. Results and Discussion

### 2.3.1. Synthesis

Reaction of benzoylhydrazone of *2*-hydroxybenzaldehyde (H$_2$L) with [MoO$_2$(acac)$_2$] (**Scheme 2.1**) proceeds smoothly in refluxing ethanol to afford a orange complex in a decent yield. Though the preliminary characterization data (microanalysis, $^1$H NMR and IR) indicated the presence of the ligand, two oxo, and an ethanol in this complex, they could not point to any definite stereochemistry of the complex, as well as the coordination mode of H$_2$L in it. These compounds are highly soluble in aprotic solvents, viz. DMF or DMSO and are sparingly soluble in alcohol, CH$_3$CN and CHCl$_3$. All these complexes are diamagnetic, indicating the presence of molybdenum in the + 6 oxidation state, and are nonconducting in solution.
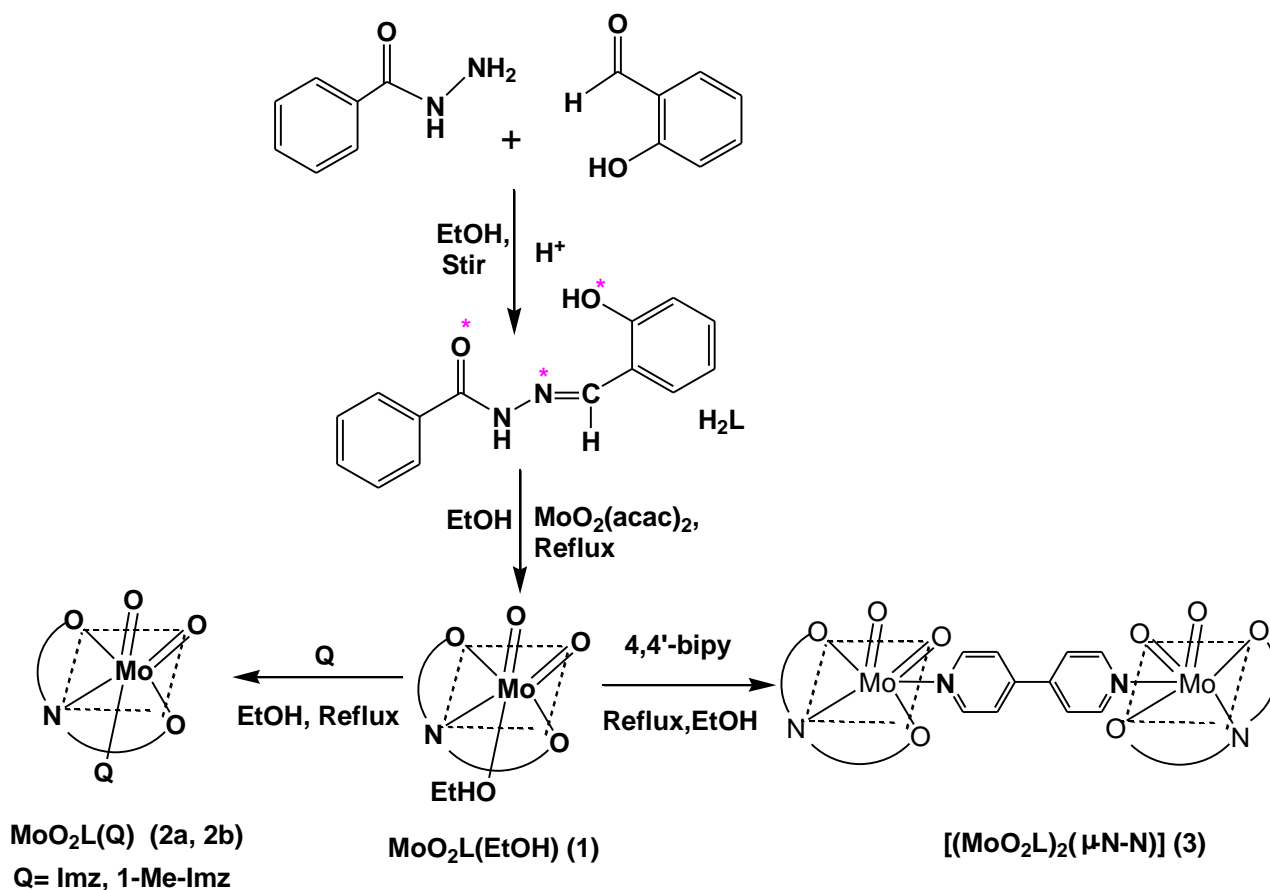


**Scheme 2.1**

*2.3.2. Spectral Characteristics*

Spectral characteristics of compounds **1–3** are listed in **Table 2.2**. Infrared spectra of all the complexes are mostly similar. The ligand exhibit the IR bands of minimum intensity at 3269 cm$^{-1}$ [$\nu$(OH)], 3057 cm$^{-1}$ [$\nu$(NH)], and 1673 cm$^{-1}$ [$\nu$(C=O)] [27–33] . Characteristic strong bands at 1607 cm$^{-1}$ and 1576 cm$^{-1}$ region due to $\nu$(C=C/aromatic) and $\nu$(C=N) stretching modes of the ligand [23,29] are located in the spectra of both the ligand and the complexes. The Mo=O stretching modes occur as a pair of sharp strong peaks in the 937–892 cm$^{-1}$ range [23,25–29]. The representative IR spectra of ligand H$_2$L and complex **1** are shown in **Figs. 2.1** and **2.2**, respectively.

 A number of absorption bands are observed in the UV-vis region. The DMSO solution of all the complexes display a shoulder in the 410–402 nm region and two strong absorptions are located in the 316–311 and 270–219 nm range, which are assignable to L→Mo(d$\pi$) LMCT and intraligand transitions respectively [23,28,29]. Electronic absorption spectra of [(MoO$_2$L)$_2$ ($\mu$-4,4'-bipy)] (**3**) is shown in **Fig. 2.3** as the representative one.

The $^1$H and $^{13}$C NMR spectroscopic data of the free ligand and all the complexes are given in the experimental section. The $^1$H NMR spectrum of the free ligand exhibits an –OH (phenolic) resonance at $\delta$ = 12.14 ppm, –NH resonance at $\delta$ = 11.32 ppm and –CH resonance at $\delta$ = 8.66 ppm. All the aromatic proton signals of ligands and complexes are observed in the expected region $\delta$ = 8.71–6.87 ppm. The signal for the –OH and –NH protons disappeared, indicating the deprotonation of the phenolic –OH and –NH groups in the complexes (**1-3**) [23–29]. The chemical shift of the coordinated EtOH of complex **1** exhibits an –OH (enolic) resonance at $\delta$ = 4.37 ppm, –CH$_2$ resonance at $\delta$ = 3.43 ppm and –CH$_3$ resonance at $\delta$ = 1.05 ppm. These data are different compared to the chemical shifts found [46] for free molecule at 4.63, 3.44 and 1.06 ppm respectively. The $^{13}$C signals expected from coordinated EtOH are clearly observed in the expected region. Therefore, the NMR data of complex **1** clearly indicates that the labile solvent molecule e.g. EtOH stay coordinated during the solution study. The representative NMR spectra of complex **1** and complex **2b** are shown in **Figs. 2.4** and **2.5**, respectively.

**Table 2.2** Characteristic IR[a] bands and electronic spectral data[b] for the studied ligand and complexes

| Compounds | ν(–OH) | ν(C=N) | ν(Mo=O)/cm$^{-1}$ | $\lambda_{max}$/nm ($\varepsilon$/dm$^3$mol$^{-1}$cm$^{-1}$) |
|---|---|---|---|---|
| H$_2$L | 3269 | 1576 | -- | 327 (23614), 217 (15785) |
| [MoO$_2$L (C$_2$H$_5$OH)] (**1**) | -- | 1555 | 937, 913 | 402 (9439), 316 (25123), 219 (16352) |
| [MoO$_2$L(Imz)] (**2a**) | -- | 1556 | 935, 892 | 403 (9569), 316 (26126), 220 (15711) |
| [MoO$_2$L(1-MeImz)] (**2b**) | -- | 1596 | 912,898 | 410 (10801), 315 (23470), 266 (16352) |
| [(MoO$_2$L)$_2$(μ-4,4'-bipy)] (**3**) | -- | 1556 | 932, 910 | 404 (6393), 311 (22768), 270 (16939) |

[a] In KBr pellet; [b] In DMSO

41
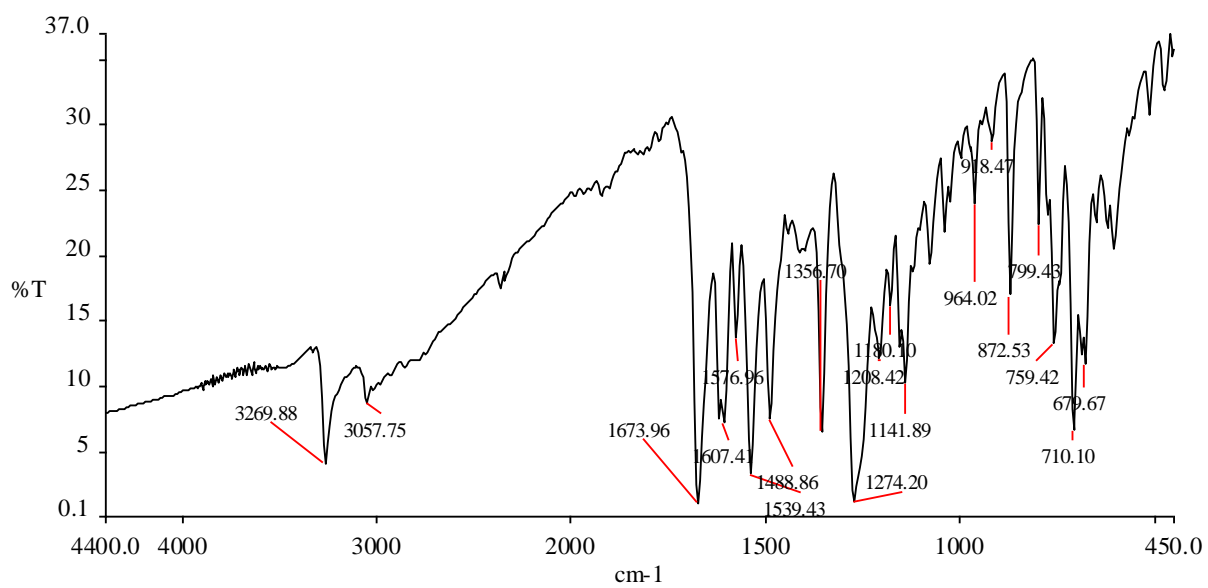
**Fig. 2.1** IR spectrum of H$_2$L
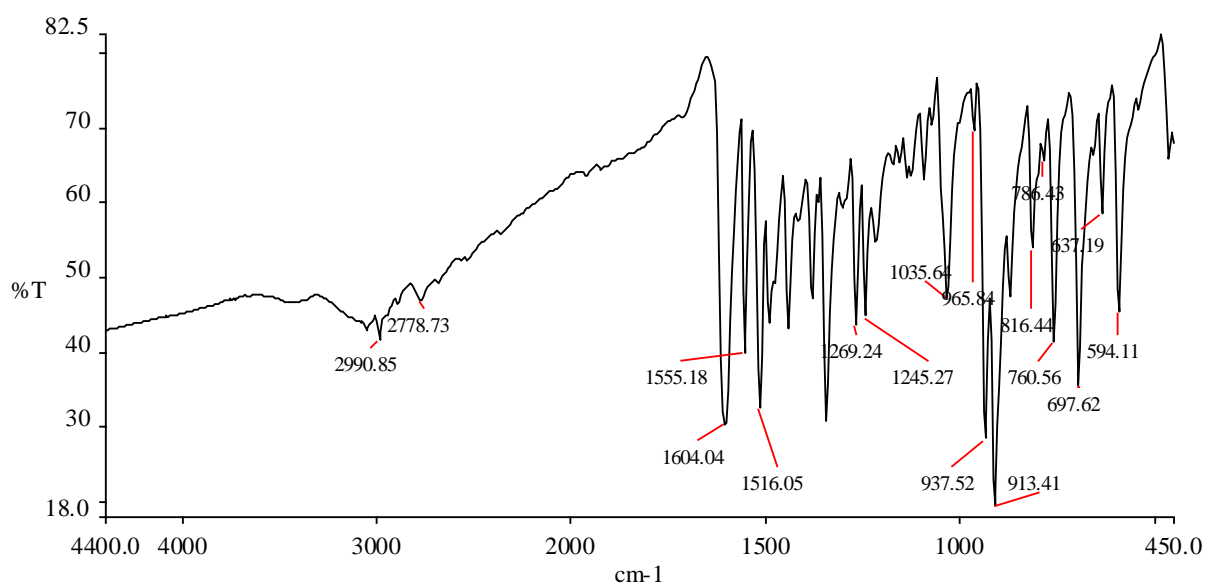
**Fig. 2.2** IR spectrum of [MoO$_2$L(EtOH)] (**1**)
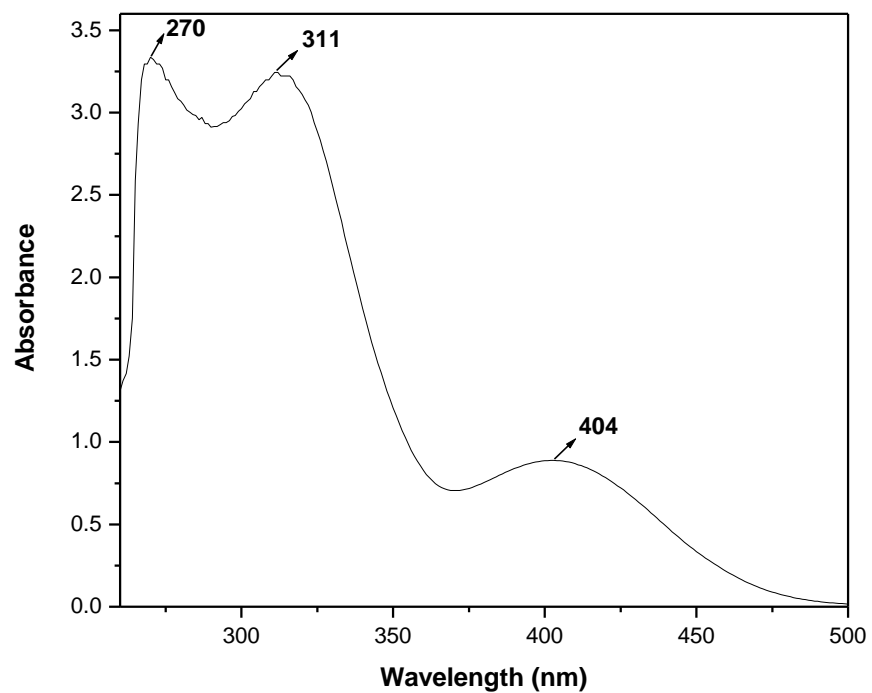
**Fig. 2.3** Electronic absorption spectra of $[(MoO_2L)_2 (\mu\text{-}4,4'\text{-bipy})]$ (**3**) in DMSO, at $25^0$ C
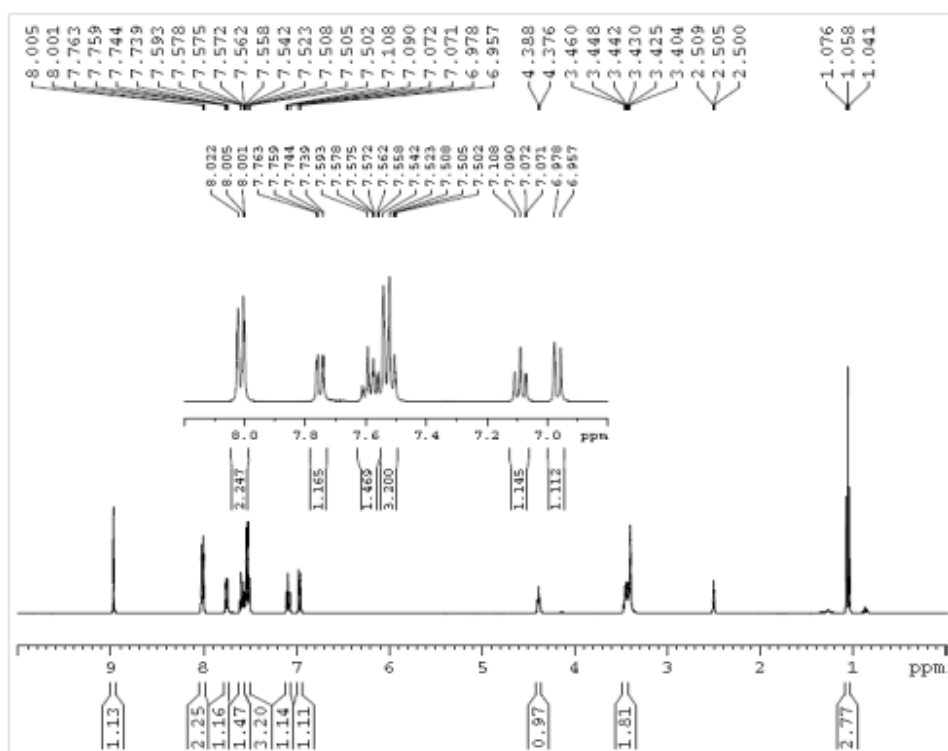
**Fig. 2.4** $^1$H NMR spectrum of [MoO$_2$L(EtOH)] (**1**) in DMSO d$_6$.
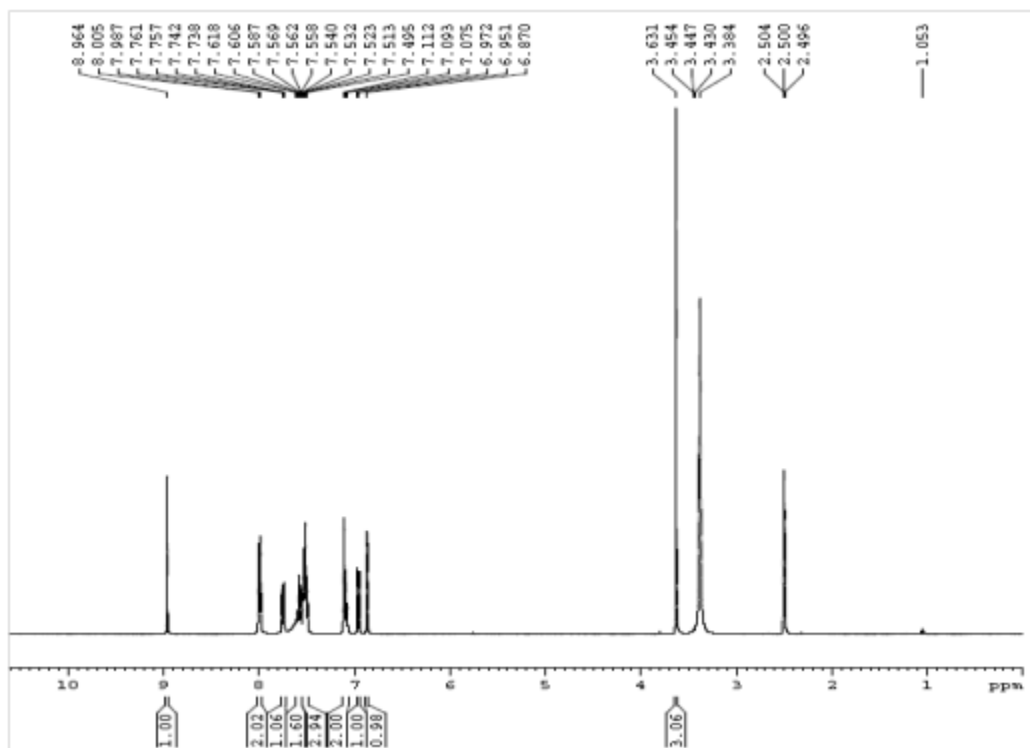
**Fig. 2.5** $^1$H NMR spectrum of [MoO$_2$L(1-MeImz)] (**2b**) in DMSO d$_6$.

*2.3.3. Electrochemical properties*

Electrochemical properties of the complexes have been studied by cyclic voltammetry in DMF solution (0·1 M TBAP). Voltammetric data are given in **Table 2.3**. The CV trace of complex **1** exhibits one irreversible reductive response at –0.81 V, which may be assigned to $Mo^{VI}/Mo^V$ process [23]. But the CV traces of complexes **2a** and **2b** exhibit two irreversible reductive responses within the potential window –0.71 to –0.73 V and –0.92 to –1.00 V, which are possibly assigned to $Mo^{VI}/Mo^V$ and $Mo^V/Mo^{IV}$ processes respectively [28].

The dinuclear complex **3** exhibit three successive irreversible one-electron reductions within the potential window –0.79 to –1.61 V versus Ag/AgCl in DMF which are assigned to $Mo^{VI}–Mo^{VI}/Mo^V–Mo^{VI}$ and $Mo^V–Mo^{VI}/Mo^V–Mo^V$ processes and the ligand (bridging)-centered reduction, respectively [29]. The cyclic voltammogram of $MoO_2L(C_2H_5OH)$ (**1**) and $[(MoO_2L)_2(\mu\text{-}4,4'\text{-bipy})]$ (**3**) are displayed in **Figs. 2.6** and **2.7** as the representative.

**Table 2.3** Cyclic voltammetric results for dioxomolybdenum (VI) complexes at 298 K

| Complex | $E$pc [V][a] |
|---|---|
| $[MoO_2L(C_2H_5OH)]$ (**1**) | –0.81 |
| $[MoO_2L(Imz)]$ (**2a**) | –0.71, –0.92 |
| $[MoO_2L(1\text{-MeImz})]$ (**2b**) | –0.73, –1.00 |
| $[(MoO_2L)_2(\mu\text{-}4,4'\text{-bipy})]$ (**3**) | –0.79, –1.35, –1.61 |

[a] Solvent: DMF; working electrode: platinum; auxiliary electrode: platinum; reference electrode: Ag/AgCl; supporting electrolyte: 0.1 M TBAP; scan rate: 50 mV/s. $E$pc is the cathodic peak potential.
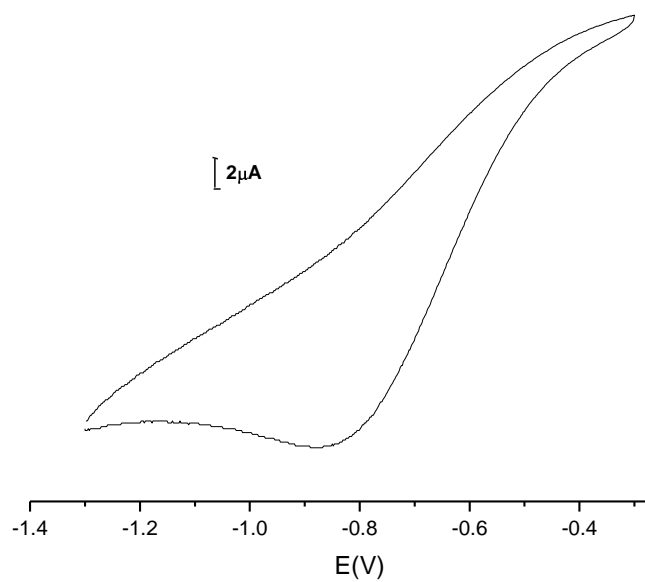
**Fig. 2.6** Cyclic voltammogram of [MoO$_2$L(C$_2$H$_5$OH)] (**1**) in DMF
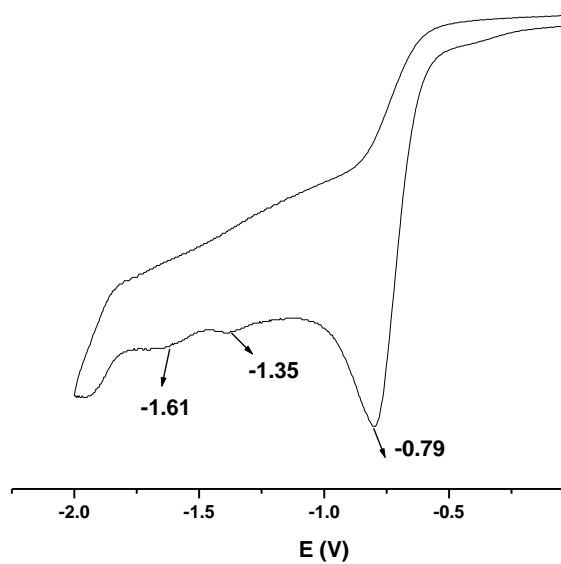


**Fig. 2.7** Cyclic voltammogram of [(MoO$_2$L)$_2$(μ-4,4'-bipy)] (**3**) in DMF

*2.3.4. Description of the X-ray structure of complex [MoO₂L(C₂H₅OH)] (1)*

Reaction of benzoylhydrazone of *2*-hydroxybenzaldehyde (H₂L) with [MoO₂(acac)₂] proceeds smoothly in refluxing ethanol to afford a orange complex in a decent yield. Though the preliminary characterization data (microanalysis, $^1$H NMR and IR) indicated the presence of the ligand, two oxo, and an ethanol in this complex, they could not point to any definite stereochemistry of the complex, as well as the coordination mode of H₂L in it. For an unambiguous characterization of this complex, its structure has been determined by X-ray crystallography. The structure is shown in **Fig. 2.8** and some relevant bond parameters are listed in **Table 2.4**. The structure shows that the ligand is coordinated to MoO₂$^{+2}$ as a ONO-donor, with bite angles of 81.08(5)° [N(1)–Mo(1)–O(1)] and 71.11(5)° [O(2)–Mo(1)–N(1)]. One ethanol molecule is also coordinated to the metal center. This complex is therefore formulated as [MoO₂L(C₂H₅OH)] (**1**), where L refers to the benzoylhydrazone of 2-hydroxybenzaldehyde ligand coordinated as in **Scheme 2.1**. The observed microanalytical data are also consistent with this composition. In this [MoO₂L(C₂H₅OH)] complex molybdenum is sitting in a NO₅ coordination sphere, which is significantly distorted from ideal octahedral geometry as reflected in the bond parameters around the metal center. The Mo=O distance is quite normal [4,23,28,29] and so are the Mo–O, Mo–N, C=N and N–N bond lengths within the Mo(L) fragment. The Mo–O(C₂H₅OH) bond lengths in complex **1** is longer than the normal single bond lengths [2.362(2) Å against 1.928 (1)–2.020 (1) Å] and that indicates the labile site available for substitutions. This possibility is realized in the facile formation of adducts of the general formula [MoO₂L(Q)] (**2a** and **2b**).

*2.3.5. X-ray structures of complexes [MoO₂L(Imz)] (2a), [MoO₂L(1-MeImz)] (2b) and [(MoO₂L)₂(μ-4,4'-bipy)] (3)*

The formation of mixed-ligand mononuclear [MoO₂L(Q)] complexes have been achieved by the reaction of **1** with different Lewis bases {Q = imidazole (**2a**), 1-methylimidazole (**2b**)} in excellent yield. The dinuclear dioxomolybdenum(VI) complex [(MoO₂L)₂(μ-4,4'-bipy)] (**3**) was achieved by the reaction of **1** and 4,4'-bipyridine as exo-bidentate ligand under reflux condition. The common characteristic of these structures is the absence of a metal-coordinating solvent molecule, and its replacement by a heterocyclic bases through the nitrogen atom. The atom numbering schemes for the complexes **2a** and **2b** are given in **Figs. 2.9** and **2.10** with the

relevant bond distances and angles collected in **Tables 2.5** and **2.6** respectively. The molecular structures of complexes, [MoO$_2$L(Imz)] (**2a**) and [MoO$_2$L(1-MeImz)] (**2b**) have shown that the dinegative hydrazone ligands (H$_2$L) bind to the molybdenum(VI) center by O(1), N(1), O(2)– donor atoms. The fourth coordination site around molybdenum (VI) is occupied by imidazole ligand in complex **2a** and by 1-methylimidazole in **2b** through its tertiary nitrogen N(3), forming distorted octahedral complexes. The rather large Mo(1)–N(3) distance are [2.348(4) Å (**2a**) and 2.353(3) Å (**2b**)] revealed that the imidazole and 1-methylimidazole moiety are also rather weakly coordinated to the MoO$_2$$^{2+}$ core [4,23,28,29]. The Mo–O (oxo) bond distances of the MoO$_2$$^{2+}$ group are unexceptional [23,29] and almost equal [1.695(2)–1.706(3) Å] for both the complexes (**2a** and **2b**). The ligand coordinates to the MoO$_2$$^{2+}$ core in the deprotonated enolate form because in complexes **1, 2a** and **2b** the C–O bond distances [C(8)–O(2)] exhibit values of 1.311(2), 1.335(4) and 1.325(5) Å respectively and are nearer to a C–O single bond than to a C–O double bond distance. However, it falls short of the pure C–O single bond distance of 1.42 Å because of the delocalization of electrons.

The dinuclear complex, **3** (**Fig. 2.11, Table 2.7**) crystallizes in the monoclinic space group *P2$_1$/n* with the molecule sitting across a crystallographic center of inversion. Each half of the dinuclear complex [(MoO$_2$L)$_2$(μ-4,4'-bipy)] closely resembles the structure of the other half of the complex. The coordination environment around the Mo (VI) center is octahedral and highly distorted. The ligand H$_2$L is dianionic and tridentate, with its meridionally situated donor sites O(1), N(1), and O(2) lying in the equatorial plane along with the oxo oxygen O(4). The bond distances about Mo(1) reveal the magnitude of the distortions, as can be seen in **Table 2.7**. The Mo–O distances range from 1.688(4) Å for the oxo ligand O(3), located in an axial position, to 1.990(3) Å for the enolate oxygen O(2). The Mo(1)–O(1) (phenolate) distance is slightly shorter at 1.923(4) Å. The second axial position is occupied by a nitrogen atom of the bridging 4,4'-bipyridine ligand, which is significantly farther from the Mo center than the other five ligated atoms. Mo(1)–N(3), at 2.487(4) Å, is undoubtedly the weakest of the six Mo–L bonds and consequently the most susceptible to ligand exchange [29]. The chelate bite angles for the five- and six-membered rings have values within the expected ranges [O(2)–Mo(1)–N(1), 71.61(1)°; O(1)–Mo(1)–N(1), 81.2(1)°].

**Table 2.4** Selected Bond Distances (Å) and Bond Angles (°) for Complex **1**

| | | Distances | | |
|---|---|---|---|---|
| Mo(1)-O(1) | 1.928(1) | | Mo(1)-O(2) | 2.020(1) |
| Mo(1)-O(3) | 1.698(2) | | Mo(1)-O(4) | 1.702(1) |
| Mo(1)-O(5) | 2.362(2) | | Mo(1)-N(1) | 2.237(1) |
| | | Angles | | |
| O(1)-Mo(1)-O(2) | 149.09(5) | | O(1)-Mo(1)-O(3) | 99.19(7) |
| O(1)-Mo(1)-O(4) | 102.65(6) | | O(1)-Mo(1)-O(5) | 82.08(5) |
| O(1)-Mo(1)-N(1) | 81.08(5) | | O(2)-Mo(1)-O(3) | 96.54(6) |
| O(2)-Mo(1)-O(4) | 98.39(6) | | O(2)-Mo(1)-O(5) | 78.51(5) |
| O(2)-Mo(1)-N(1) | 71.11(5) | | O(3)-Mo(1)-O(4) | 105.81(7) |
| O(3)-Mo(1)-O(5) | 171.06(6) | | O(3)-Mo(1)-N(1) | 95.12(7) |
| O(4)-Mo(1)-O(5) | 82.41(6) | | O(4)-Mo(1)-N(1) | 157.69(6) |
| O(5)-Mo(1)-N(1) | 76.28(5) | | | |

**Table 2.5** Selected Bond Distances (Å) and Bond Angles (°) for Complex **2a**

|  |  |  |  |
|---|---|---|---|
| Distances | | | |
| Mo(1)-O(1) | 1.929(4) | Mo(1)-O(2) | 2.028(3) |
| Mo(1)-O(3) | 1.697(3) | Mo(1)-O(4) | 1.695(2) |
| Mo(1)-N(1) | 2.251(3) | Mo(1)-N(3) | 2.348(4) |
| Angles | | | |
| O(1)-Mo(1)-O(2) | 150.0(1) | O(1)-Mo(1)-O(3) | 100.8(2) |
| O(1)-Mo(1)-O(4) | 104.4(1) | O(1)-Mo(1)-N(1) | 81.4(1) |
| O(1)-Mo(1)-N(3) | 83.7(1) | O(2)-Mo(1)-O(3) | 93.2(1) |
| O(2)-Mo(1)-O(4) | 97.5(1) | O(2)-Mo(1)-N(1) | 71.6(1) |
| O(2)-Mo(1)-N(3) | 78.5(1) | O(3)-Mo(1)-O(4) | 104.3(2) |
| O(3)-Mo(1)-N(1) | 92.4(1) | O(3)-Mo(1)-N(3) | 169.0(1) |
| O(4)-Mo(1)-N(1) | 160.7(1) | O(4)-Mo(1)-N(3) | 84.0(1) |
| N(1)-Mo(1)-N(3) | 78.3(1) | | |

**Table 2.6** Selected Bond Distances (Å) and Bond Angles (°) for Complex **2b**

|  |  |  |  |
|---|---|---|---|
| | | Distances | |
| Mo(1)-O(1) | 1.905(3) | Mo(1)-O(2) | 2.010(3) |
| Mo(1)-O(3) | 1.703(3) | Mo(1)-O(4) | 1.706(3) |
| Mo(1)-N(1) | 2.239(3) | Mo(1)-N(3) | 2.353(3) |
| | | Angles | |
| O(1)-Mo(1)-O(2) | 150.4(1) | O(1)-Mo(1)-O(3) | 100.2(1) |
| O(1)-Mo(1)-O(4) | 103.9(1) | O(1)-Mo(1)-N(1) | 82.1(1) |
| O(1)-Mo(1)-N(3) | 81.5(1) | O(2)-Mo(1)-O(3) | 94.3(1) |
| O(2)-Mo(1)-O(4) | 96.7(1) | O(2)-Mo(1)-N(1) | 71.9(1) |
| O(2)-Mo(1)-N(3) | 79.6(1) | O(3)-Mo(1)-O(4) | 106.0(1) |
| O(3)-Mo(1)-N(1) | 91.0(1) | O(3)-Mo(1)-N(3) | 168.8(1) |
| O(4)-Mo(1)-N(1) | 160.4(1) | O(4)-Mo(1)-N(3) | 84.2(1) |
| N(1)-Mo(1)-N(3) | 78.2(1) | | |

**Table 2.7** Selected Bond Distances (Å) and Bond Angles (˚) for Complex **3**

| | Distances | | |
|---|---|---|---|
| Mo(1)-O(1) | 1.923(4) | Mo(1)-O(2) | 1.990(3) |
| Mo(1)-O(3) | 1.688(4) | Mo(1)-O(4) | 1.703(4) |
| Mo(1)-N(1) | 2.249(4) | Mo(1)-N(3) | 2.487(4) |
| | Angles | | |
| O(1)-Mo(1)-O(2) | 148.5(1) | O(1)-Mo(1)-O(3) | 98.8(2) |
| O(1)-Mo(1)-O(4) | 104.2(2) | O(1)-Mo(1)-N(1) | 81.2(1) |
| O(1)-Mo(1)-N(3) | 80.7(1) | O(2)-Mo(1)-O(3) | 99.0(2) |
| O(2)-Mo(1)-O(4) | 95.5(2) | O(2)-Mo(1)-N(1) | 71.61(1) |
| O(2)-Mo(1)-N(3) | 77.8(1) | O(3)-Mo(1)-O(4) | 106.2(2) |
| O(3)-Mo(1)-N(1) | 94.6(2) | O(3)-Mo(1)-N(3) | 171.3(2) |
| O(4)-Mo(1)-N(1) | 157.2(2) | O(4)-Mo(1)-N(3) | 82.2(2) |
| N(1)-Mo(1)-N(3) | 76.8(1) | | |
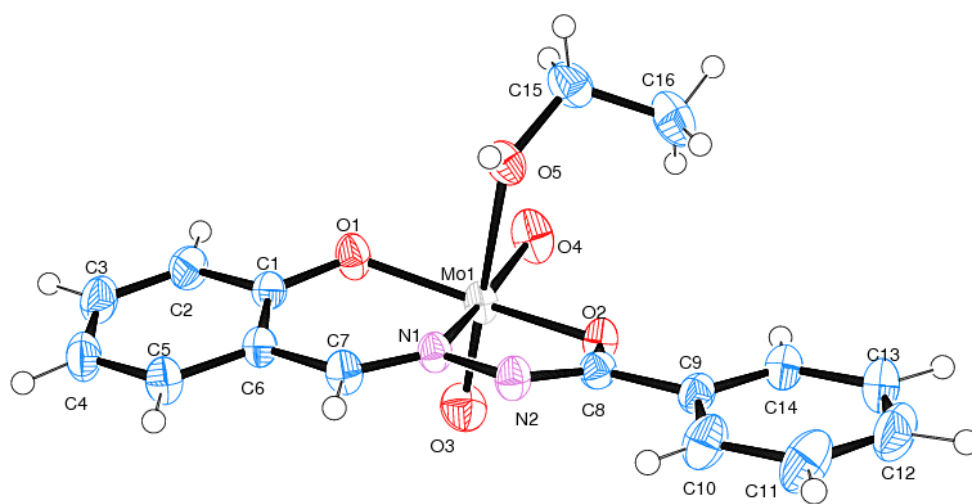
**Fig. 2.8.** ORTEP diagram of [MoO$_2$L(C$_2$H$_5$OH)] (**1**) with atom labeling scheme at 50% probability
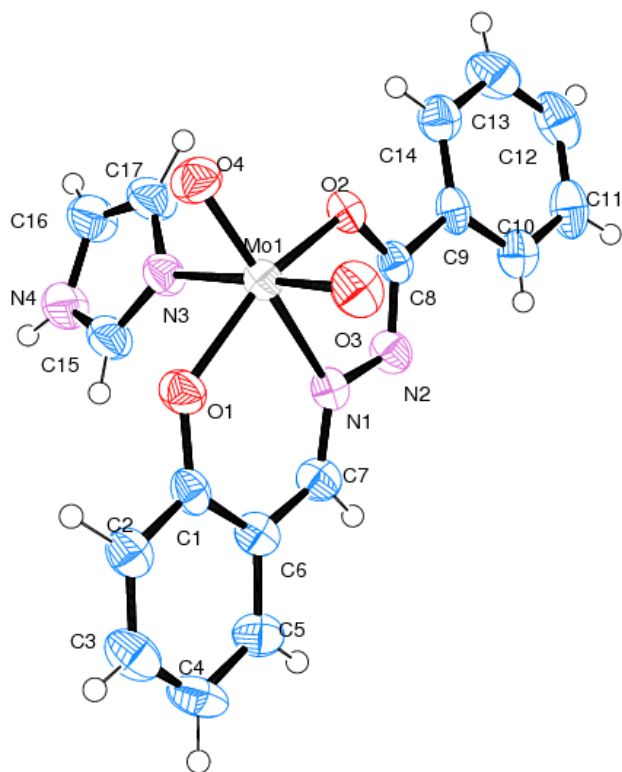
**Fig. 2.9.** ORTEP diagram of [MoO$_2$L(Imz)] (**2a**) with atom labeling scheme at 50% probability
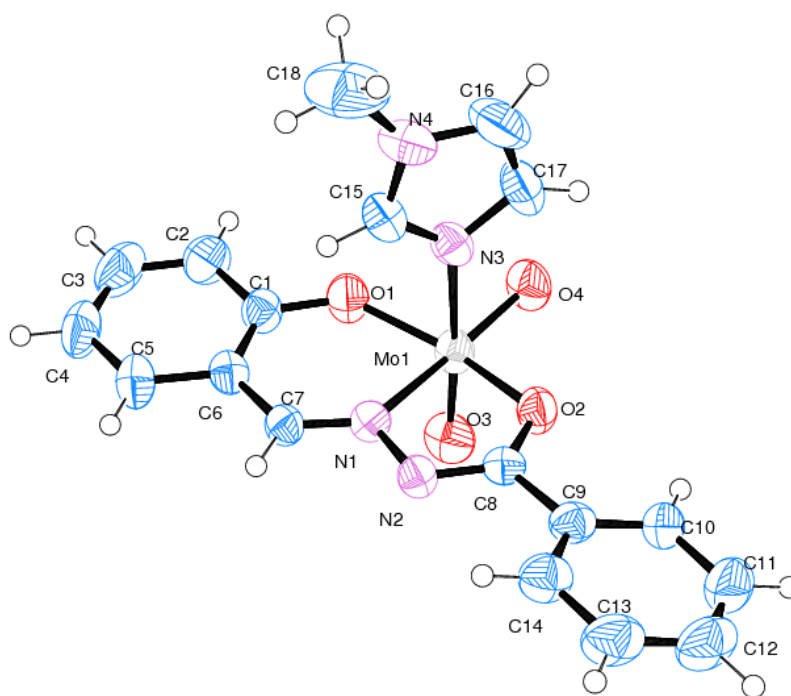
**Fig. 2.10.** ORTEP diagram of [MoO$_2$L(1-MeImz)] (**2b**) with atom labeling scheme at 50% probability
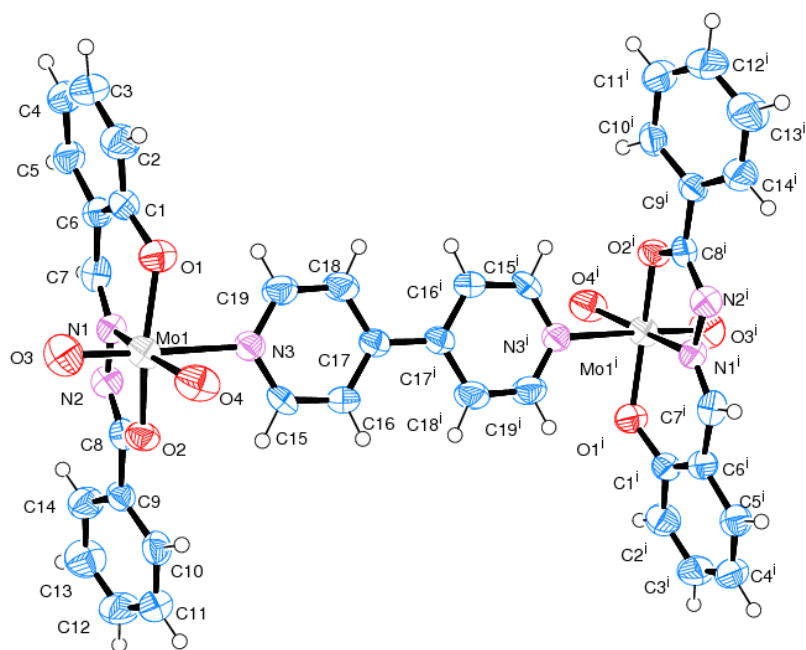
**Fig. 2.11.** ORTEP diagram of [(MoO$_2$L)$_2$ (μ-4,4'-bipy)] (**3**) with atom labeling scheme at 50% probability

*2.3.6. Antibacterial activity*

*In vitro* antimicrobial activity of the synthesized oxomolybdenum(VI) complexes (**1–3)** have been tested against the pathogenic strains of *Escherichia coli, Bacillus subtilis* and *Pseudomonas aeruginosa* by agar well-diffusion method and in some cases they showed promising results by giving the MIC value lesser than the standard drug examined. The results (**Table 2.8**) also indicate that the corresponding oxomolybdenum(VI) complexes showed much better antibacterial activity with respect to the individual ligand against the same microorganism under identical experimental conditions which is in agreement with the previous results [16,41,45,47–49]. A possible explanation is that, by coordination, the polarity of the ligand and the central metal ion are reduced through the charge equilibration, which favors permeation of the complexes through the lipid layer of the bacterial cell membrane [16,41,45,47–49].

From the zone of inhibition, it is observed that the complex **2a** and **2b** showed most promising results as compared to the other compounds (**1** and **3**) of this study and the difference in value may be attributed to the nature of compounds synthesized with imidazole as co-ligands [50,51]. Imidazole is a five membered planar ring, which is soluble in water and other polar solvent and also highly polar due to its dipole moment. Therefore, the liophilicity of the compounds (**2a** and **2b**) is increased due to these above factors and it may be the possible reasons for increasing the zone of inhibition. The result for the octahedral complex (**1**) is least promising especially for *E.coli* as compared to **2a** and **2b**, probably due to the presence of ethanol molecule in the coordination sphere. Against some of the tested bacterial species the inhibitory action for **3** has no significant effect may be because of its dimeric structure. Antibacterial activity of the similar type oxo-metal complexes has also been reported by Sharma *et al.* [52] , Chohan *et al.* [53] and Prasad *et al.* [54] using agar well diffusion technique against *Escherichia coli*, *Shigella flexenari*, *Pseudomonas aeruginosa*, *Salmonella typhi*, *Staphylococcus aureus* and *Bacillus subtilis* and the present results are in accordance with the reported values.

**Table 2.8** Minimum Inhibitory Concentration (MIC) value in µg/mL of the Schiff base ligand (H$_2$L), oxomolybdenum(VI) complexes (**1–3**) and standard drugs against pathogenic strains

| | *E.coli* | *Bacillus subtilis* | *Pseudomonas aeruginosa* |
|---|---|---|---|
| H$_2$L | 125 | 500 | -- |
| [MoO$_2$L(C$_2$H$_5$OH)] (**1**) | 125 | 62.5 | -- |
| [MoO$_2$L(Imz)] (**2a**) | 15.6 | 15.6 | 1000 |
| [MoO$_2$L(1-MeImz)](**2b**) | 15.6 | 125 | 1000 |
| [(MoO$_2$L)$_2$ (µ-4,4'-bipy)] (**3**) | 125 | -- | 500 |
| Vancomycin | 30 | 30 | -- |

## 2.4. Conclusions

In summary, this chapter presents the synthesis and structures of a mononuclear Schiff base complex (**1**), some mixed-ligand mononuclear (**2a** and **2b**) and diimine bridged dinuclear (**3**) oxomolybdenum(VI) complexes, and sheds some light on their antibacterial activity. The coordinated ethanol of oxomolybdenum(VI) complex $[MoO_2L(C_2H_5OH)]$ (**1**) with aroylhydrazone is found to act as a substrate-binding site, and mixed-ligand six-coordinate adducts, like $[MoO_2L(Imz)]$ (**2a**), $[MoO_2L(1\text{-MeImz})]$ (**2b**) and $[(MoO_2L)_2(\mu\text{-}4,4'\text{-bipy})]$ (**3**) are easily formed by the attachment of imidazole, 1-methylimidazole and 4,4'-bipyridine to this position as co-ligand respectively. The complexes have been screened for their antibacterial activity against *Escherichia coli, Bacillus subtilis* and *Pseudomonas aeruginosa*. The minimum inhibitory concentration of these complexes and antibacterial activity indicates the compound (**2a**) and (**2b**) as the potential lead molecule for drug designing.

**References**

[1] A.J. Burke, Coord. Chem. Rev. 252 (2008) 170.

[2] K.R. Jain, W.A. Herrmann, F.E. Kuhn, Coord. Chem. Rev. 252 (2008) 556.

[3] K. C. Gupta, A.K. Sutar, Coord. Chem. Rev. 252 (2008) 1420.

[4] J.H. Enemark, J.J.A. Cooney, J.J. Wang, R.H. Holm, Chem. Rev. 104 (2004) 1175.

[5] B. Frédéric, Coord. Chem. Rev. 236 (2003) 71.

[6] E.I. Stiefel, Met. Ions Biol. Syst. 39 (2002) 727.

[7] R. Hille, Chem. Rev. 96 (1996) 2757.

[8] D. Collison, C.D. Garner, J.A. Joule, Chem. Soc. Rev. 25 (1996) 25.

[9] A. Syamal, M.R. Maurya, Coord. Chem. Rev. 95 (1989) 183.

[10] R.D. Chakravarthy, K. Suresh, V. Ramkumar, D.K. Chand, Inorg. Chim. Acta 376 (2011) 57.

[11] Z. Hu, X. Fu, Y. Li, Inorg. Chem. Comm. 14 (2011) 497.

[12] N.R. Pramanik, S. Ghosh, T.K. Raychaudhuri, R.J. Butcher, S.S.Mandal, J. Coord. Chem. 64 (2011) 1207.

[13] A. Rezaeifard, I. Sheikhshoaie, N. Monadi, M. Alipour, Polyhedron 29 (2010) 2703.

[14] I. Sheikhshoaie, A. Rezaeifard, N. Monadi, S. Kaafi, Polyhedron 28 (2009) 733.

[15] V. Vrdoljak, I. Đilovic′, M. Cindric′, D.M. Čalogović, N. Strukan, A.G. Ivšic′, P. Novak, Polyhedron 28 (2009) 959.

 [16] A. Tarushi, E.K. Efthimiadou, P. Christofis, G. Psomas. Inorg. Chim. Acta 360 (2007) 3978.

[17] F.E. Inscore, S.Z. Knottenbelt, N.D. Rubie, H.K. Joshi, M.L. Kirk, J.H. Enemark, Inorg. Chem. 45 (2006) 967.

[18] J.T. Hoffman, S. Einwaechter, B.S. Chohan, P. Basu, C.J. Carrano, Inorg. Chem., 43 (2004) 7573.

[19] A. Sigel, H. Sigel (Eds.), Metal Ions in Biological Systems 39, Molybdenum and Tungsten: Their Roles in Biological Processes, Marcel Dekker, New York, (2002).

[20] R.C. Bray, B. Adams, A.T. Smith, B. Bennett, S. Bailey, Biochemistry 39 (2000) 11258.

[21] G. Lyashenko, G. Saischek, M. E. Judmaier, M. Volpe, J. Baumgartner, F. Belaj, V. Jancik, R. Herbst-Irmer, N.C. Moesch-Zanetti, Dalton Trans. 29 (2009) 5655.

[22] N.C. Mosch-Zanetti, D.Wurm, M. Volpe, G. Lyashenko, B.Harum, F. Belaj, J. Baumgartner, Inorg. Chem. 49 (2010) 8914.

[23] R. Dinda, P. Sengupta, S. Ghosh, W.S. Sheldrick, Eur. J. Inorg. Chem. (2003) 363.

[24] T. Glowiak, L. Jerzykiewicz, J.M. Sobczak, J.J. Ziolkowski, Inorg. Chim. Acta 356 (2003) 387.

[25] C.P. Rao, A. Sreedhara, P.V. Rao, M.B. Verghese, K. Rissanen, E. Kolehmainen, N.K. Loknath, M.A. Sridhar, J.S. Prasad, J. Chem. Soc., Dalton Trans. (1998) 2383.

[26] O.A. Rajan, A. Chakravarthy, Inorg. Chem. 20 (1981) 660.

[27] E.B. Seena, M.R. Prathapachandra Kurup, Polyhedron 26 (2007) 3595.

[28] S. Purohit, A.P. Koley, L.S. Prasad, P.T. Manoharan, S. Ghosh, Inorg. Chem. 28 (1989) 3735.

[29] R. Dinda, S. Ghosh, L.R. Falvello, M. Tomás, T.C.W. Mak, Polyhedron 25 (2006) 2375.

[30] L.H.A. Terra, M.C. Areias, I. Gaubeur, M.E.V. Suez-Iha, Spectrosc. Lett. 32 (1999) 257.

[31] M.R. Maurya, S. Agarwal, M. Abid, A. Azam, C. Bader, M. Ebel, D. Rehder, Dalton Trans. (2006) 937.

[32] A.C. Cunha, J.M. Figueiredo, J.L.M. Tributino, A.L.P. Miranda, H.C. Castro, R.B. Zingali, C.A.M. Fraga, M.C.B.V. Souza, V.F. Ferreira, E.J. Barreiro, Bioorg. Med. Chem. 11 (2003) 2051.

[33] S.P. Dash, S. Pasayat, Saswati, H.R. Dash, S. Das, R.J. Butcher, R. Dinda, Polyhedron 31 (2012) 524.

[34] M.V. Angelusiu, S.F. Barbuceanu, C.Draghici, G.L. Almajan, Eur. J. Med. Chem. 45 (2010) 2055.

[35] I. Babahan, E.P. Çoban, A.Özmen, H. Biyik, B. Işman, Afri. J. Microbiol. 5 (2011) 271.

[36] L. Mitu, N. Raman, A. Kriza, N. Stănică , M. Dianu, J. Serb. Chem. Soc. 74 (2009)1075.

[37] D.K. Johnson, T.B. Murphy, N.J. Rose, W.H. Goodwin, L. Pickart, Inorg. Chim. Acta 67 (1982) 159.

[38] S. El-Tabl Abdou , A.A. Farag , M.E.S. Mohamad , M.E.S. Adel, J. Coord. Chem. 63 (2010) 700.

[39] R. Garg, M.K. Saini, N. Fahmi, R.V. Singh, Transition Met. Chem. 31 (2006) 362.

[40] M.L.H. Nair, D. Thankamani, J. Ind. Chem. Soc. 87 (2010) 1029.

[41] A.R. Yaul, V.V. Dhande, S.G. Bhadange, A.S. Aswar, Russ. J. Inorg. Chem. 56 (2011) 549.

[42] R. Dinda, P.K. Majhi, P. Sengupta, S. Pasayat, S. Ghosh, L.R. Falvello, T.C.W. Mak, Polyhedron 29 (2010) 248.

[43] G.M. Sheldrick, SHELXS-97, Program for Crystal Structure Determination, Universitäet Göttingen, Göttingen, Germany, (1997).

[44] G.M. Sheldrick, SHELXL-97, Program for Refinement of Crystal Structures, Universitäet Göttingen, Göttingen, Germany, (1997).

[45] A.A. Abdel Aziz, J. Mol. Struct. 979 (2010) 77.

[46] G.R. Fulmer, A.J.M. Miller, N.H. Sherden, H.E. Gottlieb, A. Nudelman, B.M. Stoltz, J.E. Bercaw, K.I. Goldberg, Organometallics 29 (2010) 2176.

[47] E.K. Efthimiadou, Y. Sanakis, N. Katsaros, A. Karaliota, G. Psomas, Polyhedron 26 (2007) 1148.

[48] A.M. Ramadan, J. Inorg. Biochem. 65 (1997) 183.

[49] P.G. Avaji, C.H.V. Kumar, S.A. Patil, K.N. Shivananda, C. Nagaraju, Eur. J. Med. Chem. 44 (2009) 3552.

[50] E.B. Anderson, T.E. Long, Polymer 51 (2010) 2447.

[51] R. Dahiya, H. Gautam, Afri. J. Pharm. Pharmacol. 5 (2011) 447.

[52] N. Sharma, M. Kumari, V. Kumar, J. Coord. Chem. 63 (2010) 1940.

[53] Z.H. Chohan, S.H. Sumrra, M.H. Youssoufi, Eur. J. Med. Chem. 45 (2010) 2739.

[54] K.S. Prasad, L.S. Kumar1, S.C. Shekar, M. Prasad, H.D. Revanasiddappa, Chem. Sci. J.(2011) CSJ-12.

# Chapter 3

**Synthesis, Structural Studies, Biological and Catalytic Activity of Dioxomolybdenum(VI) Complexes with Aroylhydrazones of Naphthol-Derivative**

# Chapter 3

**Synthesis, Structural Studies, Biological and Catalytic Activity of Dioxomolybdenum(VI) Complexes with Aroylhydrazones of Naphthol-Derivative**

## Abstract

Reaction of the salicyloylhydrazone of 2-hydroxy-1-naphthaldehyde ($H_2L^1$), anthranylhydrazone of 2-hydroxy-1-naphthaldehyde ($H_2L^2$), benzoylhydrazone of 2-hydroxy-1-acetonaphthone ($H_2L^3$) and anthranylhydrazone of 2-hydroxy-1-acetonaphthone ($H_2L^4$; general abbreviation $H_2L$) with [$MoO_2(acac)_2$] afforded a series of 5- and 6- coordinate Mo(VI) complexes of the type [$MoO_2L(ROH)$] [where R = $C_2H_5$ (**1**) and $CH_3$ (**2**)], and [$MoO_2L$] (**3** and **4**). The substrate binding capacity of **1** has been demonstrated by the formation of one mononuclear mixed-ligand dioxomolybdenum complex [$MoO_2L^1(Q)$] {where Q = γ-picoline (**1a**)}. Molecular structure of all the complexes (**1**, **1a**, **2**, **3** and **4**) is determined by X-ray crystallography, demonstrating the dibasic tridentate behaviour of ligands. All the complexes show two irreversible reductive responses within the potential window –0.73 to –1.08 V, due to $Mo^{VI}/Mo^V$ and $Mo^V/Mo^{IV}$ processes. The complexes have been screened for their antibacterial activity against *Escherichia coli, Bacillus subtilis, Proteus vulgaris* and *Klebsiella pneumoniae*. Minimum inhibitory concentration of these complexes and antibacterial activity indicates **1** and **1a** as the potential lead molecule for drug designing. Catalytic potential of these complexes was tested for the oxidation of benzoin using 30% aqueous $H_2O_2$ as an oxidant in methanol. At least four reaction products benzoic acid, benzaldehyde-dimethylacetal, methylbenzoate and benzil were obtained with the 95-99% conversion under optimized reaction conditions. Oxidative bromination of salicylaldehyde, a functional mimic of haloperoxidases, in aqueous $H_2O_2$/KBr in the presence of $HClO_4$ at room temperature has also been carried out successfully.

## 3.1. Introduction

Schiff bases, characterized by the azomethine group (–RC=N–), form a significant class of compounds in medicinal and pharmaceutical chemistry and are known to have biological applications due to their antibacterial [1–6], antifungal [3–6] and antitumor [7,8] activity. The incorporation of transition metals into these compounds leads to the enhancement of their biological activities and decrease in the cytotoxicity of both the metal ion and Schiff base ligand [9–11]. On the other hand, aroylhydrazones are excellent multidentate ligands for transition metals. They have been shown to exhibit a range of biological e.g. antiamoebic activity [12] and DNA synthesis inhibition or antiproliferative behavior [13–15]. For quite some time, our group has been engaged in a program aimed at credible synthesis of oxygen and nitrogen co-ordinated transition metal compounds in order to approach the biological co-ordination units as potential lead molecules for drug designing. Accordingly, our group has synthesized and examined a number of transition metal-Schiff base compounds using aroylhydrazone as tridentate ONO– donor ligand [16–18]. Their properties can be tuned by modification of either the aromatic aldehyde or the hydrazide component. Our aim was to increase lipophilicity using bulky aromatic groups and to investigate the influence on the coordination sphere as well as reactivity by the use of aroylhydrazone of naphthol-derivatives.

The coordination chemistry of molybdenum has become a fascinating area of research in recent years because of the presence of molybdenum in metalloenzymes [19–25]. Catalytic applications of molybdenum complexes in organic transformations, particularly in the epoxidation of alkenes have been explored much as evidenced by number of publications [26–39]. The catalytic activity of molybdenum complexes are sensitive to the donor/acceptor ability of the ligand, and to steric and strain factors. Therefore, we have designed sterically hindered/ bulky ONO donor aroylhydrazones of naphthol-derivative (**Scheme 3.1**) in the light of above factors to prepare dioxomolybdenum(VI) complexes. Varying the steric bulk of the aroylhydrazone ligands also controls the coordination number of the molybdenum in these complexes. Novel structural features, reactivity patterns of these complexes and their catalytic activity for the oxidation of benzoin are reported here. Selective transformation of $\alpha$-hydroxyketone to the corresponding $\alpha$-diketone is one of the most important fundamental reactions in organic chemistry [40–41]. The catalytic potential of dioxomolybdenum(VI) complexes for the oxidative bromination of salicylaldehyde, as functional mimic of haloperoxidase has also been explored.

### 3.2. Experimental

#### 3.2.1. Materials

[$MoO_2(acac)_2$] was prepared as described in the literature [42]. Reagent grade solvents were dried and distilled prior to use. All other chemicals were reagent grade, available commercially and used as received. Commercially available TBAP (tetra butyl ammonium perchlorate) was dried and used as a supporting electrolyte for recording cyclic voltammograms of the complexes.

#### 3.2.2. Physical Measurements

Elemental analyses were performed on a Vario ELcube CHNS Elemental analyzer. IR spectra were recorded on a Perkin-Elmer Spectrum RXI spectrometer. ^{1}H NMR spectra were recorded with a Bruker Ultra shield 400 MHz spectrometer using $SiMe_4$ as an internal standard. Electronic spectra were recorded on a Lamda25, PerkinElmer spectrophotometer. Electrochemical data were collected using a PAR electrochemical analyzer and a PC-controlled Potentiostat/Galvanostat (PAR 273A) at 298 K in a dry nitrogen atmosphere. Cyclic voltammetry experiments were carried out with a platinum working electrode, platinum auxiliary electrode, Ag/AgCl as reference electrode and TBAP as supporting electrolyte. A Shimadzu 2010 plus gas-chromatograph fitted with an Rtx-1 capillary column (30 m × 0.25 mm × 0.25 μm) and a FID detector was used to analyze the reaction products and their quantifications were made on the basis of the relative peak area of the respective product. The identity of the products was confirmed using a GC-MS model Perkin-Elmer, Clarus 500 and comparing the fragments of each product with the library available. The percent conversion of substrate and selectivity of products was calculated from GC data using the formulae:

$$\% \text{ Conversion of substrate } = 100 - \frac{\text{Peak area of a substrate}}{\text{Total area of substrate + products}} \text{ X } 100$$

$$\% \text{ Selectivity of a product} = \frac{\text{Peak area of a product}}{\text{Total area of products}} \text{ X } 100$$

#### 3.2.2.1. Product Quantification

For oxidation of benzoin, the percentage of substrate and oxidation products are usually quantified by GC itself from the relative peak area of the respective product. For bromination of salicylaldehyde, white products form in solution where HBr, $Br_2$ etc. are present hence it requires extraction with $CH_2Cl_2$ and the crude mass is dissolved in methanol and then subjected to GC.

Some researchers are usually used internal standard, but this is a very tedious method. Therefore, the substrate and products both were analysed by GC using the formulae discussed as above.

### 3.2.3. Synthesis of Ligands ($H_2L^{1-4}$)

Schiff base ligands, $H_2L^{1-4}$ were prepared by the condensation of carbonyl compounds and the respective acidhydrazide in equimolar ratio in ethanol medium by a standard procedure [43]. The resulting yellowish- white compounds were filtered, washed with ethanol and dried over fused $CaCl_2$.

*$H_2L^1$:* Yield: 0.22 g (72%). Anal. Calcd for $C_{18}H_{14}N_2O_3$: C, 70.58; H, 4.61; N, 9.15. Found: C, 70.59; H, 4.59; N, 9.12%. $^1H$ NMR (DMSO-$d_6$, 400 MHz): $\delta$ = 12.74 (s, 1H, naphthyl–OH), 12.07 (s, 1H, NH), 11.87 (s, 1H, aryl-OH), 9.54 (s, 1H, HC=N), 8.33–6.62 (m, 10H, Aromatic) ppm. $^{13}C$ NMR (DMSO-$d_6$, 100 MHz): $\delta$ = 163.72, 158.51, 157.89, 147.44, 133.78, 132.68, 131.44, 128.69, 128.55, 127.57, 127.50, 123.33, 120.73, 118.92, 118.65, 117.05, 115.48, 108.36.

*$H_2L^2$:* Yield: 0.19 g (62%). Anal. Calcd for $C_{18}H_{15}N_3O_2$: C, 70.81; H, 4.95; N, 13.76. Found: C, 70.78; H, 4.92; N, 13.77%. $^1H$ NMR (DMSO-$d_6$, 400 MHz): $\delta$ = 12.97 (s, 1H, naphthyl–OH), 12.04 (s, 1H, NH), 9.47 (s, 1H, HC=N), 8.18–6.64 (m, 10H, Aromatic), 6.61 (s, 2H, NH$_2$) ppm. $^{13}C$ NMR (DMSO-$d_6$, 100 MHz): $\delta$ =165.12, 158.33, 150.93, 146.33, 133.18, 132.91, 132.07, 129.45, 128.57, 128.25, 128.16, 123.96, 120.88, 119.42, 117.12, 115.14, 112.62, 109.06.

*$H_2L^3$:* Yield: 0.18 g (63%). Anal. Calcd for $C_{19}H_{16}N_2O_2$: C, 74.98; H, 5.30; N, 9.20. Found: C, 74.97; H, 5.32; N, 9.18%. $^1H$ NMR (DMSO-$d_6$, 400 MHz): $\delta$ = 10.31 (s, 1H, naphthyl–OH), 9.55 (s, 1H, NH), 7.91–7.27 (m, 11H, Aromatic), 2.34 (s, 3H, CH$_3$) ppm. $^{13}C$ NMR (DMSO-$d_6$, 100 MHz): $\delta$ = 153.71, 152.63, 134.24, 131.82, 131.51, 130.21, 129.06, 128.76, 128.36, 128.23, 127.86, 127.43, 126.99, 123.67, 123.19, 118.99, 118.71, 113.74, 24.30.

*$H_2L^4$:* Yield: 0.21 g (65%). Anal. Calcd for $C_{19}H_{17}N_3O_2$: C, 71.47; H, 5.36 ; N, 13.16. Found: C, 71.45; H, 5.33; N, 13.15%. $^1H$ NMR (DMSO-$d_6$, 400 MHz): $\delta$ = 10.35 (s, 1H, naphthyl–OH), 9.17 (s, 1H, NH), 7.91–6.23 (m, 10H, Aromatic), 6.05 (s, 2H, NH$_2$), 2.35 (s, 3H, CH$_3$) ppm. $^{13}C$ NMR (DMSO-$d_6$, 100 MHz): $\delta$ =153.98, 152.47, 152.36, 149.84, 132.47, 131.56, 130.22, 129.09, 128.34, 127.98, 127.67, 123.78, 123.14, 118.94, 117.04, 115.46, 114.69, 113.59, 24.15.

*3.2.4. Synthesis of complexes (**1**–**4**)*

These complexes were prepared modifying a previously published procedure [44–46]. To a refluxing solution of ligand, $H_2L^{1-4}$ (1.0 mmol) in 30 mL of alcohol {ethanol (**1** and **2**) and methanol (**3** and **4**)}, 1.0 mmol of $MoO_2(acac)_2$ was added. The color of the solution changed to dark red. The mixture was then refluxed for 3 hr. After leaving the solution for 2 days at room temperature, fine red colored crystals were isolated. Crystals of most complexes were suitable for single crystal X-ray analysis.

*[MoO$_2$L$^1$(C$_2$H$_5$OH)](**1**):* Yield: 0.29 g (60%). Anal. Calcd for $C_{20}H_{18}N_2O_6Mo$: C, 50.20; H, 3.76; N, 5.85. Found: C, 50.18; H, 3.77; N, 5.84%. $^1H$ NMR (DMSO-d$_6$, 400 MHz): $\delta$ = 11.41 (s, 1H, aryl–OH), 10.07 (s, 1H, HC=N), 8.61–6.99 (m, 10H, Aromatic), 4.36 (s, 1H, OH–ethanol), 3.42 (q, 2H, CH$_2$–ethanol), 1.05 (s, 3H, CH$_3$–ethanol) ppm. $^{13}C$ NMR (DMSO-d$_6$, 100 MHz): $\delta$ = 168.19, 160.20, 158.59, 152.76, 136.14, 134.01, 132.51, 129.03, 128.99, 128.89, 128.49, 124.91, 121.87, 120.25, 119.38, 117.10, 113.21, 111.65, 56.00, 18.54.

*[MoO$_2$L$^2$(CH$_3$OH)] (**2**):* Yield: 0.23 g (53%). Anal. Calcd for $C_{19}H_{17}N_3O_5Mo$: C, 49.26; H, 3.70; N, 9.07. Found: C, 49.25; H, 3.68; N, 9.08%. $^1H$ NMR (DMSO-d$_6$, 400 MHz): $\delta$ = 9.92 (s, 1H, HC=N), 8.57–6.65 (m, 10H, Aromatic), 7.12 (s, 2H, NH$_2$), 4.10 (s, 1H, OH-methanol), 3.15 (s, 3H, CH$_3$- methanol) ppm. $^{13}C$ NMR (DMSO-d$_6$, 100 MHz): $\delta$ = 169.06, 160.58, 151.88, 150.05, 135.93, 133.01, 132.91, 130.33, 129.44, 129.25, 128.77, 125.15, 122.16, 120.86, 116.51, 115.18, 112.26, 109.63, 49.07.

*[MoO$_2$L$^3$](**3**):* Yield: 0.26 g (54%). Anal. Calcd for $C_{19}H_{14}N_2O_4Mo$: C, 53.04; H, 3.28; N, 6.51. Found: C, 53.06; H, 3.26; N, 6.50%. $^1H$ NMR (DMSO-d$_6$, 400 MHz): $\delta$ = 8.11–7.18 (m, 11H, Aromatic), 2.93 (s, 3H, CH$_3$), ppm. $^{13}C$ NMR (DMSO-d$_6$,100 MHz): $\delta$ = 169.36, 165.06, 163.01, 152.34, 134.25, 132.43, 131.88, 130.98, 130.13, 129.41, 129.24, 128.52, 127.84, 126.07, 125.02, 120.38, 119.84, 116.46, 24.23.

*[MoO$_2$L$^4$](**4**):* Yield: 0.21 g (52%). Anal. Calcd for $C_{19}H_{15}N_3O_4Mo$: C, 51.23; H, 3.37; N, 9.43. Found: C, 51.24; H, 3.35; N, 9.44%. $^1H$ NMR (DMSO-d$_6$, 400 MHz): $\delta$ = 8.01–6.87 (m, 10H, Aromatic), 7.04 (s, 2H, NH$_2$), 2.86 (s, 3H, CH$_3$) ppm. $^{13}C$ NMR (DMSO-d$_6$,100 MHz): $\delta$ =

170.36, 162.91, 162.82, 150.17, 134.03, 133.14, 131.87, 130.36, 130.07, 129.37, 127.77, 126.08, 124.96, 120.38, 119.82, 116.53, 115.47,110.15, 24.40.

### 3.2.5. Synthesis of mixed-ligand complex [{MoO₂L¹(Q)}, where Q = γ-picoline (1a)]

To a clear red solution of (**1**) (0.50 mmol) in $CH_3CN$ (30 mL), γ-picoline (0.73 mmol) was added and the mixture was refluxed for 3 hr. Slow evaporation of the red filtrate over 2 days produced dark red crystals. These were separated by filtration. Yield 0.25 g (57%). Anal. Calcd for $C_{24}H_{19}N_3O_5Mo$: C, 54.85; H, 3.61; N, 8.00. Found: C, 54.86; H, 3.59; N, 8.01%. ¹H NMR (DMSO-d₆, 400 MHz): $\delta$ = 11.42 (s, 1H, aryl–OH), 10.08 (s, 1H, HC=N), 8.62–6.99 (m, 10H, Aromatic), 7.24–6.97 (m, 4H, Aromatic–γ–picoline), 2.31 (s, 3H, CH₃–γ–picoline) ppm. ¹³C NMR (DMSO-d₆, 100 MHz): $\delta$ = 168.69, 160.70, 159.09, 153.26, 149.76, 147.22, 136.62, 134.49, 133.00, 129.52, 129.47, 129.38, 128.97, 125.38, 125.11, 122.35, 120.73, 119.85, 117.58, 114.35, 113.71, 112.15, 110.15, 19.02.

### 3.2.6. Crystallography

Suitable single crystal of **1**, **1a** and **2-4** was chosen for X-ray diffraction studies. Crystallographic data and details of refinement are given in **Table 3.1**. The unit cell parameters and the intensity data for the complexes (**1**, **2**, **3** and **4**) were collected at ~ 293 K, on a Bruker Smart Apex CCD diffractometer and complex (**1a**) was collected at 100 K, on a Bruker Smart Apex II CCD diffractometer using graphite monochromated Mo Kα radiation ($\lambda$ = 0.71073 Å), employing the ω–2θ scan techniques. The intensity data were corrected for Lorentz, polarization and absorption effects. The structures were solved using the SHELXS97 [47] and refined using the SHELXL97 [48] computer programs. The non-hydrogen atoms were refined anisotropically.

### 3.2.7. Antibacterial activity

Antibacterial activity of the compounds (ligands and complexes) was studied against *Escherichia coli (E. coli), Bacillus subtilis, Proteus vulgaris* and *Klebsiella pneumoniae* by agar well diffusion technique. Mueller Hinton-agar (containing 1% peptone, 0.6% yeast extract, 0.5% beef extract and 0.5% NaCl, at pH 6.9–7.1) plates were prepared and 0.5–McFarland culture (1.5 × $10^8$ cells/mL) of the test organisms were swabbed onto the agar plate (as per CLSI guidelines,

2006) [49]. Test compounds were dissolved in DMSO at several concentrations ranging from 1000 μg/mL–1.95 μg/mL. 9 mm wide wells were dug on the agar plate using a sterile cork borer. A solution of 100 μg/mL of each test compound from each dilution was added into each of the well using a micropipette. These plates were incubated for 24 h at 35 ± 2 °C. The growth of the test organisms was inhibited by diffusion of the test compounds and then the inhibition zones developed on the plates were measured [16,50–51]. The effectiveness of an antibacterial agent in sensitivity is based on the diameter of the zones of inhibition which is measured to the nearest millimeter (mm). The standard drug Vancomycin and Amoxycillin were also tested for their antibacterial activity at the same concentration under the conditions similar to that of the test compounds as +ve control. DMSO alone was used as a –ve control under the same conditions for each organism.

### 3.2.8. Catalytic Reactions

### 3.2.8.1. Oxidation of benzoin

In a typical oxidation reaction, benzoin (1.06 g, 5 mmol), aqueous 30% $H_2O_2$ (1.71 g, 15 mmol) and catalyst (0.0005 g) were mixed in methanol (10 mL). The reaction mixture was heated under reflux with stirring for 4 hr. The progress of the reaction was monitored by withdrawing samples at different time intervals and samples were extracted with n-hexane and then analysed quantitatively by gas chromatography. The effect of various parameters such as amount of catalyst, amount of oxidant, and solvent were checked to optimize the conditions for the best performance of the catalyst. The identity of the products was confirmed by GC-mass.

### 3.2.8.2. Oxidative bromination of salicylaldehyde

Salicylaldehyde (0.610 g, 5 mmol) was added to an aqueous solution (20 mL) of KBr (1.785 g, 15 mmol), followed by addition of aqueous 30% $H_2O_2$ (1.71 g, 15 mmol) in a 100 mL reaction flask. The catalyst (0.0005 g) and 70% $HClO_4$ (0.715 g, 5 mmol) were added, and the reaction mixture was stirred at room temperature (20 $^0$C). Three additional 5 mmol portions of 70% $HClO_4$ were further added to the reaction mixture in three equal portions at 45 minutes intervals under continuous stirring. After 3 hr, the separated white products were extracted with $CH_2Cl_2$ and dried. The crude mass was dissolved in methanol and was subjected to gas chromatography. The identity of the products was confirmed as mentioned above.

**Table 3.1** Crystal and Refinement Data of Complexes **1**, **1a**, **2**, **3** and **4**

| Compound | 1 | 1a | 2 | 3 | 4 |
|---|---|---|---|---|---|
| Formula | $C_{20}H_{18}N_2O_6Mo$ | $C_{24}H_{19}N_3O_5Mo$ | $C_{19}H_{17}N_3O_5Mo$ | $C_{19}H_{14}N_2O_4Mo$ | $C_{19}H_{15}N_3O_4Mo$ |
| M | 478.30 | 525.36 | 463.30 | 430.26 | 445.28 |
| Crystal symmetry | Triclinic | Monoclinic | Triclinic | Monoclinic | Monoclinic |
| Space group | $P$-1 | $P\,2_1/c$ | $P$-1 | $P2_1/c$ | $P2_1/n$ |
| $a(\check{A})$ | 7.8196(2) | 13.313(2) | 8.1198(5) | 4.0623(12) | 7.8923(3) |
| $b(\check{A})$ | 11.1222(3) | 8.0476(14) | 9.9276(6) | 25.842(8) | 13.8894(5) |
| $c(\check{A})$ | 11.4265(3) | 21.357(3) | 12.3349(8) | 15.761(5) | 15.3314(6) |
| $\alpha$ (°) | 80.0650(10) | 90 | 101.8430(10) | 90 | 90 |
| $\beta$ (°) | 85.1030(10) | 68.156(11) | 103.7180(10) | 98.332(16) | 100.355(2) |
| $\gamma$ (°) | 82.1190(10) | 90 | 91.6650(10) | 90 | 90 |
| $V(\check{A}^3)$ | 967.69(4) | 2123.9(6) | 942.23(10) | 1637.1(9) | 1653.24(11) |
| Z | 2 | 4 | 2 | 4 | 4 |
| $D_{calc}(g.cm^{-3})$ | 1.642 | 1.643 | 1.633 | 1.746 | 1.789 |
| $F(000)$ | 484 | 1064 | 468 | 864 | 896 |
| $\mu$(Mo-K$\alpha$) (mm$^{-1}$) | 0.718 | 0.661 | 0.732 | 0.830 | 0.827 |
| max./min.trans. | 0.9514 / 0.8999 | 0.9934 / 0.9804 | 0.9370 / 0.8981 | 0.9755 / 0.9366 | 0.9918 / 0.9598 |
| 2θ(max)(°) | 30.00 | 25.42 | 26.00 | 26.00 | 25.99 |
| Reflections collected / unique | 20284 / 5821 | 3820 / 3820 | 9689 / 3671 | 26708 / 3181 | 26992 / 3249 |
| $R_1^a$[I>2σ(I)] | R1 = 0.0335, wR2=0.0781 | R1 = 0.0670, wR2= 0.0974 | R1 = 0.0250, wR2 = 0.0669 | R1 = 0.0676, wR2 = 0.1673 | R1 = 0.0387, wR2 = 0.0881 |
| wR$_2^b$[all data] | R1 = 0.0432, wR2=0.0836 | R1 = 0.1298, wR2= 0.1143 | R1 = 0.0267, wR2=0.0681 | R1 = 0.0789, wR2 = 0.1730 | R1 = 0.0633, wR2=0.0992 |
| S[goodness of fit] | 1.044 | 1.044 | 1.099 | 1.157 | 1.089 |
| min./max. res.(e.Å$^{-3}$) | 0.691 / -0.535 | 1.041/-0.667 | 0.333 / -0.233 | 2.007 / -1.890 | 0.372 / -0.467 |

$^aR_1 = \Sigma\,|\,F_O\,|\,-\,|\,F_C\,|\,/\,\Sigma\,|\,F_O\,|$.

$^bwR_2 = \{\Sigma\,[\,w\,(F_O{}^2 - F_C{}^2)^2]/\Sigma\,[\,w\,(F_O{}^2)^2]\}^{\frac{1}{2}}$.

### 3.3. Results and Discussion

*3.3.1. Synthesis*

Reactions of the selected aroylhydrazones (*c.f.* **Scheme 3.1**) with $[MoO_2(acac)_2]$ in refluxing alcohol afforded two different types of $Mo^{VI}$ complexes, $[MoO_2L(ROH)]$ and $[MoO_2L]$; Equations 1 and 2. The formation of mixed-ligand mononuclear complex $[MoO_2L(Q)]$ {where Q = γ-picoline (**1a**)} has been achieved by the reaction of **1** with γ-picoline; Equation 3. Proposed structures of these complexes (**Scheme 3.2**) are based on their spectroscopic characterization (IR, electronic and $^1H$ NMR spectroscopy), elemental analyses and single crystal X-ray diffraction studies. The ligands coordinate through their dianionic $(ONO)^{2-}$ enolate tautomeric forms.

$$[MoO_2(acac)_2] + H_2L + ROH \rightarrow [MoO_2L(ROH)] + 2Hacac \qquad (1)$$

$$[H_2L = H_2L^1, R = C_2H_5: (\mathbf{1}) \text{ and } H_2L = H_2L^2, R = CH_3: (\mathbf{2})]$$

$$[MoO_2(acac)_2] + H_2L \rightarrow [MoO_2L]_n + 2Hacac \qquad (2)$$

$$[H_2L = H_2L^3, n = \infty: (\mathbf{3}) \text{ and } H_2L = H_2L^4, n = 1: (\mathbf{4})]$$

$$[MoO_2L^1(C_2H_5OH)] + Q \rightarrow [MoO_2L^1Q] + C_2H_5OH \qquad (3)$$

$$[Q = \text{γ-picoline}: (\mathbf{1a})]$$
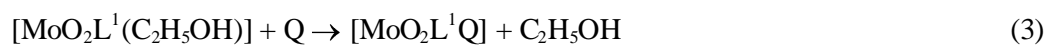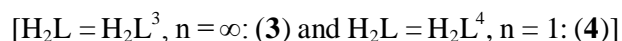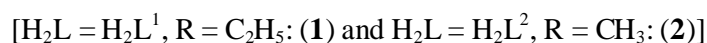
All these complexes are highly soluble in aprotic solvents, viz. DMF or DMSO and are sparingly soluble in alcohol, $CH_3CN$ and $CHCl_3$. All these complexes are diamagnetic, indicating the presence of molybdenum in the +6 oxidation state, and are nonconducting in solution.

$R^1 = H$,  R = OH, $H_2L^1$

$R^1 = H$,  R = $NH_2$, $H_2L^2$

$R^1 = CH_3$,  R = H, $H_2L^3$

$R^1 = CH_3$,  R = $NH_2$, $H_2L^4$
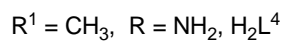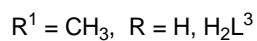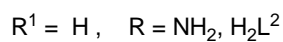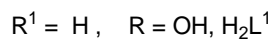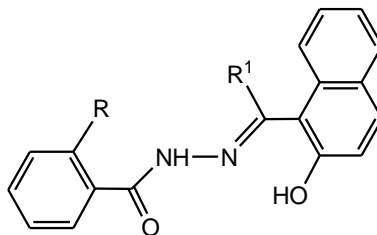
**Scheme 3.1.** Schematic representation of Ligand.
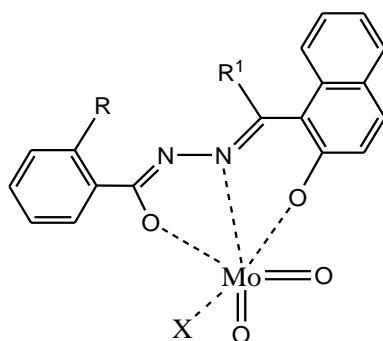


| Ligand | X | Complex |
|--------|---|---------|
| $H_2L^1$ | $C_2H_5OH$ | [$MoO_2L^1$ ($C_2H_5OH$)] (**1**) |
| $H_2L^1$ | γ-picoline | [$MoO_2L^1$ (γ -pic)] (**1a**) |
| $H_2L^2$ | $CH_3OH$ | [$MoO_2L^2$($CH_3OH$)] (**2**) |
| $H_2L^3$ | -- | [$MoO_2L^3$]$_n$ (**3**) |
| $H_2L^4$ | -- | [$MoO_2L^4$] (**4**) |

**Scheme 3.2.** Possible bonding modes of Mo(VI) complexes

## 3.3.2. Spectral properties

Spectral characteristics of compounds are listed in **Table 3.2**. All the ligands exhibit the bands at 3368–3323 cm$^{-1}$ [ν(OH)], 3135–3022 cm$^{-1}$ [ν(NH)] and 1652–1623 cm$^{-1}$ [ν(C=O)] region, are disappeared in complexes [16, 52-53]. Characteristic strong bands at 1622–1592 cm$^{-1}$ and 1555–1605 cm$^{-1}$ due to ν(C=C/aromatic) and ν(C=N) stretching modes of the ligand are located in the spectra of both the ligands and the complexes [16,52–53]. In addition, **1, 1a, 2** and **4** display two strong peaks in the range 937–902 cm$^{-1}$ due to terminal ν(M=O$_t$) stretch [16,52–54]. There are two relatively strong and broad peaks around 863–821 cm$^{-1}$ due to weakened (Mo–O→Mo) for oligomeric complex **3**, observed. The representative IR spectra of ligand H$_2$L$^1$ and complex **1** are shown in **Figs. 3.1** and **3.2** respectively.

The DMSO solution of all the complexes display a medium intensity band in the 468–423 nm region and two strong absorptions in the 340–256 nm range which are assignable to ligand to molybdenum (pπ–dπ) charge transfer (LMCT) and intraligand transitions, respectively [16,52–53]. Electronic spectra of all the complexes are shown in **Fig. 3.3**.

The $^1$H and $^{13}$C NMR (DMSO-d$_6$) data of all the free ligands and their corresponding dioxomolybdenum(VI) complexes are given in the experimental section. The spectra of the free ligands exhibit a resonance at δ = 12.97–10.31 ppm due to naphthyl –OH (H$_2$L$^{1-4}$), at δ = 9.54–9.47 ppm due to –HC=N protons (H$_2$L$^{1-2}$) and at δ = 2.35–2.34 ppm due to –CH$_3$ protons (H$_2$L$^{3-4}$), respectively. All the aromatic protons of ligands are clearly observed in the expected region δ = 8.33–6.23 ppm. In the NMR spectra of complexes, the absence of signal due to aromatic (naphthyl) –OH indicates that the phenolic group is coordinated to the metal centre after proton replacement [16,52–53]. Similarly, the absence of signal due to –NH proton in the complexes suggests that the ligands are coordinated to the metal center via enolic form. The representative NMR spectra of ligand H$_2$L$^2$ and complex **2** are shown in **Figs.3.4** and **3.5** respectively.

**Table 3.2** Characteristic IR[a] bands and electronic spectral data[b] for the studied complexes (**1, 1a** and **2–4**)

| Compounds | $\nu$(C=O) | $\nu$(C=N) | $\nu$(Mo=O) | $\lambda_{max}$/nm ($\varepsilon$/dm$^3$ mol$^{-1}$ cm$^{-1}$) |
|---|---|---|---|---|
| H$_2$L$^1$ | 1621 | 1570 | -- | 327 (2064), 257 (5321) |
| H$_2$L$^2$ | 1637 | 1555 | -- | 323 (1925), 257 (5246) |
| H$_2$L$^3$ | 1652 | 1572 | -- | 335 (1854), 256 (5136) |
| H$_2$L$^4$ | 1652 | 1583 | -- | 337 (1938), 257 (5148) |
| [MoO$_2$L$^1$(C$_2$H$_5$OH)] (**1**) | -- | 1602 | 937, 913 | 447 (5890), 340 (1591), 257 (1915) |
| [MoO$_2$L$^1$($\gamma$-pic)] (**1a**) | -- | 1595 | 923, 902 | 446 (5505), 339 (1361), 257 (1770) |
| [MoO$_2$L$^2$(CH$_3$OH)] (**2**) | -- | 1597 | 931, 902 | 468 (51649), 329 (12711), 256 (13024) |
| [MoO$_2$L$^3$]$_n$ (**3**) | -- | 1593 | 863, 821 | 423 (10701), 329 (23470), 258 (20373) |
| [MoO$_2$L$^4$] (**4**) | -- | 1590 | 935, 915 | 442 (10433), 329 (14886), 258 (27667) |

[a] In KBr pellet; [b] In DMSO
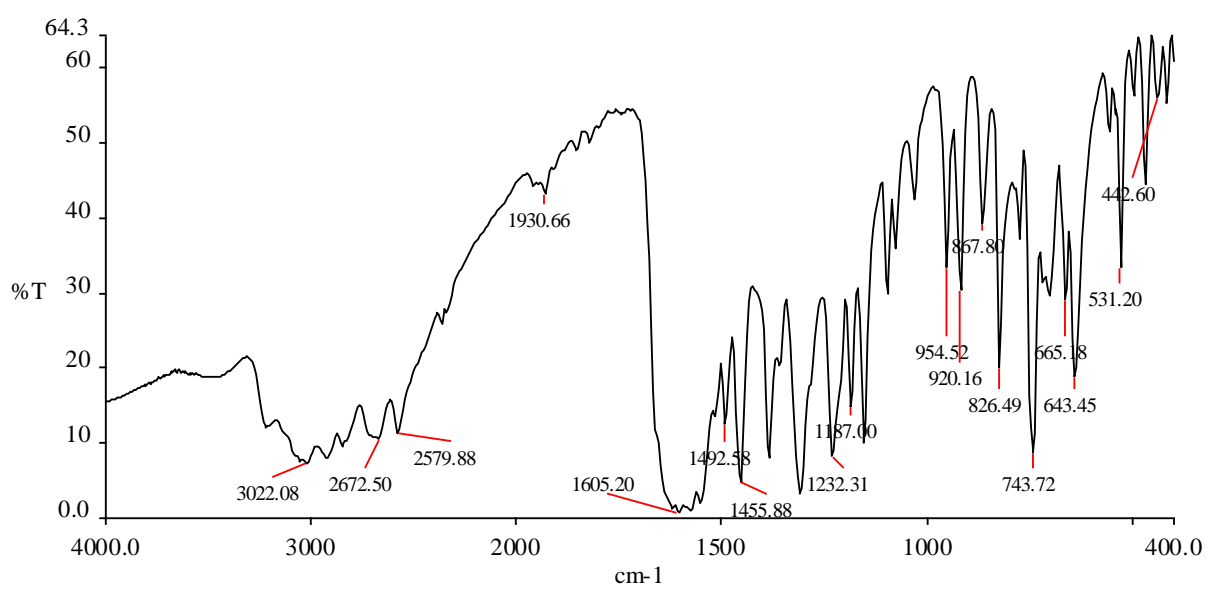
**Fig. 3.1** IR spectrum of $H_2L^1$
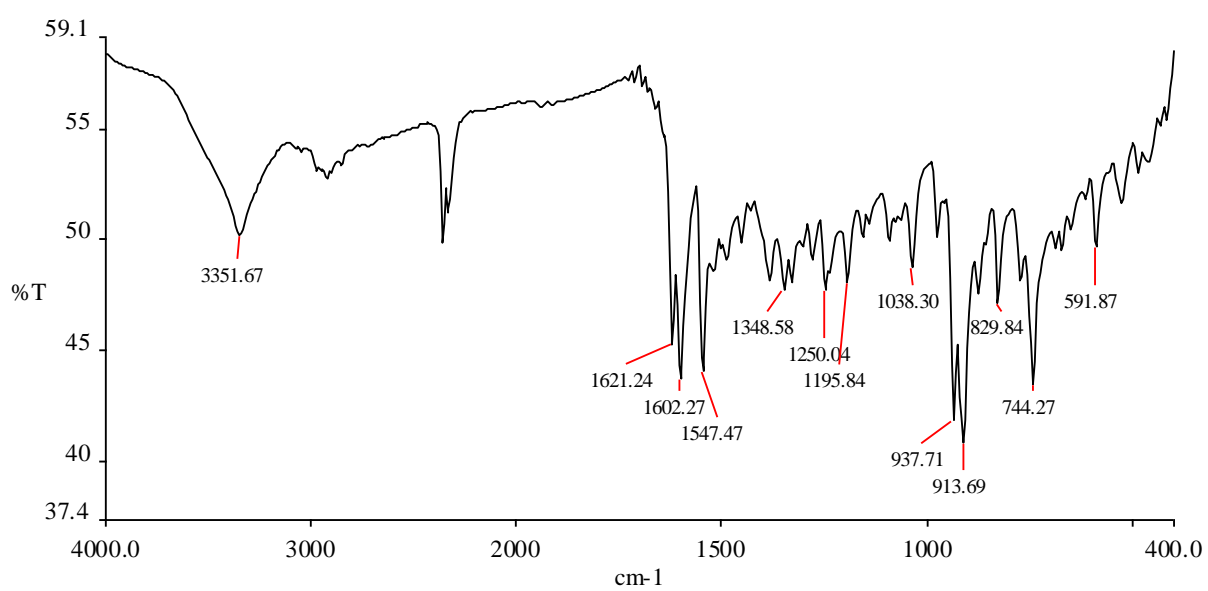
**Fig. 3.2** IR spectrum of $[MoO_2L^1(C_2H_5OH)]$ (**1**)
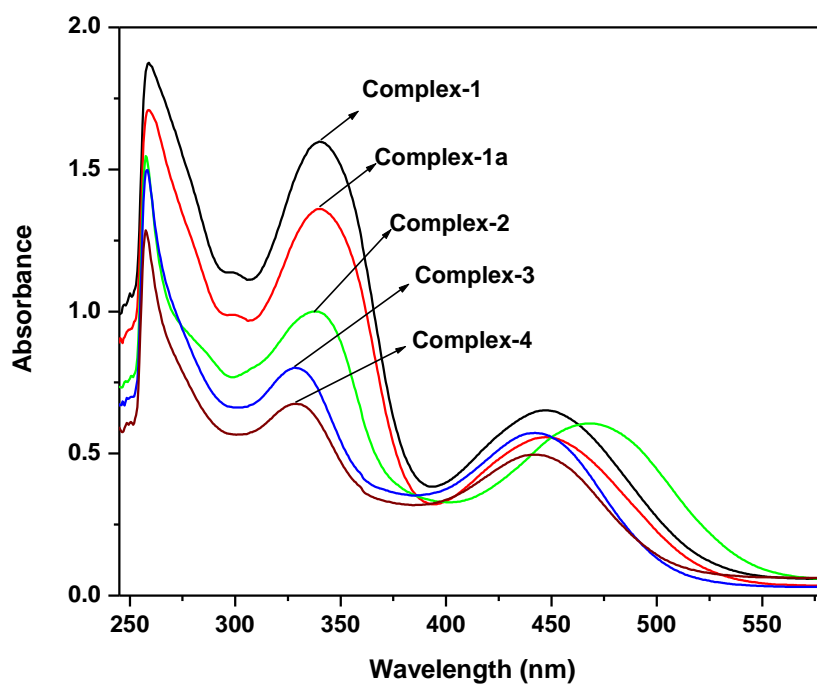
**Fig. 3.3** Electronic absorption spectra of Complexes (**1**, **1a** and **2–4**) in DMSO, at $25^0$ C
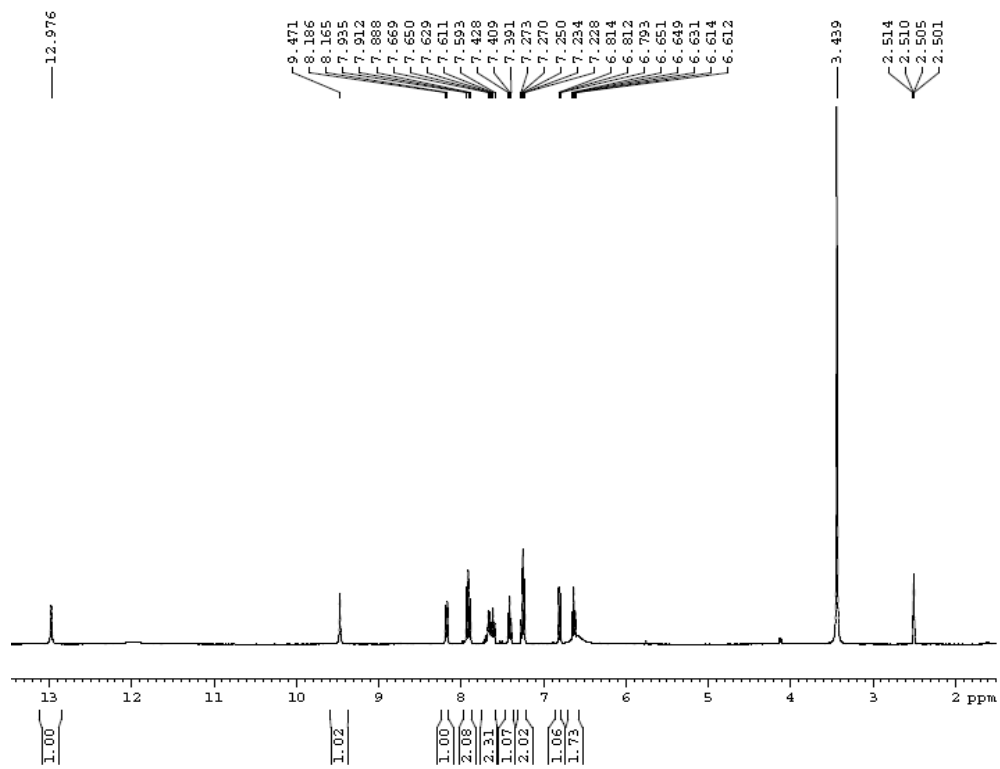
**Fig. 3.4** $^1$H NMR spectrum of [$H_2L^2$] in DMSO $d_6$
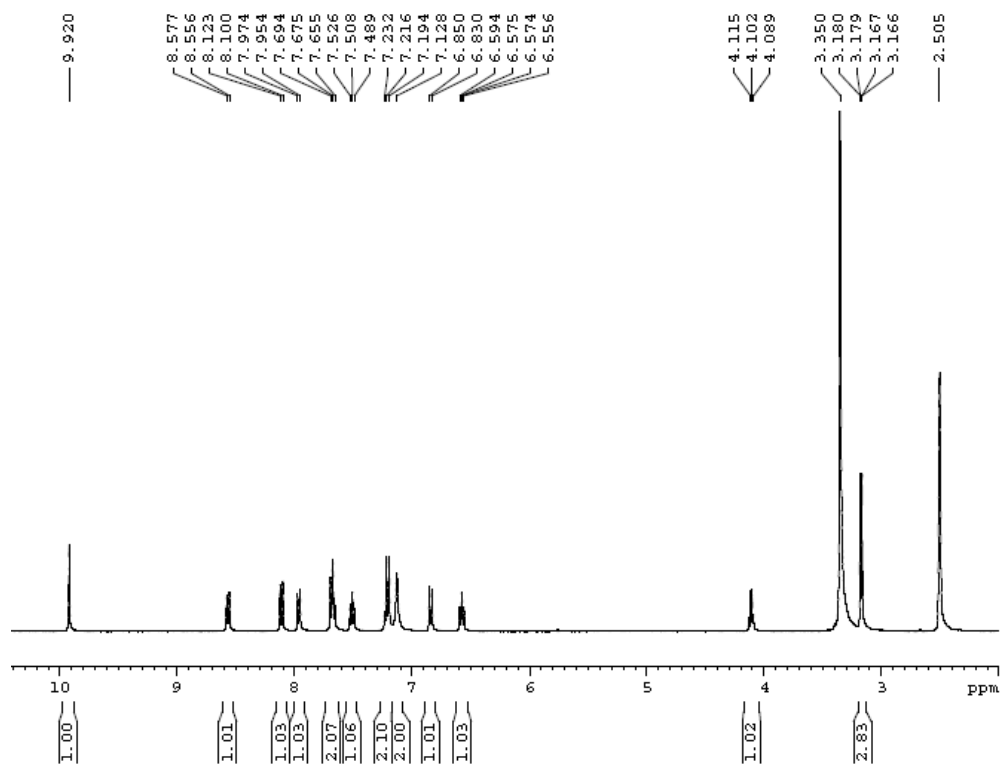
**Fig. 3.5** $^1$H NMR spectrum of [MoO$_2$L$^2$(CH$_3$OH] (**2**) in DMSO d$_6$

*3.3.3. Electrochemical properties*

Electrochemical properties of the complexes have been studied by cyclic voltammetry in DMF solution (0.1 M TBAP). Voltammetric data are given in **Table 3.3** and the cyclic voltamogram of $MoO_2L^2(CH_3OH)$ (**2**) is displayed in **Fig. 3.6** as the representative one. The CV traces of complexes (**1–5**) exhibit two irreversible reductive responses within the potential window –0.73 to –0.81 V and –1.03 to –1.08 V, which are assigned to $Mo^{VI}/Mo^V$ and $Mo^V/Mo^{IV}$ processes respectively. The lack of anodic response, even at a high scan rate, is clearly due to rapid decomposition of the reduced species [16,52–53].

**Table 3.3** Cyclic voltammetric results for dioxomolybdenum (VI) complexes (**1**, **1a** and **2–4**) at 298 K

| Complex | $E$pc [V][a] |
|---|---|
| $[MoO_2L^1(C_2H_5OH)]$ (**1**) | –0.81, –1.03 |
| $[MoO_2L^1(\gamma\text{-pic})]$ (**1a**) | –0.79, –1.06 |
| $[MoO_2L^2(CH_3OH)]$ (**2**) | –0.73, –1.08 |
| $[MoO_2L^3]_n$ (**3**) | –0.75, –1.07 |
| $[MoO_2L^4]$ (**4**) | –0.77, –1.06 |

[a] Solvent: DMF; working electrode: platinum; auxiliary electrode: platinum; reference electrode: Ag/AgCl; supporting electrolyte: 0.1 M TBAP; scan rate: 50 mV/s. $E$pc is the cathodic peak potential
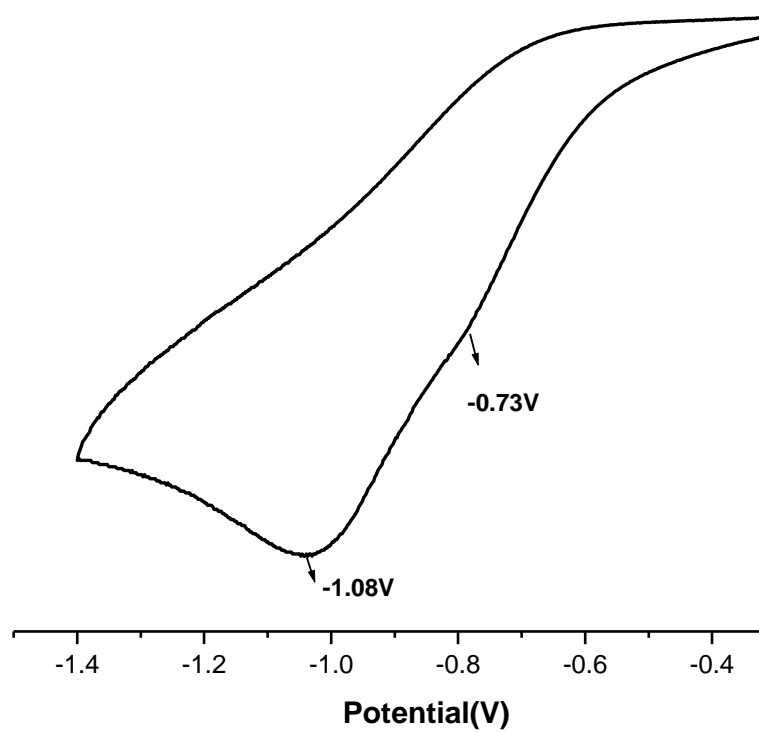
**Fig. 3.6** Cyclic voltammogram of [MoO$_2$L$^2$(CH$_3$OH)] (**2**) in DMF

*3.3.4. Description of the X-ray structure of complexes [MoO$_2$L$^1$(C$_2$H$_5$OH)] (**1**), [MoO$_2$L$^2$(CH$_3$OH)] (**2**) and [MoO$_2$L$^3$] (**3**)*

The molecular structure and the atom numbering schemes for the complex [MoO$_2$L$^1$(C$_2$H$_5$OH)] (**1**), [MoO$_2$L$^2$(CH$_3$OH)] (**2**) and [MoO$_2$L$^3$] (**3**) are shown in **Figs 3.7–3.9** respectively, with the relevant bond distances and angles collected in **Table 3.4**. The coordination geometry around the molybdenum (VI) atom in **1**, **2** and **3** reveals a distorted octahedral environment with an NO$_5$ coordination sphere (**Scheme 3.2**). Each ligand molecule behaves as dianionic tridentate one binding through the phenolate oxygen O(1), the enolate oxygen O(2) and the imine nitrogen N(1). In all three complexes, one of the two oxo group O(4) is located trans to the imine nitrogen in the same plane. For complexes **1** and **2** the other oxo group O(3) is located in the axial plane with the solvent molecule [C$_2$H$_5$OH (**1**) and CH$_3$OH (**2**)]. Whereas in complex **3** along with the two oxo-oxygens, O(3) and O(4), the three ONO donor points of the ligand complete the five coordinate environment around the Mo(VI) acceptor center, the disposition of the donor points being roughly square pyramidal. The sixth coordination site, trans to the oxo-oxygen O(3), is occupied by an oxo-oxygen O(3$^!$) of the next neighboring complex molecule and this pattern is repeated leading to a chain of MoO$_2$L$^3$ molecules (**Fig. 3.10**). This may be visualized as an effect of stacking of the complex molecules along the z-axis [55]. The length of the Mo–O(3$^!$) bond (2.374Å) is considerably longer than the other Mo–O bonds, the longest of which [Mo–O(2)] is 1.982(5) Å which suggest that this should be explained as oligomeric structure where one of the oxygen of one molybdenum weakly interacts with other. The bond between Mo and the azomethine nitrogen in the complexes are within a range of 2.225–2.234 Å which is comparatively longer than other Mo–N single bonds. This is due to the trans effect generated by the oxo group trans to the Mo–N bond [52].

The angular distortion in the octahedral environment around Mo comes from the bites taken by the Schiff base ligand, angles O(1)–Mo(1)–N(1) is [80.56(6)° (**1**), 80.12(6)° (**2**), 79.2(2)° (**3**)] and angles O(2)–Mo(1)–N(1) is [72.33(6)° (**1**), 71.88(6)° (**2**) and 72.4(2)° (**3**)]. For the same reason the *trans* angles O(1)–Mo(1)–O(2) and O(4)–Mo(1)–N(1) are significantly reduced from the ideal value of 180°, the *trans*-axial angle O(3)–Mo(1)–O(5) is 172.09(7)° (complex **1**) and 171.46(8)° (complex **2**). The two oxo oxygen of MoO$_2$ groups is almost equal [average 1.696(2) & 1.697(2)]. The Mo–O(alcohol) bond [2.383(2) Å (**1**) and 2.294(2) Å (**2**)] is significantly longer than the other Mo–O bonds [1.694(2)–2.001(2) Å (**1**) and 1.693(2)–1.992(1) (**2**) Å] indicating

85

that the alcohol molecule is weakly bonded to the $MoO_2^{2+}$ core and this position holds the possibility of functioning as a substrate-binding site of the general formula $[MoO_2L(Q)]$.

### 3.3.5. Description of the X-ray structure of complex $[MoO_2L^1(\gamma\text{-pic})]$ (*1a*)

The atom numbering scheme for the complex **1a** is given in **Fig. 3.11** with the relevant bond distances and angles collected in **Table 3.4**. The molecular structures of complex, $[MoO_2L^1(\gamma\text{-pic})]$ has shown that the dinegative hydrazone ligand $(H_2L^1)$ bind to the molybdenum(VI) center by O(1), N(1), O(2)–donor atoms. The fourth coordination site around molybdenum (VI) is occupied by $\gamma$-picoline ligand in complex **1a** through its tertiary nitrogen N (3), forming distorted octahedral complex. The rather large Mo(1)–N(3) distance is [2.427(5) Å] revealed that the $\gamma$-picoline moiety is also rather weakly coordinated to the $MoO_2^{2+}$ core [16,19,53]. The Mo–O (oxo) bond distances of the $MoO_2^{2+}$ group is unexceptional [16,19,53] and almost equal [1.698(4)–1.713(3) Å]. The ligand coordinate to the $MoO_2^{2+}$ core in the deprotonated enolate form because, in complexes (**1**) and (**1a**) the C–O bond distances [C(12)–O(2)] exhibit values of 1.314(3) and 1.329(6) Å respectively and are nearer to a C–O single bond than to a C–O double bond distance. However, it falls short of the pure C–O single bond distance of 1.42 Å because of the delocalization of electrons.

### 3.3.6. Description of the X-ray structure of complex $[MoO_2L^4]$ (*4*)

We have employed the steric bulk on aroylhydrazones ligand $(H_2L^4)$ (**Scheme 3.1**) to gain control of the coordination number around the Mo(VI) center. Structural studies indicate that, with increasing steric bulk, control of the coordination number around the Mo(VI) center is achieved by the formation of 5-coordinate dioxomolybdenum(VI) complex of the type $[MoO_2L^4]$ (**4**) (**Scheme 3.2**). The molecular structure and the atom numbering schemes of **4** is shown in **Fig. 3.12**. In this compound $(MoO_2L^4)$ the coordination geometry of Mo(VI) is similar to that observed earlier [53], which consist of two oxo oxygen atoms, one enolate oxygen, one phenolate oxygen, and an azomethine nitrogen atom. This is the rare example of a five–coordinate Mo(VI) complex [53,56]. No structural evidence for the achievement of hexacoordination through Mo–O···Mo bridging is observed. The molecular geometry of $[MoO_2L^4]$ is best represented as a square-pyramid with one axial oxo oxygen atom [O(3)], and three O atoms [O(1,2,4)] and the N(1) atom describing the equatorial plane, which is slightly

distorted from an ideal geometry, as reflected in the bond parameters (**Table 3.4**) around the metal center. The length of the Mo–O(4) bond lying *trans* to N(1) is practically equal to Mo-O(3); the position *trans* to O(3) remains unoccupied. The other Mo–O and Mo–N distances are normal, as observed in other structurally characterized complexes of molybdenum containing these bonds [52–53]. The bite angles of the ligand at Mo, O(2)–Mo(1)–N(1) and O(1)–Mo(1)–N(1), are 72.3(1)° and 80.2(1)°, respectively, generating five-membered and six-membered chelate rings at the $Mo^{VI}$ center.

**Table 3.4.** Selected Bond Distances [Å] and Bond Angles [˚] for Complex **1**, **1a**, **2**, **3** and **4**

|  | Complex **1** | Complex **1a** | Complex **2** | Complex **3** | Complex **4** |
|---|---|---|---|---|---|
| Bond lengths |  |  |  |  |  |
| Mo(1)-O(1) | 1.918(1) | 1.915(4) | 1.925(1) | 1.892(5) | 1.924(3) |
| Mo(1)-O(2) | 2.001(2) | 2.015(5) | 1.992(1) | 1.982(5) | 1.992(3) |
| Mo(1)-O(3) | 1.694(2) | 1.698(4) | 1.693(2) | 1.701(5) | 1.689(3) |
| Mo(1)-O(4) | 1.697(2) | 1.713(3) | 1.706(2) | 1.689(5) | 1.700(3) |
| Mo(1)-O(5) | 2.383(2) | -- | 2.294(2) | -- | -- |
| Mo(1)-N(1) | 2.225(2) | 2.219(4) | 2.234(2) | 2.231(5) | 2.222(3) |
| Mo(1)-O(3)#1 | -- |  | -- | 2.374(5) | -- |
|  |  |  |  |  |  |
| Bond Angles |  |  |  |  |  |
| O(1)-Mo(1)-O(2) | 149.49(6) | 148.9(2) | 146.78(6) | 146.8(2) | 147.0(1) |
| O(1)-Mo(1)-O(3) | 99.78(7) | 101.1(2) | 99.25(8) | 101.0(2) | 99.9(1) |
| O(1)-Mo(1)-O(4) | 102.68(7) | 101.9(2) | 104.25(7) | 100.8(2) | 101.7(1) |
| O(1)-Mo(1)-O(5) | 80.24(6) | -- | 79.38(7) | -- | -- |
| O(1)-Mo(1)-N(1) | 80.56(6) | 80.0(2) | 80.12(6) | 79.2(2) | 80.2(1) |
| O(2)-Mo(1)-O(3) | 97.25(7) | 95.9(2) | 99.37(7) | 99.3(2) | 100. 9(1) |
| O(2)-Mo(1)-O(4) | 96.68(7) | 98.4(2) | 97.07(7) | 98.6(2) | 96.3(1) |
| O(2)-Mo(1)-O(5) | 79.49(6) | -- | 78.15(6) | -- | -- |
| O(2)-Mo(1)-N(1) | 72.33(6) | 72.5(2) | 71.88(6) | 72.4(2) | 72.3(1) |
| O(3)-Mo(1)-O(4) | 105.95(8) | 105.4(2) | 105.19(8) | 105.7(3) | 107.1(1) |
| O(3)-Mo(1)-O(5) | 172.09(7) | -- | 171.46(8) | -- | -- |
| O(3)-Mo(1)-N(1) | 97.11(7) | 95.5(2) | 92.28(7) | 97.5(2) | 96.4(1) |
| O(4)-Mo(1)-O(5) | 81.67(7) | -- | 83.28(7) | -- | -- |
| O(4)-Mo(1)-N(1) | 155.65(7) | 158.0(2) | 160.84(7) | 156.2(2) | 155.6(1) |
| O(5)-Mo(1)-N(1) | 75.06(6) | -- | 79.18(6) | -- | -- |
| O(3)-Mo(1)-O(3)#1 | -- | -- | -- | 170.8(2) | -- |
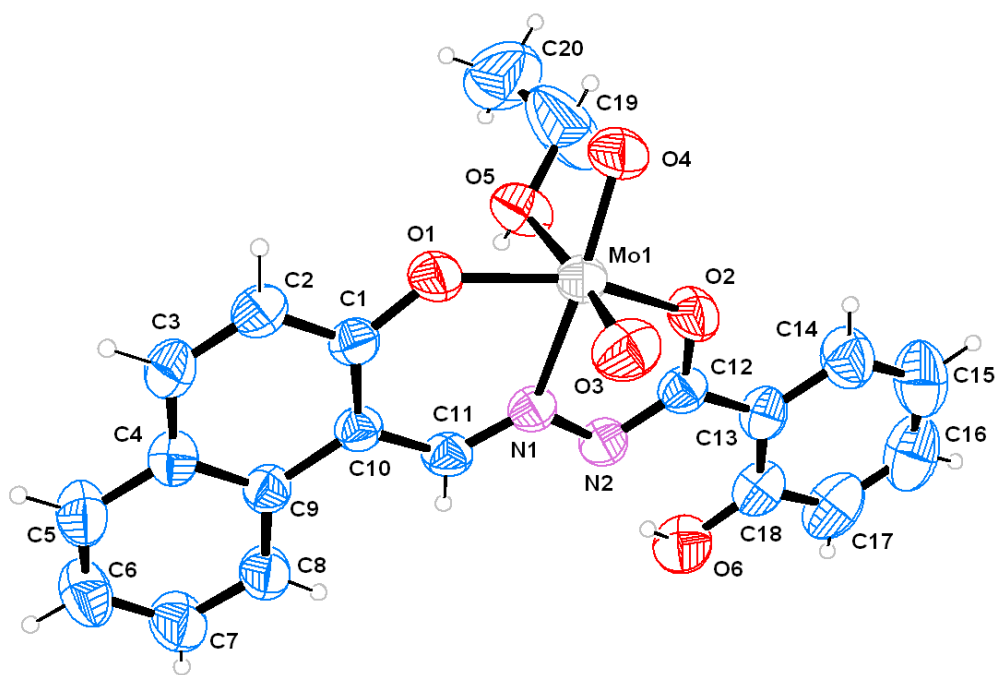
**Fig. 3.7.** ORTEP diagram of [MoO$_2$L$^1$(C$_2$H$_5$OH)] (**1**) with atom labeling scheme at 50% probability.
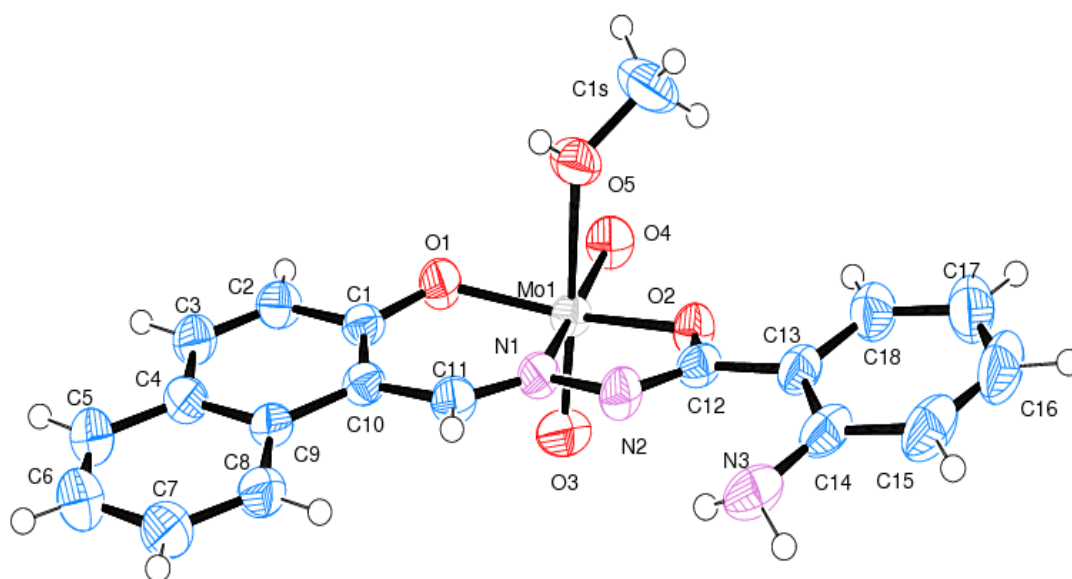
**Fig. 3.8.** ORTEP diagram of [MoO$_2$L$^2$(CH$_3$OH)] (**2**) with atom labeling scheme at 50% probability.
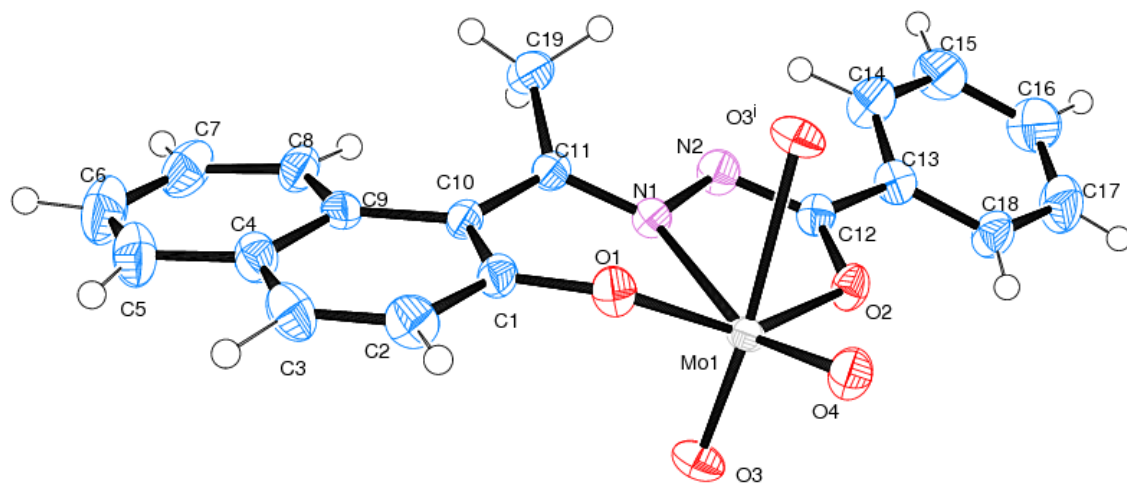
**Fig. 3.9.** ORTEP diagram of asymmetry unit of $[MoO_2L^3]_n$ (**3**) with atom labeling scheme at 50% probability.

.
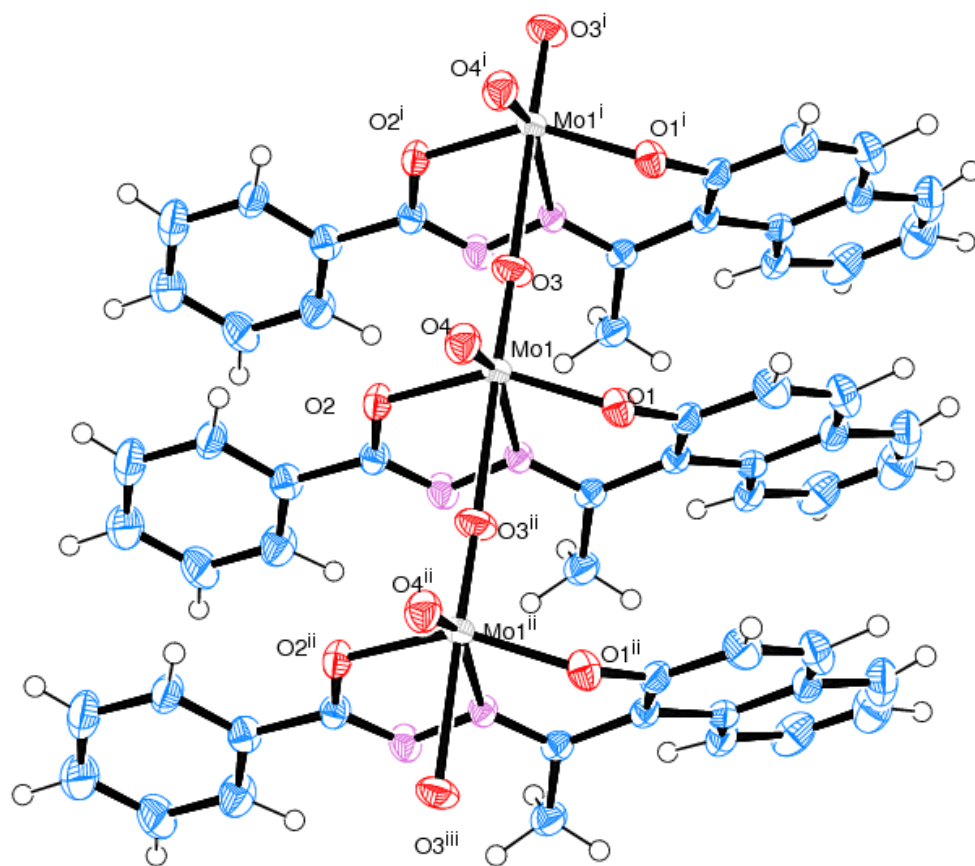
**Fig. 3.10.** One dimensional polymeric diagram of $[MoO_2L^3]_n$ (**3**)
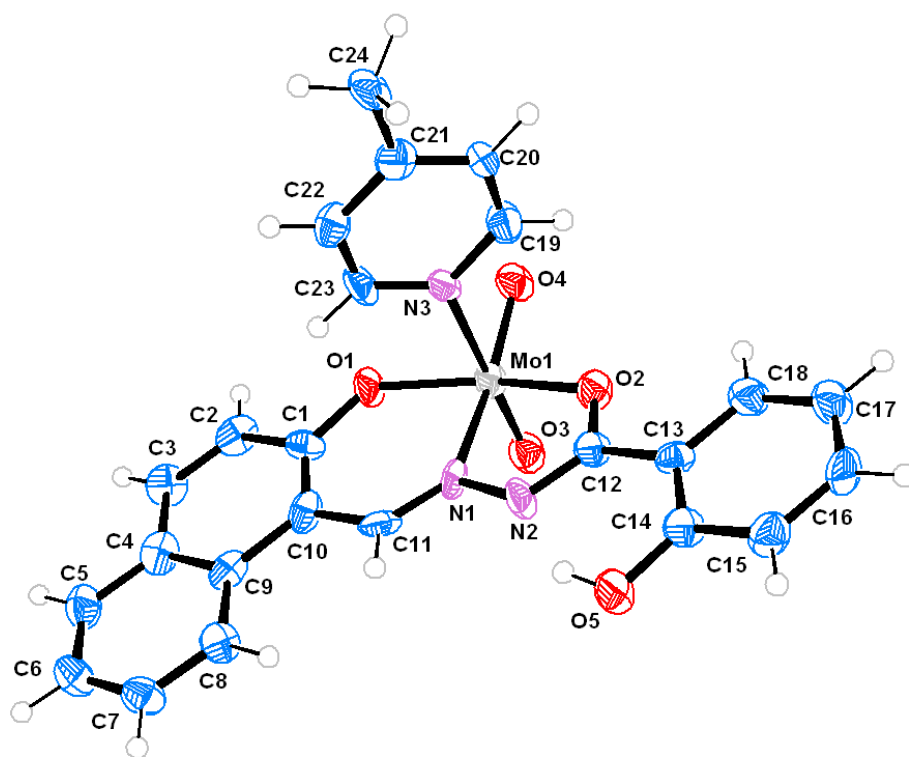
**Fig. 3.11.** ORTEP diagram of [MoO$_2$L$^1$(γ-pic)] (**1a**) with atom labeling scheme at 50% probability.

.
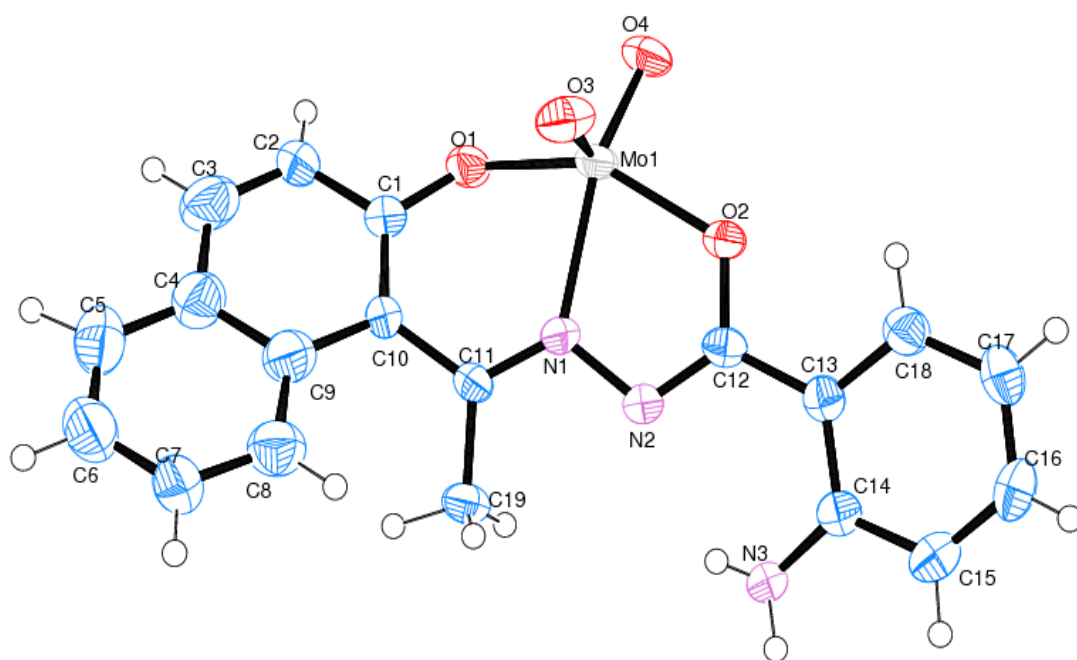
**Fig. 3.12.** ORTEP diagram of [MoO$_2$L$^4$ ] (**4**) with atom labeling scheme at 50% probability.

.

*3.3.7. Antibacterial activity*

All synthesized ligands and complexes were evaluated for their *in vitro* antimicrobial activity against the pathogenic strains of *Escherichia coli, Bacillus subtilis, Proteus vulgaris* and *Klebsiella pneumoniae* by agar well-diffusion method and their MIC values are represented in **Table 3.5** and **Fig.3.13**. It is clearly observed that in some cases they showed promising results by giving the MIC value lesser than the standard drug examined. The results also indicate that the corresponding dioxomolybdenum(VI) complexes showed much better antibacterial activity with respect to the individual ligand against the same microorganism under identical experimental conditions which is in agreement with the previous results [16,50–51,57–60]. A possible explanation is that, by coordination, the polarity of the ligand and the central metal ion are reduced through the charge equilibration, which favors permeation of the complexes through the lipid layer of the bacterial cell membrane [16,50–51,57–60].

From the zone of inhibition, it is observed that the complex **1** and **1a** showed most promising results as compared to the other compounds (**2**, **3** and **4**) of this study and the difference in value may be attributed to their distorted octahedral geometry and nature of compounds synthesized in presence of one molecule of ethanol in the coordination sphere of the metallic ion (**1**) and with γ-picoline as co-ligand (**1a**) [61–62]. The result for the octahedral complex (**2**) is least promising as compared to (**1**) and (**1a**), probably due to the presence of methanol in the coordination sphere. Against some of the tested bacterial species the inhibitory action for complex (**3**) and (**4**) are less significant may be because of their polymeric and square pyramidal structure respectively.

Antibacterial activity of the similar type oxo-metal complexes has also been reported by our group [16,17] Sharma *et al.* [63], Chohan *et al.* [64] and Prasad *et al.* [65] using agar well diffusion technique against *Escherichia coli*, *Shigella flexenari*, *Pseudomonas aeruginosa*, *Salmonella typhi*, *Staphylococcus aureus* and *Bacillus subtilis* and the present results are in accordance with the reported values. However, the difference in value may be attributed to the nature of compounds synthesized with different ligands.

**Table 3.5** Minimum Inhibitory Concentration (MIC) value in µg/mL of the Schiff base ligand (**H₂L$^{1-4}$**), dioxomolybdenum (VI) complexes (**1**, **1a** and **2–4**) and standard drugs against pathogenic strains

|  | *E.coli* | *Bacillus subtilis* | *Proteus vulgari* | *Klebsiella pneumoniae* |
|---|---|---|---|---|
| H₂L$^1$ | -- | 62.5 | 125 | -- |
| H₂L$^2$ | -- | -- | -- | -- |
| H₂L$^3$ | -- | 125 | 250 | -- |
| H₂L$^4$ | -- | 125 | 500 | -- |
| [MoO₂L$^1$(C₂H₅OH)] (**1**) | 62.5 | 15.6 | 15.6 | 15.6 |
| [MoO₂L$^1$ (γ-pic)] (**1a**) | 15.6 | 62.5 | 15.6 | 15.6 |
| [MoO₂L$^2$ (CH₃OH)] (**2**) | -- | 15.6 | 125 | -- |
| [MoO₂L$^3$]ₙ (**3**) | -- | 62.5 | 62.5 | -- |
| [MoO₂L$^4$] (**4**) | 15.6 | 15.6 | 62.5 | -- |
| Vancomycin | 30 | 30 | -- | 30 |
| Amoxycillin | -- | -- | 25 | -- |
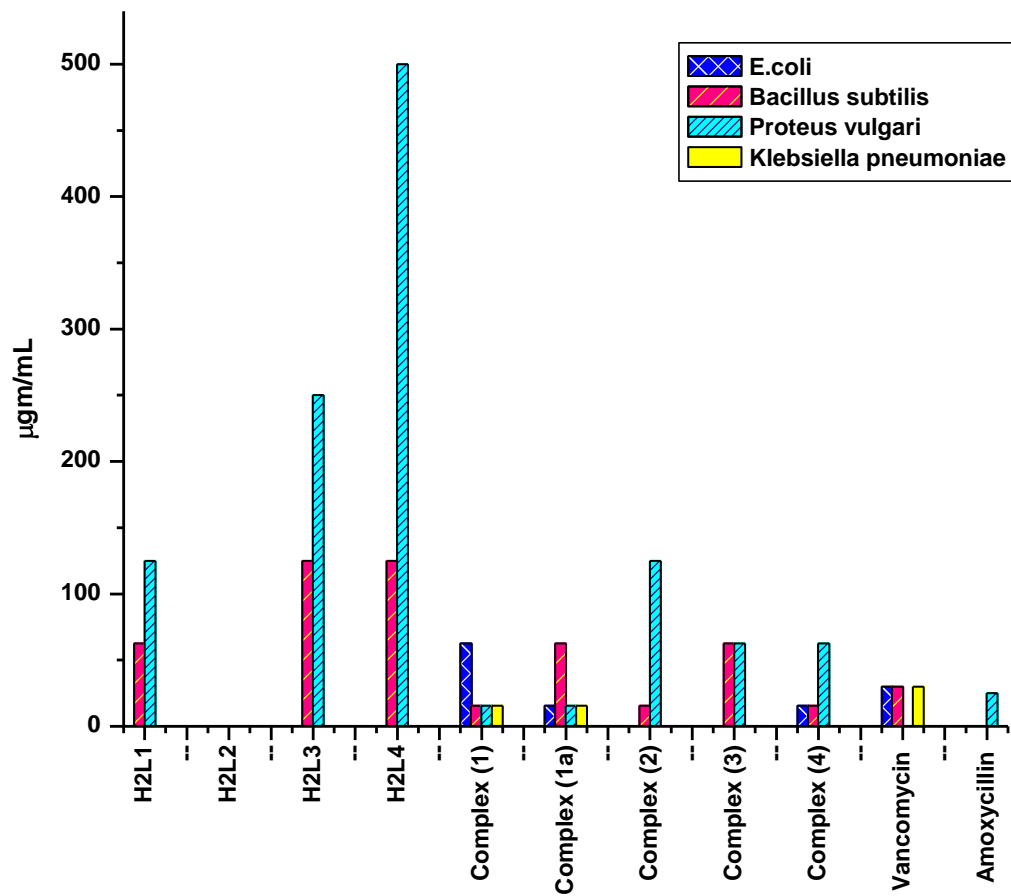
**Fig. 3.13** Minimum Inhibitory Concentration (MIC) of the Schiff base ligand ($\mathbf{H_2L^{1-4}}$), their corresponding Mo(VI) complexes (**1–4**) and standard drugs against pathogenic strains.

*3.3.8. Catalytic Activity Studies*

*3.3.8.1. Oxidation of benzoin*

The oxidation of benzoin has attracted the attention of researchers because one of its oxidized product, benzil, is a very useful intermediate for the synthesis of heterocyclic compounds and benzylic acid rearrangements [66]. The oxidation of benzoin was successfully achieved with the molybdenum complexes using 30% aqueous $H_2O_2$ as oxidant. The products mainly obtained were benzoic acid, benzaldehyde-dimethylacetal, methylbenzoate and benzil (**Scheme 3.3**).
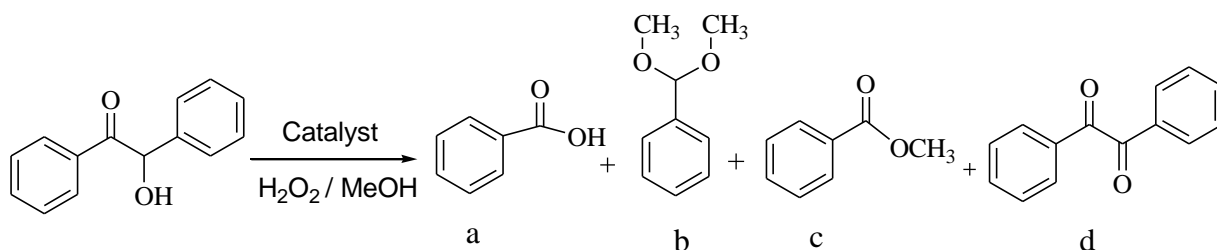


**Scheme 3.3.** Various oxidation products of benzoin. (a) benzoic acid, (b) benzaldehyde-dimethylacetal, (c) methylbenzoate and (d) benzil.

To optimize the reaction conditions for the maximum oxidation of benzoin, $[MoO_2L^2(CH_3OH)]$ (**2**) was considered as a representative catalyst. The effect of oxidant was studied by considering the substrate to oxidant ratios of 1 : 1, 1 : 2 and 1 : 3 for the fixed amount of catalyst (0.0005 g) and substrate (1.06 g, 5 mmol) in 10 mL of refluxing methanol. As shown in **Fig. 3.14** and entry no. 3 of **Table 3.6**, a maximum of 96 % conversion of benzoin was achieved at the substrate to oxidant ratio of 1:3, in 4 hr of reaction time. Lowering the amount of oxidant decreases the conversion. The effect of amount of catalyst on the oxidation of benzoin was studied considering three different amounts of $[MoO_2L^2(CH_3OH)]$ (**2**) viz. 0.0005, 0.001 and 0.0015 g for the fixed amount of benzoin (1.06 g, 5 mmol) and 30% $H_2O_2$ (1.7 g, 15 mmol) in 10 mL of methanol and reaction was monitored at reflux temperature of methanol. A maximum of 96 % conversion was achieved with 0.0005 g of catalyst. This conversion improved only marginally to 98% whereas 0.0015 g of catalyst gave a maximum conversion of 99 % in 4 hr of reaction time (**Fig. 3.15**). Thus at the expense of catalyst, only 0.0005 g of catalyst can be considered sufficient to optimize other reaction conditions. The amount of solvent also influences on the oxidation of benzoin. It was concluded (**Fig. 3.16** and entry no. 3, 4 and 5 of **Table 3.6**) that 10 mL methanol was

sufficient to effect maximum conversion under above optimized reaction conditions. **Table 3.6** summarizes conversion of benzoin under different experimental conditions. Thus, from these experiments, the best reaction conditions for the maximum oxidation of benzoin as concluded are: catalyst $[MoO_2L^2(CH_3OH)]$ (**2**) (0.0005 g), benzoin (1.06 g, 5 mmol) and 30% $H_2O_2$ (1.7 g, 15 mmol) and refluxing methanol (10 mL).

**Fig. 3.17** presents the selectivity of products along with the conversion of benzoin as a function of time (4 hr) under the optimal experimental conditions as concluded above, *i.e.* benzoin (1.06 g, 5 mmol), 30% $H_2O_2$ (1.7 g, 15 mmol), $[MoO_2L^2(CH_3OH)]$ (**2**) (0.0005 g) and methanol (10 mL) under reflux condition. It is clear from the plot that all products form with the conversion of benzoin. The highest selectivity of benzoic acid (*ca.* 51%) was observed in the first one hour. With the elapse of time its selectivity slowly decreases and finally becomes almost constant and reaches 47 % after 4hr. Similar results have been observed in case of methyl benzoate and benzil and reach 23 and 16 %, respectively. The selectivity of benzaldehyde-dimethylacetal increases continuously from 3 to 14 %. Thus, with the maximum benzoin oxidation of 96 % after 4 hr of reaction time, the selectivity of the reaction products varies in the order: benzoic acid (47 %) > methyl benzoate (23 %), > benzil (16 %) > benzaldehyde-dimethylacetal (14 %).

Under these reaction conditions other catalysts were also tested and results are compared in **Fig. 3.18** while **Table 3.7** provides turnover frequency (TOF) and selectivity details. The data presented in table show that other complexes are also catalytically active and show equally good activity with very high turnover frequency (TOF: 1021–1301 $h^{-1}$) but the selectivity order of various products slightly differs. In the absence of the catalyst, the reaction mixture showed 60% conversion where selectivity of different products follows the order: benzil (48%) > benzoic acid (27%) > benzaldehyde-dimethylacetal (20%) > methyl benzoate (5%). Thus, these complexes not only enhance the catalytic action, they also alter the selectivity of the products.

**Table 3.6** Conversion of benzoin (1.06 g, 5 mmol) using $[MoO_2L^2(CH_3OH)]$ (**2**) as catalyst in 4 hr of reaction time under different reaction conditions.

| Entry No. | Catalyst [g] | $H_2O_2$ [g, mmol] | $CH_3OH$ [ml] | Conversion [%] |
|-----------|--------------|--------------------|----------------|-----------------|
| 1 | 0.0005 | 0.57, 05 | 10 | 83 |
| 2 | 0.0005 | 1.14, 10 | 10 | 88 |
| 3 | 0.0005 | 1.71, 15 | 10 | 96 |
| 4 | 0.0005 | 1.71, 15 | 15 | 89 |
| 5 | 0.0005 | 1.71, 15 | 20 | 81 |
| 6 | 0.001 | 1.71, 15 | 10 | 98 |
| 7 | 0.0015 | 1.71, 15 | 10 | 99 |

**Table 3.7** Effect of different catalysts on the oxidation of benzoin, TOF and product selectivity

| Catalyst [g] | TOF [h$^{-1}$] | Conversion [%] | Selectivity [%][a] | | | |
|---|---|---|---|---|---|---|
| | | | a | b | c | d |
| [MoO$_2$L$^1$(C$_2$H$_5$OH)] (**1**) | 1148 | 96 | 29 | 22 | 31 | 18 |
| [MoO$_2$L$^1$(γ-pic)] ( **1a**) | 1301 | 99 | 31 | 26 | 26 | 17 |
| [MoO$_2$L$^2$(CH$_3$OH)] (**2**) | 1110 | 96 | 47 | 14 | 23 | 16 |
| [MoO$_2$L$^3$]$_n$ (**3**) | 1021 | 95 | 40 | 25 | 22 | 13 |
| [MoO$_2$L$^4$] (**4**) | 1073 | 96 | 40 | 24 | 22 | 14 |
| Without catalyst | | 60 | 27 | 20 | 5 | 48 |

[a] (a) benzoic acid, (b) benzaldehyde-dimethylacetal, (c) methylbenzoate and (d) benzil.
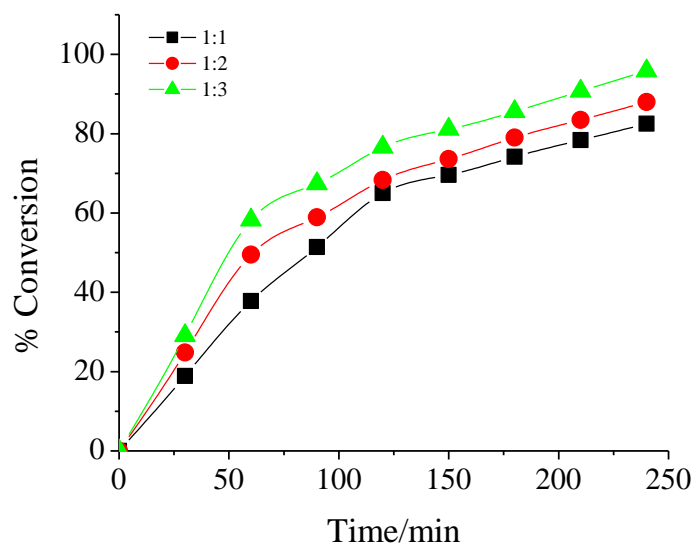
**Fig. 3.14.** Effect of oxidant amount on the oxidation of benzoin. Reaction conditions: benzoin (1.06 g, 5 mmol), catalyst amount (0.0005 g) and methanol (10 mL).
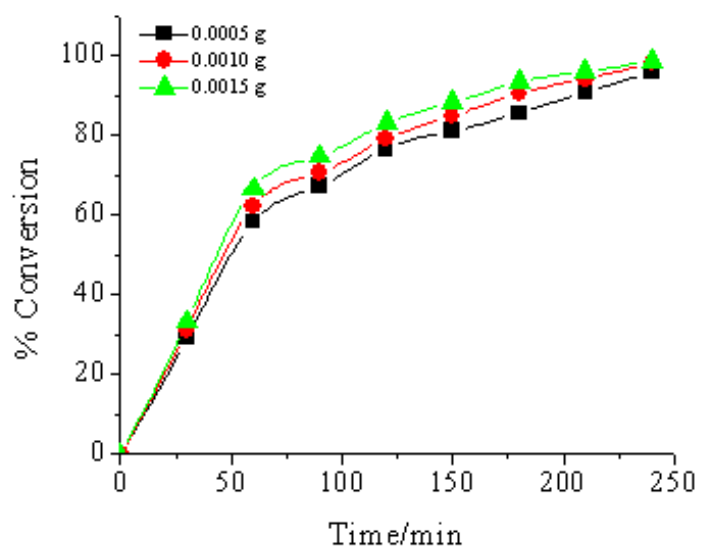
**Fig. 3.15.** Effect of catalyst amount on the oxidation of benzoin. Reaction conditions: benzoin (1.06 g, 5 mmol), 30 % $H_2O_2$ (1.7 g, 15 mmol) and methanol (10 mL).
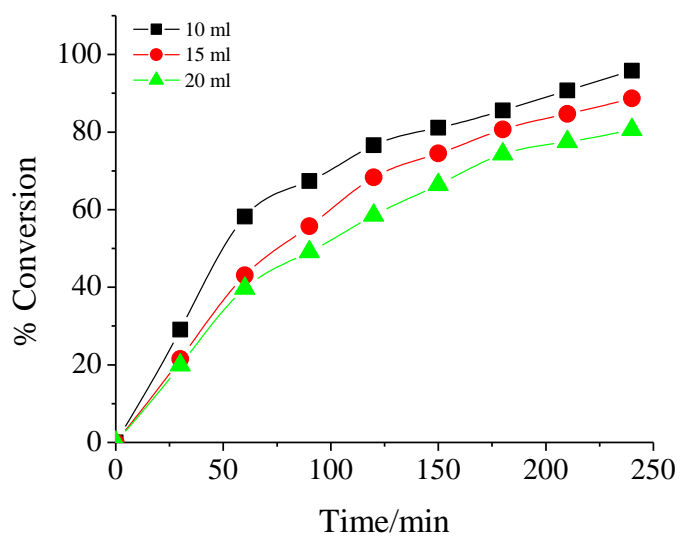
**Fig. 3.16**. Effect of solvent (methanol) amount on the oxidation of benzoin. Reaction conditions: benzoin (1.06 g, 5 mmol), catalyst amount (0.0005 g) and 30% $H_2O_2$ (1.7 g, 15 mmol).
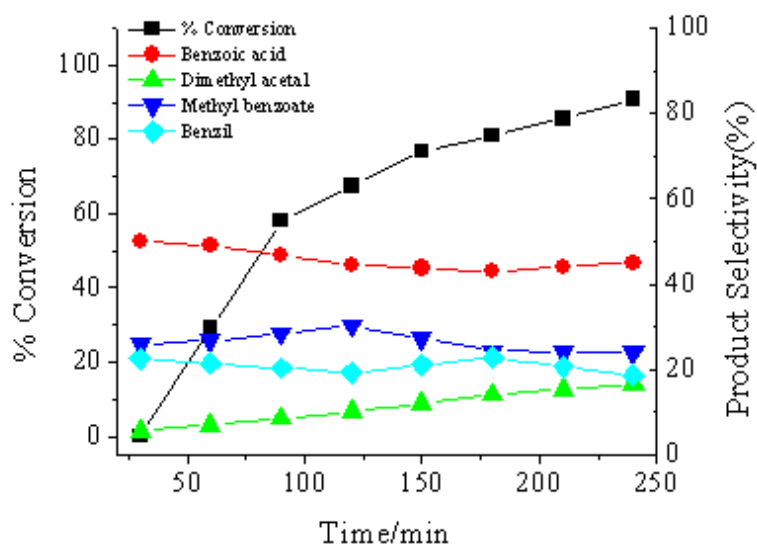
**Fig. 3.17.** Plot showing percentage conversion of benzoin and the selectivity of benzoic acid, benzaldehyde dimethylacetal, methyl benzoate and benzil formation as a function of time. Reaction condition: benzoin (1.06 g, 5 mmol), $H_2O_2$ (1.7 g, 15 mmol), $[MoO_2L^2(CH_3OH)]$, **2** (0.0005 g) and 10 mL methanol.
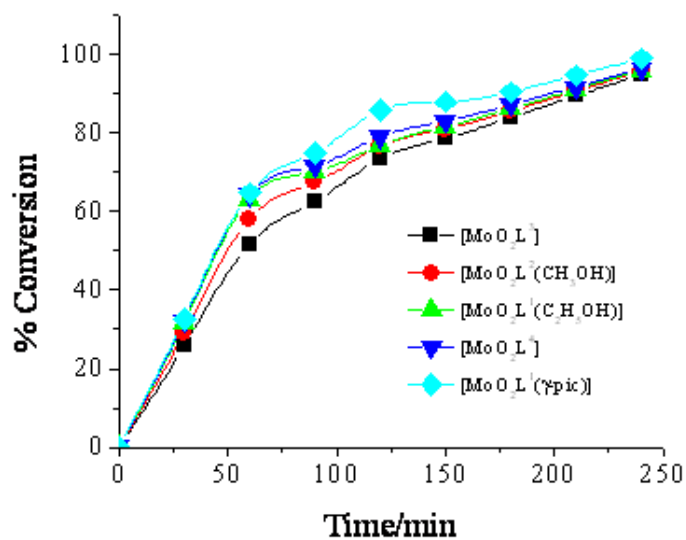
**Fig. 3.18.** Comparison of various catalysts on the oxidation of benzoin. Reaction conditions: benzoin (1.06 g, 5 mmol), 30% $H_2O_2$ (1.7 gm, 15 mmol), catalyst amount (0.0005 gm) and methanol (10 mL).

*3.3.8.2. Oxidative bromination of salicylaldehyde*

Oxidative bromination of salicylaldehyde, a functional mimic of haloperoxidases, in aqueous solution at room temperature has also been carried out successfully. By using these dioxomolybdenum(VI) complexes as catalyst precursors in the presence of KBr, $HClO_4$ and $H_2O_2$ gave mainly three products, namely 5-bromosalicylaldehyde, 3,5-dibromosalicylaldehyde and 2,4,6- tribromophenol; (**Scheme 3.4**).
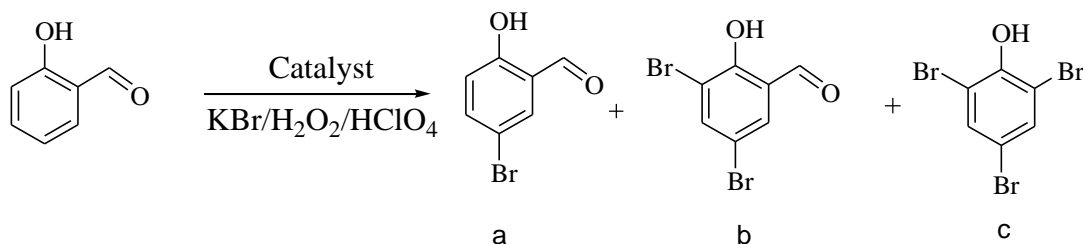


**Scheme 3.4.** Main products obtained upon oxidative bromination of salicylaldehyde. (a) 5-bromosalicylaldehyde, (b) 3,5-dibromosalicylaldehyde and (c) 2,4,6- tribromophenol.

After several trials (**Table 3.8**), the best suited reaction conditions obtained for the maximum conversion of 5 mmol (0.610 g) of salicylaldehyde were: KBr (1.785 g, 15 mmol), aqueous 30% $H_2O_2$ (1.71 g, 15 mmol), catalyst (0.0005), aqueous 70% $HClO_4$ (2.86 g, 20 mmol) and water (20 mL). However, the addition of $HClO_4$ in four equal portions (at t = 0, 45, 90 and 135 min. of reaction time) was necessary to improve the conversion of the substrate and to avoid decomposition of the catalyst. A total of 3 hr was required to complete the reaction. Under the above conditions, a maximum of 96% conversion was achieved with $[MoO_2L^2(CH_3OH)]$ (**2**) and all three products were identified; **Table 3.8**. The presence of three equivalent of $H_2O_2$ facilitates not only the formation of HOBr which ultimately helps in the oxidative bromination of salicylaldehyde but also affects on the selectivity of different products. Other catalysts gave similar results. Lowering the amount of $H_2O_2$ increased the formation of 5-bromosalicylaldehyde. In the absence of the catalyst, the reaction mixture gave *ca.* 40% conversion of salicylaldehyde where selectivity of the formation of 5-bromosalicylaldehyde is 89%.

Other complexes have also been tested under similar reaction conditions and the obtained results are summarized in **Table 3.9**. It is clear from the table that all complexes have equally good catalytic potential with high turnover frequency. The selectivity of the 5-bromosalicylaldehyde (56.5–75%) is much high for most complexes except for [MoO$_2$L$^4$] (**4**) which exhibits only 47.5 % selectivity. The overall selectivity of three products follows the order: 5-bromosalicylaldehyde > 2,4,6- tribromophenol > 3,5-dibromosalicylaldehyde.
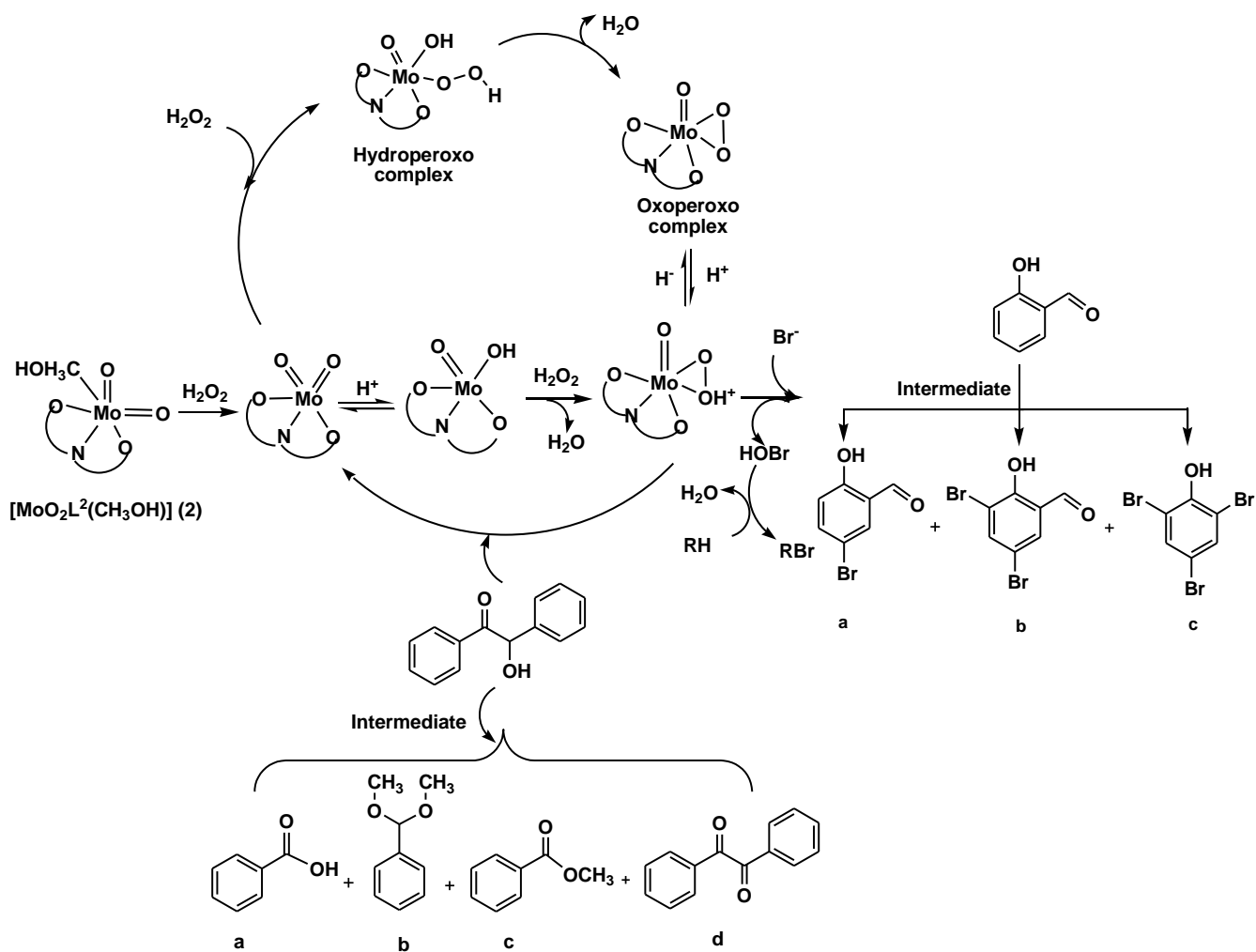


**Scheme 3.5.** Mechanism of the catalytic oxidation of benzoin and oxidative bromination of salicylaldehyde

**Table 3.8**. Results of oxidative bromination of salicylaldehyde catalyzed by [MoO$_2$L$^2$(CH$_3$OH)] (**2**) after 3 hr of contact time

| Entry no. | Catalyst [g] | H$_2$O$_2$ [g, mmol] | KBr [g, mmol] | HClO$_4$ [g, mmol] | Conversion [%] |
|---|---|---|---|---|---|
| 1 | 0.0005 | 0.57, 5 | 1.78, 15 | 2.86, 20 | 66 |
| 2 | 0.0005 | 1.14, 10 | 1.78, 15 | 2.86, 20 | 81 |
| 3 | 0.0005 | 1.71, 15 | 1.78, 15 | 2.86, 20 | 96 |
| 4 | 0.0005 | 1.71, 15 | 0.59, 5 | 2.86, 20 | 57 |
| 5 | 0.0005 | 1.71, 15 | 1.19, 10 | 2.86, 20 | 77 |
| 6 | 0.0005 | 1.71, 15 | 1.78, 15 | 1.43, 10 | 67 |
| 7 | 0.0005 | 1.71, 15 | 1.78, 15 | 2.14, 15 | 89 |
| 8 | 0.0010 | 1.71, 15 | 1.78, 15 | 2.86, 20 | 98 |
| 9 | 0.0015 | 1.71, 15 | 1.78, 15 | 2.86, 20 | 99 |

**Table 3.9.** Effect of different catalysts on the oxidative bromination of salicylaldehyde, TOF and product selectivity.

| Catalyst (g) | TOF [h$^{-1}$] | Conversion [%] | Selectivity [%][a] | | |
|---|---|---|---|---|---|
| | | | monobromo | Dibromo | Tribromo |
| [MoO$_2$L$^1$(C$_2$H$_5$OH)] (**1**) | 1555 | 98 | 60.6 | 1.6 | 37.8 |
| [MoO$_2$L$^1$($\gamma$-pic)] ( **1a**) | 1673 | 95 | 75 | 4.4 | 20.5 |
| [MoO$_2$L$^2$(CH$_3$OH)] (**2**) | 1482 | 96 | 75 | 12.1 | 12.6 |
| [MoO$_2$L$^3$]$_n$ (**3**) | 1415 | 99 | 56.6 | 1.7 | 41.7 |
| [MoO$_2$L$^4$] (**4**) | 1470 | 99 | 47.5 | 1.6 | 51.0 |
| Without catalyst | | 40 | 89 | 0.2 | 10.8 |

[a] (a) 5-bromosalicylaldehyde, (b) 3,5-dibromosalicylaldehyde and (c) 2,4,6- tribromophenol

*3.3.8.3. Reactivity of complexes with $H_2O_2$*

Dioxomolybdenum (VI) complexes are known to react with $H_2O_2$ to form the corresponding oxoperoxo complexes [67]. In order to throw some light on the reaction mechanism of catalytic reactions (**Scheme 3.5**), complex $[MoO_2L^2(CH_3OH)]$ (**2**) dissolved in DMSO was reacted with $H_2O_2$ and spectral changes were monitored by electronic absorption spectroscopy. Thus, the stepwise additions of $H_2O_2$ (1.47 g, 13 mmol) of 30% $H_2O_2$ dissolved in 5 mL of DMSO to 25 mL of ca. $6.7 \times 10^{-3}$ M solution of $[MoO_2L^2(CH_3OH)]$ (**2**) in DMSO causes the decrease in the intensities of the 468 nm band and finally disappear (**Fig. 3.19**). Simultaneously, two bands start appearing at 369 and 383 nm and become intense after addition of excess of $H_2O_2$. The intensity of the 337 nm band decreases slowly along with the appearance of a shoulder band at ca. 312 nm. We have interpreted this result in terms of the formation of the oxoperoxomolybdenum(VI) complex. The new bands at 383 and 368 nm may be assigned to LMCT and n–$\pi$* transitions, respectively. The later one was not visible in $[MoO_2L^2(CH_3OH)]$ (**2**) while the band at 312 nm is assignable to $\pi - \pi$* transition. Exact mechanism for the catalytic oxidation of benzoin catalysed by dioxomolybdenum(VI) complex in presence of $H_2O_2$ is not clear at present. However, based on the oxidation products obtained and experiments carried out above it is concluded that the reaction used the following pathway. Where, $[MoO_2L^2(CH_3OH)]$ (**2**) reacts with $H_2O_2$ to give Mo(oxo)peroxo $[MoO(O_2)-]$ complex which finally catalyses abstraction of hydrogen from alcoholic group of benzoin to give benzil. By oxidative cleavage benzil produces benzoic acid which on subsequent esterification gives methylbenzoate. The acid produced by hydrogen peroxide during catalytic reaction catalyses the esterification [68].

During bromination process, molybdenum reacts with 1 or 2 equiv. of $H_2O_2$, forming oxoperoxo species, which ultimately oxidise bromide, possibly by formation of a hydroperoxo intermediate. The oxidised bromine species ($Br_2$, $Br_3^-$ and/or HOBr) then brominates the substrate. The presence of acid was found to be essential during catalytic oxidative bromination reaction [69].
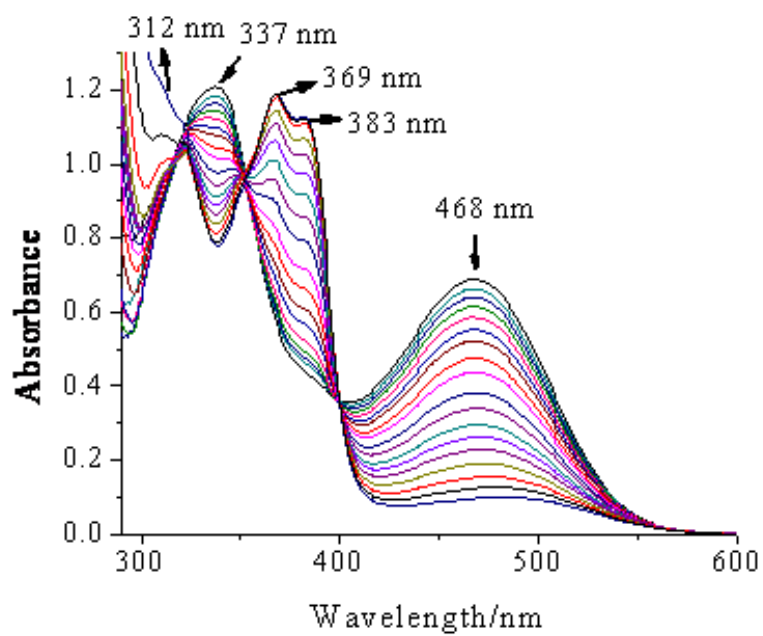
**Fig. 3.19.** UV–Vis spectral changes observed during titration of $[MoO_2L^2(CH_3OH)]$ (**2**) with $H_2O_2$. The spectra were recorded after successive additions of 1-drop portions of 30% $H_2O_2$ (13 mmol) dissolved in 5 mL of DMSO to 25 mL of $6.7 \times 10^{-3}$ M solution in DMSO.

**3.4. Conclusions**

Synthesis of four new dioxomolybdenum(VI) complexes with aroylhydrazone of naphthol-derivative (**1**, **2**, **3** and **4**) and one mixed-ligand mononuclear complex (**1a**) have been prepared and characterized. The complexes have been screened for their antibacterial activity against *Escherichia coli, Bacillus subtilis, Proteus vulgaris and Klebsiella pneumoniae*. Minimum inhibitory concentration of these complexes and antibacterial activity indicates the complexes (**1**) and (**1a**) as the potential lead molecule for drug designing. The one labile binding site in these complexes has an added advantage as has been shown by reacting complex (**2**) with $H_2O_2$ to give corresponding peroxo species without changing original coordinating sites i.e. ONO coordination of ligands. Again the labile peroxo group of complexes has an added advantage as they transfer oxygen in catalytic oxidation as has been demonstrated for the oxidation, by peroxide, of benzoin using these complexes as catalysts. Under optimized reaction conditions benzoin gives 95-99% conversion with four reaction products benzoic acid, benzaldehyde-dimethylacetal, methyl benzoate and benzil. The functional mimic of haloperoxidase is demonstrated by the oxidative bromination of salicylaldehyde where these complexes have shown 95–99% conversion of salicylaldehyde to brominated and other products with high turnover frequency.

**References**

[1] A.A.A. Abu-Hussen, J. Coord. Chem. 59 (2006) 157.

[2] M.S. Karthikeyan, D.J. Prasad, B. Poojary, K.S. Bhat, Bioorg. Med. Chem. 14 (2006) 7482.

[3] K. Singh, M.S. Barwa, P. Tyagi, Eur. J. Med. Chem. 41 (2006) 147.

[4] P. Pannerselvam, R.R. Nair, G. Vijayalakshmi, E.H. Subramanian, S.K. Sridhar, Eur. J. Med. Chem. 40 (2005) 225.

[5] S.K. Sridhar, M. Saravanan, A. Ramesh, Eur. J. Med. Chem. 36 (2001) 615.

[6] S.N. Pandeya, D. Sriram, G. Nath, E. De Clercq, Eur. J. Pharm. Sci. 9 (1999) 25.

[7] R. Mladenova, M. Ignatova, N. Manolova, T.S. Petrova, I. Rashkov, Eur. Polym. J. 38 (2002) 989.

[8] O.M. Walsh, M.J. Meegan, R.M. Prendergast, T.A. Nakib, Eur. J. Med. Chem. 31 (1996) 989.

[9] Z. Trávníček, M. Maloň, Z. Šindelář, K. Doležal, J. Rolčik, V. Kryštof, M. Strnad, J. Marek, J. Inorg. Biochem. 84 (2001) 23.

[10] U. El-Ayaan, A.A.M. Abdel-Aziz, Eur. J. Med. Chem. 40 (2005) 1214.

[11] M. Sönmez, I. Berber, E. Akbaş, Eur. J. Med. Chem. 41 (2006) 101.

[12] M.R. Maurya, S. Agarwal, M. Abid, A. Azam, C. Bader, M. Ebel, D. Rehder, Dalton Trans. (2006) 937.

[13] D.K. Johnson, T.B. Murphy, N.J. Rose, W.H. Goodwin, L. Pickart, Inorg. Chim. Acta 67 (1982) 159.

[14] T.B. Chaston, D.B. Lovejoy, R.N. Watts, D.R. Richardson, Clin. Cancer Res. 9 (2003) 402.

[15] G. Link, P. Ponka, A.M. Konijn, W. Breuer, Z.I. Cabantchik, C. Hershko, Blood 101 (2003) 4172.

[16] S. Pasayat, S.P. Dash, Saswati, P.K. Majhi, Y.P. Patil, M. Nethaji, H.R. Dash, S. Das , R. Dinda, Polyhedron 38 (2012) 198.

[17] S.P. Dash, S. Pasayat, Saswati, H.R. Dash, S. Das, R.J. Butcher, R. Dinda, Polyhedron 31 (2012) 524.

[18] R. Dinda, P.K. Majhi, P. Sengupta, S. Pasayat, S. Ghosh, L.R. Falvello, T.C.W. Mak, Polyhedron 29 (2010) 248.

[19] J.H. Enemark, J.J.A. Cooney, J.J. Wang, R.H. Holm, Chem. Rev. 104 (2004) 1175.

[20] E.I. Stiefel, Met. Ions Biol. Syst. 39 (2002) 727.

[21] R. Hille, Chem. Rev. 96 (1996) 2757.

[22] D. Collison, C.D. Garner, J.A. Joule, Chem. Soc. Rev. 25 (1996) 25.

[23] J.T. Hoffman, S. Einwaechter, B.S. Chohan, P. Basu, C.J. Carrano, Inorg. Chem. 43 (2004) 7573.

[24] A. Sigel, H. Sigel (Eds.), Metal Ions in Biological Systems 39, Molybdenum and Tungsten: Their Roles in Biological Processes, Marcel Dekker, New York, (2002)

[25] R.C. Bray, B. Adams, A.T. Smith, B. Bennett, S. Bailey, Biochemistry 39 (2000) 11258.

[26] K. Jeyakumar, D.K. Chand, J. Chem. Sci. 121 (2009) 111.

[27] M.R. Maurya,Curr. Org. Chem. 16 (2012) 73.

[28] R.D. Chakravarthy, K. Suresh, V. Ramkumar, D.K. Chand, Inorg. Chim. Acta 376 (2011) 57.

[29] Z. Hu, X. Fu, Y. Li, Inorg. Chem. Commun. 14 (2011) 497.

[30] M. Herbert, F. Montilla, A. Galindo, J. Mol. Catal. A: Chem. 338 (2011) 111.

[31] A. Rezaeifard, I. Sheikhshoaie, N. Monadi, M. Alipour, Polyhedron 29 (2010) 2703.

[32] I. Sheikhshoaie, A. Rezaeifard, N. Monadi, S. Kaafi, Polyhedron 28 (2009) 733.

[33] A. Gunyara, D. Betzb, M. Dreesb, E. Herdtweck, F.E. Kuhna, J. Mol. Catal. A: Chem. 331 (2010) 117.

[34] M.R. Maurya , S. Sikarwar , P. Manikandan , Appl. Catal., A 315 (2006) 74.

[35] A.J. Burke, Coord. Chem. Rev. 252 (2008) 170.

[36] K.R. Jain, W.A. Herrmann, F.E. Kuhn, Coord. Chem. Rev. 252 (2008) 556.

[37] K.C. Gupta, A.K. Sutar, Coord. Chem. Rev. 252 (2008) 1420.

[38] B. Frédéric, Coord. Chem. Rev. 236 (2003) 71.

[39] A. Syamal, M.R. Maurya, Coord. Chem. Rev. 95 (1989) 183.

[40] R.A. Sheldon, J.K. Kochi, Metal Catalyzed Oxidations of Organic Compounds, Academic Press, New York, (1981).

[41] B.M. Trost, I. Fleming, S.V. Ley (Eds.), Comprehensive Organic Synthesis, Pergamon, Oxford, 7 (1991) 251.

[42] G.J.-J. Chen, J.W. McDonald, W.E. Newton, Inorg. Chem. 15 (1976) 2612.

[43] I. Kızılcıklı, S. Eğlence, A. Gelir, B. Ülküseven, Transition Met. Chem. 33 (2008) 775.

[44] A. Syamal, D. Kumar, Transition Met. Chem. 7 (1982) 118.

[45] A. Syamal, D. Kumar, J. Ind. Chem. Soc. 65 (1988) 112.

[46] R.L.Dutta, A.K. Pal, Ind. J. Chem. A. 22 (1983) 871.

[47] G.M. Sheldrick, SHELXS-97, Program for Crystal Structure Determination, Universitäet Gö ttingen, Gö ttingen, Germany, (1997).

[48] G.M. Sheldrick, SHELXL-97, Program for Refinement of Crystal Structures, Universitäet Gö ttingen, Gö ttingen, Germany, (1997).

[49] Clinical and Laboratory Standards Institute Methods for Dilution Antimicrobial Susceptibility Tests for Bacteria That Grow Aerobically—Seventh Edition: Approved Standard M7-A7. CLSI, Wayne, PA, USA, (2006).

[50] A.A. Abdel Aziz, J. Mol. Struct. 979 (2010) 77.

[51] A.R. Yaul, V.V. Dhande, S.G. Bhadange, A.S. Aswar, Russ. J. Inorg. Chem. 56 (2011) 549.

[52] R. Dinda, P. Sengupta, S. Ghosh, H.M. Figge, W.S. Sheldrick, Dalton Trans. (2002) 4434.

[53] R. Dinda, P. Sengupta, S. Ghosh, W.S. Sheldrick, Eur. J. Inorg. Chem. (2003) 363.

[54] R.D.R.S. Manian, R. Leino, O. Wichmann, A. Lehtonen, Inorg. Chem. Commun. 12 (2009) 1004.

[55] N.R. Pramanik, S. Ghosh, T.K. Raychaudhuri, S. Ray, R.J. Butcher, S.S. Mandal, Polyhedron 23 (2004) 1595.

[56] T.A. Hanna, A.K. Ghosh, C. Ibarra, M.A. Mendez-Rojas, A.L. Rheingold, W.H. Watson, Inorg. Chem. 43 (2004) 1511.

[57] A. Tarushi, E.K. Efthimiadou, P. Christofis, G. Psomas. Inorg. Chim. Acta 360 (2007) 3978.

[58] E.K. Efthimiadou, Y. Sanakis, N. Katsaros, A. Karaliota, G. Psomas, Polyhedron 26 (2007) 1148.

[59] A.M. Ramadan, J. Inorg. Biochem. 65 (1997) 183.

[60] P.G. Avaji, C.H.V. Kumar, S.A. Patil, K.N. Shivananda, C. Nagaraju, Eur. J. Med. Chem. 44 (2009) 3552.

[61] E.B. Anderson, T.E. Long, Polymer 51 (2010) 2447.

[62] R. Dahiya, H. Gautam, Af. J. Pharm. Pharmacol. 5 (2011) 447.

[63] N. Sharma, M. Kumari, V. Kumar, J. Coord. Chem. 63 (2010) 1940.

[64] Z.H. Chohan, S.H. Sumrra, M.H. Youssoufi, Eur. J. Med. Chem. 45 (2010) 2739.

[65] K.S. Prasad, L.S. Kumar, S.C. Shekar, M. Prasad, H.D. Revanasiddappa, Chem. Sci. J. (2011) 12.

[66] G.B. Gill, in Comprehensive Organic Synthesis, ed. G. Pattenden, Pergamon Press, New York 3 (1991) 821.

[67] M.R. Maurya, M. Kumar, U. Kumar, J. Mol. Catal. A: Chem. 273 (2007) 133.

[68] M.R. Maurya, S. Sikarwar, P. Manikandan, Appl. Catal., A 315 (2006) 74.

[69] A. Butler, M.J. Clague, G.E. Meister, Chem. Rev. 94 (1994) 625.

# Chapter 4

**Synthesis, Structure and Characterization of Dimeric and Tetrameric Dioxomolybdenum(VI) Complexes of *N,N*'-disalicyloylhydrazine**

# Chapter 4

**Synthesis, Structure and Characterization of Dimeric and Tetrameric Dioxomolybdenum(VI) Complexes of *N,N'*-Disalicyloylhydrazine**

**Abstract**

The *in situ* reaction of salicyloylhydrazide and its corresponding hydrazone with $[MoO_2(acac)_2]$ afforded two novel and unusual type dimeric $[(Mo^{VI}O_2)_2L]$ (**1**) and tetrameric $[\{(C_2H_5OH)LO_3Mo_2^{VI}\}_2(\mu\text{-}O)_2]\cdot C_2H_5OH$ (**2**) dioxomolybdenum(VI) complexes with *N,N'*–disalicyloylhydrazine ($H_2L$). These binucleating ligands were formed by the self-combination of acid hydrazide or corresponding hydrazone. The complexes were characterized by various spectroscopic techniques (IR, UV and NMR) and also by electrochemical study. The molecular structures of both have been confirmed by X-ray crystallography. The above studies indicate that the *N,N'*–disalicyloylhydrazine ($H_2L$) has the normal tendency to form both dimeric and tetrameric complexes coordinated through the dianionic tridentate manner.

## 4.1. Introduction

The coordination chemistry of transition metals with ligands from the hydrazine family has been of interest due to different bonding modes shown by them with both electron rich and electron poor metals. Acylhydrazones have been extensively investigated by chemists for the synthesis of coordination polymers owing to their inherent coordination and hydrogen-bonding donor/acceptor functionalities, as well as their biological activities [1,2].

However, the research on the compounds with symmetrical diaroylhydrazine ligands is limited [3–10]. The *N,N′*–diacylhydrazines have value as structural components of heterocyclic ring systems [11], and as tuberculostatic agents [12]. The *N,N′*–bis-salicylhydrazine [13], which had previously been known to chelate a variety of metal ions [13,14], has been shown to exhibit potent inhibition of the human immunodeficiency virus (HIV) integrase [15]. This enzyme is a potential target for the development of new anti-HIV therapeutics [16]. On the other hand, among all the transition metals, the coordination chemistry of high-valent molybdenum(VI) with Schiff base ligand has attracted wide interests due to its biochemical significance [17−19], as well as for the involvement of molybdenum(VI) compounds as catalysts in several industrial processes such as amoxidation of propene, epoxidation of olefins, etc. [20,21]. In this chapter, we report the synthesis and structural studies of two novel di- and tetranuclear dioxomolybdenum(VI) complexes of *N,N′*–disalicyloylhydrazine. These complexes are fully characterized by various physicochemical techniques.

## 4.2. Experimental

### 4.2.1. Materials

$[MoO_2(acac)_2]$ and salicyloyl hydrazide were prepared as described in the literature [22,23]. Reagent grade solvents were dried and distilled prior to use. All other chemicals were reagent grade, available commercially and used as received. Commercially available TBAP (tetra butyl ammonium perchlorate) was properly dried and used as a supporting electrolyte for recording cyclic voltammograms of the complexes.

### 4.2.2. Physical Measurements

Elemental analyses were performed on a Vario ELcube CHNS Elemental analyzer. IR spectra were recorded on a Perkin-Elmer Spectrum RXI spectrometer. $^1$H NMR spectra were recorded with a Bruker Ultrashield 400 MHz spectrometer using $SiMe_4$ as an internal standard. Electronic spectra were recorded on a Lamda25, PerkinElmer spectrophotometer. Magnetic susceptibility was measured with a Sherwood Scientific AUTOMSB sample magnetometer. Electrochemical data were collected using a PAR electrochemical analyzer and a PC-controlled Potentiostat/Galvanostat (PAR 273A) at 298 K in a dry nitrogen atmosphere. Cyclic voltammetry experiments were carried out with a platinum working electrode, platinum auxiliary electrode, Ag/AgCl as reference electrode and TBAP as supporting electrolyte. X-band EPR measurements were performed on a JEOL JES-FA 200 instrument.

### 4.2.3. Synthesis of salicyloylhydrazone of acetophenone

The ligand salicyloylhydrazone of acetophenone was prepared by the condensation of equimolar ratio of salicyloylhydrazide 2.72 g (20.00 mmol) and acetophenone 2.38 g (20.00 mmol) in stirring ethanol (25 ml) for 2 hr following a standard procedure [24]. The resulting yellowish-white compound was filtered, washed with ethanol and dried over fused $CaCl_2$. M.P. 160$^o$C. Yield: 0.18 g (75%). Anal. Calcd. for $C_{15}H_{14}N_2O_2$: C, 70.88; H, 5.55; N, 11.08. Found: C, 70.90; H, 5.54; N, 11.06%. $^1$H NMR (400 MHz, DMSO-$d_6$): $\delta$ = 11.83 (s, 1H, OH), 11.35 (s, 1H, NH), 8.03–6.97 (m, 9H, Aromatic), 2.33 (s, 3H, $CH_3$),.$^{13}$C NMR (DMSO-$d_6$, 100 MHz): $\delta$ = 164.99, 159.50, 157.99, 149.49, 134.44, 132.08, 129.04, 128.83, 126.89, 119.85, 119.08, 117.77, 116.92, 116.06, 14.34.

*4.2.4. Synthesis of complex [(Mo<sup>VI</sup>O₂)₂L] (1)*

*4.2.4. Synthesis of complex [(Mo$^{VI}$O$_2$)$_2$L] (**1**)*

To the refluxing solution of 0.15 g (1.0 mmol) of salicyloylhydrazide in 30 mL of ethanol 0.32 g (1.0 mmol) of MoO$_2$(acac)$_2$ was added [25]. The color of the solution changed to dark red. The mixture was then refluxed for 3 hr. After leaving the solution for 2 days at room temperature, fine dark red colored crystals were isolated and a suitable single crystal was selected for X-ray analysis. *[(Mo$^{VI}$O$_2$)$_2$L] (**1**):* Yield: 0.36g (68%). Anal. Calcd for C$_{14}$H$_8$N$_2$O$_8$Mo$_2$: C, 32.08; H, 1.53; N, 5.34. Found: C, 32.06; H, 1.55; N, 5.37%. $^1$H NMR (DMSO-d$_6$, 400 MHz): $\delta$ = 7.94–7.02 (m, 4H, Aromatic). $^{13}$C NMR (DMSO-d$_6$, 100 MHz): $\delta$ = 163.55, 162.00, 135.42, 129.87, 122.53, 120.03, 115.80.

*4.2.5. Synthesis of complex [{(C$_2$H$_5$OH)LO$_3$Mo$_2$$^{VI}$}$_2$(μ-O)$_2$]·C$_2$H$_5$OH (**2**)*

0.24 g (1.00 mmol) of salicyloylhydrazone of acetophenone was dissolved in 30 mL ethanol. When 0.32 g (1.00 mmol) of MoO$_2$(acac)$_2$ was added to the solution, the color changed to dark orange [24]. The solution mixture was then refluxed for 3 hr. After leaving the solution for 2 days at room temperature, fine dark orange crystals were isolated and a suitable single crystal was selected for X-ray analysis. *[{(C$_2$H$_5$OH)LO$_3$Mo$_2$$^{VI}$}$_2$(μ-O)$_2$]·C$_2$H$_5$OH (**2**):* Yield: 0.19g (73%). Anal. Calcd for C$_{36}$H$_{40}$N$_4$O$_{20}$Mo$_4$: C, 35.06; H, 3.27; N, 4.55. Found: C, 35.08; H, 3.25; N, 4.56%. $^1$H NMR (DMSO-d$_6$, 400 MHz): $\delta$ = 8.14–7.06 (m, 8H, Aromatic), 4.36 (s, 1H, OH), 3.42 (q, 2H, CH$_2$), 1.05 (s, 3H, CH$_3$). $^{13}$C NMR (DMSO-d$_6$, 100 MHz): $\delta$ = 163.58, 163.46, 162.42, 162.02, 135.58, 134.67, 129.87, 128.69, 122.67, 121.22, 120.10, 118.87, 115.67, 114.96, 56.49, 55.95, 19.10, 19.00.

*4.2.6. Crystallography*

Suitable single crystal of **1** and **2** were chosen for X-ray diffraction studies. Crystallographic data and details of refinement are given in **Table 4.1**. Both the compounds crystallized in the Triclinic space group *P*-1. The unit cell parameters and the intensity data for the complexes were collected at ~293 K, on a Bruker Smart Apex CCD diffractometer using graphite monochromated Mo K$\alpha$ radiation (k = 0.71073 Å), employing the $\omega$–$2\theta$ scan technique. The intensity data were corrected for Lorentz, polarization and absorption effects. The structures were solved using the SHELXS97 [26] and refined using the SHELXL97 [27] computer programs. The non-hydrogen atoms were refined anisotropically.

**Table 4.1** Crystal and Refinement Data of Complexes **1** and **2**

| Compound | 1 | 2 |
|---|---|---|
| Formula | $C_{14}H_8Mo_2N_2O_8$ | $C_{36}H_{40}Mo_4N_4O_{20}$ |
| M | 524.10 | 1232.50 |
| Crystal symmetry | Triclinic | Triclinic |
| Space group | $P$ -1 | $P$ -1 |
| $a(\text{Å})$ | 3.96540(10) | 9.5892(3) |
| $b(\text{Å})$ | 9.5080(2) | 10.7151(4) |
| $c(\text{Å})$ | 10.1683(2) | 11.4986(4) |
| $\alpha$ (°) | 76.167(10) | 68.042(10) |
| $\beta$ (°) | 87.856(10) | 73.353(10) |
| $\gamma$ (°) | 82.230(10) | 81.152(2) |
| $V(\text{Å}^3)$ | 368.834(14) | 1048.39(6) |
| Z | 1 | 1 |
| $D_{calc}(g.cm^{-3})$ | 2.360 | 1.952 |
| $F(000)$ | 254 | 612 |
| $\mu(Mo\text{-}K\alpha)(mm^{-1})$ | 1.753 | 1.256 |
| $2\theta(max)(°)$ | 26.37 | 25.50 |
| Reflections collected / unique | 11936/ 1498 | 9430 / 3870 |
| $R_1^a[I>2\sigma(I)]$ | R1 = 0.0224, wR2= 0.0782 | R1 = 0.0413, wR2 = 0.0790 |
| $wR_2^b[all\ data]$ | R1 = 0.0214, wR2= 0.0815 | R1 = 0.0285, wR2= 0.0736 |
| S[goodness of fit] | 0.793 | 1.062 |
| min./max. res.(e.$\text{Å}^{-3}$) | 0.843/ -0.649 | 0.920/ -0.873 |

$^aR_1 = \Sigma \left| F_O \right| - \left| F_C \right| / \Sigma \left| F_O \right|$

$^bwR_2 = \{\Sigma [w (F_O{}^2 - F_C{}^2)^2]/\Sigma [w (F_O{}^2)^2]\}^{1/2}$

## 4.3. Results and Discussion

### 4.3.1. Synthesis

**Scheme 4.1** summarizes the synthesis of dioxomolybdenum(VI) complexes (**1**) and (**2**) from the common ligand, *N,N'*–disalicyloylhydrazine (H$_2$L) employed in the present study. According to the demand, to provide the exact stereo and electronic environment for the stability of well known penta- and hexa coordinated dioxomolybdenum(VI) complexes, the *N,N'*–disalicyloylhydrazine ligand (H$_2$L) was synthesized by the self-combination of salicyloylhydrazide and subsequently transformed to the corresponding dioxomolybdenum(VI) complexes through *in situ* reaction of corresponding hydrazide or hydrazone and metal precursor MoO$_2$(acac)$_2$. The metal precursor in ethanol may provide the acidic medium (P$_H$ = 3.5) required for this self-combination.



**Scheme 4.1**

124
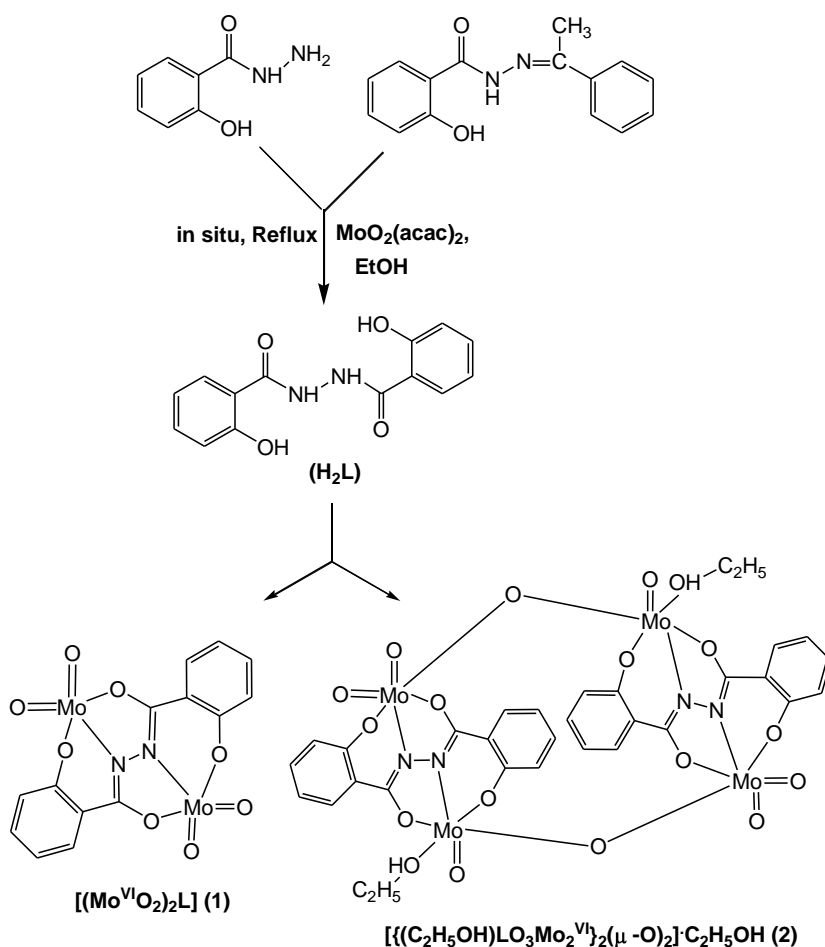
Methods used for synthesis of the precursor hydrazide, hydrazone and dioxomolybdenum complexes (**1** and **2**) are given in experimental section. These compounds are highly soluble in aprotic solvents, viz. DMF or DMSO and are sparingly soluble in alcohol, $CH_3CN$ and $CHCl_3$. Both the complexes are diamagnetic and EPR inactive, indicating the presence of molybdenum in the +6 oxidation state, and are nonconducting in solution.

### 4.3.2. Spectral properties

Spectral characteristics of precursor salicyloylhydrazone of acetophenone and complexes **1**–**2** are listed in **Table 4.2**. The IR spectra of the hydrazone ligand exhibits the peak at 3267 $cm^{-1}$, 1611$cm^{-1}$ and 1581 $cm^{-1}$ due to $v(-OH)$, $v(C=C/aromatic)$ and $v(C=N)$ stretching modes respectively. During metallation reaction the hydrazide and its hydrazone are transformed to the intermediate ligand *N,N'*–disalicyloylhydrazine and produce the corresponding dioxomolybdenum(VI) complexes (**1** and **2**). The spectra of complexes exhibit two peaks in the range 1602–1601 $cm^{-1}$ and 1579–1549 $cm^{-1}$ due to $v(C=C/aromatic)$ and $v(C=N)$ stretching modes [24] respectively. New bands at 662–644 $cm^{-1}$ for **1** and **2** are assigned to $v(Mo-N)$ [28,29]. In addition, **1**–**2** display strong and a moderately strong band in the range 944–943 $cm^{-1}$ and 921–918 $cm^{-1}$ due to terminal $v(M=O_t)$ stretch [24]. A strong band at 752 $cm^{-1}$ for complex **2** may be assigned to (Mo–O–Mo) [30]. The representative IR spectra of precursor ligand and complex **2** are given in **Figs. 4.1** and **4.2**, respectively.

The DMSO solution of all the complexes display a shoulder in the 426–423 nm region and two strong absorptions are located in the 314–312 and 274–260 nm range, which are assignable to L→Mo(dπ) LMCT and intraligand transitions respectively [24]. The electronic spectrum of complex **2** is shown in **Fig. 4.3** as the representative one.

The $^1H$ and $^{13}C$ NMR data of the precursor ligand and complexes are given in the experimental section. The spectrum of the free ligand exhibits an –OH (phenolic) resonance at δ = 11.83 ppm and one –NH proton resonance at δ = 11.35 ppm. All the aromatic proton signals of the precursor ligand are clearly observed at δ = 8.03–6.97 ppm and the $CH_3$ proton resonance is observed at δ = 2.33 ppm. The NMR spectra of the metal complexes show no resonance for –OH proton due to coordination. The aromatic protons of **1** and **2** are observed at δ = 8.14–7.02 ppm [31]. The chemical shift of the coordinated $C_2H_5OH$ of complex (**2**) exhibits an –OH resonance at δ = 4.36 ppm, –$CH_2$ resonance at δ = 3.42 ppm and –$CH_3$ resonance at δ = 1.05 ppm. The representative

NMR spectrum of precursor ligand and [(Mo$^{VI}$O$_2$)$_2$L] (**1**) is displayed in **Figs. 4.4** and **4.5**, respectively.

**Table 4.2** Characteristic IR[a] bands and electronic spectral data[b] for the studied ligand and complexes (**1–2**)

| Compounds | $\nu$(C=N) | $\nu$(Mo=O)/cm$^{-1}$ | $\lambda_{max}$/nm ($\varepsilon$/dm$^3$ mol$^{-1}$ cm$^{-1}$) |
|---|---|---|---|
| Salicyloylhydrazone of acetophenone | 1581 | -- | 331 (23524), 292 (15624) |
| [(Mo$^{VI}$O$_2$)$_2$L] (**1**) | 1579 | 944, 918 | 426 (9439), 314 (25123), 274 (16352) |
| [{(C$_2$H$_5$OH)LO$_3$Mo$_2$$^{VI}$}$_2$($\mu$-O)$_2$]·C$_2$H$_5$OH (**2**) | 1549 | 943, 921 | 423 (9569), 312 (26126), 260 (15711) |

[a] In KBr pellet; [b] In DMSO

**Fig. 4.1** IR spectrum of Salicyloylhydrazone of acetophenone

**Fig. 4.2** IR spectrum of $[\{(C_2H_5OH)LO_3Mo_2^{VI}\}_2(\mu\text{-}O)_2]\cdot C_2H_5OH$ (**2**)

**Fig. 4.3**. Electronic absorption spectrum of $[\{(C_2H_5OH)LO_3Mo_2{}^{VI}\}_2(\mu\text{-}O)_2]\cdot C_2H_5OH$ (**2**) in DMSO, at $25^0$ C

**Fig. 4.4** ^{1}H NMR spectrum of Salicyloylhydrazone of acetophenone

**Fig. 4.5** $^1$H NMR spectrum of $[(Mo^{VI}O_2)_2L]$ (**1**) in DMSO $d_6$

### 4.3.3. Electrochemical properties

Electrochemical properties of the complexes have been studied by cyclic voltammetry in DMSO solution (0.1 M TBAP). Voltammetric data are given in **Table 4.3**. The CV traces of complexes (**1–2**) exhibit two irreversible reductive responses within the potential window –0.05 to –0.15 V and –1.01 to –1.06 V, which are assigned to $Mo^{VI}/Mo^V$ and $Mo^V/Mo^{IV}$ processes respectively [24]. An oxidation wave at positive potentials in the range of +1.45 V to +1.48 V, which is assigned to the oxidation of the coordinated ligands [32]. As the Mo(VI) complex cannot undergo a metal-centered oxidation, this is attributed to a ligand-centered process [31]. The cyclic voltammogram of $[(Mo^{VI}O_2)_2L]$ (**1**) is displayed in **Fig.4.6** as the representative one.

**Table 4.3** Cyclic voltammetric results for dioxomolybdenum (VI) complexes (**1–2**) at 298 K

| Complexes | $E$pc [V][a] |
|---|---|
| $[(Mo^{VI}O_2)_2L]$ (**1**) | –0.05, –1.01 |
| $[\{(C_2H_5OH)LO_3Mo_2^{VI}\}_2(\mu\text{-}O)_2]\cdot C_2H_5OH$ (**2**) | –0.15, –1.06 |

[a] Solvent: DMSO; working electrode: platinum; auxiliary electrode: platinum; reference electrode: Ag/AgCl; supporting electrolyte: 0.1 M TBAP; scan rate: 50 mV/s. $E$pc is the cathodic peak potential

**Fig.4.6** Cyclic voltammogram of $[(Mo^{VI}O_2)_2L]$ (**1**) in DMSO

*4.3.4. Description of the X-ray structure of complex [(Mo$^{VI}$O$_2$)$_2$L] (**1**) and [{(C$_2$H$_5$OH)LO$_3$Mo$_2$$^{VI}$}$_2$($\mu$-O)$_2$]·C$_2$H$_5$OH (**2**)*
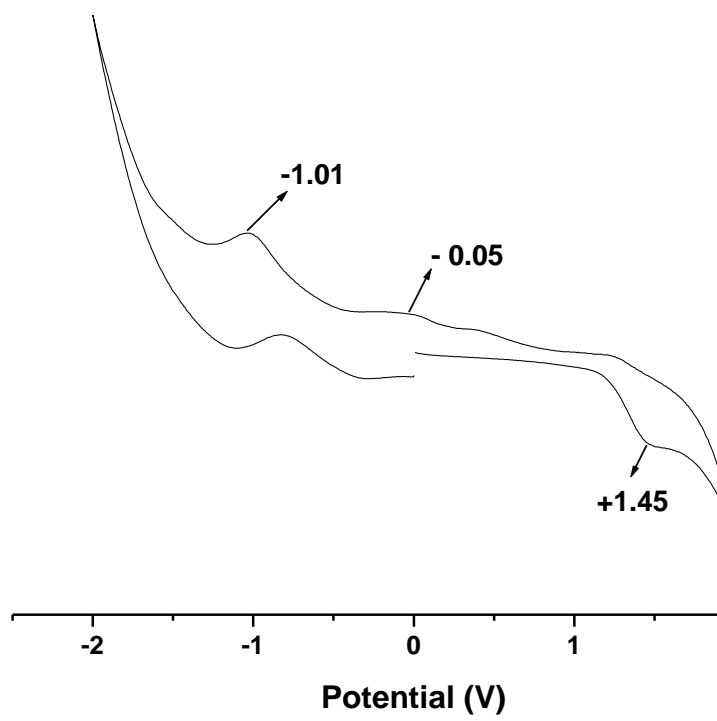
The reaction of salicyloylhydrazide and its corresponding hydrazone with metal precursor does not produce the expected complexes **I** and **II** (**Scheme 4.2**). However, during *in situ* reaction the hydrazide and its hydrazone are being transformed to *N,N'*–disalicyloylhydrazine (H$_2$L), which subsequently reacts with MoO$_2$(acac)$_2$ and produced two novel di- and tetranuclear oxomolybdenum(VI) complexes [(MoO$_2$)$_2$L] (**1**) and [{(C$_2$H$_5$OH)LO$_3$Mo$_2$$^{VI}$}$_2$($\mu$-O)$_2$]·C$_2$H$_5$OH (**2**) respectively (**Scheme 4.1**).
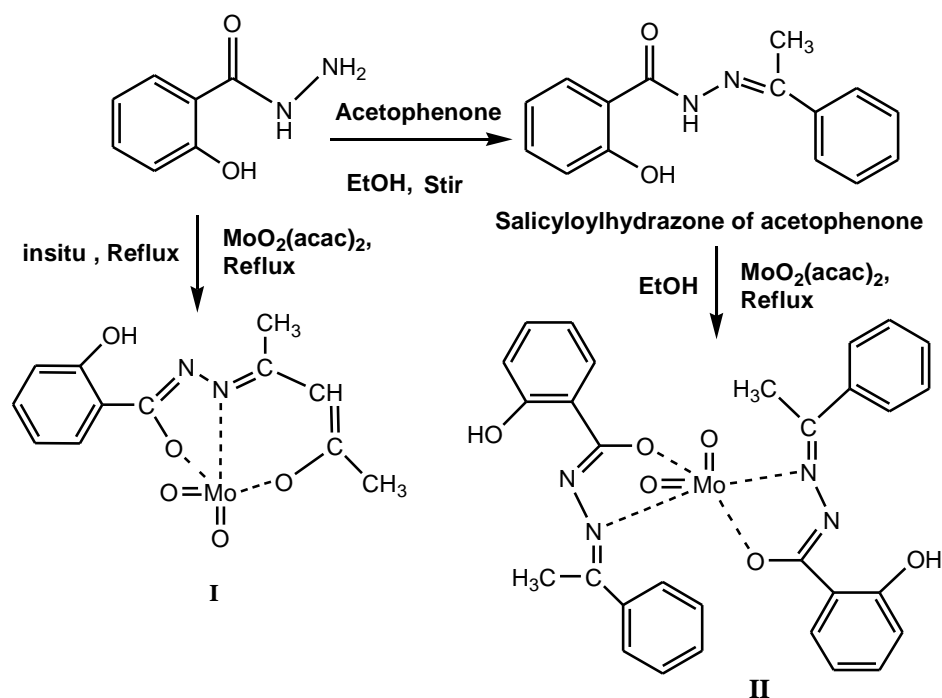


**Scheme 4.2**

The molecular structure and the atom numbering schemes for the complex **1** is shown in **Fig 4.7**, with the relevant bond distances and angles collected in **Table 4.4**. X-ray diffraction indicates complex **1** crystallizes in the triclinic system with space group *P*-1. Each molybdenum atom coordinated with 'NO$_4$' chromophore adopts a distorted tetragonal pyramidal geometry.

Both sides of the ligand behave as a tridentate (ONO) binegative one, where one side of the ligand offers two oxygens as donors to the Mo(1) center–one from the enolate oxygen O(1), another from the phenolate oxygen O(2) and the last two oxo O(3) and O(4) atoms with bite angles of 71.90(7) [O(1)–Mo(1)–N(1)] and 80.50(8) [O(2)–Mo(1)–N(1)] forming one five- and

one six-membered chelate ring. The planar structure of the chelating groups of ligand $H_2L$ in compound **1** favors the delocalization of the double bonds. Due to this, the N(1)–N(1A) bond (1.380 Å) is shorter than the standard ordinary nitrogen–nitrogen bond (1.45 Å) [33]. At the same time, the C(1)–N(1A) bond length (1.309 Å) is close to the length of the standard double carbon–nitrogen bond (1.340 Å) [13]. The lengths of other bonds and the values of bond angles in the organic ligands are close to standard values [33].

Reaction of $MoO_2(acac)_2$ with salicyloylhydrazone of acetophenone can lead to $[\{(C_2H_5OH)LO_3Mo_2^{VI}\}_2(\mu\text{-}O)_2]\cdot C_2H_5OH$ **(2)**, a novel di-$\mu$-oxo tetrameric structure (**Fig.4.8**) with the relevant bond distances and angles collected in **Table 4.5**. The molecular structure of **2** is almost similar to complex **1** and crystallizes in the triclinic system with space group *P*-1. The two halves of **2** are crystallographically equivalent with closely matching structural dimensions bridged by two oxygen atoms; hence, the structure of one half of the complex is described in detail.

Both the Mo centers [Mo(1) and Mo(2)] are six coordinated having 'NO$_5$' chromophore, giving a distorted octahedral structure. The ligand *N,N'*–disalicyloylhydrazine coordinates to the molybdenum in the same way as complex (**1**). As expected from its structure, the tridentate ligand is bonded to the Mo(1) centre in a planar fashion involving the *xy*–plane, coordinating through the phenolate oxygen O(4), the enolate oxygen O(1), the imine nitrogen atom N(2) and an oxo group O(5) lying *trans* to N(2). The fifth and sixth position of the distorted octahedron is occupied by the bridging oxygen O(6) and free ethanol molecule respectively. The coordination around Mo(2) centre is same except the sixth position which is occupied by an oxo group O(8). The Mo(1)–O(9) (alcohol) bond [2.272(3) Å] is significantly longer than the other Mo(1)–O bonds [1.692(3)–2.029(2) Å] indicating that the alcohol molecule is weakly bonded to the $MoO_2^{2+}$ core. The lengths of other bonds and the values of bond angles in the organic ligands are close to standard values [33]. In this complex (**2**) the molecules are bridged by O-H...O hydrogen bonds (dashed lines, **Fig.4.9**) involving the coordinated and solvent molecules of ethanol, forming chains propagating along the c axis direction. Detail of the classical hydrogen bonding of complex **2** is given in **Table 4.6**.

**Table 4.4** Selected Bond Distances (Å) and Bond Angles (˚) for Complex **1**

| | Distances | | |
|---|---|---|---|
| Mo(1)-O(1) | 2.037(2) | Mo(1)-O(2) | 1.900(2) |
| Mo(1)-O(3) | 1.728(2) | Mo(1)-O(4) | 1.693(2) |
| Mo(1)-N(1) | 2.211(2) | N(1)-N(1A) | 1.380(3) |
| C(1)–N(1A) | 1.309(3) | | |

| | Angles | | |
|---|---|---|---|
| O(1)-Mo(1)-O(2) | 150.01(8) | O(1)-Mo(1)-O(3) | 95.59(9) |
| O(1)-Mo(1)-O(4) | 98.08(9) | O(1)-Mo(1)-N(1) | 71.90(7) |
| O(2)-Mo(1)-O(3) | 98.85(9) | O(2)-Mo(1)-O(4) | 103.20(9) |
| O(2)-Mo(1)-N(1) | 80.50(8) | O(3)-Mo(1)-O(4) | 83.49(9) |
| O(3)-Mo(1)-N(1) | 96.15(9) | O(4)-Mo(1)-N(1) | 157.24(9) |

**Table 4.5** Selected Bond Distances (Å) and Bond Angles (°) for Complex **2**

| | | | |
|---|---|---|---|
| | | Distances | |
| Mo(1)-O(1) | 2.029(2) | Mo(2)-O(2) | 1.920(3) |
| Mo(1)-O(4) | 1.919(3) | Mo(2)-O(3) | 2.043(3) |
| Mo(1)-O(5) | 1.692(3) | Mo(2)-O(7) | 1.704(3) |
| Mo(1)-O(6) | 1.715(2) | Mo(2)-O(8) | 1.694(3) |
| Mo(1)-O(9) | 2.272(3) | Mo(2)-O(6)# | 2.409(2) |
| Mo(1)-N(2) | 2.204(3) | Mo(2)-N(1) | 2.199(3) |
| | | | |
| | | Angles | |
| O(1)-Mo(1)-O(4) | 150.1(1) | O(2)-Mo(2)-O(3) | 147.9(1) |
| O(1)-Mo(1)-O(5) | 97.2(1) | O(2)-Mo(2)-O(8) | 101.4(1) |
| O(1)-Mo(1)-O(6) | 96.1(1) | O(2)-Mo(2)-O(7) | 102.0(1) |
| O(1)-Mo(1)-O(9) | 82.2(1) | O(2)-Mo(2)-N(1) | 80.3(1) |
| O(1)-Mo(1)-N(2) | 72.3(1) | O(2)-Mo(2)-O(6) # | 81.1(1) |
| O(4)-Mo(1)-O(5) | 104.3(1) | O(3)-Mo(2)-O(7) | 96.8(1) |
| O(4)-Mo(1)-O(6) | 98.0(1) | O(3)-Mo(2)-O(8) | 98.2(1) |
| O(4)-Mo(1)-O(9) | 80.5(1) | O(3)-Mo(2)-N(1) | 71.8(1) |
| O(4)-Mo(1)-N(2) | 80.2(1) | O(3)-Mo(2)-O(6) # | 75.92(9) |
| O(5)-Mo(1)-O(6) | 105.2(1) | O(7)-Mo(2)-O(8) | 105.6(1) |
| O(5)-Mo(1)-O(9) | 82.1(1) | O(7)-Mo(2)-N(1) | 154.4(1) |
| O(5)-Mo(1)-N(2) | 157.5(1) | O(7)-Mo(2)-O(6) # | 82.1(1) |
| O(6)-Mo(1)-O(9) | 172.6(1) | O(8)-Mo(2)-N(1) | 98.8(1) |
| O(6)-Mo(1)-N(2) | 95.8(1) | O(7)-Mo(2)-O(6) # | 171.0(1) |
| O(9)-Mo(1)-N(2) | 76.8(1) | N(1)-Mo(2)-O(6) # | 73.0(1) |

**Table 4.6** Hydrogen bond distances (A) and angles ($^o$) for Complex **2**

| D–H…A | D–H(Å) | H...A(Å) | D...A(Å) | <D–H…A (∘) |
|---|---|---|---|---|
| O9–H90…O10 | 0.873(19) | 1.81(2) | 2.601(4) | 137.7(19) |
| O10–H100…O4 | 0.82 | 2.27 | 2.988(4) | 147 |
| O10–H100…O9 | 0.82 | 2.49 | 3.189(4) | 143 |

*Symmetry transformations used to generate equivalent atoms:*

(a) -x, -y, 2-z
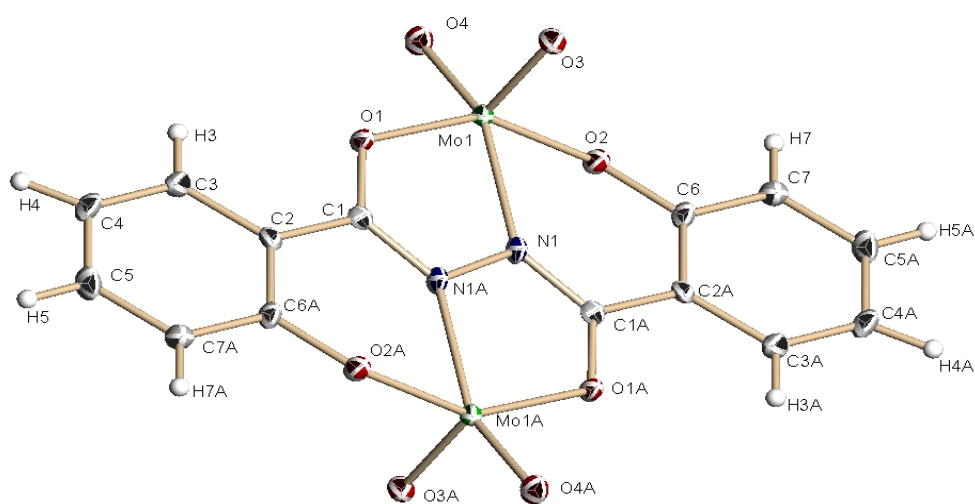
**Fig. 4.7.** ORTEP diagram of [(Mo$^{VI}$O$_2$)$_2$L] (**1**) with atom labeling scheme at 50% probability.
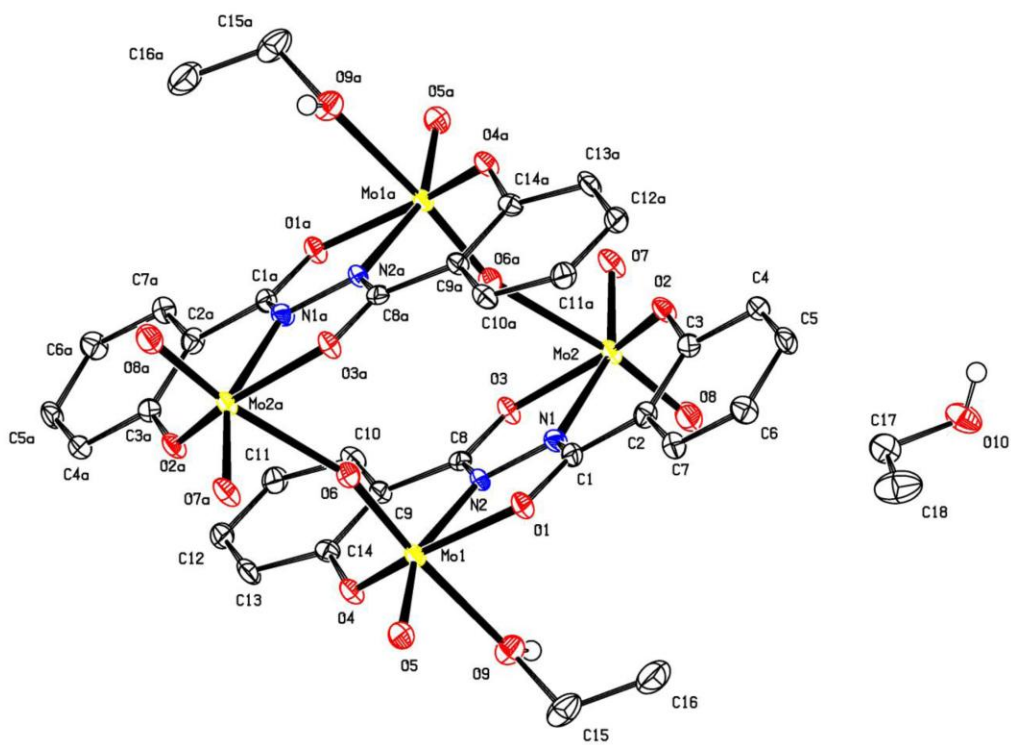
**Fig. 4.8.** PLATON diagram of $[\{(C_2H_5OH)LO_3Mo_2{}^{VI}\}_2(\mu\text{-}O)_2]\cdot C_2H_5OH$ (**2**) with atom labeling scheme at 50% probability.
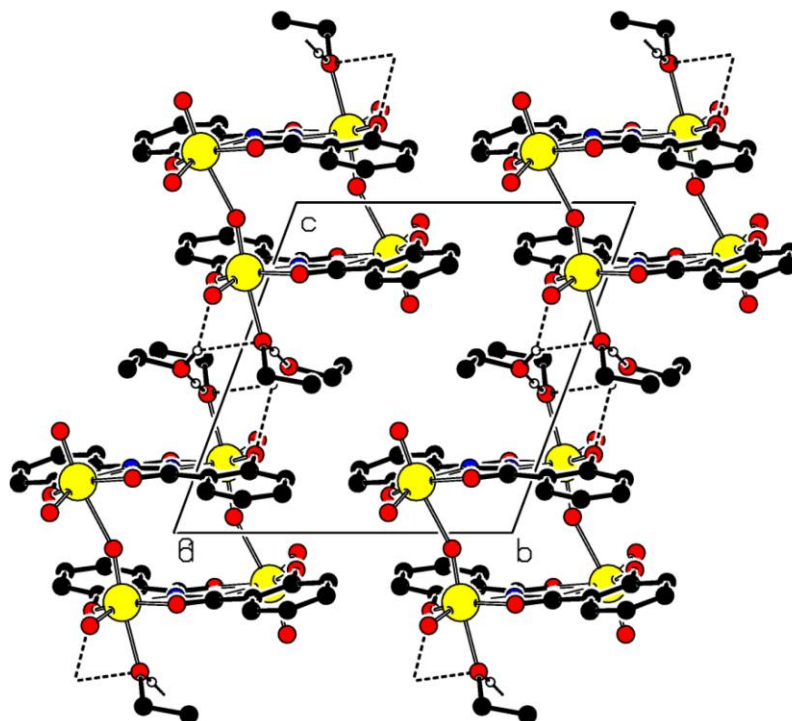
**Fig.4.9.** Packing diagram of complex **2** along a axis

## 4.4. Conclusions

Two novel and unusual type dimeric $[(Mo^{VI}O_2)_2L]$ (**1**) and tetrameric $[\{(C_2H_5OH)LO_3Mo_2^{VI}\}_2(\mu–O)_2]\cdot C_2H_5OH$ (**2**) dioxomolybdenum(VI) complexes with *N,N'*–disalicyloylhydrazine have been synthesized and fully characterized. These binucleating ligands were formed by the selfcombination of acid hydrazide or corresponding hydrazone. The complexes were characterized by various spectroscopic techniques (IR, UV-Vis and NMR) and also by electrochemical study. The molecular structures of both have been confirmed by X-ray crystallography. The above studies indicate that the *N,N'*–disalicyloylhydrazine (H$_2$L) has the normal tendency to form both dimeric and tetrameric complexes coordinated through the dianionic tridentate manner.

**References**

[1] S. Dutta, V. Manivannan, L.G. Babu, S. Pal, Acta Crystallogr. Sect. C 51 (1995) 813.

[2] Z.-X. Lian, P. Liu, J.-M. Zhang, T.-J. Lou, T.-X. Wang, H.-H. Li, Chin. J. Struct. Chem. 27 (2008) 639.

[3] V.F. Shul'gin, E.A. Sarnit, O.V. Konnik, E.B. Rusanov, A.S. Bogomyakov, V.I. Ovcharenko, V.V. Minin, Russ. J. Coord. Chem. 38 (2012) 44.

[4] Y.-T. Chen, D.-C. Li, Acta Cryst. 64 (2008) 1466.

[5] P.V. Bernhardt, P. Chin, P.C. Sharpe, J.C. Wang, D.R. Richardson, J. Biol. Inorg. Chem. 10 (2005) 761.

[6] Y.-T. Chen, J.-M. Dou, D.-C. Li, D.-Q. Wang, Y.-H. Zhu, Acta Cryst. 63 (2007) 2503.

[7] J.M. Dou, M.L. Liu, D.C. Li, D.Q. Wang, Eur. J. Inorg. Chem. 23 (2006) 4866.

[8] D. Li, S. Wang, H. Xu, Y. Yang, S. Zeng, J. Zhao, D. Wang, J. Dou, Inorg. Chim. Acta 365 (2011) 85.

[9] R.P. John, J. Park, D. Moon, K. Lee, M.S. Lah, Chem. Commun. (2006) 3699.

[10] Z. Huang, Q. Cui, L. Xiong, Z. Wang, K. Wang, Q. Zhao, F. Bi, Q. Wang, J. Agric. Food Chem. 57 (2009) 2447.

[11] J.K. Daniel, N.P. Peet, J. Heterocyclic Chem. 15 (1978) 1309.

[12] H.H.Fox, J.T. Gibas, J. Org. Chem. 18 (1953) 1375.

[13] W. Von Gentzkow, H. Formanek, I. Dietrich, E. Knapek, Siemens Forsch.-Entwicklungsber 12 (1983) 149.

[14] S.R.Tewari, S.K. Bajpai, S.K. Misra, G.N. Shukla, V.N. Misra, J. Indian Chem. Soc. 59 (1983) 891.

[15] H. Zhao, N. Neamati, S. Sunder, H. Hong, S. Wang, G.W.A. Milne, Y. Pommier, T.R. Burke Jr, J. Med. Chem. 40 (1997) 937.

[16] DeClercq, E. J. Med. Chem. 38 (1995) 2491.

[17] O.A. Rajan, A. Chakravorty, Inorg. Chem. 20 (1981) 660.

[18] M.M. Abu-omar, A. Loaiza, N. Hontzeas, Chem. Rev. 105 (2005) 2227.

[19] J. Topich, Inorg. Chem. 20 (1981) 3704.

[20] R.K. Grasselli, Catal. Today 49 (1999) 141.

[21] R.J. Cross, P.D. Newman, R.D. Peacock, D. Stirling, J. Mol. Catal. 144 (1999) 273.

[22] G.J.-J. Chen, J.W. McDonald, W.E. Newton, Inorg. Chem. 15 (1976) 2612.

[23] E.H. Rodd, in Chemistry of Carbon Compounds, Elsevier, London, 3 (1954) 556.

[24] R. Dinda, P. Sengupta, S. Ghosh, W.S. Sheldrick, Eur. J. Inorg. Chem. (2003) 363.

[25] A. Sarkar, S. Pal, Inorg. Chim.Acta 362 (2009) 3807.

[26] G.M. Sheldrick, *SHELXS-97*, Program for Crystal Structure Determination, Universitäet Gö ttingen, Gö ttingen, Germany, (1997).

[27] G.M. Sheldrick, *SHELXL-97*, Program for Refinement of Crystal Structures, Universitäet Gö ttingen, Gö ttingen, Germany, (1997).

[28] S.K. Dutta, D.B. McConville, W.J. Youngs, M. Chaudhury. Inorg. Chem. 36 (1997) 2517.

[29] Y.-L. Zhai, X.-X. Xu, X. Wang. Polyhedron 11 (1992) 415.

[30] C.C.L. Pereira, S.S. Balula, F.A. Almeida Paz, A.A. Valente, M. Pillinger, J. Klinowski, I.S. Goucalves, Inorg. Chem. (Communication) 46 (2007) 8508.

[31] R. Dinda, P. Sengupta, S. Ghosh, H.M. Figge, W.S. Sheldrick, Dalton Trans. (2002) 4434.

[32] S.F. Gheller, W.E. Newton, L.P. de Majid, J.R. Bradbury, F.A. Schultz, Inorg. Chem., 27 (1988) 359.

[33] F.H. Allen, O. Kennard, D.G. Watson, J. Chem. Soc., Perkin Trans. 12 (1987) 1.

# Chapter 5

**Synthesis and Structural Characterization of Novel Dioxomolybdenum(VI) Complexes: Unexpected Coordination Due to Ligand Rearrangement Through Metal Mediated Interligand C–C Bond Formation**

# Chapter 5

**Synthesis and Structural Characterization of Novel Dioxomolybdenum(VI) Complexes: Unexpected Coordination Due to Ligand Rearrangement Through Metal Mediated Interligand C–C Bond Formation**

## Abstract

Two novel dioxomolybdenum(VI) complexes containing the $MoO_2^{2+}$ motif are reported where unexpected coordination due to ligand rearrangement through metal mediated interligand C–C bond formation is observed. The ligand transformations are probably initiated by molybdenum assisted C–C bond formation in the reaction medium. The ligands ($H_2L'^{1-2}$) are tetradentate C–C coupled $O_2N_2-$ donor systems formed *in situ* during the synthesis of the complexes by the reaction of bis(acetylacetonato)dioxomolybdenum(VI) with Schiff base ligands of 2-aminophenol with 2-pyridinecarboxaldehyde ($HL^1$) and 2-quinolinecarboxaldehyde ($HL^2$). The reported dioxomolybdenum(VI) complexes $[MoO_2L'^1]$ (**1**) and $[MoO_2L'^2]$ (**2**) coordinated with the $O_2N_2-$ donor rearranged ligand are expected to have better stability of the molybdenum in +6 oxidation state than the corresponding $ON_2-$donor ligand precursor. Both the complexes are fully characterized by several physicochemical techniques and the novel structural features through single crystal X-ray crystallography.

## 5.1. Introduction

The coordination chemistry of transition metal complex with nitrogen-oxygen donor ligands has become an interesting area of research in recent times because of their ability to possess unusual configurations, be structurally labile and their sensitivity to molecular environments [1]. Many transition metal complexes of Schiff base ligands have received considerable attention in biological field, as antibacterial [2–4] and anticancer [5] drugs, including DNA-cleavage systems [6,7], and also have catalytic applications, such as in polymerization [8], olefin oxidation [6] and Suzuki-Miyaura coupling [7]. On the other hand, the coordination chemistry of molybdenum has been a subject of enthusiastic research due to the presence of molybdenum in metalloenzymes [8–10] and its biochemical as well as catalytic importance [11–25].

Transition metal complexes of 2-aminophenol based Schiff base ligands have been widely reported [26–31]. But the Schiff base ligands with carbonyl compounds such as 2-pyridine carboxaldehyde and 2-quinolinecarboxaldehyde have not been reported much [32–34]. These ligands are uninegative tridentate one and coordinate with Mo(VI) precursors $MoO_2(acac)_2$ forming the $\mu$-oxomolybdenum compounds $[MoO_2(L^1)]_2(\mu\text{-}O)$ [35].

In this chapter two novel dioxomolybbdenum(VI) complexes containing the $MoO_2^{2+}$ motif are reported where unexpected coordination due to ligand rearrangement through metal mediated interligand C–C bond formation is observed. The ligand transformations are probably initiated by molybdenum assisted C–C bond formation in the reaction medium. The ligands ($H_2L^{'1-2}$) are tetradentate C–C coupled $O_2N_2-$ donor systems formed *in situ* during the synthesis of the complexes by the reaction of bis(acetylacetonato)dioxomolybdenum(VI) with Schiff-base ligands of 2-aminophenol with 2-pyridine carboxaldehyde ($HL^1$) and 2-quinolinecarboxaldehyde ($HL^2$). The reported dioxomolybdenum(VI) complexes coordinated with the $O_2N_2$-donor rearranged ligand are expected to have better stability of molybdenum in +6 oxidation state than the corresponding $ON_2$-donor ligand precursor [36]. Both the complexes are fully characterized by several physicochemical techniques and the novel structural features through single crystal X-ray crystallography.

## 5.2. Experimental

### 5.2.1. Materials

[MoO$_2$(acac)$_2$] was prepared as described in the literature [37]. Reagent grade solvents were dried and distilled prior to use. All other chemicals were reagent grade, available commercially and used as received. Commercially available TBAP (tetra butyl ammonium perchlorate) was properly dried and used as a supporting electrolyte for recording cyclic voltammograms of the complexes.

### 5.2.2. Physical Measurements

Elemental analyses were performed on a Vario ELcube CHNS Elemental analyzer. IR spectra were recorded on a Perkin-Elmer Spectrum RXI spectrometer. $^1$H NMR spectra were recorded with a Bruker Ultra shield 400 MHz spectrometer using SiMe$_4$ as an internal standard. Electronic spectra were recorded on a Lamda25, PerkinElmer spectrophotometer. Magnetic susceptibility was measured with a Sherwood Scientific AUTOMSB sample magnetometer. Electrochemical data were collected using a PAR electrochemical analyzer and a PC-controlled Potentiostat/Galvanostat (PAR 273A) at 298 K in a dry nitrogen atmosphere. Cyclic voltammetry experiments were carried out with a platinum working electrode, platinum auxiliary electrode, Ag/AgCl as reference electrode and TBAP as supporting electrolyte.

### 5.2.3. Synthesis of Ligands (*HL$^{1-2}$*)

Schiff base ligands HL$^{1-2}$ were prepared by the condensation of 2-aminophenol with 2-pyridine carboxaldehyde (HL$^1$) and 2-quinolinecarboxaldehyde (HL$^2$) in equimolar ratio in ethanol medium following a standard procedure [38]. The resulting brown compounds were filtered, washed with ethanol and dried over fused CaCl$_2$.

*HL$^1$:* Yield: 0.13 g (65%). Anal. Calcd for C$_{12}$H$_{10}$N$_2$O: C, 72.72; H, 5.05; N, 14.14. Found: C, 72.76; H, 5.07; N, 14.09%. $^1$H NMR (DMSO-d$_6$, 400 MHz): $\delta$ = 9.25 (s, 1H, OH), 8.71 (s, 1H, CH), 8.69–6.86 (m, 8H, Aromatic). $^{13}$C NMR (DMSO-d$_6$, 100 MHz): $\delta$ = 159.33, 154.49, 151.37, 149.45, 136.82, 136.80, 128.21, 125.37, 121.49, 119.66, 119.57, 116.31.

*HL²:* Yield: 0.18 g (72%). Anal. Calcd for $C_{16}H_{12}N_2O$: C, 77.4; H, 4.87; N, 11.28. Found: C, 77.38; H, 4.89; N, 11.26%. $^1$H NMR (DMSO-$d_6$, 400 MHz): $\delta$ = 9.36 (s, 1H, OH), 8.91 (s, 1H, CH), 8.58–6.87 (m, 10H, Aromatic). $^{13}$C NMR (DMSO-$d_6$,100 MHz): $\delta$ = 167.79, 157.14, 154.32, 152.92, 136.86, 134.43, 132.44, 130.90, 129.52, 128.91, 127.88, 127.81, 120.38, 118.34, 116.29, 115.49.

## *5.2.4. Synthesis of complexes [MoO₂L'¹](1) and [MoO₂L'²](2)*

To the refluxing solution of 1.0 mmol ligand $HL^{1-2}$ in 30 mL of ethanol, 1.0 mmol of $MoO_2(acac)_2$ was added. The color of the solution changed to dark red. The mixture was then refluxed for 3 hr. After leaving the solution for 2 days at room temperature, fine yellow colored crystals were isolated and suitable single crystals were selected for X-ray analysis.

*[MoO₂L'¹](1):* Yield: 0.25 g (57%). Anal. Calcd for $C_{17}H_{17}N_2O_{5.50}Mo$: C, 47.13; H, 3.95; N, 6.47. Found: C, 47.14; H, 3.94; N, 6.48%. $^1$H NMR (DMSO-$d_6$, 400 MHz): $\delta$ = 8.87–6.63 (m, 8H, Aromatic), 8.68 (s, 1H, NH), 5.81 (s, 1H, CH), 2.57 (s, 3H, CH$_3$), 2.22 (s, 3H, CH$_3$). $^{13}$C NMR (DMSO-$d_6$, 100 MHz): $\delta$ = 195.90, 173.66, 162.00, 157.43, 148.49, 141.49, 133.32, 129.55, 126.36, 125.50, 122.49, 121.16, 117.31, 116.29, 63.71, 31.39, 24.42.

*[MoO₂L'²](2):* Yield: 0.31 g (65%). Anal. Calcd for $C_{21}H_{18}N_2O_5Mo$: C, 53.16; H, 3.83; N, 5.90. Found: C, 53.15; H, 3.84; N, 5.90%. $^1$H NMR (DMSO-$d_6$, 400 MHz): $\delta$ = 9.27–6.64 (m, 10H, Aromatic), 8.79 (s, 1H, NH), 6.03 (s, 1H, CH), 2.59 (s, 3H, CH$_3$), 2.23 (s, 3H, CH$_3$). $^{13}$C NMR (DMSO-$d_6$, 100 MHz): $\delta$ = 195.49, 174.28, 162.43, 158.44, 143.31, 141.18, 132.84, 131.48, 128.96, 128.44, 128.28, 127.43, 126.59, 125.63, 120.78, 119.58, 116.91, 116.01, 63.71, 30.75, 23.42.

## 5.2.5. Crystallography

Suitable single crystals of **1** and **2** were chosen for X-ray diffraction studies. Crystallographic data and details of refinement are given in **Table 5.1**. These compounds crystallize in the triclinic space group $P$ -1 (**1**) and $P$ $\bar{1}$ (**2**). The unit cell parameters and the intensity data for the complexes were collected at ~ 293 K, on a Bruker Smart Apex CCD diffractometer using graphite monochromated Mo K$\alpha$ radiation (k = 0.71073 Å), employing the $\omega$–2$\theta$ scan technique. The intensity data were corrected for Lorentz, polarization and absorption effects. The structures were solved using the SHELXS97 [39] and refined using the SHELXL97 [40] computer programs. The non-hydrogen atoms were refined anisotropically.

**Table 5.1** Crystal and Refinement Data of Complexes **1** and **2**

| Compound | 1 | 2 |
|---|---|---|
| Formula | $C_{17}H_{17}MoN_2O_{5.50}$ | $C_{21}H_{18}MoN_2O_5$ |
| M | 433.27 | 474.31 |
| Crystal symmetry | Triclinic | Triclinic |
| Space group | $P$ -1 | $P$ 1 |
| $a(\check{A})$ | 8.4739(5) | 9.1187(19) |
| $b(\check{A})$ | 9.6684(5) | 9.6426(19) |
| $c(\check{A})$ | 11.5506(7) | 11.841(2) |
| $\alpha$ (°) | 94.10(10) | 73.432(8) |
| $\beta$ (°) | 109.95(10) | 84.460(9) |
| $\gamma$ (°) | 96.81(10) | 66.820(9) |
| $V(\check{A}^3)$ | 876.87(9) | 917.2(3) |
| Z | 2 | 2 |
| $D_{calc}(g.cm^{-3})$ | 1.641 | 1.717 |
| F(000) | 438 | 480 |
| $\mu$(Mo-K$\alpha$)(mm$^{-1}$) | 0.781 | 0.753 |
| max./min.trans. | 0.9546 / 0.9053 | 0.9285 / 0.8639 |
| 2$\theta$(max)(°) | 26.00 | 28.65 |
| Reflections collected / unique | 9144/ 3434 | 48181 / 4651 |
| $R_1^a$[I>2$\sigma$(I)] | R1 = 0.0274, wR2= 0.0787 | R1 = 0.0188, wR2 = 0.0492 |
| wR$_2^b$[all data] | R1 = 0.0294, wR2=0.0803 | R1 = 0.0197, wR2=0.0498 |
| S[goodness of fit] | 1.074 | 1.067 |
| min./max. res.(e.$\check{A}^{-3}$) | 0.831 / -0.245 | 0.435 / -0.409 |

$^aR_I = \Sigma \left| F_O \right| - \left| F_C \right| / \Sigma \left| F_O \right|$

$^bwR_2 = \{\Sigma [w (F_O^2 - F_C^2)^2]/\Sigma [w (F_O^2)^2]\}^{½}$

## 5.3. Results and Discussion

### 5.3.1. Synthesis

The precursor ligands ($HL^{1-2}$) were synthesized by Schiff base condensation of equimolar amounts of 2-aminophenol and corresponding carbonyl compounds [2-pyridinecarboxaldehyde ($HL^1$) and 2-quinolinecarboxaldehyde ($HL^2$)] in absolute ethanol at room temperature (**Scheme 5.1**). Detail methods used for the syntheses of precursor ligands ($HL^{1-2}$) and corresponding dioxomolybdenum(VI) complexes (**1–2**) are given in the experimental section. Reactions of the 2-aminophenol based Schiff base ligands ($HL^{1-2}$) with $MoO_2(acac)_2$ proceed in refluxing ethanol and each of these reactions afford yellow color products $[MoO_2L^{'1}]$ (**1**) and $[MoO_2L^{'2}]$ (**2**) in decent yield (**Scheme 5.2**). Both the reactions are also performed catalytically and results and yield completely matched well with the original compounds. These compounds are highly soluble in aprotic solvents, viz. DMF or DMSO and are sparingly soluble in alcohol, $CH_3CN$ and $CHCl_3$. All these complexes are diamagnetic, indicating the presence of molybdenum in the +6 oxidation state, and are nonconducting in solution.
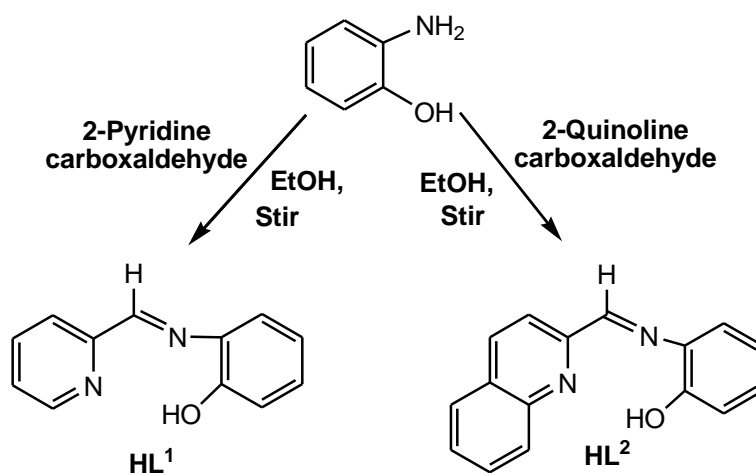


**Scheme 5.1**. Synthesis of tridentate Schiff base ligands
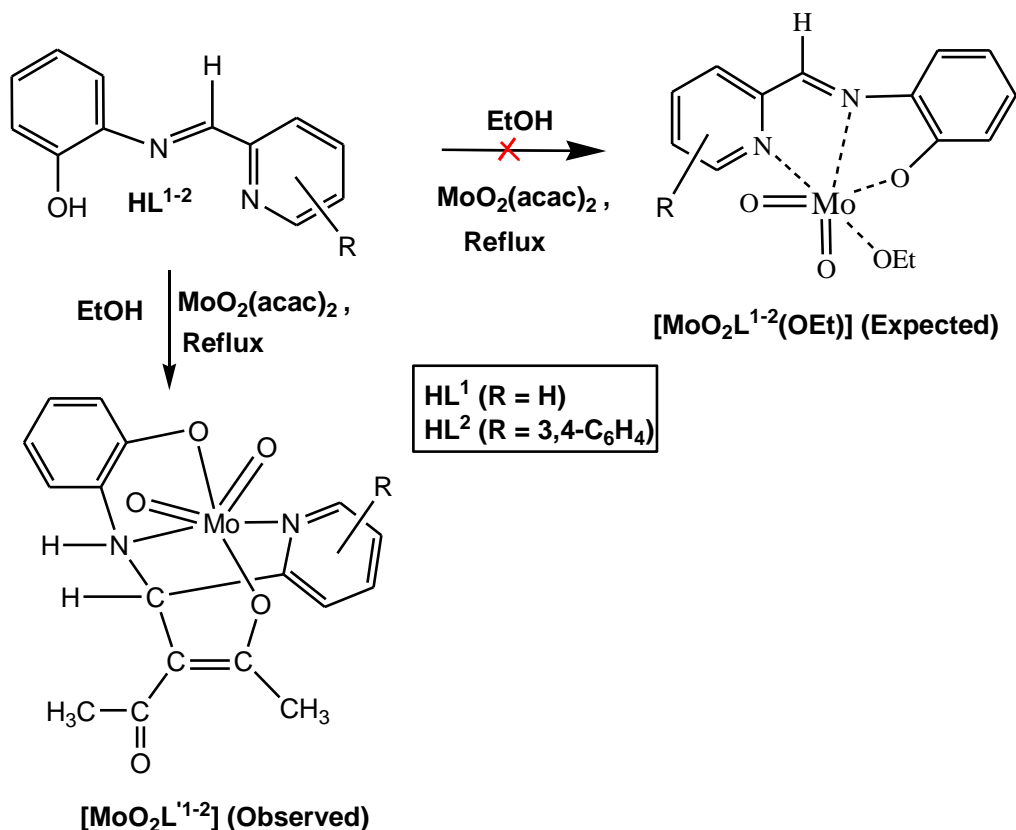
**Scheme 5.2**. Synthesis of dioxomolybdenum(VI) complexes (**1** and **2**)

### 5.3.2. Description of the X-ray structures of [MoO₂L¹] (1) and [MoO₂L²] (2)

The structure of **1** and **2** (**Figs. 5.1** and **5.2**) reveals an unexpected coordination due to ligand rearrangement, which amounts to an interligand C–C bond coupling between two methylenic carbon atoms $C_8$ and $C_9$, leading to the formation of novel dioxomolybdenum(VI) complexes. The rearranged ligands ($H_2L'^{1-2}$) are formed (**Scheme 5.3**) due to template reactions between one of the metal coordinated acetylacetonate in [MoO₂(acac)₂] and the corresponding Schiff base ligand ($HL^{1-2}$). These ligand transformations are highly specific and probably initiated by a Mo mediated C–C bond formation in the reaction medium. It is checked and confirmed that, the reactions using other metal precursors [VO(acac)₂ or Cu(acac)₂] do not initiate this type of ligand rearrangement.

In the structure of **1** and **2**, the corresponding rearranged ligand $H_2L^{'1-2}$ is coordinated to molybdenum as a dianionic tetradentate $N_2O_2$–donor, forming one six-membered and two five-membered rings with bite angles of $80.80(4)°$–$80.89(8)°$, $76.32(8)°$–$77.27(4)°$ and $69.40(8)°$–$70.07(4)°$ respectively. The complexes (**1** and **2**) have a six-coordinated distorted octahedral geometry where Mo–O(3) and Mo–O(4) bond distances of the $MoO_2^{2+}$ group are unexceptional [11, 36] and almost equal in the range [1.698(2)–1.711(1) Å]. The Mo–O and Mo–N distances are close to typical values (**Table 5.2**) [11, 36].
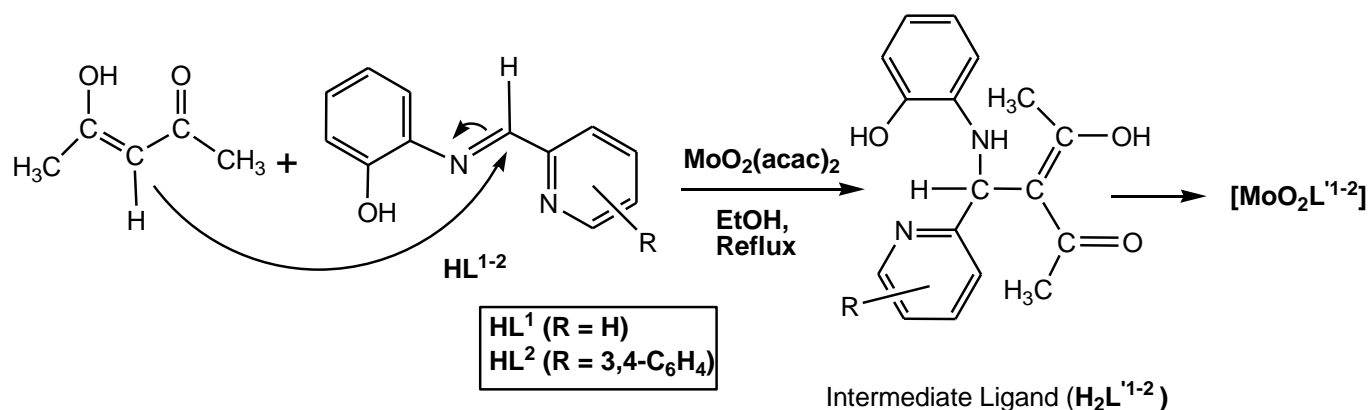


**Scheme 5.3**. Synthesis of C–C σ bonded rearranged ligands

Both the molecules are found to show inter molecular hydrogen bonding. Two $[MoO_2L^{'1}]$ (**1**) molecules form a dimeric unit via a pair of reciprocal hydrogen bonds between the N(1)–H proton of one molecule and the acetylacetonate oxygen O(5) of other moiety. On the other hand, the dimeric unit of **2** is formed through a pair of reciprocal hydrogen bonds between the oxo oxygen O(3) of one molecule with the N(1)–H proton of the neighboring molecule. The representative hydrogen-bonded dimeric structure of $[MoO_2L^{'1}]$ (**1**) is shown in **Fig. 5.3**.

**Table 5.2** Selected Bond Distances (Å) and Bond Angles (°) for Complex **1** and **2**

|  | Complex **1** | Complex **2** |
|---|---|---|
| Bond lengths | | |
| Mo(1)-O(1) | 1.946(2) | 1.941(1) |
| Mo(1)-O(2) | 1.980(2) | 1.953(9) |
| Mo(1)-O(3) | 1.703(2) | 1.711(1) |
| Mo(1)-O(4) | 1.698(2) | 1.703(1) |
| Mo(1)-N(1) | 2.325(2) | 2.327(2) |
| Mo(1)-N(2) | 2.338(2) | 2.417(1) |
| C(7)-C(13) | 1.522(3) | 1.507(2) |
| | | |
| Bond Angles | | |
| O(1)-Mo(1)-O(2) | 153.00(8) | 152.89(5) |
| O(1)-Mo(1)-O(3) | 99.91(9) | 99.29(5) |
| O(1)-Mo(1)-O(4) | 97.72(9) | 97.71(5) |
| O(1)-Mo(1)-N(1) | 76.32(8) | 77.27(4) |
| O(1)-Mo(1)-N(2) | 81.86(8) | 81.20(4) |
| O(2)-Mo(1)-O(3) | 95.97(9) | 95.85(5) |
| O(2)-Mo(1)-O(4) | 98.4(1) | 99.33(5) |
| O(2)-Mo(1)-N(1) | 80.89(8) | 80.80(4) |
| O(2)-Mo(1)-N(2) | 76.67(8) | 76.44(4) |
| O(3)-Mo(1)-O(4) | 106.8(1) | 106.58(5) |
| O(3)-Mo(1)-N(1) | 94.15(9) | 88.50(5) |
| O(3)-Mo(1)-N(2) | 162.69(9) | 158.02(5) |
| O(4)-Mo(1)-N(1) | 158.92(9) | 95.06(5) |
| O(4)-Mo(1)-N(2) | 89.85(9) | 164.77(5) |
| N(1)-Mo(1)-N(2) | 69.40(8) | 70.07(4) |
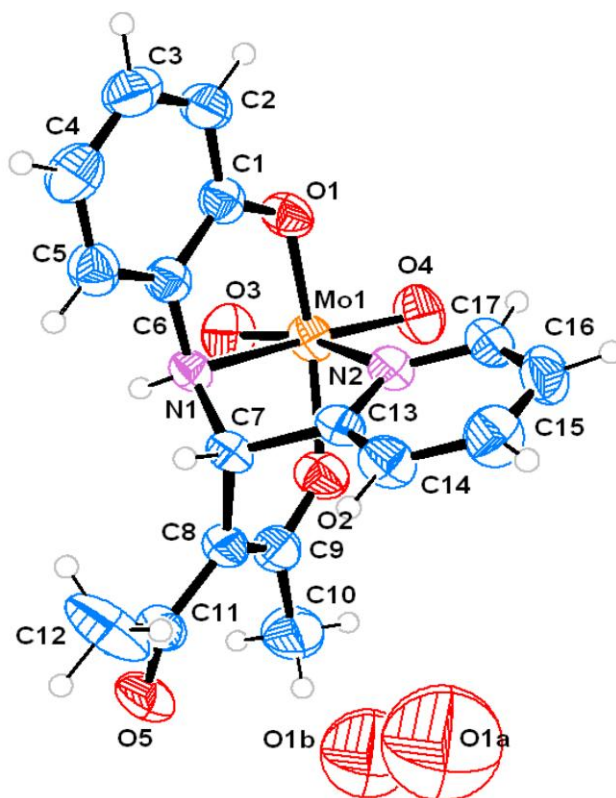
**Fig. 5.1.** ORTEP diagram of [MoO$_2$L$^{'1}$] (**1**) with atom labeling scheme
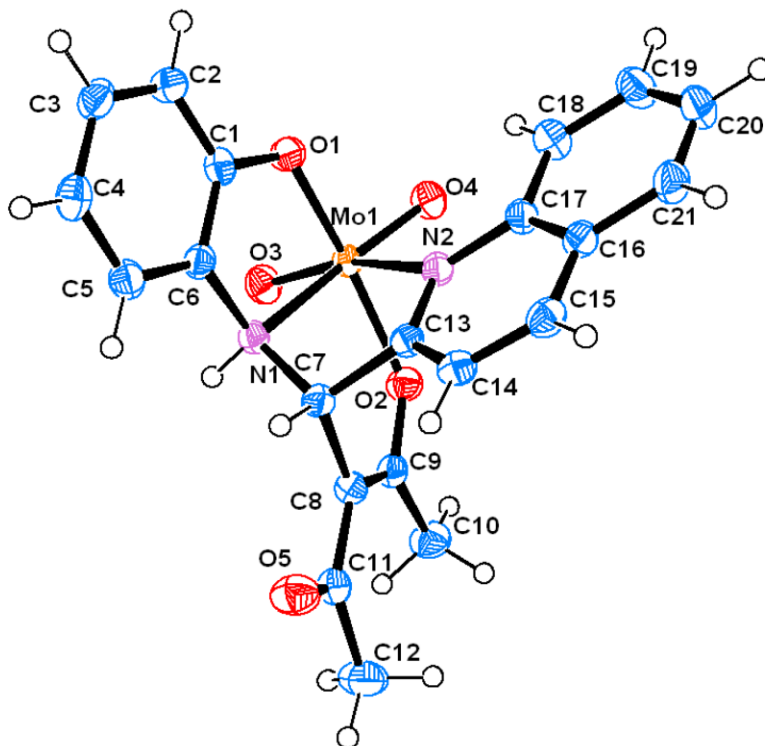
at 50% probability

**Fig. 5.2.** ORTEP diagram of $[MoO_2L^{'2}]$ (**2**) with atom labeling scheme

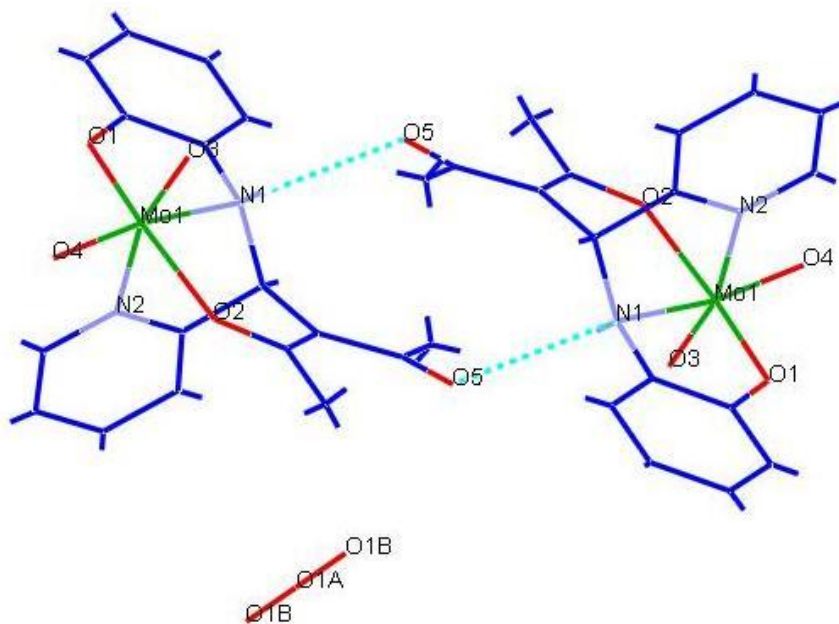at 50% probability

**Fig. 5.3.** The hydrogen-bonded dimer of $[MoO_2L^{/1}]$ (**1**) (side view)

*5.3.3. Spectral properties*

Spectral characteristics of both the ligands and compounds (**1–2**) are listed in **Table 5.3**. Both the ligands exhibit the IR band of minimum intensity in the 3197–3164 cm$^{-1}$ region due to $\nu$(OH) stretching [27–33]. Characteristic strong bands at 1622–1611 cm$^{-1}$ and 1583–1581cm$^{-1}$ region due to $\nu$(C=C/aromatic) and $\nu$(C=N) stretching modes of the ligands [11,36] are located in the spectra of both the ligands and the complexes. In addition, complexes (**1** and **2)** display a pair of sharp strong peaks in the range 931–924 cm$^{-1}$ and 910–907 cm$^{-1}$ due to terminal $\nu$(M=O$_t$) stretch [11,36]. The representative IR spectra of ligand HL$^1$ and complex **1** are shown in **Figs. 5.4** and **5.5** respectively.

The DMSO solution of both the complexes display a shoulder in the 423–417 nm region and two strong absorptions in the 329–252 nm range which are assignable to LMCT and intraligand transitions, respectively [11,36]. The electronic spectrum of complex **2** is shown in **Fig. 5.6** as the representative one.

The $^1$H and $^{13}$C NMR data of the free ligands and dioxomolybdenum(VI) complexes are given in the experimental section. The spectrum of the free ligands exhibits a resonance in the range $\delta$ = 9.36–9.25 ppm due to phenolic OH and at $\delta$ = 8.71–8.91 ppm due to –CH protons. All the aromatic protons from ligands are clearly observed in the expected region $\delta$ = 8.69–6.85 ppm. The spectra of complexes **1–2** display two singlets in the range $\delta$ = 2.23–2.22 ppm and $\delta$ = 2.59–2.57 ppm [41]. These are assigned to the protons of the two methyl groups present in the acetylacetone fragment of the rearranged ligand. The –NH and –CH= proton resonance are observed in the range of $\delta$ = 8.86–8.79 and $\delta$ = 6.03–5.81 ppm, respectively [41]. In the NMR spectra of complexes, the aromatic –OH proton disappeared due to the deprotonation of phenolic group [11,36]. The representative NMR spectra of ligand HL$^2$ and complex **2** are shown in **Figs. 5.7** and **5.8**, respectively.

**Table 5.3** Characteristic IR[a] bands and electronic spectral data[b] for the studied ligands and complexes (**1–2**)

| Compounds | $\nu(-OH)$ | $\nu(C=N)$ | $\nu(Mo=O)/cm^{-1}$ | $\lambda_{max}/nm\ (\varepsilon/dm^3\ mol^{-1}\ cm^{-1})$ |
|---|---|---|---|---|
| HL$^1$ | 3197 | 1583 | -- | 355 (20154), 256 (15625) |
| HL$^2$ | 3164 | 1581 | -- | 366 (20184), 256 (15463) |
| [MoO$_2$L$^{'1}$] (**1**) | -- | 1604 | 924, 907 | 417 (30124), 320 (25123), 252 (16352) |
| [MoO$_2$L$^{'2}$] (**2**) | -- | 1593 | 931, 910 | 423 (30125), 329 (25126), 257 (16350) |

[a] In KBr pellet; [b] In DMSO
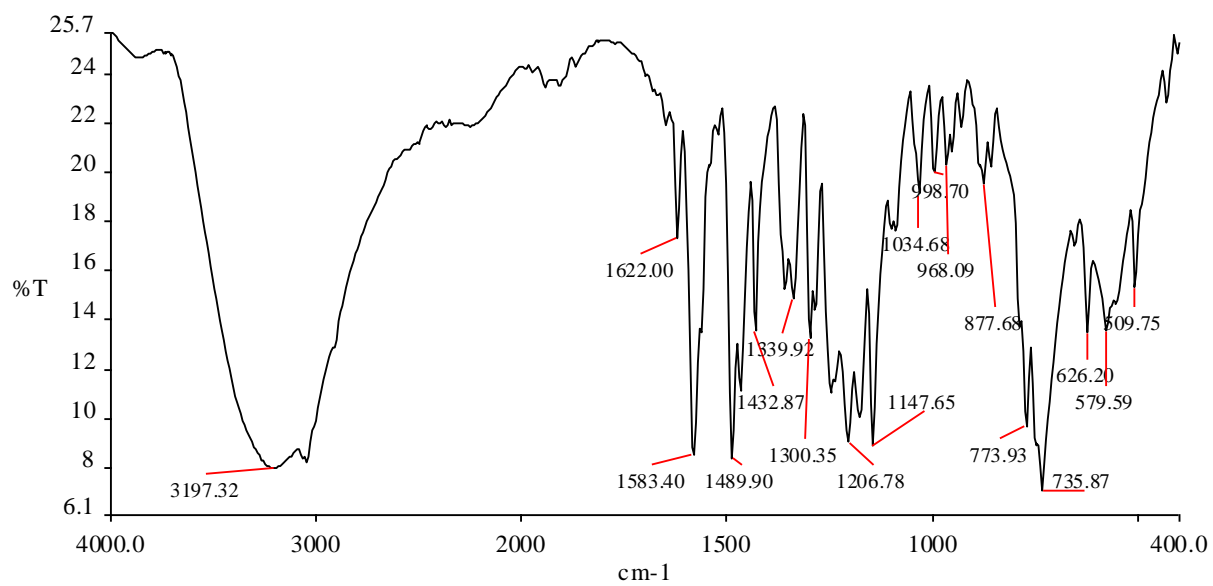
**Fig. 5.4.** IR spectrum of [HL$^1$]
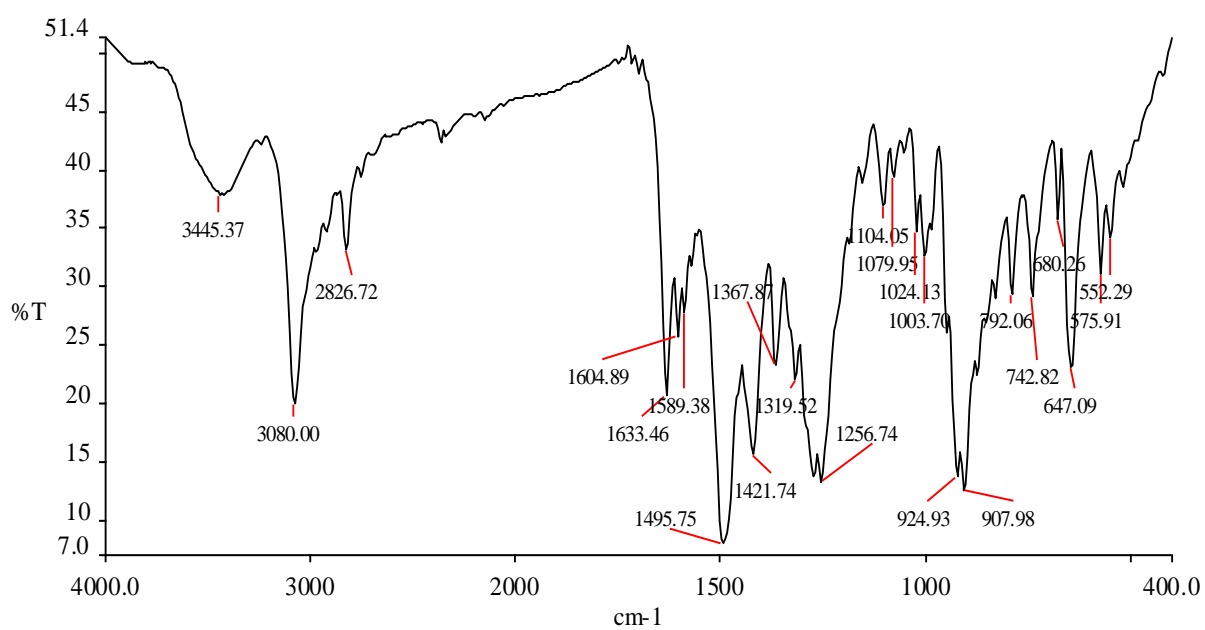
**Fig. 5.5.** IR spectrum of $[MoO_2L'^1]$ (**1**)
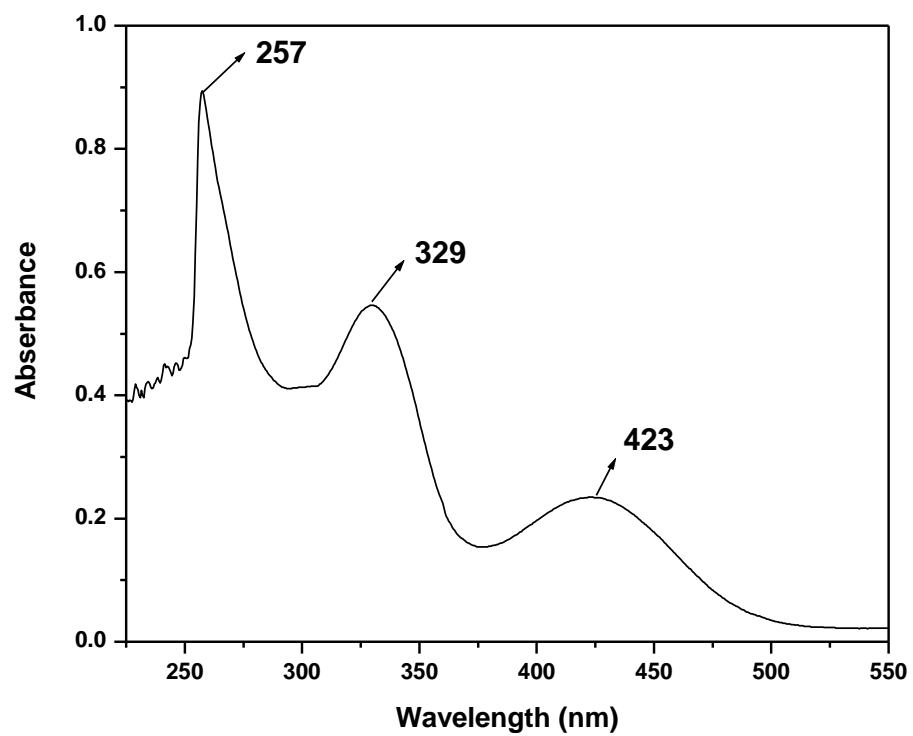
**Fig. 5.6.** Electronic absorption spectrum of [MoO$_2$L$^2$] (**2**) in DMSO, at 25$^0$ C
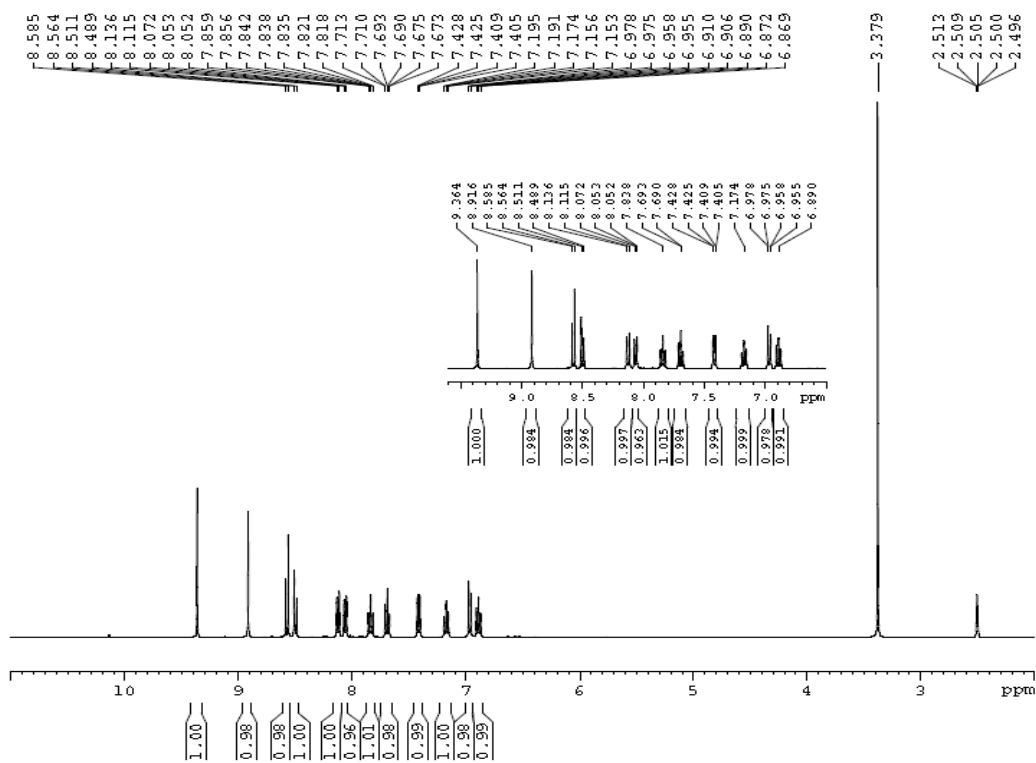
**Fig. 5.7.** $^1$H NMR spectrum of [HL$^2$] in DMSO d$_6$.
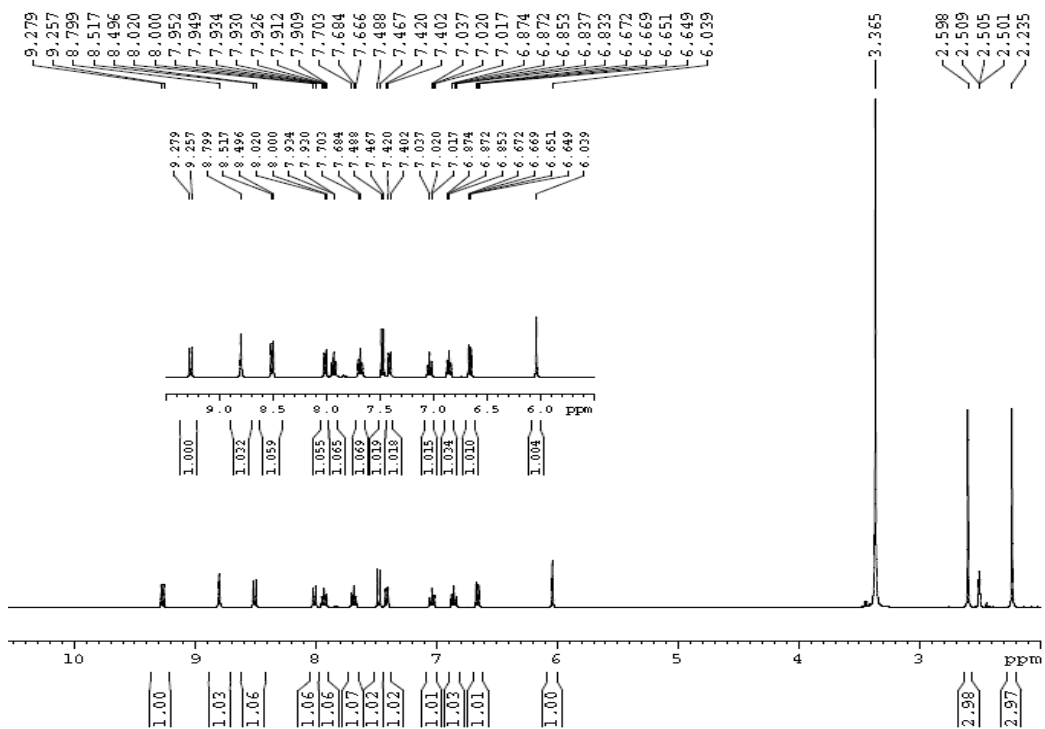
**Fig. 5.8.** $^{1}$H NMR spectrum of [MoO$_2$L$^{2}$] (**2**) in DMSO d$_6$.

### 5.3.4. Electrochemical properties

Electrochemical properties of the complexes have been studied by cyclic voltammetry in DMF solution (0.1 M TBAP). Voltammetric data are given in **Table 5.4** and the cyclic voltamogram of [MoO$_2$L$^{-1}$] (**1**) is displayed in **Fig.5.9** as the representative one. The CV traces of complexes (**1–2**) exhibit two irreversible reductive responses within the potential window –1.05 to –1.14 V and –1.58 to –1.69 V, which are assigned to Mo$^{VI}$/Mo$^{V}$ and Mo$^{V}$/Mo$^{IV}$ processes respectively [11]. An oxidation wave at positive potentials in the range of +1.14 to +1.23 V is assigned to the oxidation of the coordinated ligands [11]. As the Mo(VI) complex cannot undergo a metal-centered oxidation, this is attributed to a ligand-centered process [11].

**Table 5.4** Cyclic voltammetric results for dioxomolybdenum (VI) complexes (**1–2**) at 298 K

| Complex | $E$pc [V][a] |
|---|---|
| [MoO$_2$L$^{-1}$] (**1**) | –1.14, –1.69 |
| [MoO$_2$L$^{-2}$] (**2**) | –1.05, –1.58 |

[a] Solvent: DMF; working electrode: platinum; auxiliary electrode: platinum; reference electrode: Ag/AgCl; supporting electrolyte: 0.1 M TBAP; scan rate: 50 mV/s. $E$pc is the cathodic peak potential
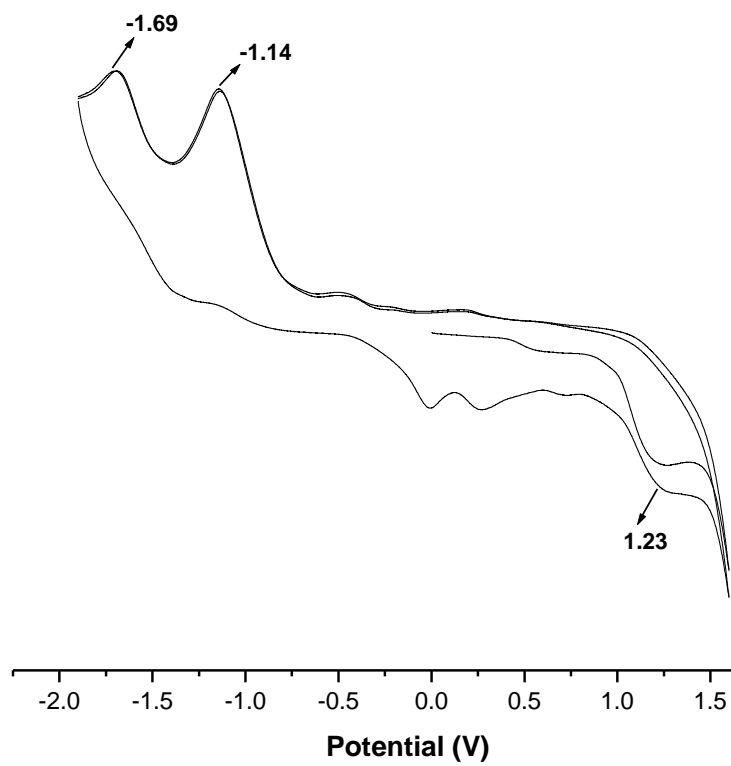
**Fig. 5.9.** Cyclic voltammogram of [MoO$_2$L$^{\prime 1}$] (**1**) in DMF

## 5.4. Conclusions

Two novel dioxomolybdenum(VI) complexes (**1** and **2**) containing C–C coupled rearranged ligand have been synthesized and successfully characterized. The C–C σ bond formation is highly specific and dependent on the metal precursor $[MoO_2(acac)_2]$ as suggested from the tentative reaction mechanism. It is checked and confirmed that, the reactions using other metal precursors $[VO(acac)_2$ or $Cu(acac)_2]$ do not initiate this type of ligand rearrangement. Both the complexes (**1** and **2**) are diamagnetic and electrically non-conducting in solution. The microanalysis, electrochemical study and spectroscopic characteristics are consistent with their molecular formula. The molecular structures of both have been confirmed by X-ray crystallography.

**References**

[1] A. Golcu, M. Tumer, H. Demirelli, R.A. Wheatley, Inorg. Chim. Acta 358 (2005) 1785.

[2] V. Patroniak, A.R. Stefankiewicz, J.-M. Lehn, M. Kubicki, Eur. J. Inorg. Chem 10 (2005) 4168

[3] A. Balamurugan, G. Balossier, D. Laurent-Maquin, S. Pina, A.H.S. Rebelo, J. Faure, J.M.F. Ferreira, Dent. Mater. 24 (2008) 1343.

[4] Z.H. Chohan, S. Kausar, Chem. Pharm. Bull. 41 (1993) 951.

[5] M. Kurtoglu, F. Purtas, S. Toroglu, Trans. Met. Chem. 33 (2008) 705.

[6] C. Adhikary, R. Bera, B. Dutta, S. Jana, G. Bocelli, A. Cantoni, S. Chaudhuri, S. Koner, Polyhedron 27 (2008) 1556.

[7] P.R. Kumar, S. Upreti, A.K. Singh, Polyhedron 27 (2008) 1610.

[8] T. Opstal, F. Verpoort, Angew. Chem., Int. Ed. 42 (2003) 2876.

[9] G. Lyashenko, G. Saischek, M.E. Judmaier, M. Volpe, J. Baumgartner, F. Belaj, V. Jancik, R. Herbst-Irmer, N.C. Moesch-Zanetti, Dalton Transactions 29 (2009) 5655.

[10] N.C. Mosch-Zanetti, D. Wurm, M. Volpe, G. Lyashenko, B. Harum, F. Belaj, J. Baumgartner, Inorg. Chem. 49 (2010) 8914.

[11] R. Dinda, P. Sengupta, S. Ghosh, W.S. Sheldrick, Eur. J. Inorg. Chem. (2003) 363.

[12] K. Jeyakumar, D.K. Chand, J. Chem. Sci. 121 (2009) 111.

[13] M.R. Maurya,Curr. Org. Chem. 16 (2012) 73.

[14] R.D. Chakravarthy, K. Suresh, V. Ramkumar, D.K. Chand, Inorg. Chim. Acta 376 (2011) 57.

[15] Z. Hu, X. Fu, Y. Li, Inorg. Chem. Commun. 14 (2011) 497.

[16] M. Herbert, F. Montilla, A. Galindo, J. Mol. Catal. A: Chem. 338 (2011) 111.

[17] A. Rezaeifard, I. Sheikhshoaie, N. Monadi, M. Alipour, Polyhedron 29 (2010) 2703.

[18] I. Sheikhshoaie, A. Rezaeifard, N. Monadi, S. Kaafi, Polyhedron 28 (2009) 733.

[19] A. Gunyara, D. Betzb, M. Dreesb, E. Herdtweck, F.E. Kuhna, J. Mol. Catal. A: Chem. 331 (2010) 117.

[20] M.R. Maurya, S. Sikarwar, P. Manikandan, Appl. Catal., A 315 (2006) 74.

[21] A.J. Burke, Coord. Chem. Rev. 252 (2008) 170.

[22] K.R. Jain, W.A. Herrmann, F.E. Kuhn, Coord. Chem. Rev. 252 (2008) 556.

[23] K.C. Gupta, A.K. Sutar, Coord. Chem. Rev. 252 (2008) 1420.

[24] B. Frédéric, Coord. Chem. Rev. 236 (2003) 71.

[25] A. Syamal, M.R. Maurya, Coord. Chem. Rev. 95 (1989) 183.

[26] S. Bhattacharya, T. Ghosh, Trans. Met. Chem. 27 (2002) 89.

[27] S. Basu, G. Gupta, B. Das, K.M. Rao, J. Organomet. Chem. 695 (2010) 2098.

[28] S. Priyarega, M.M. Tamizh, R. Karvembu, R. Prabhakaran, K. Natarajan, J. Chem. Sci. 123 (2011) 319.

[29] M.H. Habibi, E. Shojaee, Y. Yamane , T. Suzuki, J. Inorg. Organomet. Polym. 22 (2012) 190.

[30] A.A. Abdel Aziz, A.N.M. Salem, M.A. Sayed, M.M. Aboaly, J. Mol. Struct. 1010 (2012) 130.

[31] J. Joseph, K. Nagashri, G.B. Janaki, Eur. J. Med. Chem. 49 (2012) 151.

[32] A. Majumder, G.M. Rosair, A. Mallick, N. Chattopadhyay, S. Mitra, Polyhedron 25 (2006) 1753.

[33] A.R. Stefankiewicz , M. Wałęsa-Chorab , H.B. Szcześniak , V. Patroniak , M. Kubicki, Z. Hnatejko, J. Harrowfield, Polyhedron 29 (2010) 178.

[34] D. Chatterjee, J. Mol. Catal. A: Chem. 310 (2009) 174.

[35] Y. Wong, D.K.P. Ng, H.K. Lee, Inorg. Chem., 41 (2002) 5276.

[36] S. Pasayat, S.P. Dash, Saswati, P.K. Majhi, Y.P. Patil, M. Nethaji, H.R. Dash, S. Das, R. Dinda, Polyhedron 38 (2012) 198.

[37] G.J.-J. Chen, J.W. McDonald, W.E. Newton, Inorg. Chem. 15 (1976) 2612.

[38] C. G. Pitt, Y. Bao, J. Thompson, M. C. Wani, H. Rosenkrantz, J. Metterville, J. Med. Chem. 29 (1986) 1231.

[39] G.M. Sheldrick, *SHELXS-97*, Program for Crystal Structure Determination, Universitäet Gö ttingen, Gö ttingen, Germany, (1997).

[40] G.M. Sheldrick, *SHELXL-97*, Program for Refinement of Crystal Structures, Universitäet Gö ttingen, Gö ttingen, Germany, (1997).

[41] A. Sarkar, S. Pal, Inorg. Chim. Acta 362 (2009) 3807.

# Chapter 6

**Crystal Engineering with Aroyl Hydrazones of Acetylacetone –**
**Molecular and Supramolecular Structures of Some**
**Oxomolybdenum(VI) Complexes in Relation to Biological Activity**

# Chapter 6

**Crystal Engineering with Aroyl Hydrazones of Acetylacetone – Molecular and Supramolecular Structures of Some Oxomolybdenum(VI) Complexes in Relation to Biological Activity**

**Abstract**

In this chapter we present a detailed account of the synthesis, structure, spectroscopic, electrochemical properties and study of biological activity of some oxomolybdenum(VI) complexes with special reference to their H–bonded molecular and supramolecular structures. Reaction of bis(acetylacetonato)dioxomolybdenum(VI) with three different hydrazides (isonicotinoyl hydrazide, anthraniloyl hydrazide and 4-nitrobenzoyl hydrazide) afforded two di-oxomolybdenum(VI) complexes $\{[MoO_2L^1(CH_3OH)]$ (**1**) and $[MoO_2L^3]$ (**3**)$\}$ and one mono-oxomolybdenum(VI) complex $\{[MoOL^2(O–N)]$ (**2**)$\}$ (where L = Intermediate *in situ* ligand formed by the reaction between acetyl acetone and the corresponding acid hydrazide, and O–N = 4-nitrobenzoylhydrazide). All the complexes have been characterized by elemental analysis, electrochemical and spectroscopic (IR, UV–Vis and NMR) measurements. Molecular structures of all the complexes (**1**, **2** and **3**) have been determined by X-ray crystallography. The complexes have been screened for their antibacterial activity against *Escherichia coli*, *Bacillus subtilis* and *Pseudomonas aeruginosa*. The Minimum inhibitory concentration of these complexes and antibacterial activity indicates **1** as the potential lead molecule for drug designing.

## 6.1. Introduction

Crystal engineering and the design of solid-state architectures has become an area of increasing interest over recent years [1–4]. Much study has been centered upon the use of supramolecular contacts, particularly hydrogen-bonding, between suitable molecules to generate multi-dimensional arrays or networks [1–3]. Variation in the ligand architecture coupled with a change in the geometric disposition of the ligands induced by metal nodes may give rise to a number of one-, two- and three-dimensional infinite frameworks, such as diamondoid [5,6], helix [7,8], brick wall [9,10], ladder [9–13], honeycomb [9,10], square grid and parquet [14], and other three-dimensional frameworks. Some supramolecular assemblies are also known to exhibit interesting redox, magnetic and optical [15,16] properties.

In some previous work [17,18], our group have reported several supramolecular architecture of oxovanadium(V) aroyl hydrazone and mixed-ligand Ni(II) thiosemicarbazone complexes by slight modification of the substituents attached to the ligand framework. In this chapter, I would like to examine the possible change in the coordination behavior of the ligands and its concomitant effect on the solid state supramolecular assembly of the complexes, when aliphatic carbonyl functionality is used instead of the aromatic carbonyls that were used for Schiff base formation in the previous studies [17–19]. Chattopadhyay et al. has recently highlighted the special role of aroyl hydrazones by systematic variation in the H-bond forming abilities of their aroyl moiety. Which can influences the formation of supramolecular assembly of transition metal complexes in generating varied molecular architectures [20–22].

Keeping this in mind, we have synthesized Schiff bases of acetyl acetone with isonicotinoyl hydrazide, benzoyl hydrazide and anthraniloyl hydrazide to study the supramolecule forming abilities of these Schiff bases. These aroyl hydrazones have been chosen in such a way that the aroyl moiety varies from being a H–bond donor (anthraniloyl), a H-bond acceptor (isonicotinoyl) and one which has no H–bond donor and acceptor ability (benzoyl). We shall show below that such a systematic variation of the H–bond forming ability has a profound effect on the supramolecular structures of these molecules (**Scheme 6.1**).

The hydrazone compounds along with their metal complexes have been extensively investigated for their versatile coordination modes [23–25] with prospective biological activities [26–28]. On the other hand, the coordination chemistry of molybdenum has been a subject of enthusiastic research due to its proven role of catalytic activity [29–42] in various biological and industrial

processes, and the potential medicinal effect as therapeutic agents such as antiamoebic activity [43] and DNA synthesis inhibition [44–46]. Our group has been studying the coordination complexes of penta- and hexavalent molybdenum with aroyl hydrazones derived from various acid hydrazides over the past several years [47–50]. Accordingly, in this chapter we present a detailed account of the synthesis, structure, spectroscopic, electrochemical properties and study of biological activity of some dioxomolybdenum(VI) complexes with special reference to their H–bonded molecular and supramolecular structures.
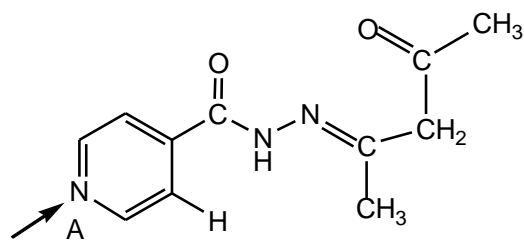
$H_2L^1$:The aroyl moiety is a H-bond acceptor only
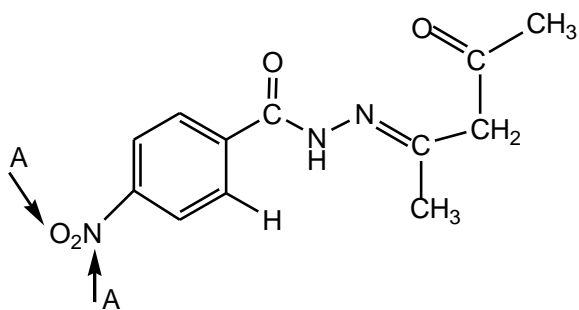


$H_2L^2$:The aroyl moiety is a H-bond acceptor only
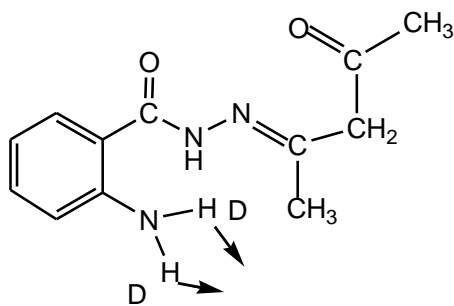


$H_2L^3$:The aroyl moiety is a H-bond donor only
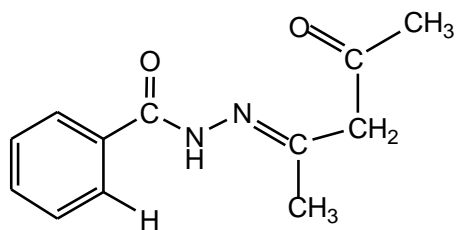


The aroyl moiety has no H-bonding ability

**Scheme 6.1.** Possible H-bond donor acceptor sites on the ligand containing aroyl moiety

## 6.2. Experimental

### 6.2.1. Materials

[MoO$_2$(acac)$_2$] and acid hydrazides were prepared as described in the literature [51,52]. Reagent grade solvents were dried and distilled prior to use. All other chemicals were reagent grade, available commercially and used as received. Commercially available TBAP (tetra butyl ammonium perchlorate) was properly dried and used as a supporting electrolyte for recording cyclic voltammograms of the complexes.

### 6.2.2. Physical Measurements

Elemental analyses were performed on a Vario ELcube CHNS Elemental analyzer. IR spectra were recorded on a Perkin-Elmer Spectrum RXI spectrometer. $^1$H NMR spectra were recorded with a Bruker Ultra shield 400 MHz spectrometer using SiMe$_4$ as an internal standard. Electronic spectra were recorded on a Lamda25, PerkinElmer spectrophotometer. Magnetic susceptibility was measured with a Sherwood Scientific AUTOMSB sample magnetometer. Electrochemical data were collected using a PAR electrochemical analyzer and a PC-controlled Potentiostat/Galvanostat (PAR 273A) at 298 K in a dry nitrogen atmosphere. Cyclic voltammetry experiments were carried out with a platinum working electrode, platinum auxiliary electrode, Ag/AgCl as reference electrode and TBAP as supporting electrolyte.

### 6.2.3. Synthesis of complexes (1–3)

To the refluxing solution of 1.0 mmol of hydrazides [Isonicotinoylhydrazide (**1**), 4-nitrobenzoylhydrazide (**2**) and anthraniloylhydrazide (**3**)] in 30 mL of methanol, 1.0 mmol of MoO$_2$(acac)$_2$ was added [53]. The color of the solution changed to dark red. The mixture was then refluxed for 3 hr. After leaving the solution for 2 days at room temperature, fine dark red colored crystals were isolated and a suitable single crystal was selected for X-ray analysis.

*[MoO$_2$L$^1$(CH$_3$OH)](1):* Yield: 0.25g (66%). Anal. Calcd for C$_{12}$H$_{15}$N$_3$O$_5$Mo: C, 38.21; H, 4.01; N, 11.14. Found: C, 38.23; H, 4.02; N, 11.12%. $^1$H NMR (DMSO-d$_6$, 400 MHz): $\delta$ = 8.70–7.79 (m, 4H, Aromatic), 5.53 (s, 1H, CH), 4.11 (s, 1H, OH–methanol), 3.16 (s, 3H, CH$_3$–methanol), 2.35 (s, 3H, CH$_3$), 2.01 (s, 3H, CH$_3$). $^{13}$C NMR (DMSO-d$_6$, 100 MHz): $\delta$ = 170.87, 165.30, 162.93, 150.78, 138.38, 121.79, 115.48, 110.28, 103.31, 49.05, 24.07, 20.57.

*[MoOL²(O–N)](2; O-N = 4-nitrobenzoylhydrazide):* Yield: 0.32g (57%). Anal. Calcd for $C_{19}H_{16}N_6O_8Mo$: C, 41.31; H, 2.91; N, 15.21. Found: C, 41.28; H, 2.93; N, 15.17%. $^1$H NMR (DMSO-$d_6$, 400 MHz): $\delta$ = 8.71 (s, 1H, NH), 8.10–8.33 (m, 8H, Aromatic), 5.84 (s, 1H, CH), 2.58 (s, 3H, CH$_3$), 2.16 (s, 3H, CH$_3$). $^{13}$C NMR (DMSO-$d_6$, 100 MHz): $\delta$ = 170.89, 166.28, 165.24, 162.94, 150.52, 149.25, 136.97, 136.82, 131.18, 129.28, 124.34, 124.22, 121.67, 120.42, 119.48, 117.28, 103.37, 24.07, 20.61.

*[MoO₂L³](3):* Yield: 0.23g (64%). Anal. Calcd for $C_{12}H_{13}N_3O_4Mo$: C, 40.11; H, 3.62; N, 11.69. Found: C, 40.08; H, 3.64; N, 11.67%. $^1$H NMR (DMSO-$d_6$, 400 MHz): $\delta$ = 6.60–7.67 (m, 4H, Aromatic), 6.84 (s, 2H, NH$_2$), 5.56 (s, 1H, CH), 2.42 (s, 3H, CH$_3$), 2.06 (s, 3H, CH$_3$). $^{13}$C NMR (DMSO-$d_6$, 100 MHz): $\delta$ = 169.52, 165.79, 161.91, 149.26, 132.33, 130.08, 116.24, 115.38, 110.60, 103.12, 23.97, 21.08.

### 6.2.4. Crystallography

Suitable single crystal of **1**, **2** and **3** were chosen for X-ray diffraction studies. Crystallographic data and details of refinement are given in **Table 6.1**. Details of the classical hydrogen bonding are given in **Table 6.2**. The compound **1** crystallized in monoclinic space group *C 1 c 1* and compounds **2** and **3** crystallized in triclinic space group *P $\bar{1}$* and *P2$_1$/c* respectively. Single crystal X-ray diffraction data collection and analysis were performed on a Bruker SMART APEX II diffractometer with a sealed tube, K$_\alpha$ Mo source ($\lambda$=0.71073 A), graphite monochrometer and CCD detector. An Oxford 700 Cryostream N$_2$ open-flow temperature system was used. The unit cell refinement and the integration of the diffraction frames were done with Bruker SAINT. Intensity data were corrected for Lorentz and polarization effects. Absorption corrections were applied using SADABS, and the structures were solved by direct methods and refined using least squares with the SHELXL–97 [54] software program.

### 6.2.5. Antibacterial activity

Antibacterial activity of the complexes was studied against *Escherichia coli (E. coli), Bacillus subtilis* and *Pseudomonas aeruginosa* by agar well diffusion technique. Mueller Hinton-agar (containing 1% peptone, 0.6% yeast extract, 0.5% beef extract and 0.5% NaCl, at pH 6.9−7.1) plates were prepared and 0.5–McFarland culture (1.5 x 10$^8$ cells /mL) of the test organisms were

swabbed onto the agar plate (as per CLSI guidelines, 2006) [55]. Test compounds were dissolved in DMSO at several concentrations ranging from 1000 μg/mL–1.95 μg/mL. 9 mm wide wells were dug on the agar plate using a sterile cork borer. 100 μg/mL of the solutions of each test compound from each dilution were added into each of the wells using a micropipette. These plates were incubated for 24 h at 35 ± 2 °C. The growth of the test organisms was inhibited by diffusion of the test compounds and then the inhibition zones developed on the plates were measured [18,19,56,57]. The effectiveness of an antibacterial agent in sensitivity is based on the diameter of the zones of inhibition which is measured to the nearest millimeter (mm). The standard drug Vancomycin was also tested for their antibacterial activity at the same concentration under the conditions similar to that of the test compounds as +ve control. DMSO alone was used as a –ve control under the same conditions for each organism.

**Table 6.1** Crystal and refinement data of complexes **1**, **2** and **3**

| Compound | 1 | 2 | 3 |
|---|---|---|---|
| Formula | $C_{12}H_{15}MoN_3O_5$ | $C_{19}H_{16}MoN_6O_8$ | $C_{12}H_{13}MoN_3O_4$ |
| M | 377.21 | 552.32 | 359.19 |
| Crystal symmetry | Monoclinic | Triclinic | Monoclinic |
| Space group | *C 1 c 1* | *P $\bar{1}$* | *P2$_1$/c* |
| $a(\AA)$ | 14.1081(10) | 7.5791(3) | 6.7999(5) |
| $b(\AA)$ | 7.5782(10) | 11.4060(4) | 13.2638(8) |
| $c(\AA)$ | 13.9670(10) | 13.2523(4) | 15.5050(8) |
| $\alpha$ (°) | 90.00 | 73.825(2) | 90.00 |
| $\beta$ (°) | 111.59 | 84.423(2) | 116.012(2) |
| $\gamma$ (°) | 90.00 | 81.4190(10) | 90.00 |
| $V(\AA^3)$ | 1388.5(2) | 1086.09(7) | 1256.78(14) |
| Z | 4 | 2 | 4 |
| $D_{calc}(g.cm^{-3})$ | 1.804 | 1.689 | 1.898 |
| F(000) | 760 | 556 | 720 |
| $\mu(Mo\text{-}K\alpha)(mm^{-1})$ | 0.970 | 0.664 | 1.061 |
| max./min.trans. | 0.8005 / 0.6530 | 0.8516 / 0.6914 | 0.999 / 0.829 |
| $2\theta(max)(°)$ | 26.99 | 28.25 | 25.50 |
| Reflections collected / unique | 24336/ 3031 | 8574 / 5105 | 3275 / 2933 |
| $R_1^a[I>2\sigma(I)]$ | R1 = 0.0128, wR2 = 0.0514 | R1 = 0.0379, wR2 = 0.0960 | R1 = 0.0283, wR2 = 0.0527 |
| $wR_2^b[all\ data]$ | R1 = 0.0128, wR2 = 0.0512 | R1 = 0.0515, wR2 = 0.1022 | R1 = 0.0238, wR2 = 0.0514 |
| S[goodness of fit] | 0.506 | 1.048 | 0.990 |
| min./max. res.(e.$\AA^{-3}$) | 0.233/ -0.430 | 0.580 / -0.617 | 0.534/-0.578 |

$^aR_1 = \Sigma \left| F_O \right| - \left| F_C \right| / \Sigma \left| F_O \right|$

$^bwR_2 = \{\Sigma [w (F_O^2 - F_C^2)^2]/\Sigma [w (F_O^2)^2]\}^{1/2}$

**Table 6.2** Hydrogen bond distances (A) and angles ($^o$) for **1** & **3**

| D–H…A | D–H(Å) | H…A(Å) | D…A(Å) | <D–H…A (∘) |
|---|---|---|---|---|
| *[MoO₂L¹(CH₃OH)](1)* | | | | |
| O5–H5…N3 | 0.915(18) | 1.742(19) | 2.655(2) | 175.2(16) |

*Symmetry transformations used to generate equivalent atoms:*

(a) x, y, z' ; (b) 'x, -y, z + 1/2'; (c) 'x + 1/2, y + 1/2, z'; (d) 'x + 1/2, -y + 1/2, z + 1/2'

| | | | | |
|---|---|---|---|---|
| *[MoO₂L³] (3)* | | | | |
| N3–H3B…N2 | 0.873(19) | 2.02(2) | 2.734(3) | 137.7(19) |
| C1–H1C…O3 | 0.96 | 2.57 | 3.491(3) | 162 |
| C5–H5B…O1 | 0.96 | 2.56 | 3.443(3) | 154 |
| C5–H5C…O4 | 0.96 | 2.58 | 3.144(3) | 117 |
| C11–H11…O1 | 0.93 | 2.44 | 3.224(3) | 142 |

*Symmetry transformations used to generate equivalent atoms:*

(a) x, y, z ; (b) -x, 1/2 + y, 1/2 - z ; (c) -x, -y, -z ; (d) x, 1/2 - y, 1/2 + z

## 6.3. Results and Discussion

### 6.3.1. Synthesis

The potentially tridentate diprotic ONO donor ligands used in the present work are generally abbreviated as $H_2((L^n)^{2-})$. The ligands $((L^n)^{2-})$ are thus formed due to template reactions between one of the metal coordinated acetylacetonate in $[MoO_2(acac)_2]$ and the corresponding acid hydrazide. The *in situ* ligands are formed as intermediate during the metallation reactions. Methods used for syntheses of the oxomolybdenum complexes (**1–3**) are given in experimental section. Reactions of the selected acidhydrazide with $MoO_2(acac)_2$ proceed in refluxing methanol and each of these reactions (**Scheme 6.2**) afford dark red color products in decent yields. These compounds are highly soluble in aprotic solvents, viz. DMF or DMSO and are sparingly soluble in alcohol, $CH_3CN$ and $CHCl_3$. All these complexes are diamagnetic, indicating the presence of molybdenum in the + 6 oxidation state, and are nonconducting in solution.



R = H, X =N, Y=.... (n = 1),   $H_2L^1$

R = H, X=C, Y=NO$_2$ (n = 2), $H_2L^2$

R = NH$_2$, X=C, Y=H (n =3), $H_2L^3$

O-N = *4*-nitrobenzoylhydrazide

Ligand formed in insitu reaction

(Intermediate $H_2L^n$)

$[Mo^{VI}O_2L^1(CH_3OH)]$ (1)    $[Mo^{VI}OL^2(O-N)]$ (2)    $[Mo^{VI}O_2L^3]$ (3)
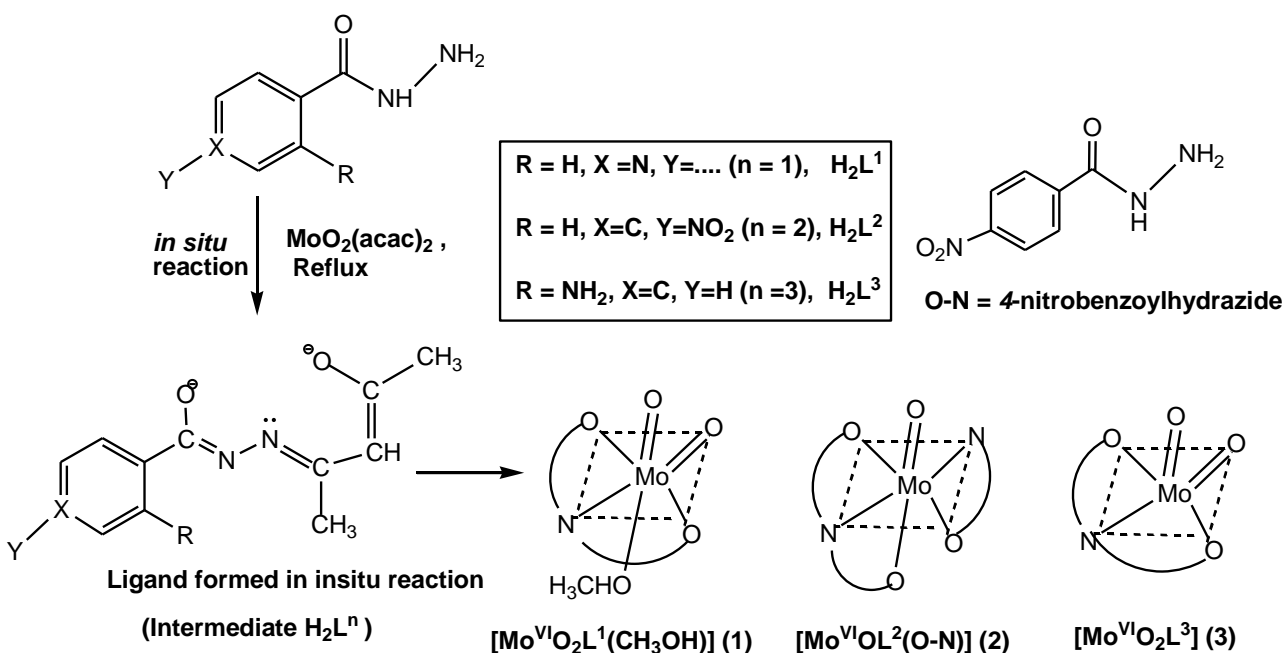
**Scheme 6.2**

*6.3.2. Spectral properties*

Spectral characteristics of all the compounds (**1–3**) are listed in **Table 6.3**. Infrared spectra of the complexes in KBr disks do not display the characteristic bands associated with the C=O and the N–H functionalities of the free Schiff base system $H_2L^n$. Thus in each complex both the acetylacetone and the amide fragments of the metal coordinated tridentate ligand $((L^n)^{2-})$ are in enolate form. All the complexes display a strong band within 1579–1554 cm$^{-1}$. This band is attributed to the C=N–N=C fragment of the *in situ* ligand [53]. Complexes **1** and **3** display a strong and a moderately strong band in the range 939–931 cm$^{-1}$ and 909–899 cm$^{-1}$ respectively due to terminal $v(M=O_t)$ stretch [45–50]. Whereas, the complex **2** exhibits only one such peak at 950 cm$^{-1}$, which is because of monooxo species. The infrared spectrum of the complex **1** is shown in **Fig. 6.1** as the representative one.

The DMSO solution of all the complexes display a shoulder in the 436–422 nm region and two strong absorptions in the 327–264 nm range which are assignable to L→Mo(dπ) (LMCT) and intraligand transitions respectively [45–50]. The electronic spectrum of complex **2** is shown in **Fig. 6.2** as the representative one.

The $^1$H and $^{13}$C NMR spectroscopic data of all the complexes are given in the experimental section. NMR spectrum of complex **3** is shown in **Fig. 6.3** as the representative one. The NMR spectra of **1–3** display two singlets in the ranges δ = 2.16–2.01 ppm and δ = 2.58–2.35 ppm [53]. These are assigned to the protons of the two methyl groups present in the acetylacetone fragment of the tridentate ligand [53]. The –CH= proton of the acetylacetone fragment appears as a singlet within δ = 5.84–5.53 ppm [53]. The complex **2** exhibits one –NH proton resonance at δ =8.71 ppm, due to the coordination of the hydrazide moiety (co-ligand). The aromatic protons are observed in the range δ = 8.70–6.60 ppm. The chemical shift of the coordinated $CH_3OH$ of complex **1** exhibits an OH resonance at δ = 4.11 ppm and $CH_3$ resonance at δ = 3.16 ppm [45–50].

**Table 6.3** Characteristic IR$^{[a]}$ bands and electronic spectral data$^{[b]}$ for the studied complexes (**1-3**)

| Complex | $\nu$(C=N) | $\nu$(Mo=O)/cm$^{-1}$ | $\lambda_{max}$/nm ($\varepsilon$/dm$^3$ mol$^{-1}$ cm$^{-1}$) |
|---------|------------|------------------------|-----------------------------------------------------------------|
| [MoO$_2$L$^1$(CH$_3$OH)] (**1**) | 1579 | 939, 909 | 422 (9439), 314 (25123), 269 (16352) |
| [MoOL$^2$(O–N)] (**2**) | 1575 | 950 | 436 (9434), 267 (16350) |
| [MoO$_2$L$^3$] (**3**) | 1554 | 931, 899 | 431 (9569), 327 (26126), 264 (15711) |

$^{[a]}$ In KBr pellet; $^{[b]}$ In DMSO
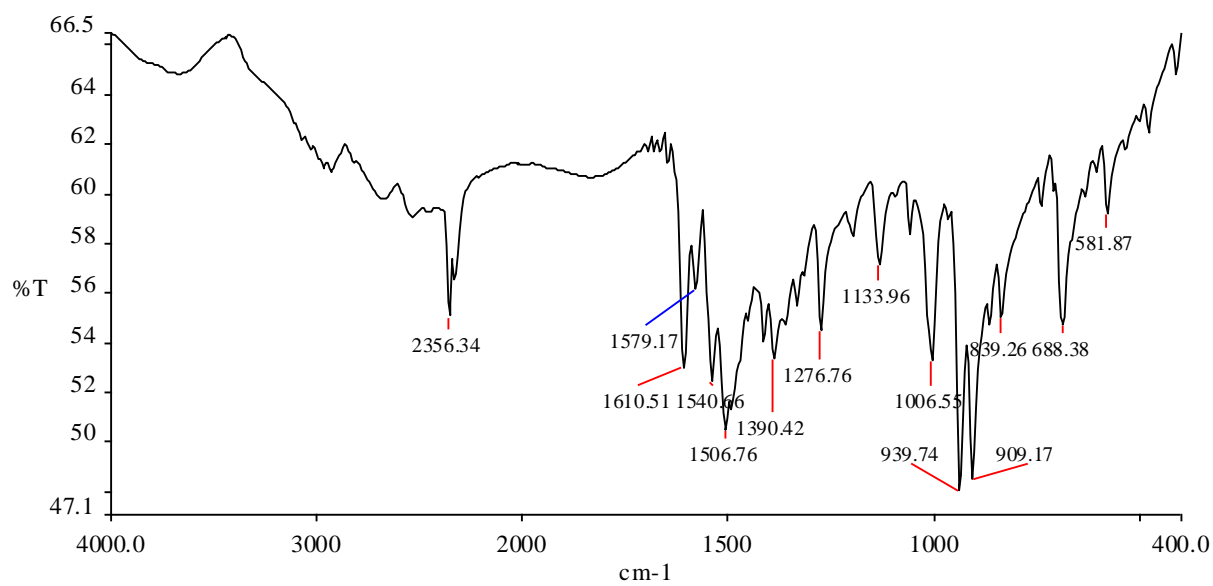
**Fig.6.1.** IR spectrum of [MoO$_2$L$^1$(CH$_3$OH)] (**1**)
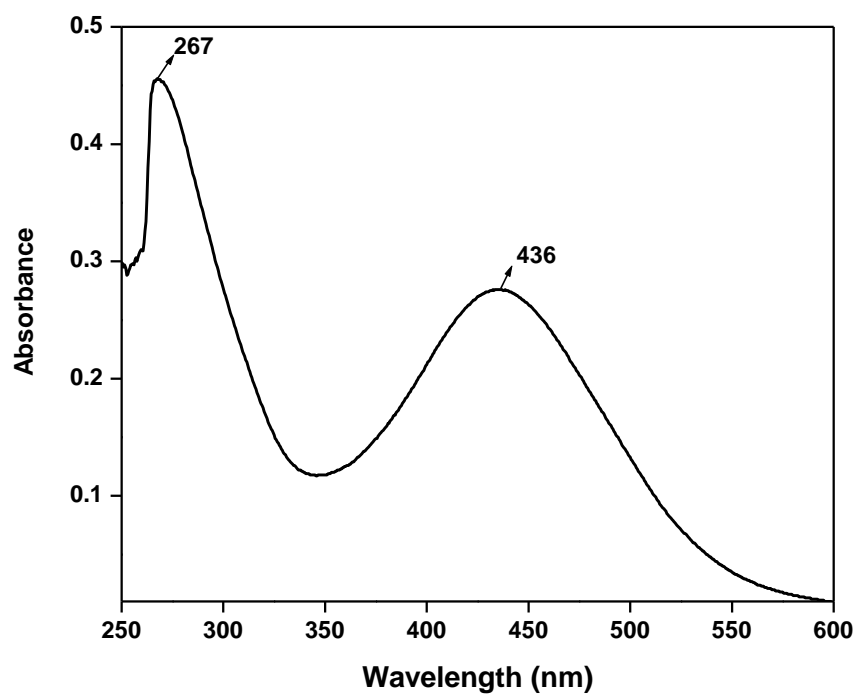
**Fig.6.2.** Electronic absorption spectra of $[MoOL^2(O–N)]$ (**2**) in DMSO, at $25^0$ C

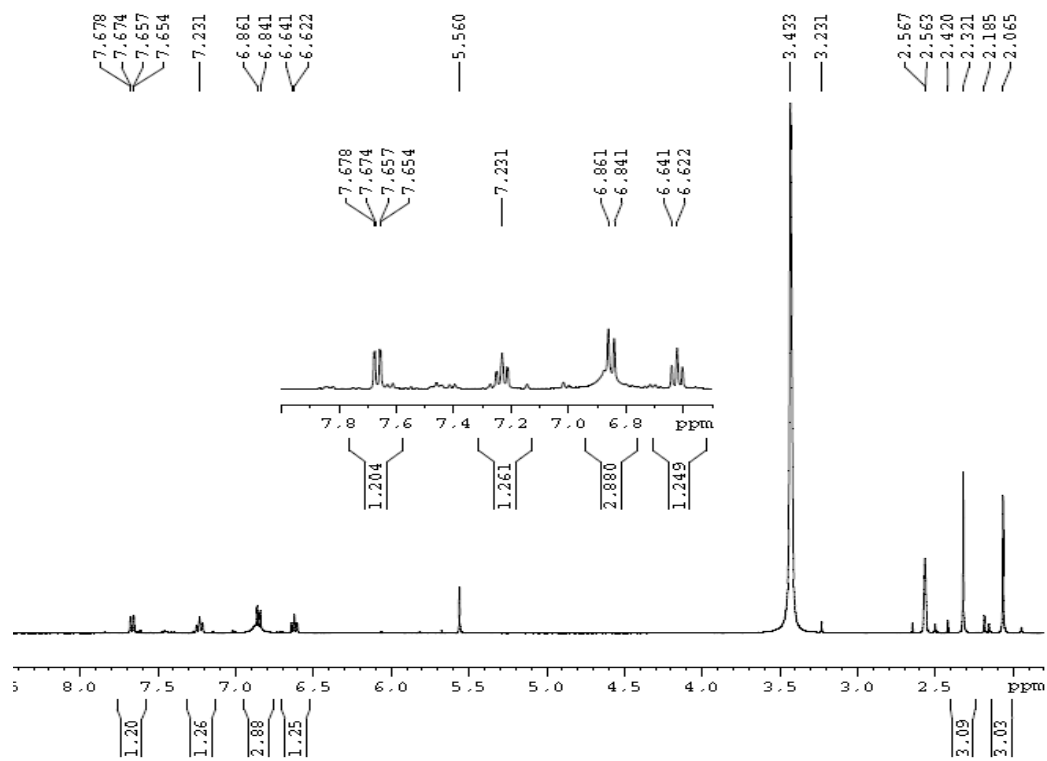**Fig.6.3.** $^1$H NMR spectra of [MoO$_2$L$^3$] (**3**) in DMSO d$_6$.

## 6.3.3. Electrochemical properties

Electrochemical properties of the complexes have been studied by cyclic voltammetry in DMSO solution (0.1 M TBAP). Voltammetric data are given in **Table 6.4** and the cyclic voltamogram of $MoO_2L^1(CH_3OH)$ (**1**) is displayed in **Fig.6.4** as the representative one. The CV traces of complexes (**1–3**) exhibit two irreversible reductive responses within the potential window –0.17 to –0.25 V and –1.02 to –1.08 V, which are assigned to $Mo^{VI}/Mo^{V}$ and $Mo^{V}/Mo^{IV}$ process respectively [48]. An oxidation wave at positive potentials in the range of +1.43 V to +1.47 V, which is assigned to oxidation of the coordinated ligands [48]. As the Mo(VI) complex cannot undergo a metal-centered oxidation, this is attributed to a ligand-centered process [48].

**Table 6.4** Cyclic voltammetric results for dioxomolybdenum (VI) complexes (**1–3**) at 298 K

| Complex | $E$pc [V][a] |
|---------|--------------|
| $[MoO_2L^1(CH_3OH)]$ (**1**) | –0.17, –1.02 |
| $[MoOL^2(O–N)]$ (**2**) | –0.20, –1.06 |
| $[MoO_2L^3]$ (**3**) | –0.25, –1.08 |

[a] Solvent: DMSO; working electrode: platinum; auxiliary electrode: platinum; reference electrode: Ag/AgCl; supporting electrolyte: 0.1 M TBAP; scan rate: 50 mV/s. $E$pc is the cathodic peak potential
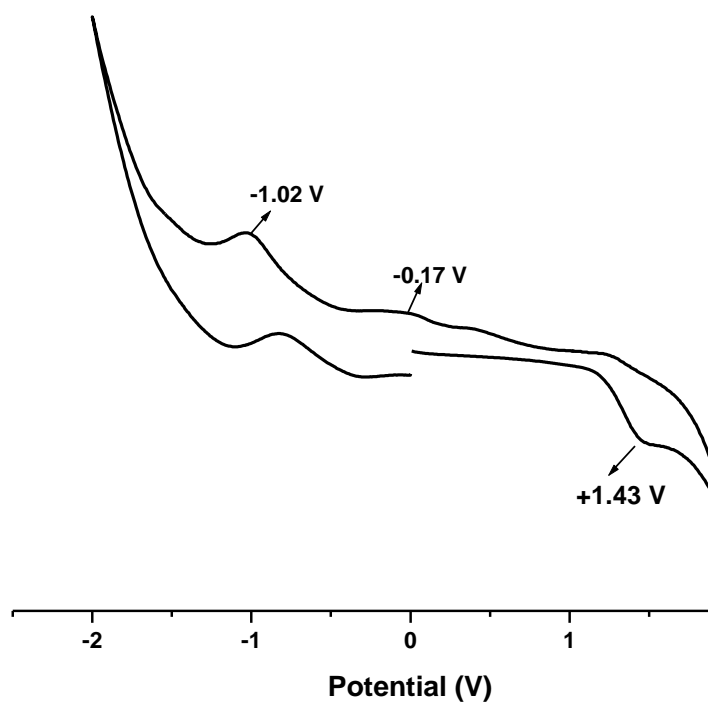
**Fig. 6.4**. Cyclic voltammogram of $[MoO_2L^1(CH_3OH)]$ (1) in DMSO

*6.3.4. Description of the X-ray structure of complex [MoO₂L¹(CH₃OH)](**1**) and [MoOL²(O–N)](**2**)*

The molecular structure and the atom numbering schemes for the complex [MoO$_2$L$^1$(CH$_3$OH)] (**1**) and [MoOL$^2$(O–N)] (**2**) are shown in **Figs 6.5** and **6.6** respectively, with the relevant bond distances and angles collected in **Table 6.5**. In each complex, the tridentate intermediate *in situ* ligand coordinates the metal ion via the enolate –O, the imine –N and the deprotonated amide –O atoms, with bite angles of 72.68(4)–74.26(8) [N(1)–Mo(1)–O(3)] and 82.20(6)–83.50(9) [N(1)–Mo(1)–O(4)] forming one five- and one six-membered chelate ring. The coordination geometry around the molybdenum(VI) atom in **1** and **2** reveals a distorted octahedral environment with an NO$_5$ and N$_2$O$_4$ coordination sphere respectively.

In complex **1**, one of the two oxo group O(2) is located trans to the imine nitrogen in the same plane and the other oxo group O(1) is located in the axial plane with the solvent molecule [CH$_3$OH (**1**)]. The common characteristic of the structure **2** is the absence of one oxo group and a metal–coordinating solvent molecule, and these are replaced by a co-ligand (O–N = *4-nitrobenzoylhydrazide*). The fifth and sixth coordination sites are occupied by this co-ligand through the enolate oxygen –O(2) and amine nitrogen –N(4) atoms (**Scheme 6.2**), forming a distorted octahedral complex (**Fig 6.6**) with the bond distances 2.138(2) [Mo(1)–O(2)] and 1.983(2) [Mo(1)–N(4)] respectively. The bond between Mo and the azomethine nitrogen in the complexes are within a range of 2.127–2.225 Å which is comparatively longer than the Mo–N(4) single bond in **2**. This is due to the trans effect generated by the oxo group trans to the Mo–N bond [49]. The C(6)–O(3) bond lengths for complex **1** and **2** are 1.324–1.330 Å, which is closer to single bond length rather than C=O double bond length. However, the short bond length compared to C–O single bond may be attributed to extended electron delocalization in the ligands. Similarly shortening of C(6)–N(2) length in complex **1** and **2** are 1.291–1.294 Å instead of normal 1.385Å.

The angular distortion in the octahedral environment around Mo comes from the bites taken by the Schiff base ligand. For the same reason the *trans* angles O(3)–Mo(1)–O(4) and O(2)–Mo(1)–N(1) are significantly reduced from the ideal value of 180°; the *trans*-axial angle O(1)–Mo(1)–O(5) is 172.36(5)° (complex **1**). The bond length of two oxo oxygen of MoO$_2$ group (complex **1**) is unexceptional and almost equal [1.697(1) & 1.708(1)]. The Mo–O(5) (alcohol) bond [2.330(1) Å (**1**)] is significantly longer than the other Mo–O bonds [1.697(1)–2.011(8) Å] indicating that

the alcohol molecule (complex **1**) is weakly bonded to the $MoO_2^{2+}$ core and this position holds the possibility of functioning as a substrate-binding site [19].

Both the molecules (**1** & **2**) are found to show inter molecular hydrogen bonding and it is observed in this complexes that due to variation in the H-bond donor acceptor properties of the ligands leads to considerable diversity in their supramolecular architecture [17,18,20–22]. Complex **1** form a polymeric unit via a hydrogen bond between the isonicotinoyl nitrogen N(3) of one molecule and the methanolic proton O(5)–H(5) of another moiety. Complex **2** is also found to show such supramolecular arrangement via a pair of reciprocal hydrogen bonds between the N(4)–H proton of one molecule and the imine nitrogen N(5) of other moiety. Some of the drawings of the corresponding H-bonded supramolecular arrangement of complex **1** & **2** as example of novel features of crystal engineering are shown in **Figs. 6.7–6.13**.

### 6.3.5. Description of the X-ray structure of complex [MoO₂L³] (3)

*6.3.5. Description of the X-ray structure of complex [MoO$_2$L$^3$] (3)*

The molecular structure and the atom numbering schemes of **3** is shown in **Fig. 6.14** with the relevant bond distances and angles collected in **Table 6.5**. The crystallographic analysis of a suitable crystal of **3** revealed a five-coordinate mononuclear complex, one structural type quite uncommon for dioxomolybdenum(VI) complexes [58], that are generally six-coordinate showing a distorted octahedral coordination sphere. For related dioxomolybdenum(VI) species bearing a tridentate ligand, the sixth position is typically occupied by a donor ligand [59–61]. In some cases, the supposed five-coordinate mononuclear complexes are weakly associated by unsymmetrical Mo–O…Mo interactions to give an essentially ''binuclear'' structure [62] or a ''linear polymeric''structure [61]. The molecular geometry of $MoO_2L^3$ is best represented as a square-pyramid with one axial oxo oxygen atom O(1), and three O atoms [O(2,3,4)] and the N(1) atom describing the equatorial plane, which is slightly distorted from an ideal geometry, as reflected in the bond parameters around the metal center. The length of the Mo–O(2) bond lying *trans* to N(1) is practically equal to Mo–O(1); the position *trans* to O(1) remains unoccupied. The other Mo–O and Mo–N distances are normal, as observed in other structurally characterized complexes of molybdenum containing these bonds [19,47–50].

Complex **3** is found to show both inter and intra molecular hydrogen bonding. $[MoO_2L^3]$ (**3**) molecules form a supramolecular three-dimensional network via four different intermolecular hydrogen bonds (**Fig.6.15**). A pair of intermolecular hydrogen bonds between the enolic oxygen

O(4) and O(3) of one molecule and the methyl ($CH_3$) proton C(5)–H(5C) and C(1)–H(1C) of another moiety, respectively. Another pair of intermolecular hydrogen bonds between the oxo oxygen O(1) of one molecule and the methyl ($CH_3$) proton C(5)–H(5B) and C(11)–H(11) of another moiety. Another hydrogen bonding interaction between the imine nitrogen N(2) and the amine ($NH_2$) hydrogen, N(3)–H(3B), is also observed to constitute an intramolecular hydrogen bond (**Fig. 6.14**).

**Table 6.5** Selected Bond Distances (Å) and Bond Angles (°) for Complex **1**, **2** and **3**

|  | Complex **1** | Complex **2** | Complex **3** |
|---|---|---|---|
| Bond lengths |  |  |  |
| Mo(1)-O(1) | 1.697(1) | 1.671(2) | 1.700(2) |
| Mo(1)-O(2) | 1.708(1) | 2.138(2) | 1.648(2) |
| Mo(1)-O(3) | 2.011(8) | 2.011(2) | 2.079(1) |
| Mo(1)-O(4) | 1.960(2) | 1.986(2) | 2.034(1) |
| Mo(1)-O(5) | 2.330(1) | -- | -- |
| Mo(1)-N(1) | 2.225(1) | 2.127(2) | 2.110(2) |
| Mo(1)–N(4) | -- | 1.983(2) | -- |
| Bond Angles |  |  |  |
| O(1)-Mo(1)-O(2) | 105.81(5) | 159.87(9) | 107.94(9) |
| O(1)-Mo(1)-O(3) | 97.45(4) | 100.2(1) | 97.10(8) |
| O(1)-Mo(1)-O(4) | 98.33(6) | 99.9(1) | 100.57(8) |
| O(1)-Mo(1)-O(5) | 172.36(5) | -- | -- |
| O(1)-Mo(1)-N(1) | 97.29(5) | 108.3(1) | 96.58(9) |
| O(2)-Mo(1)-O(3) | 95.98(4) | 83.59(8) | 95.26(8) |
| O(2)-Mo(1)-O(4) | 102.02(6) | 83.33(8) | 99.91(8) |
| O(2)-Mo(1)-O(5) | 81.68(4) | -- | -- |
| O(2)-Mo(1)-N(1) | 155.51(5) | 91.78(8) | 154.53(8) |
| O(3)-Mo(1)-O(4) | 151.77(6) | 153.74(9) | 151.83(7) |
| O(3)-Mo(1)-O(5) | 80.01(4) | -- | -- |
| O(3)-Mo(1)-N(1) | 72.68(4) | 74.26(8) | 74.47(7) |
| O(4)-Mo(1)-O(5) | 81.27(6) | -- | -- |
| O(4)-Mo(1)-N(1) | 82.20(6) | 83.50(9) | 81.83(7) |
| O(5)-Mo(1)-N(1) | 75.08(4) | -- | -- |
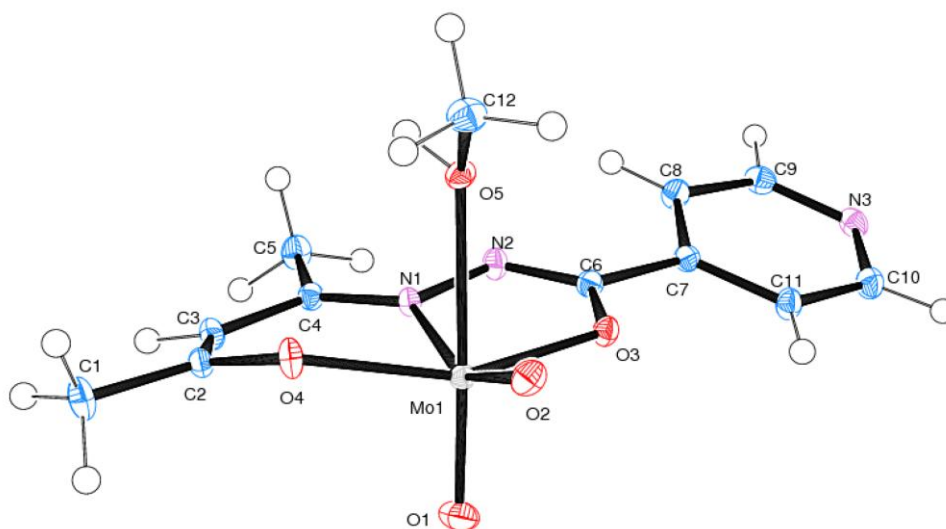
**Fig.6.5.** ORTEP diagram of [MoO$_2$L$^1$(CH$_3$OH)] (**1**) with atom labeling scheme
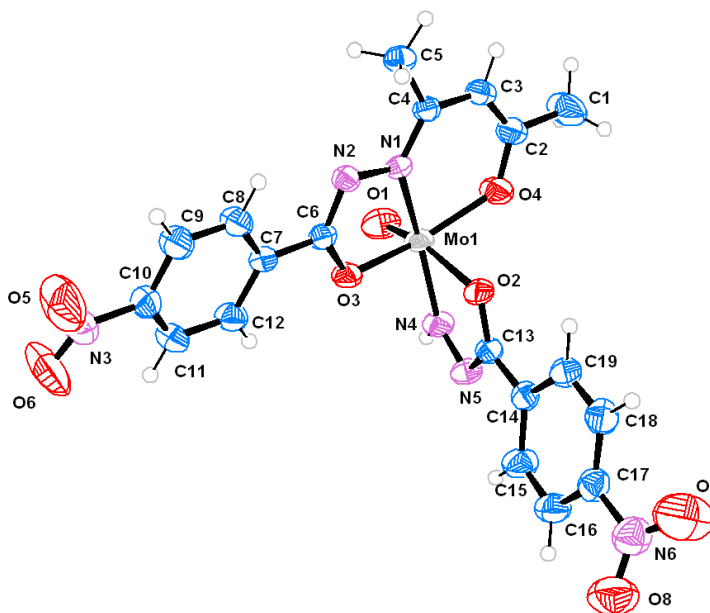
at 50% probability

.



**Fig. 6.6.** ORTEP diagram of [MoOL$^2$ (O–N)] (**2**) with atom labeling scheme
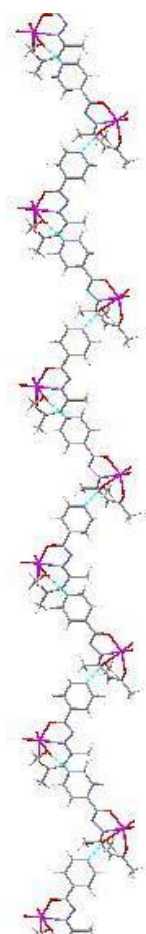
at 50% probability

.



**Fig.6.7.** H-bonded supramolecular single stranded helix of complex **1** view along c axis
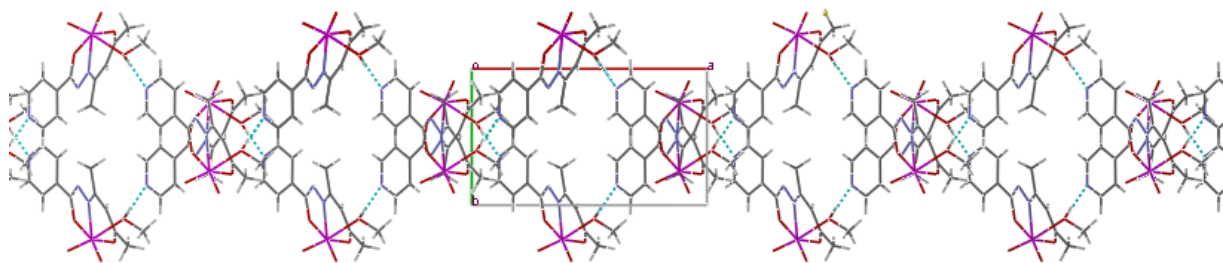
**Fig.6.8.** Spider net like packing of complex **1** view along c axis
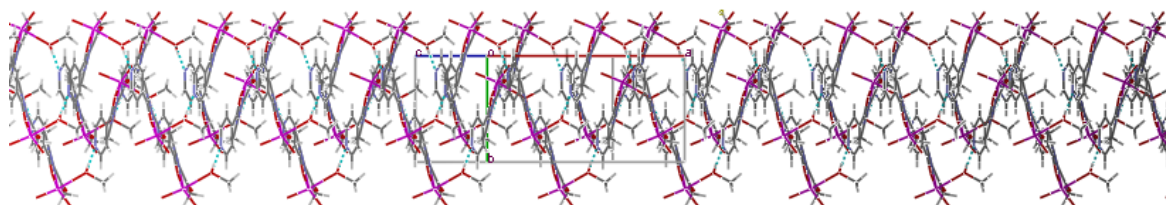


**Fig.6.9.** Cylindrical packing of complex **1** view perpendicular to c axis
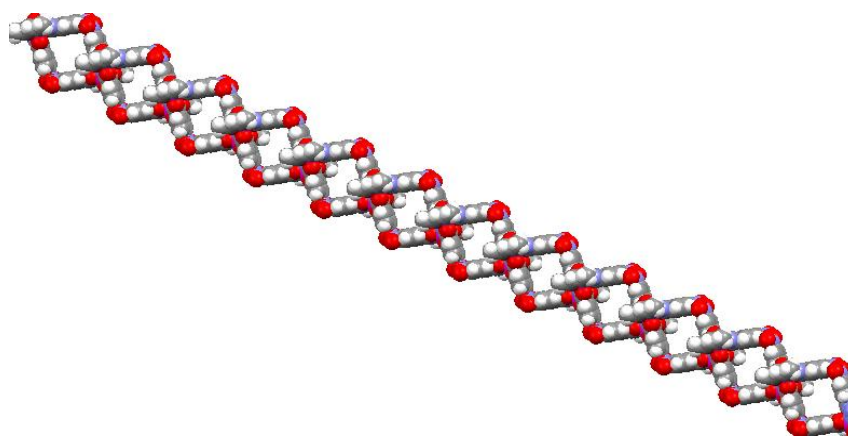


**Fig.6.10.** Chain like packing of complex **1** view perpendicular to c axis
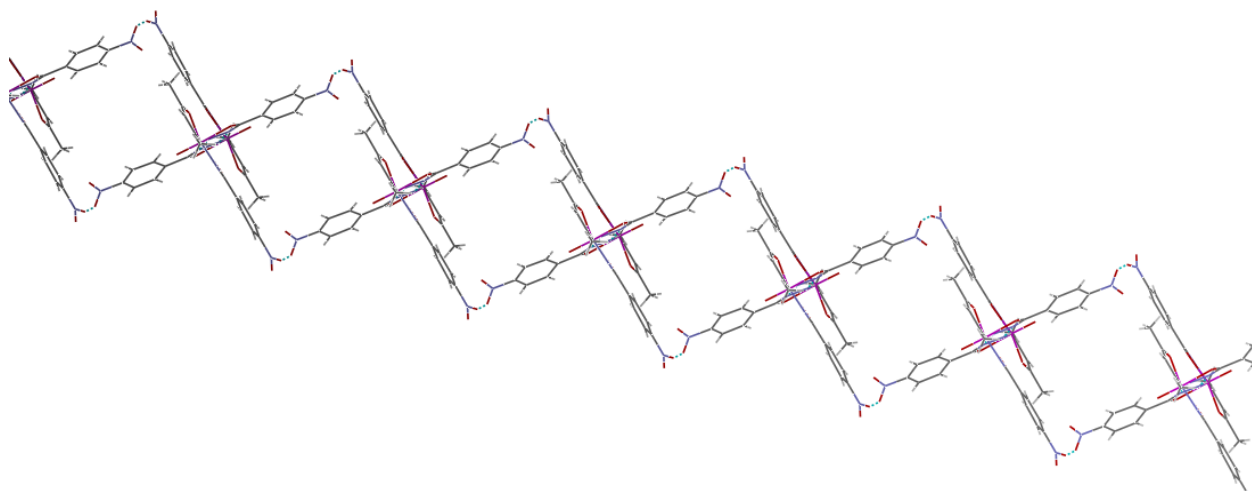
**Fig.6.11.** Two interpenetrating one-dimensional zig-zag chains through complementary pairs of hydrogen bonding in **2** view along the c axis.
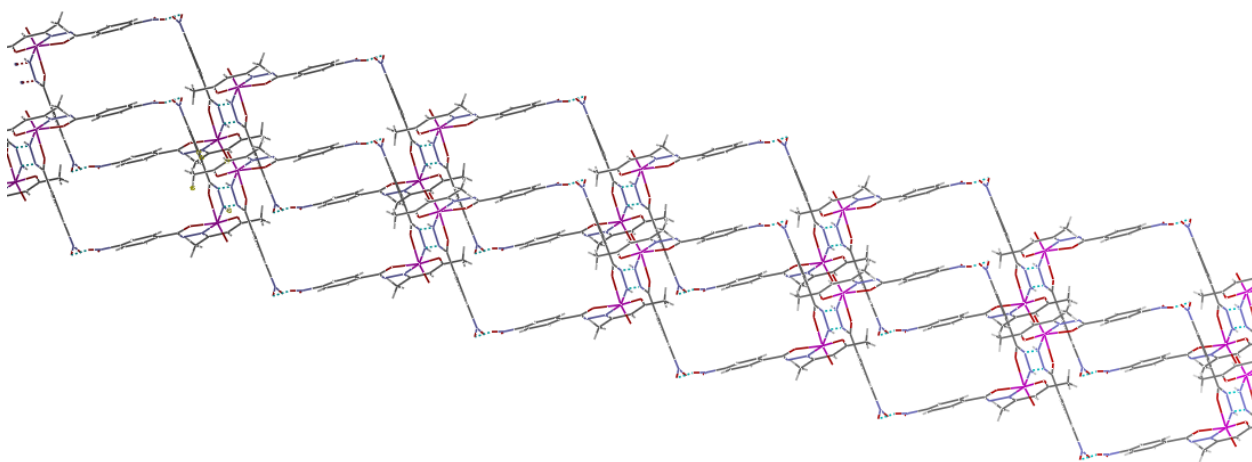


**Fig.6.12.** Four interpenetrating one-dimensional zig-zag chains through complementary pairs of hydrogen bonding in **2** view along the c axis.
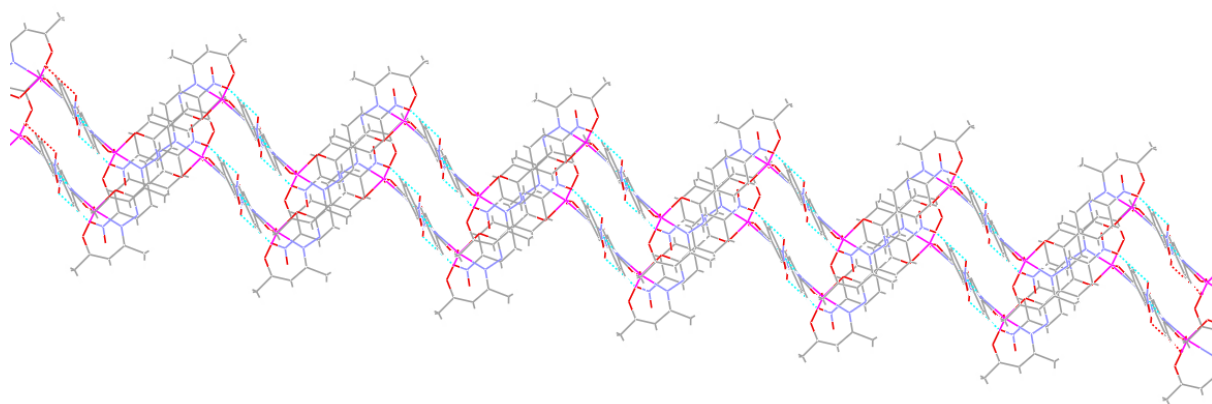
**Fig.6.13.** Staircase like packing arrangement of complex **2** view along a axis

**Fig.6.14.** PLATON diagram of $[MoO_2L^3]$ (**3**) with atom labeling scheme

at 50% probability

.

**Fig.6.15.** Packing diagram of $[MoO_2L^3]$ (**3**) along b axis

*6.3.6. Antibacterial activity*

The synthesized oxomolybdenum(VI) complexes (**1-3**) were screened for antimicrobial activity against the pathogenic strains of *Escherichia coli, Bacillus subtilis* and *Pseudomonas aeruginosa* by agar well-diffusion method and their MIC values are represented in **Table 6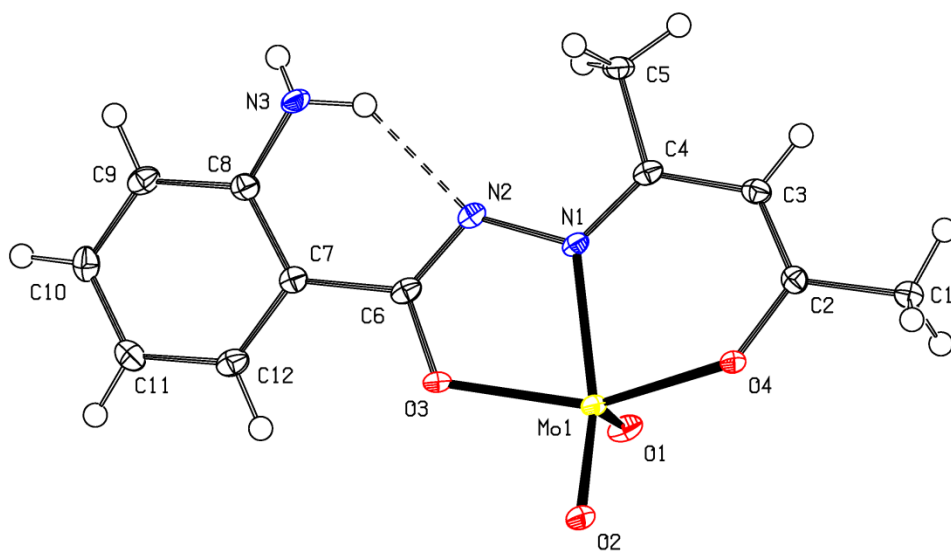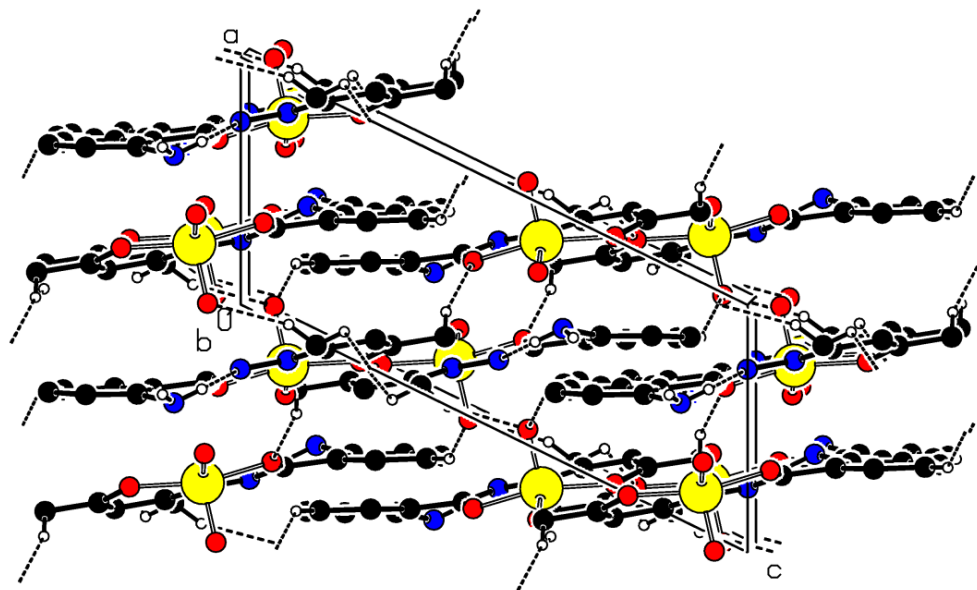.6** and **Fig. 6.16**. In some cases they showed promising results by giving the MIC value lesser than the standard drug examined. The results also indicate that the corresponding oxomolybdenum(VI) complexes showed much better antibacterial activity with respect to the individual hydrazide against the same microorganism under identical experimental conditions which is in agreement with the previous results [18,19,63–67]. A possible explanation is that, by coordination, the polarity of the ligand and the central metal ions are reduced through the charge equilibration, which favors permeation of the complexes through the lipid layer of the bacterial cell membrane [18,19,63–67].

From the zone of inhibition, it is observed that the complex **1** showed most promising results especially for *E.coli* compared to the other compounds (**2** and **3**) of this study and the difference in value may be attributed to the nature of compounds synthesized [68]. Antibacterial activity of the similar type oxo-metal complexes has also been reported by Sharma *et al.* [69] , Chohan *et al.* [70] and Prasad *et al.* [71] using agar well diffusion technique against *Escherichia coli*, *Shigella flexenari*, *Pseudomonas aeruginosa*, *Salmonella typhi*, *Staphylococcus aureus* and *Bacillus subtilis* and the present results are in accordance with the reported values. However, the difference in value may be attributed to the nature of compounds synthesized with different ligands.

**Table 6.6** Minimum Inhibitory Concentration (MIC) value in μg/mL of the oxomolybdenum(VI) complexes (**1–3**) and standard drugs against pathogenic strains

| | E.coli | Bacillus subtilis | Pseudomonas aeruginosa |
|---|---|---|---|
| $[MoO_2L^1(CH_3OH)]$ (**1**) | 15.6 | 62.5 | -- |
| $[MoOL^2(O–N)]$ (**2**) | -- | -- | -- |
| $[MoO_2L^3]$(**3**) | 31.2 | 31.2 | 250 |
| Vancomycin | 30 | 30 | -- |
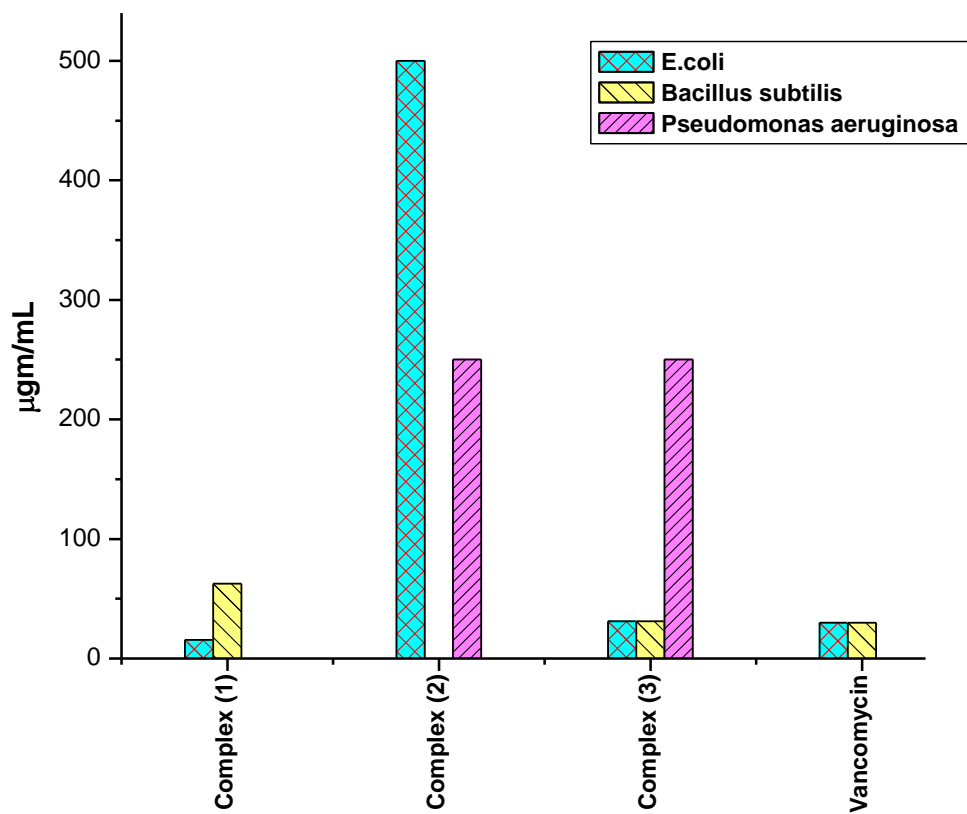
**Fig.6.16.** Minimum Inhibitory Concentration (MIC) of Mo(VI) complexes (**1–3**) and

standard drug

## 6.4. Conclusions

The synthesis of three new oxomolybdenum(VI) complexes (**1**, **2** and **3**) with aroyl hydrazones has been achieved in excellent yield and is characterized by various spectroscopic techniques, electrochemistry and X-ray crystallography. The special role of different hydrazones by systematic variation in the H-bond forming abilities of their aroyl moiety is successfully highlighted by the formation of supramolecular assembly of oxomolybdenum complexes in generating varied molecular architectures. The complexes have been screened for their antibacterial activity against *Escherichia coli, Bacillus subtilis* and *Pseudomonas aeruginosa*. Minimum inhibitory concentration of these complexes and antibacterial activity indicates the compound **1** as the potential lead molecule for drug designing.

**References**

[1] G.R. Desiraju, in *Crystal Engineering: Design of Organic Solids*, Elsevier, Amsterdam, (1989).

[2] The Crystal as a Supramolecular Entity, ed. G.R. Desiraju, Wiley, (1995).

[3] G.R. Desiraju, Angew. Chem., Int. Ed. Engl. 34 (1995) 2311.

[4] R.Robson, B.F. Abrahams, S.R. Batten, R.W. Gable, B.F. Hoskins, J. Liu, Supramolecular Architecture, ACS publications, (1992), ch. 19.

[5] S.S.M. Chung, W.S.Li, M. Schröder, Chem. Commun. (1997) 1005.

[6] A.J. Blake, N.R. Champness, A.N. Khlobystov, D.A. Lemenovskii, W.S. Li, M. Schröder, Chem. Commun. (1997) 1339.

[7] L. Carlucci, G. Ciani, D.W.V. Gudenberg, D.M. Proserpio, Inorg. Chem. 36 (1997) 3812.

[8] D. Wang, K. Kim, J. Am. Chem. Soc. 119 (1997) 451.

[9] M. Fujita, Y.J. Kwon, O. Sasaki, K. Yamaguchi, K. Ogura, J. Am. Chem. Soc. 117 (1995) 7287.

[10] H.J. Choi, M.P. Suh, J. Am. Chem. Soc. 120 (1998) 10622.

[11] T.L. Hennigar, D.C. MacQuarrie, P. Losier, R.D. Rogers, M.J. Zaworotko, Angew. Chem., Int. Ed. Engl. 36 (1997) 972.

[12] A.J. Blake, N.R. Champness, A.N. Khlobystov, D.A. Lemenovskii, W.S. Li, M. Schröder, Chem. Commun. (1997) 2027.

[13] Y.-B. Dong, R.C. Layland, M.D. Smith, N.G. Pschirer, U.H.F. Bunz, H.-C. zur Loye, Inorg. Chem. 38 (1999) 3056.

[14] M. Fujita, Y.J. Kwon, S. Wsahizu, K. Ogura, J. Am. Chem. Soc. 116 (1994) 1151.

[15] M. Ruben, J.-M. Lehn, G. Vaughan, Chem. Commun. (2003) 1338.

[16] L.H. Uppadine, J.-P. Gisselbrecht, J.-M. Lehn, Chem. Commun. (2004) 718.

[17] R. Dinda, P.K. Majhi, P. Sengupta, S. Pasayat, S. Ghosh, L.R. Falvello, T.C.W. Mak, Polyhedron 29 (2010) 248.

[18] Saswati, R. Dinda, C.S. Schmiesing, E. Sinn, Y.P. Patil, M. Nethaji, H. Stoeckli-Evans, R. Acharyya, Polyhedron 50 (2013) 354.

[19] S. Pasayat, S.P. Dash, Saswati, P.K. Majhi, Y.P. Patil, M. Nethaji, H.R. Dash, S. Das , R. Dinda, Polyhedron 38 (2012) 198.

[20] S. Naskar, D. Mishra, R.J. Butcher, S.K. Chattopadhyay, Polyhedron 26 (2007) 3703.

[21] S. Naskar, D. Mishra, S.K. Chattopadhyay, M. Corbella, A.J. Blake, Dalton Trans. (2005) 2428.

[22] S. Naskar, M. Corbella, A.J. Blake, S.K. Chattopadhyay, Dalton Trans. (2007) 1150.

[23] L.A. Saghatforoush, F. Chalabian, A. Aminkhani, G. Karimnezhad, S. Ershad, Eur. J. Med. Chem. 44 (2009) 4490.

[24] S. Pal, J. Chem. Crystallogr. 30 (2000) 329.

[25] E. Kwiatkowski, M. Kwiatkowski, A. Olechnowicz, G. Bandoli, J. Chem. Crystallogr. 23 (1993) 473.

[26] D. Sinha, A.K. Tiwari, S. Singh, G. Shukla, P. Mishra, H. Chandra, A. K. Mishra, Eur. J. Med. Chem. 43 (2008) 160.

[27] H.I. Ugras, I. Basaran, T. Kilic, U. Cakir, J. Heterocycl. Chem. 43 (2006) 1679.

[28] V. Vajpayee, Y.P. Singh, J. Coord. Chem. 61 (2008) 1622.

[29] K. Jeyakumar, D.K. Chand, J. Chem. Sci. 121 (2009) 111.

[30] M.R. Maurya, Curr. Org. Chem. 16 (2012) 73.

[31] R.D. Chakravarthy, K. Suresh, V. Ramkumar, D.K. Chand, Inorg. Chim. Acta 376 (2011) 57.

[32] Z. Hu, X. Fu, Y. Li, Inorg. Chem. Commun. 14 (2011) 497.

[33] M. Herbert, F. Montilla, A. Galindo, J. Mol. Catal. A: Chem. 338 (2011) 111.

[34] A. Rezaeifard, I. Sheikhshoaie, N. Monadi, M. Alipour, Polyhedron 29 (2010) 2703.

[35] I. Sheikhshoaie, A. Rezaeifard, N. Monadi, S. Kaafi, Polyhedron 28 (2009) 733.

[36] A. Gunyara, D. Betzb, M. Dreesb, E. Herdtweck, F.E. Kuhna, J. Mol. Catal. A: Chem. 331 (2010) 117.

[37] M.R. Maurya , S. Sikarwar , P. Manikandan , Appl. Catal., A 315 (2006) 74.

[38] A.J. Burke, Coord. Chem. Rev. 252 (2008) 170.

[39] K.R. Jain, W.A. Herrmann, F. E. Kuhn, Coord. Chem. Rev. 252 (2008) 556.

[40] K.C. Gupta, A.K. Sutar, Coord. Chem. Rev. 252 (2008) 1420.

[41] B. Frédéric, Coord. Chem. Rev. 236 (2003) 71.

[42] A. Syamal, M.R. Maurya, Coord. Chem. Rev. 95 (1989) 183.

[43] M.R. Maurya, S. Agarwal, M. Abid, A. Azam, C. Bader, M. Ebel, D. Rehder, Dalton Trans. (2006) 937.

[44] D.K. Johnson, T.B. Murphy, N.J. Rose, W.H. Goodwin, L. Pickart, Inorg. Chim. Acta 67 (1982) 159.

[45] T.B. Chaston, D.B. Lovejoy, R.N. Watts, D.R. Richardson, Clin. Cancer Res. 9 (2003) 402.

[46] G. Link, P. Ponka, A.M. Konijn, W. Breuer, Z.I. Cabantchik, C. Hershko, Blood 101 (2003) 4172.

[47] A. Rana, R. Dinda, P. Sengupta, L.R. Falvello, S. Ghosh., Polyhedron 21 (2002) 1023.

[48] R. Dinda, P. Sengupta, S. Ghosh, H.M. Figge , W.S. Sheldrick, Dalton Trans. (2002) 4434.

[49] R. Dinda, P. Sengupta, S. Ghosh, W.S. Sheldrick, Eur. J. Inorg. Chem. (2003) 363.

[50] R. Dinda, S. Ghosh, L.R. Falvello, M. Tomás, T.C.W. Mak, Polyhedron 25 (2006) 2375.

[51] G.J.-J. Chen, J.W. McDonald, W.E. Newton, Inorg. Chem. 15 (1976) 2612.

[52] E.H. Rodd, in Chemistry of Carbon Compounds, Elsevier, London, 3 (1954) 556.

[53] A. Sarkar, S. Pal, Inorg. Chim.Acta 362 (2009) 3807.

[54] G.M. Sheldrick, *SHELXL-97*, Program for Refinement of Crystal Structures, Universitäet Göttingen, Göttingen, Germany, (1997).

[55] Clinical and Laboratory Standards Institute Methods for Dilution Antimicrobial Susceptibility Tests for Bacteria That Grow Aerobically—Seventh Edition: Approved Standard M7-A7. CLSI, Wayne, PA, USA, (2006).

[56] A.A. Abdel Aziz, J. Mol. Struct. 979 (2010) 77.

[57] A.R. Yaul, V.V. Dhande, S.G. Bhadange, A.S. Aswar, Russ. J. Inorg. Chem. 56 (2011) 549.

[58] T.A. Hanna, A.K. Ghosh, C. Ibarra, M.A. Mendez-Rojas, A.L. Rheingold, W.H. Watson, Inorg. Chem. 43 (2004) 1511.

[59] J.M. Berg, R.H. Holm, Inorg. Chem.22 (1983) 1768.

[60] J.M. Berg, R.H. Holm, J. Am. Chem. Soc. 107 (1985) 917.

[61] J.M. Hawkins, J.C. Dewan, K.B. Sharpless, Inorg. Chem. 25 (1986) 1501.

[62] S. Bellemin-Laponnaz, K.S. Coleman, P. Dierkes, J.P. Masson, J.A. Osborn, Eur. J. Inorg. Chem. (2000) 1645.

[63] A. Tarushi, E.K. Efthimiadou, P. Christofis, G. Psomas. Inorg. Chim. Acta 360 (2007) 3978.

[64] E.K. Efthimiadou, Y. Sanakis, N. Katsaros, A. Karaliota, G. Psomas, Polyhedron 26 (2007) 1148.

[65] A.M. Ramadan, J. Inorg. Biochem. 65 (1997) 183.

[67] P.G. Avaji, C.H.V. Kumar, S.A. Patil, K.N. Shivananda, C. Nagaraju, Eur. J. Med. Chem. 44 (2009) 3552.

[68] M.L.H. Nair, D. Thankamani, Indian J. Chem. 48 (2009) 1212.

[69] N. Sharma, M. Kumari, V. Kumar, J. Coord. Chem. 63 (2010) 1940.

[70] Z.H. Chohan, S.H. Sumrra, M.H. Youssoufi, Eur. J. Med. Chem. 45 (2010) 2739.

[71] K.S. Prasad, L.S. Kumar, S.C. Shekar, M. Prasad, H.D. Revanasiddappa, Chem. Sci. J. (2011) 12.

# A Brief Resume of the Work Embodied in this Dissertation and Concluding Remark

# A Brief Resume of the Work Embodied in this Dissertation and Concluding Remark

The aim of this dissertation was to explore in depth certain aspects of the chemistry of oxomolybdenum(VI) ligated to a few selected multidentate NO- and/or ONO- donor systems. Major emphasis was given to the study of chemical, electrochemical, biological and catalytic activity of the complexes and structural characterization of the synthesized complexes and the products obtained from the precursor. Works described in **chapter 2-6** reveal the results of the attempt to fulfill the objectives. The following chapter-wise summary of the work presented in this dissertation reveals the extent to which the above-mentioned objectives are fulfilled.

*Chapter 2* contains synthesis and characterization of the oxomolybdenum(VI) complex $[MoO_2L(C_2H_5OH)]$ (**1**) of benzoylhydrazone of *2*-hydroxybenzaldehyde (H$_2$L). The substrate binding capacity of **1** has been demonstrated by the formation and isolation of two mononuclear $[MoO_2L(Q)]$ {where Q = imidazole (**2a**) and 1-methylimidazole (**2b**)} and one dinuclear $[(MoO_2L)_2(Q)]$ {Q = 4,4'-bipyridine (**3**)} mixed-ligand oxomolybdenum(VI) complexes. All the complexes have been characterized by elemental analysis, spectroscopic (IR, UV–Vis and NMR) and cyclic voltammetry measurements. Molecular structures of all the oxomolybdenum(VI) complexes (**1**, **2a**, **2b** and **3**) have been determined by X-ray crystallography. The complexes have been screened for their antibacterial activity against *Escherichia coli, Bacillus subtilis* and *Pseudomonas aeruginosa*. The minimum inhibitory concentration of these complexes and antibacterial activity indicates the compound **2a** and **2b** as the potential lead molecule for drug designing.

.*Chapter 3* deals with the synthesis, characterization and reactivity of a series of 5- and 6-coordinated oxomolybdenum(VI) complexes of the type $[MoO_2L(ROH)]$ [where R = C$_2$H$_5$ (**1**) and CH$_3$ (**2**)], and $[MoO_2L]$ (**3** and **4**) of four different ONO donor ligands: salicyloylhydrazone of 2-hydroxy-1-naphthaldehyde (H$_2$L$^1$), anthranylhydrazone of 2-hydroxy-1-naphthaldehyde (H$_2$L$^2$), benzoylhydrazone of 2-hydroxy-1-acetonaphthone (H$_2$L$^3$) and anthranylhydrazone of 2-hydroxy-1-acetonaphthone (H$_2$L$^4$; general abbreviation H$_2$L). The substrate binding capacity of **1** has been demonstrated by the formation of one mononuclear mixed-ligand dioxomolybdenum

complex [MoO$_2$L$^1$(Q)] {where Q = γ-picoline (**1a**)}. Molecular structure of all the complexes (**1**, **1a**, **2**, **3** and **4**) is determined by X-ray crystallography, demonstrating the dibasic tridentate behavior of ligands. The complexes have been screened for their antibacterial activity against *Escherichia coli, Bacillus subtilis, Proteus vulgaris* and *Klebsiella pneumoniae*. The minimum inhibitory concentration of these complexes and antibacterial activity indicates **1** and **1a** as the potential lead molecule for drug designing. Catalytic potential of these complexes was tested for the oxidation of benzoin using 30% aqueous H$_2$O$_2$ as an oxidant in methanol. At least four reaction products benzoic acid, benzaldehyde-dimethylacetal, methylbenzoate and benzil were obtained with the 95-99% conversion under optimized reaction conditions. Oxidative bromination of salicylaldehyde, a functional mimic of haloperoxidases, in aqueous H$_2$O$_2$/KBr in the presence of HClO$_4$ at room temperature has also been carried out successfully.

*Chapter 4* describes the report of synthesis and characterization of two novel dimeric [(Mo$^{VI}$O$_2$)$_2$L] (**1**) and tetrameric [{(C$_2$H$_5$OH)LO$_3$Mo$_2$$^{VI}$}$_2$(μ-O)$_2$]·C$_2$H$_5$OH (**2**) dioxomolybdenum (VI) complexes with *N,N'*-disalicyloylhydrazine (H$_2$L), which is formed by the self combination of acid hydrazide. Both the complex was characterized by various spectroscopic techniques (IR, UV–Vis and NMR) and also by electrochemical study. The molecular structures of both the complexes have been confirmed by X-ray crystallography. All these studies indicate that the *N,N'*-disalicyloylhydrazine (H$_2$L) has the normal tendency to form both dimeric and tetrameric complexes coordinated through the dianionic tridentate manner.

In *chapter 5* two novel dioxomolybbdenum(VI) complexes containing the MoO$_2$$^{2+}$ motif are reported where unexpected coordination due to ligand rearrangement through metal mediated interligand C–C bond formation is observed. These ligand transformations are probably initiated by molybdenum assisted C–C bond formation in the reaction medium. It is checked and confirmed that, the reactions using other metal precursors [VO(acac)$_2$ or Cu(acac)$_2$] do not initiate this type of ligand rearrangement. The ligands (H$_2$L$^{'}$) are tetradentate C–C coupled O$_2$N$_2$– donor systems formed *in situ* during the synthesis of the complexes from bis(acetylacetonato)dioxomolybdenum(VI) with Schiff base ligands of 2-aminophenol with 2-pyridinecarboxaldehyde (HL$^1$) and 2-quinolinecarboxaldehyde (HL$^2$). The reported

dioxomolybdenum(VI) complexes $[MoO_2L'^1]$ (**1**) and $[MoO_2L^2]$ (**2**) coordinated with the $O_2N_2$– donor rearranged ligand are expected to have better stability of the +6 oxidation state of molybdenum than the corresponding ONN– donor ligand precursor. Both the complexes are fully characterized by several physicochemical techniques and the novel structural features through single crystal X-ray crystallography.

The essence of the work presented in ***chapter 6*** is the detailed account of the synthesis, structure, spectroscopic, electrochemical properties and study of biological activity of some oxomolybdenum(VI) complexes with special reference to their H–bonded molecular and supramolecular structures. Reaction of bis(acetylacetonato)dioxomolybdenum(VI) with three different hydrazides (isonicotinoyl hydrazide, anthraniloyl hydrazide and 4-nitrobenzoyl hydrazide) afforded two dioxomolybdenum(VI) complexes $\{[MoO_2L^1(CH_3OH)]$ (**1**) and $[MoO_2L^3]$ (**3**)$\}$ and one mono-oxomolybdenum(VI) complex $\{[MoOL^2(O\text{-}N)]$ (**2**)$\}$ (where L = Intermediate *in situ* ligand formed by the reaction between acetyl acetone and the corresponding acid hydrazide, and O–N = 4-nitrobenzoylhydrazide). All the complexes have been characterized by elemental analysis, magnetic and spectroscopic (IR, UV–Vis and NMR) measurements. Molecular structures of all the complexes (**1**, **2** and **3**) have been determined by X-ray crystallography. The complexes have been screened for their antibacterial activity against *Escherichia coli, Bacillus subtilis* and *Pseudomonas aeruginosa*. The minimum inhibitory concentration of these complexes and antibacterial activity indicates **1** as the potential lead molecule for drug designing.

The author is very much aware of the fact that some portions of the work described in the present dissertation left scope for future work especially the biological and catalytic studies. All the reported complexes can be used for the study of several other catalytic and bio activities. This dissertation also left scope for further qualitative improvement by the utilization of some relevant instrumental data, which could have been really helpful in arriving at completely unambiguous conclusions. As those instrumental facilities were not available to us, we were rather helpless. However, the above discussion on the entire work presented in **chapter 2-6** reveals that the aims and objectives of the present dissertation are mostly fulfilled.

# Bio-data

**Sagarika Pasayat**

Research Scholar

Department of Chemistry

National Institute of Technology Rourkela

Rourkela-769008, Odisha, India

## Research experience

**A. Doctoral Research (July 2008 – Continuing)**

Supervisor: Dr. Rupam Dinda, Department of Chemistry, National Institute of Technology Rourkela, India,

**Research area**        Synthetic Inorganic Chemistry

**B. M.Sc. One Year Project (July 2006 – May 2007)**

Title of Thesis: "*Study the removal of fluoride from water by using chitin*".

Supervisor: Prof. R. K. Patel, Department of Chemistry, National Institute of Technology Rourkela, India,

**C. Summer Project (May 2006 – July 2006)**

Title of Thesis: "*Naphthalene production in Steel Plant*".

Supervisor: Dr. H. Mohanty, R & D Section, Rourkela Steel plant of India, India.

## Analytical Techniques

Spectroscopy        :  Acquisition and analysis of $^1$H, $^{13}$C NMR, Mass spectra. Recording and interpretation of GC-MS, FT-IR, UV-Vis spectra, Magnetic Susceptibility and Cyclic Voltammetry.  Interpretation of X-ray crystal structure

X-Ray Crystallography Software: **MERCURY & ORTEP**

## Education Profile

| | |
|---|---|
| 2000 | Secondary (**10$^{th}$**), BSE Board, Ispat Vidyalaya, Rourkela, Odisha, India. |
| 2002 | Higher Secondary (**+2 Science**), CHSE Board, D.A.V. Women's College, Rourkela, Odisha, India. |
| 2005 | Graduation (**B.Sc. Hons. in Chemistry**), Sambalpur University, Ispat College, Rourkela, Odisha, India |
| 2007 | Post graduation (**M.Sc. in Chemistry**), NIT, Rourkela, Odisha, India. |

## Honors and Fellowship

- Qualified Senior Research Fellowship (CSIR), Govt. of India, 2010
- Life Member of Orissa Chemical Society, Odisha, India

## Papers published in cited Journals (SCI)

1) Alkali metal (Na+ and K+)-mediated supramolecular assembly of oxovanadium(V) complexes: Synthesis and structural characterization, R. Dinda, P. K. Majhi, P. Sengupta, **S. Pasayat**, S. Ghosh, L. R. Falvello, T. C. W. Make, **Polyhedron, 2010,** *29*, 248.

2) Oxovanadium(V) complexes incorporating tridentate aroylhydrazoneoximes: Synthesis, characterizations and antibacterial activity, S. P. Dash, **S. Pasayat**, Saswati, H. R. Dash, S. Das, Ray J. Butcher, Rupam Dinda, **Polyhedron, 2012,** *38*, 524

3) Mixed-ligand aroylhydrazone complexes of molybdenum: Synthesis, structure and biological activity, **Sagarika Pasayat**, Subhashree P. Dash, Saswati, Paresh K. Majhi, Yogesh P. Patil, M. Nethaji, Hirak R. Dash, Surajit Das, Rupam Dinda, **Polyhedron, 2012,** *31*, 198.

4) Synthesis, structural studies and catalytic activity of dioxidomolybdenum(VI) complexes with aroylhydrazones of naphthol-derivative, **Sagarika Pasayat**, Subhashree P. Dash, Satabdi Roy, Rupam Dinda, Sarita Dhaka, Mannar. R. Maurya, Werner Kaminsky, Yogesh P. Patil and M. Nethaji, **Polyhedron (Accepted)**.

5) Synthesis, Structure and Characterization of Dimeric and Tetrameric Dioxomolybdenum(VI) Complexes of *N,N'*-Disalicyloylhydrazine, **Sagarika Pasayat**, Subhashree P. Dash, Rupam Dinda, E. Sinn and H. Stoeckli-Evans, **Inorg. Chim. Acta** (**Communicated**).

## Personal Profile

- Name                           Sagarika Pasayat
- Date of Birth               1$^{st}$ May 1985
- Nationality                   Indian
- Permanent Address       At-Upper Balijodi, Town- Fertilizer

  P.O.- Sonaparbat, Dist- Sundergarh,

  Odisha-769016

# Publications

**Papers published in cited Journals (SCI)**

1) Alkali metal (Na+ and K+)-mediated supramolecular assembly of oxovanadium(V) complexes: Synthesis and structural characterization, Rupam Dinda, P. K. Majhi, P. Sengupta, **S. Pasayat**, S. Ghosh, L. R. Falvello, T. C.W. Make, **Polyhedron, 2010,** *29*, 248.

2) Oxovanadium(V) complexes incorporating tridentate aroylhydrazoneoximes: Synthesis, characterizations and antibacterial activity, S. P. Dash, **S. Pasayat**, Saswati, H. R Dash, S. Das;,Ray J Butcher, Rupam Dinda, **Polyhedron, 2012,** *38*, 524.

3) Mixed-ligand aroylhydrazone complexes of molybdenum: Synthesis, structure and biological activity, **Sagarika Pasayat**, Subhashree P. Dash, Saswati Bhakat, Paresh Kumar Majhi, Yogesh P. Patil, M. Nethaji, Hirak R. Dash, Surajit Das, Rupam Dinda, **Polyhedron, 2012,** *31*, 198.

4) Synthesis, structural studies and catalytic activity of dioxidomolybdenum(VI) complexes with aroylhydrazones of naphthol-derivative, **Sagarika Pasayat** , Subhashree P. Dash , Satabdi Roy , Rupam Dinda , Sarita Dhaka , Mannar. R. Maurya , Werner Kaminsky , Yogesh P. Patil  and M. Nethaji, **Polyhedron (Accepted)**.

5) Synthesis, Structure and Characterization of Dimeric and Tetrameric  Dioxomolybdenum(VI) Complexes of *N,N*'-Disalicyloylhydrazine, **Sagarika Pasayat**, Subhashree P. Dash, Rupam Dinda, E. Sinn and H. Stoeckli-Evans, **Inorg. Chim. Acta** (**Communicated**).

**Papers published in Conference Proceedings, Popular Journals etc**

1) 'Synthesis, Structural and Biological Evaluation of Dioxomolybdenum(VI) Complexes: Metal-Mediated Metal–Metal And C–C Bond Formation', **Sagarika Pasayat**, Satabdi Roy, Subhashree P. Dash, Saswati, Werner Kaminsky and Rupam Dinda', **International Conference on Recent Trends in Organometallic Compounds and their Industrial Applications, KIIT University, Bhubaneswar, India, 5-7 February, 2013.**

2) 'Synthesis and Characterization of a Series of Hexacoordinated Non-oxo Vanadium(IV) Complex', Subhashree P. Dash, Satabdi Roy, **Sagarika Pasayat**, Saswati, Yogesh P. Patil M. Nethaji and Rupam Dinda, **15<sup>th</sup> CRSI National Symposium in Chemistry (NSC-15), BHU, India, 1-3 February, 2013**.

3) 'Dioxomolybdenum(VI) Complexes of Isonicotinoyl Hydrazide Derivatives: Synthesis, Characterizations and Antibacterial Activity', **Sagarika Pasayat**, Subhashree P. Dash, Yogesh P. Patil, M. Nethaji, Ekkehard Sinn and Rupam Dinda, **14th CRSI National Symposium in Chemistry (NSC-14), NIIST, Trivandrum, Kerala, India, 2-3 February, 2012**.

4) 'Complexation of Isoniazid and its derivatives with vanadium: synthesis, characterization and antimicrobial activity', Subhashree P. Dash, **Sagarika Pasayat**, Yogesh P. Patil, M. Nethaji and Rupam Dinda, **National Symposium on Modern Trends in Inorganic Chemistry (MTIC-XIV), University of Hyderabad, 10-13 December, 2011**.

5) 'Synthesis, Structure and Study of Reactivity of Two Novel Dioxomolybdenum(VI) complexes with Tridentate Hydrazone Ligands ', **Sagarika Pasayat**, Subhashree P. Dash, M. Nethaji and Rupam Dinda, **13th CRSI National Symposium in Chemistry (NSC-13), KIIT University, Bhubaneswar, India, 4-6 February, 2011.**

6) 'Synthesis and characterization of mono and binuclear oxovanadium(V) complexes incorporating oxime based ligand systems'. Subhashree P. Dash, **Sagarika Pasayat**, Saswati, M.Nethaji, Ray J. Butcher and Rupam Dinda, **Frontiers in Inorganic Chemistry (FIC-2010), IACS, Kolkata, 11-13 December, 2010**.

7) 'New insights into the chemistry of oxovanadium(V) oxomolybdenum(VI) complexes with tridentate hydrazone ligands', S. P. Dash, **S. Pasayat**, P. K. Majhi and R. Dinda, **National Seminar on Recent Trends in Chemical Sciences' School of Chemistry, Sambalpur University, 19-21 February, 2010**.

8) 'Complexes of oxovanadium(V) oxomolybdenum(VI) with tridentate acid hydrazide based Schiff bases', S. P. Dash, P. K. Majhi, S. Pasayat, E. Sinn and R. Dinda, **Nation Seminar on Recent Trends in Chemical Science and Technology, NIT Rourkela, 19-20 December, 2009.**

9) 'Synthesis, Characterization and Reactivity of Oxomolybdenum(IV) and (VI) Complexes Featuring O-N Donor Ligands', **S. Pasayat**, P. K. Majhi, E. Sinn, and R. Dinda, **National Symposium on Modern Trends in Inorganic Chemistry', (MTIC-XIII), IISC, Bangalore, 7-10 December, 2009**.

10) 'Studies Paving the New Way for Exploration of Mixed-Oxidation Divanadium(IV,V) Complexes', P. K. Majhi, **S. Pasayat**, N. P. Rath and R. Dinda, **12th International Symposium on Inorganic Ring Systems, Holiday Inn Resort, Goa, India, 16-21 August, 2009**.

11) 'New Mononuclear Molybdenum(VI) Complex Resembling the Active Centre of Molybdenum Oxotransferases', **S. Pasayat**, P. K. Majhi, S. Behera, P. Mitra and R. Dinda, **National Conference on Socio-Economic Development Challenges before Women Scientist, Technologists & Engineers, NIT, Rourkela, 13-15 February, 2009**.